

Table of contents

Summary	v
Abbreviations	vii
List of compounds	x
<u>Chapter 1 : Antitumor properties of cisplatin and titanium(IV) complexes</u>	1
1.1 Introduction	1
1.2 Cisplatin	4
1.3 Metallocene compounds	8
1.3.1 Titanocene dichloride	9
1.3.2 Budotitane	14
1.4 Modes of Action	16
1.4.1 Covalent bond formation of titanium(IV)	16
1.4.2 Intercalation	18
1.5 Aim of Study	20
1.6 Construction of thesis	25
<u>Chapter 2 : Titanocene derivatives with a heteroaromatic ligand containing a direct metal-carbon σ-bond</u>	26
2.1 Introduction	26
2.2 Synthesis	29
2.3 Characterization	34
• <i>Mass spectrometry</i>	34
• <i>^1H NMR and ^{13}C NMR spectroscopy</i>	38
• <i>X-ray crystallography</i>	46
2.4 Conclusions	51
<u>Chapter 3 : Titanocene derivatives with heteroaromatic thiolate ligands</u>	52
3.1 Introduction	52
3.2 Synthesis	53
3.3 Characterization	56
• <i>Mass spectrometry</i>	56
• <i>^1H NMR and ^{13}C NMR spectroscopy</i>	61
• <i>X-ray crystallography</i>	69
3.4 Conclusions	71

Chapter 4 : Bi- and trinuclear complexes of titanium(IV) and platinum(II)	72
4.1 Introduction	72
4.2 Synthesis	75
4.3 Characterization	82
• <i>Mass spectrometry</i>	82
• <i>¹H NMR and ¹³C NMR spectroscopy</i>	86
4.4 Conclusions	92
Chapter 5 : Antitumor properties, DNA interaction and ligand substitutions	93
5.1 Introduction	93
5.2 Antitumor activity	94
5.2.1 Conclusions	99
5.3 Structural features vs. antitumor activities	100
5.3.1 Conclusions	102
5.4 Ligand substitution in aqueous medium	102
5.4.1 Conclusions	108
5.5 Intercalation studies	108
5.5.1 Conclusions	112
5.6 Summary of test results and DNA interaction	113
Chapter 6 : Experimental	114
6.1 General	114
6.2 Lithiation and synthesis of heteroaromatic compounds	115
6.3 Synthesis of titanocene derivatives	119
6.4 Synthesis of bi- and trinuclear complexes	127
6.5 <i>In vitro</i> tests	135
6.6 Studies related to the antitumor activities of the complexes	135
6.7 Crystal structure determinations	136
Appendix A	141
Appendix B	149
Appendix C	155
Appendix D	161
Appendix E	163
Appendix F	165

Structure-activity relationships of titanocene complexes with antitumor properties

Candidate: Susanna Brink

Promotor: Prof Simon Lotz

Department: Chemistry

Degree: Philosophiae Doctor

Summary

This study involves the synthesis and characterization of new organometallic complexes of Ti(IV). Such complexes were modelled on titanocene dichloride and designed to act as antitumor agents incorporating ligands with specific functions. As target for biological activity, the DNA double helix was identified. The desired complexes displayed (i) a labile halogen ligand for covalent bond formation with DNA, (ii) a planar condensed 3-membered heteroaromatic ring ligand that could act as intercalator in the major groove of DNA and (iii) two bulky, non-labile stopper ligands which will control the degree of intercalation. The complexes prepared in this study were representative of two groups, namely those where the transition metal was bonded directly to a carbon of the planar ring ligand and those where a sulfur atom was located between the metal and the ring ligand. The sulfur atom acts as a spacer and causes the ring unit to lie out of the plane of the metal. Dinuclear metal complexes were also investigated and two classes of complexes were prepared. The complexes where two $[\text{TiCp}_2]$ fragments were linked and connected to two Cp rings and complexes where a [Ti] and a [Pt] fragment were connected through a Cp and ethylene diamine ligand, respectively.

New complexes $[\text{TiCp}_2(\text{R})\text{Cl}]$, $[\text{TiCp}_2(\text{R})_2]$, $[\text{TiCp}_2(\text{SR})\text{Cl}]$ and $[\text{TiCp}_2(\text{SR})_2]$ (RH = thianthrene, dibenzodioxin, dibenzofuran, benzo[b]furan, dibenzothiophene and benzo[b]thiophene) were prepared by adding the lithiated heteroaromatic precursors or the metallated thiolates to titanocene dichloride. The composition of the new complexes was determined by using NMR studies, mass spectrometry and micro analysis. The structures of $[\text{TiCp}_2(\text{Dbz})\text{Cl}]$, $[\text{TiCp}_2(\text{SDBt})\text{Cl}]$ and $[\text{TiCp}_2(\text{Dbf})_2]$ were confirmed by single crystal X-ray diffraction studies. Reaction pathways for the synthesis of $[\{\mu\text{-}\eta^5, \eta^5\text{-C}_{14}\text{H}_{16}\}\text{Ti}_2\text{Cp}_2\text{X}_2\text{Cl}_2]$ (X = Cl, SDbf) and $[\{\mu\text{-}\eta^5, \eta^5\text{-C}_{14}\text{H}_{16}\}\text{Ti}_2\text{Cp}_2\text{XCl}_3]$ (X = Dbf, SDbf) were established.

Complexes were selected for *in vitro* tests against HeLa and CoLo cells. The results were correlated with the geometry of the complexes, which made it possible to determine the antitumor structure-activity relationships. It was found that the greatest inhibition of tumor cell growth was achieved when a complex had a thiolate ligand (i.e. SDbf) for intercalation as well as a labile chloro ligand for substitution. These results supported the initial objectives and assumptions of the study. Also studied was the intercalative behaviour of selected complexes and their ligand substitution in aqueous medium. Using flow cytometry it was possible to show that the complexes did not intercalate and the high activity could probably be ascribed covalent bond formation of the complexes. Many other factors that could play a role such as the rate of substitution of ligands in aqueous medium were investigated.

Abbreviations

Nucleobases

5'-dAMP	5'-Deoxynucleoside adenosine monophosphate
5'-dCMP	5'-Deoxynucleoside thiamine monophosphate
AMP	Adenine monophosphate
dGMP	Deoxynucleoside guanine monophosphate
dTMP	Deoxynucleoside thiamine monophosphate
UMP	Uracil monophosphate
DNA	Deoxyribonucleic acid
RNA	Ribonucleic acid
A	Adenine
C	Cytosine
G	Guanine
T	Thymine
U	Uracil

Heteroaromatics

BfH/Bf	Benzo[b]furan/ Deprotonated benzo[b]furan
BtH/Bt	Benzo[b]thiophene/ Deprotonated benzo[b]thiophene
BuSDBz	1-Butylsulfanyl dibenzodioxin
DbfH/Dbf	Dibenzofuran/ Deprotonated dibenzofuran
DbfH-Me/Dbf-Me	4-Methyl dibenzofuran/ Deprotonated 4-methyl dibenzofuran
DbtH/Dbt	Dibenzothiophene/ Deprotonated dibenzothiophene
DbzH/Dbz	Dibenzo[1,4]dioxin/ Deprotonated dibenzo[1,4]dioxin
DpeH ₂ /Dpe	Diphenyl ether/ Deprotonated diphenyl ether
HSBf/SBf	Benzo[b]furan-2-thiol/ Benzo[b]furan-2-thiolate
HSBt/SBt	Benzo[b]thiophene-2-thiol/ Benzo[b]thiophene-2-thiolate
HSDbf/SDbf	Dibenzofuran-4-thiol/ Dibenzofuran-4-thiolate
HSDbf-Me/SDbf-Me	6-Methyl dibenzofuran-4-thiol/ 6-Methyl dibenzofuran-4-thiolate
HSDbt/SDbt	Dibenzothiophene-4-thiol/ Dibenzothiophene-4-thiolate
HSDbz/SDbz	Dibenzodioxin-1-thiol/ Dibenzodioxin-1-thiolate
HSThr/SThr	Thianthrene-1-thiol/ Thianthrene-1-thiolate
ThrH/Thr	Thianthrene/ Deprotonated thianthrene

Nuclear magnetic resonance spectroscopy

COSY	Correlation spectroscopy
HETCOR	Heteronuclear correlation spectroscopy
NMR	Nuclear magnetic resonance
¹ H NMR	Proton nuclear magnetic resonance
¹³ C NMR	Carbon nuclear magnetic resonance
d	Doublet
dd	Doublet of doublets
dt	Doublet of triplets
m	Multiplet
s	Singlet
t	Triplet
J	Coupling constant
δ	Chemical shift

Other techniques and instruments

<i>Anal. Calc.</i>	Micro analysis calculated values
EELS	Electron energy loss spectroscopy
ICP	Inductive coupled plasma
[M ⁺]	Molecular ion
Mp	Melting point
UV	Ultraviolet

Substituents

Bu	Butyl
Cp	Cyclopentadienyl
R	Heteroaromatic ligand
X	Labile ligand

Solvents and bases

THF	Tetrahydrofuran
TMEDA	Tetramethylethylenediamine



Tumor cell lines

CoLo	Colorectal carcinoma
EhAT	Ehrlich ascites tumour
HeLa	Human cervix epitherioid carcinoma

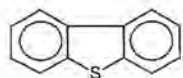
Other

FS	Forward scatter
SS	Side scatter
L	Ligand
M	Transition metal
ppm	Parts per million
Å	Angstrom (10^{-8} m)
μ	Indicates a bridged ligand
d^n	Superscript indicates the number of valence electrons in the d-orbital
η^n	Superscript indicates the number of coordinated carbons

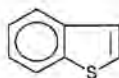
Bestpf@.com

List of Compounds

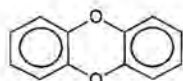
Organic Starting Compounds



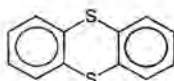
Dibenzothiophene [DbtH] L2-01



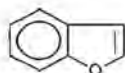
Benzo[b]thiophene [BtH] L2-02



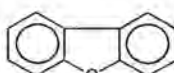
Dibenzo[1,4]dioxin [DbzH] L2-03



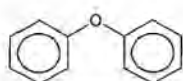
Thianthrene [ThrH] L2-04



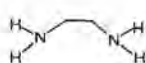
Benzo[b]furan [BfH] L2-05



Dibenzofuran [DbfH] L2-06



Diphenylether [DpeH₂] L2-08



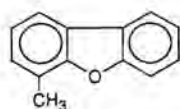
Ethylene diamine L4-01



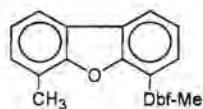
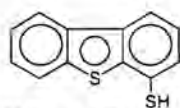
N-methyl ethylene diamine L4-02



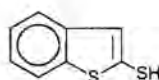
N,N'-dimethyl ethylene diamine L4-03

Organic Compounds Synthesized

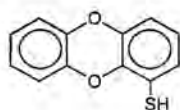
4-Methyl dibenzofuran [DbfH-Me] L2-07

4,4'-Dimethyl-6,6'-bi(dibenzofuran)
[Me-Dbf-Dbf-Me] L2-07b

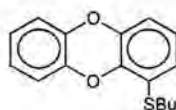
Dibenzothiophene-4-thiol [HSDbt] L3-01



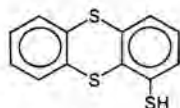
Benzo[b]thiophene-2-thiol [HSBt] L3-02



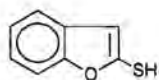
Dibenzodioxin-1-thiol [HSDbz] L3-03



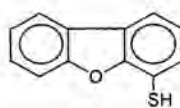
1-Butylsulfanyl dibenzodioxin [BuSDBz] L3-03b



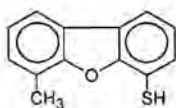
Thianthrene-1-thiol [HSThr] L3-04



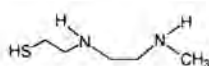
Benzo[b]furan-2-thiol [HSBf] L3-05

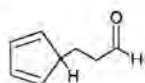
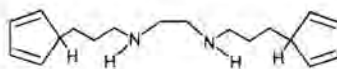
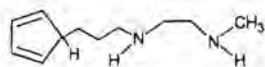
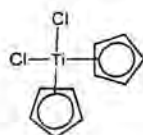
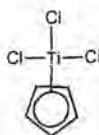
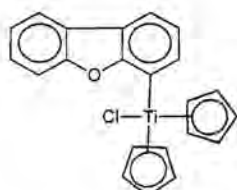
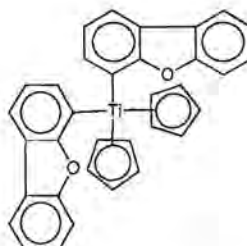
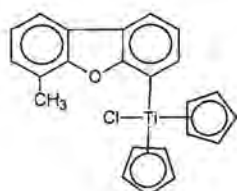
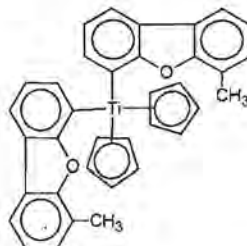


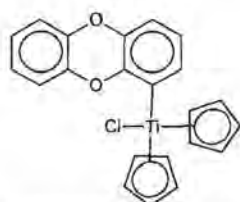
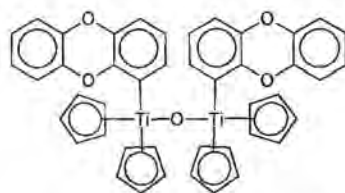
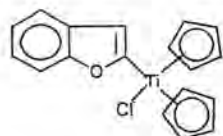
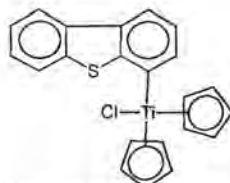
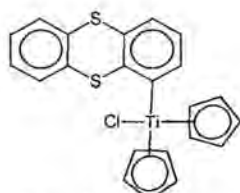
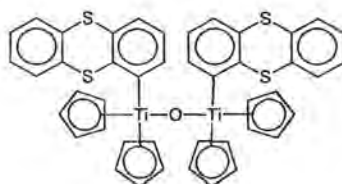
Dibenzofuran-4-thiol [HSDbf] L3-06

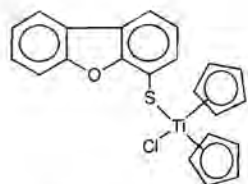
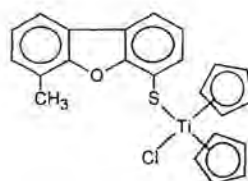
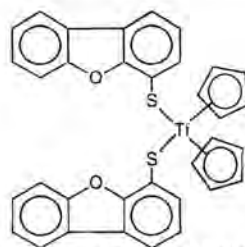
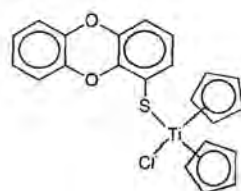
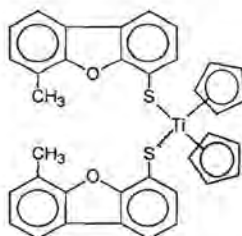
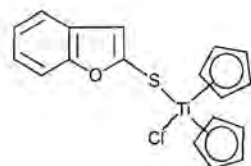
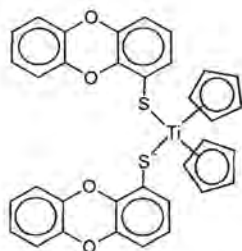
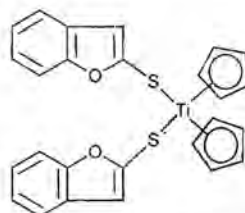


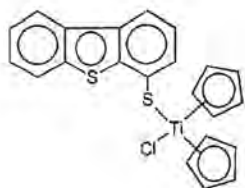
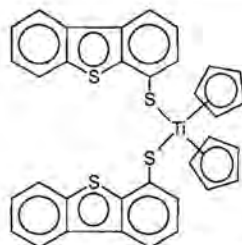
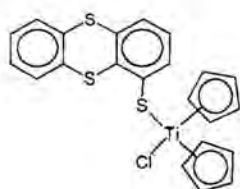
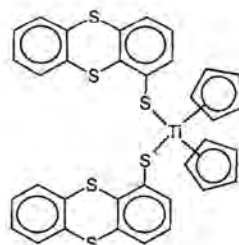
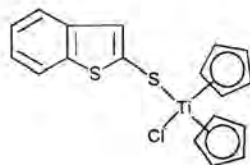
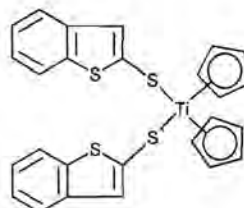
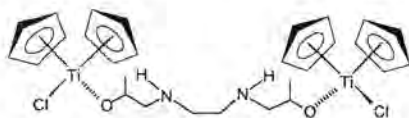
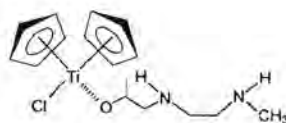
6-Methyl dibenzofuran-4-thiol [HSDbf-Me] L3-07

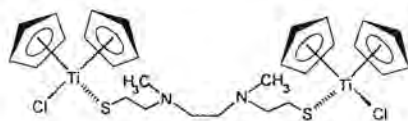
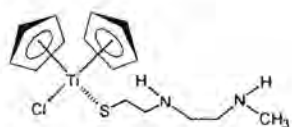
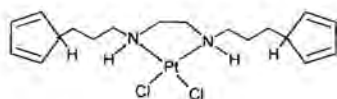
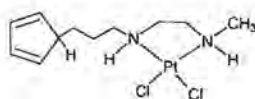
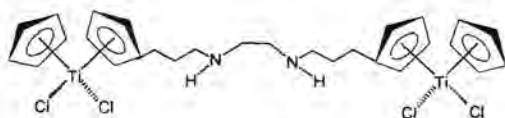
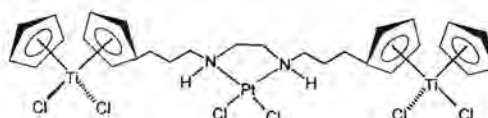
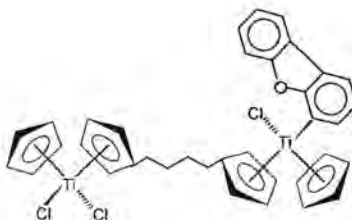
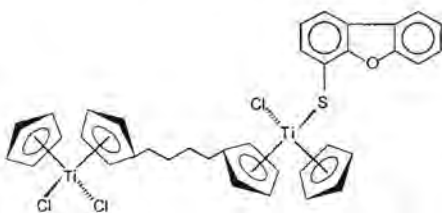
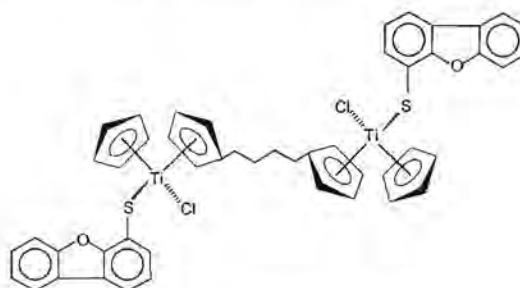
2-((2-((2-mercaptoethyl)methylamino)ethyl)methylamino)ethanethiol [C₈H₂₀N₂S] L4-042-(2-methylamino ethylamino)ethanethiol [C₅H₁₄N₂S] L4-05

3-cyclopentadienyl propionaldehyde **L4-06** N,N' -bis-(3-cyclopentadienyl propyl) ethylene diamine
L4-07N-(3-cyclopentadienyl propyl)-N'-methyl ethylene diamine **L4-08****Organometallic Starting Complexes**Titanocene dichloride $[TiCp_2Cl_2]$ **S-01**Trichloro cyclopentadienyl titanium (IV) $[TiCpCl_3]$ **Organometallic Complexes Synthesized**Chlorobis(cyclopentadienyl)(dibenzofuran-4-yl)titanium(IV) $[TiCp_2(Dbf)Cl]$ **2-01**Bis(cyclopentadienyl)bis(dibenzofuran-4-yl)titanium(IV) $[TiCp_2(Dbf)_2]$ **2-02**Chlorobis(cyclopentadienyl)(6-methyl dibenzofuran-4-yl)titanium(IV) $[TiCp_2(Dbf-Me)Cl]$ **2-03**Bis(cyclopentadienyl)bis(6-methyl dibenzofuran-4-yl)titanium(IV) $[TiCp_2(Dbf-Me)_2]$ **2-04**

Chlorobis(cyclopentadienyl)(dibenzodioxin-1-yl)titanium(IV) [TiCp₂(Dbz)Cl] **2-05** $(\mu\text{-Oxo})\text{bis}[\text{bis}(\text{cyclopentadienyl})(\text{dibenzodioxin-1-yl})\text{titanium(IV)}] [(\mu\text{-O})\{\text{TiCp}_2(\text{Dbz})\}_2]$ **2-06**(Benzofuran-2-yl)chlorobis(cyclopentadienyl)titanium(IV) [TiCp₂(Bf)Cl] **2-07**Chloro{bis(cyclopentadienyl)}(dibenzothiophen-4-yl)titanium(IV) [TiCp₂(Db)Cl] **2-08**Chlorobis(cyclopentadienyl)(thianthren-1-yl)titanium(IV) [TiCp₂(Thr)Cl] **2-09** $(\mu\text{-Oxo})\text{bis}[\text{bis}(\text{cyclopentadienyl})(\text{thianthren-1-yl})\text{titanium(IV)}] [(\mu\text{-O})\{\text{TiCp}_2(\text{Thr})\}_2]$ **2-10**Bis(cyclopentadienyl)(diphen-2,2'-yl ether)titanium(IV) [TiCp₂(Dpe)] **2-11**

Chlorobis(cyclopentadienyl)(dibenzofuran-4-ylsulfanyl)titanium(IV) [TiCp₂(SDbf)Cl] **3-01**Bis(cyclopentadienyl)bis(dibenzofuran-4-ylsulfanyl)titanium(IV) [TiCp₂(SDbf)₂] **3-02**Chlorobis(cyclopentadienyl)(6-methyl dibenzofuran-4-ylsulfanyl)titanium(IV) [TiCp₂(SDbf-Me)Cl] **3-03**Bis(cyclopentadienyl)bis(6-methyl dibenzofuran-4-ylsulfanyl)titanium(IV) [TiCp₂(SDbf-Me)₂] **3-04**Chlorobis(cyclopentadienyl)(dibenzodioxin-1-ylsulfanyl)titanium(IV) [TiCp₂(SDbz)Cl] **3-05**Bis(cyclopentadienyl)bis(dibenzodioxin-1-ylsulfanyl)titanium(IV) [TiCp₂(SDbz)₂] **3-06**(Benzofuran-2-ylsulfanyl)chlorobis(cyclopentadienyl)titanium(IV) [TiCp₂(SBf)Cl] **3-07**Bis(cyclopentadienyl)bis(benzofuran-2-ylsulfanyl)titanium(IV) [TiCp₂(SBf)₂] **3-08**

Chlorobis(cyclopentadienyl)(dibenzothien-4-ylsulfanyl)titanium(IV) [TiCp₂(SDbt)Cl] **3-09**Bis(cyclopentadienyl)bis(dibenzothien-4-ylsulfanyl)titanium(IV) [TiCp₂(SDbt)₂] **3-10**Chlorobis(cyclopentadienyl)(thianthren-1-ylsulfanyl)titanium(IV) [TiCp₂(SThr)Cl] **3-11**Bis(cyclopentadienyl)bis(thianthren-1-ylsulfanyl)titanium(IV) [TiCp₂(SThr)₂] **3-12**(Benzothien-2-ylsulfanyl)chlorobis(cyclopentadienyl)titanium(IV) [TiCp₂(SBf)Cl] **3-13**Bis(cyclopentadienyl)bis(benzothien-2-ylsulfanyl)titanium(IV) [TiCp₂(SBf)₂] **3-14**[{μ-C₈H₁₈N₂O₂} Ti₂Cp₄Cl₂] **4-01**[TiCp₂(OC₆H₁₅N₂)Cl] **4-02**

 $[\{\mu\text{-C}_8\text{H}_{18}\text{N}_2\text{S}_2\}\text{Ti}_2\text{Cp}_2\text{Cl}_2]$ **4-03** $[\text{TiCp}_2(\text{SC}_6\text{H}_{15}\text{N}_2)\text{Cl}]$ **4-04** $[\text{Pt}(\mu\text{-N,N}'\text{C}_{18}\text{H}_{28}\text{N}_2)\text{Cl}_2]$ **4-05** $[\text{Pt}(\mu\text{-N,N}'\text{C}_{11}\text{H}_{20}\text{N}_2)\text{Cl}_2]$ **4-06** $[\{\mu\text{-}\eta^5, \eta^5\text{-C}_{18}\text{H}_{26}\text{N}_2\}\text{Ti}_2\text{Cp}_2\text{Cl}_4]$ **4-07** $[\text{Ti}_2\{\mu\text{-}\eta^5, \eta^5\text{-(Pt(N,N}'\text{-C}_{18}\text{H}_{26}\text{N}_2)\text{Cl}_2)\}\text{Cp}_2\text{Cl}_4]$ **4-08** $[\{\mu\text{-}\eta^5, \eta^5\text{-C}_{14}\text{H}_{16}\}\text{Ti}_2\text{Cp}_2\text{Cl}_4]$ **4-09** $[\{\mu\text{-}\eta^5, \eta^5\text{-C}_{14}\text{H}_{16}\}\text{Ti}_2(\text{Dbff})\text{Cp}_2\text{Cl}_3]$ **4-10** $[\{\mu\text{-}\eta^5, \eta^5\text{-C}_{14}\text{H}_{16}\}\text{Ti}_2(\text{Dbff-S})\text{Cp}_2\text{Cl}_3]$ **4-11** $[\{\mu\text{-}\eta^5, \eta^5\text{-C}_{14}\text{H}_{16}\}\{\text{Ti}(\text{Dbff-S})\text{CpCl}\}_2]$ **4-12**

Chapter 1

Antitumor properties of *cisplatin* and titanium(IV) complexes

1.1. Introduction

Biomedical inorganic chemistry is a relative new research field and investigates possible applications of metal containing agents which display biological activities^{1,2}. An important part of these studies deals with compounds that display antitumor properties. The most successful anticancer drug to date containing a transition metal is *cisplatin*, [Pt(NH₃)₂Cl₂]³. The bioactivity of organometallic compounds and their anticipated application in medicine is at present a focal point of research. These studies became more relevant after the discovery that certain metallocene derivatives displayed antitumor activity⁴. The first 'International Symposium on Bioorganometallic Chemistry' was held in Paris in July 2002.

The Periodic Table in Figure 1.1 shows different metals of which some of their compounds display antitumor properties. Many of the complexes have structures, toxic properties and cellular modes of action that differ from those of *cisplatin*. Some were found to be effective on *cisplatin* resistant tumors.

1. P. J. Sadler, *Adv. Inorg. Chem.*, **1991**, 36, 1.

2. Z. Guo, P. J. Sadler, *Angew. Chem. Int. Ed.*, **1999**, 38, 1512.

3. *Cisplatin: Chemistry and Biochemistry of a Leading Anticancer Drug*, B. Lippert (Ed), Wiley-VCH, Weinheim, **1999**.

4. H. Köpf, P. Köpf-Maier, *Angew. Chem. Int. Ed. Engl.*, **1979**, 18, 477.

H																			He
Li	Be											B	C	N	O	F		Ne	
Na	Mg											Al	Si	P	S	Cl		Ar	
K	Ca	Sc	Ti	V	Cr	Mn	Fe	Co	Ni	Cu	Zn	Ga	Ge	As	Se	Br		Kr	
Rb	Sr	Y	Zr	Nb	Mo	Tc	Ru	Rh	Pd	Ag	Cd	In	Sn	Sb	Te	I		Xe	
Cs	Ba	La	Hf	Ta	W	Re	Os	Ir	Pt	Au	Hg	Tl	Pb	Bi	Po	At		Rn	
Fr	Ra	Ac	Db	Jl	Rf	Bh	Hn	Mt											

Main Group Complexes

Transition Metal Complexes

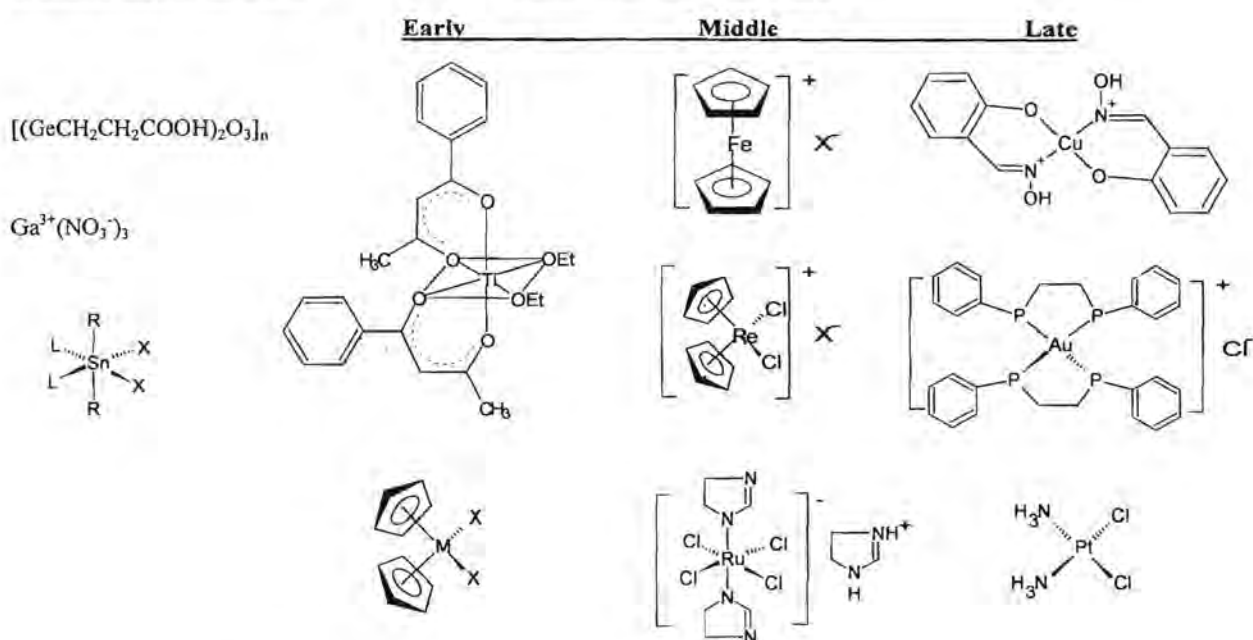


Figure 1.1. A selection of metal complexes that exhibit antitumor properties.

The antitumor active metal complexes range from the early transition metals through to the main group metals. There are basically three groups of metal containing antitumor agents.

- Inorganic complexes with classical heteroatom ligands coordinated to the metal
- Organometallic complexes where some of the ligands are directly linked to metal by carbon bonds
- Complexes with organic substituents or ligands coordinated to the metal via heteroatoms but without carbon-metal bonds

Note that many of the complexes in Figure 1.1 have two labile ligands in a *cis* configuration. It was initially accepted that the presence of readily replaceable *cis* halogen ligands was required for

antitumor activity. Also the comparable bite size of approximately 3.2Å in *cisplatin* and in active metallocene dichlorides was seen as a prerequisite for antitumor activity. These sites are vacated and taken up by donor atoms of nucleobases of DNA resulting in cytostatic activities of the compounds. The structure-activity relationship of *cisplatin* is well studied and documented³. Hence, the mechanism of action is reasonably well understood. The primary attack on DNA and formation of bifunctional intrastrand cross-links between two adjacent guanine bases by *cisplatin* was seen as the criterion for the mechanism associated with the antitumor activity.

The first non-platinum complex to enter clinical trials after *cisplatin* was budotitane, [Ti(diketonate)₂X₂], and it is presently among the most advanced antitumor complexes⁵. A few other promising complexes (like the metallocenes, germanium complexes and gallium salts) were also studied and are now in pre-clinical phase of testing or in clinical trials⁶. Since DNA is proposed as the target of most metal containing antitumor agents, there is an emphasis on those that interact with nucleic acids. Hence, some analogous derivatives were synthesized and studied to try and improve antitumor activities of the parent compounds.

New investigations in the area of antitumor drugs other than *cisplatin* are required, making studies of organometallic complexes such as titanocene derivatives an attractive alternative. Interestingly, all the organotransition metal complexes have cyclopentadienyl ligands which represent strong bonds. After the pioneering work done by Köpf and Köpf-Maier⁴ with metallocene dichlorides, this area of research has been neglected. Although the structure-activity relationship of titanocene dichloride has been studied, the mechanism of action responsible for the biological activity remains unclear.

In the short history of inorganic chemistry related to anticancer research, it is evident that the lead compound, *cisplatin*, influenced the design of most other metal complexes prepared and studied. The rest of the chapter summarizes the success story of *cisplatin* in greater detail. This will serve as an aid to understand DNA-based antitumor activity and the role of the transition metal. The titanium compounds, titanocene dichloride and budotitane are discussed to clarify the present level of understanding of the bioactivities of Ti(IV) compounds. Lastly, important interactions with DNA, such as covalent bond formation and intercalation and their role in antitumor activity, will also be explained.

5. B. K. Keppler, C. Friesen, H. Vorgerichten, E. Vogel in *Metal Complexes in Cancer Chemotherapy*, B. K. Keppler (Ed), VCH, Weinheim, 1993, 299.

6. B. K. Keppler, M. R. Berger, T. Klenner, M. E. Heim, *Adv. Drug Res.*, 1990, 19, 243.

1.2. *Cisplatin*

The serendipitous discovery of the antitumor activity of *cisplatin* (Figure 1.2) in 1969 by Barnett Rosenberg⁷ was a major achievement in bioinorganic chemistry. *Cisplatin* was the first metal complex to enter clinical trials in 1972 and after approval was introduced to clinics in 1979. This made it the first important contribution to cancer chemotherapy from the field of inorganic chemistry. Today this drug and its analogue, carboplatin (Figure 1.2), are the only inorganic complexes used on a routine clinical basis in cancer therapy. *Cisplatin* (by itself or in combination therapy) is the most extensively used drug in the treatment of certain malignant tumors.

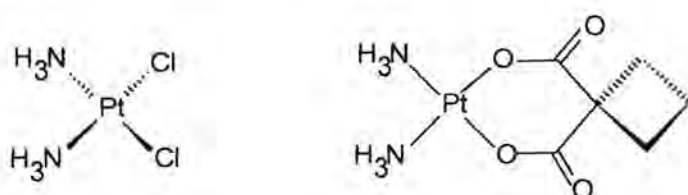


Figure 1.2. *Cisplatin* and carboplatin.

Despite the success of *cisplatin* as a drug, there are some disadvantages associated with its use. There are severe toxic side effects such as nausea, loss of hair, etc. and the ability of certain tumors to have a natural resistance to *cisplatin*, while others build up a resistance against *cisplatin* after use. In addition the spectrum of tumors inhibited by this drug is very narrow and unfortunately the high activity of *cisplatin* is limited to some very rare tumors, while most common tumors are not affected. Finally the drug has limited solubility, which makes it difficult to administer.

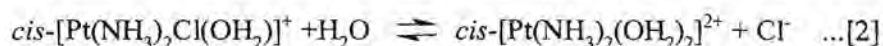
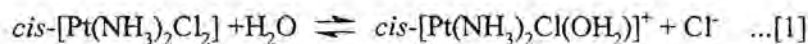
To try and minimize negative aspects associated with *cisplatin*, researchers synthesized *cisplatin* analogues. Although over 3000 second-generation platinum complexes were developed, carboplatin was the only one to receive worldwide registration⁸. The spectrum of activity of the direct derivatives of *cisplatin* largely resembles that of the mother complex due to their similar mechanism of action and some show only a limited improvement in drug toxicity.

The interaction of *cisplatin* with DNA has been studied extensively by researches using different approaches resulting in a good understanding of factors responsible for its antitumor activity. It is

7. B. Rosenberg, L. Van Camp, *Nature*, **1969**, *222*, 385.

8. R. B. Weiss, M. C. Cristian, *Drugs*, **1993**, *46*, 360.

believed that *cisplatin* is not the active species but is converted to the active drug inside the body⁹. *Cisplatin* has two chloro ligands (labile) and two ammine ligands (inert to substitution under biological conditions). The two labile chloro ligands are hydrolyzed in a stepwise manner as shown in reactions [1] and [2]^{10,11}.



In the blood plasma the chloride concentration is relatively high and this suppresses aquation, so the neutral dichloro complex is predominant outside the cell membrane¹². After entering the cell, where the chloride ion concentration is low, the hydrolysis products are formed easily. The positively charged, highly active diaquo species are attracted to the nucleophilic sites on DNA first through electrostatic attraction and thereafter by covalent bond formation.

Due to the *cis*-configuration of the complex, DNA is cross-linked as seen in Figure 1.3. (illustrating interstrand and intrastrand cross-links)⁹. It is believed that the 1,2-intrastrand cross-link of guanine bases is the critical lesion that leads to cytotoxicity, because it is specific to the *cis* isomer of the platinum complex^{13,14}. These cross-links form due to covalent bonding, preferably to two adjacent guanine bases on the N-7 position, because they are exposed in the major groove and uninvolved in Watson-Crick hydrogen bonding. Once these Pt-N adducts are formed they are very stable under physiological conditions.

9. S. E. Sherman, S. J. Lippard, *Chem. Rev.*, **1987**, 87, 1153.

10. M. E. Howe-Grant, S. J. Lippard, *Metal Ions Biol. Syst.*, **1980**, 11, 63.

11. T. G. Appleton, J. R. Hall, S. F. Ralph in *Platinum and Other Metal Coordination Compounds in Cancer Chemotherapy.*, M. Nicolini (Ed) Martinus, Nijhoff, Boston, **1988**, 643.

12. M. C. Lim, R. B. Martin, *J. Inorg. Nucl. Chem.*, **1976**, 38, 1911.

13. J. -P. Macquet, T. Theophanides, *Bioinorg. Chem.*, **1975**, 5, 59.

14. D. M. L. Goodgame, *Biochim. Biophys. Acta*, **1975**, 378, 153.

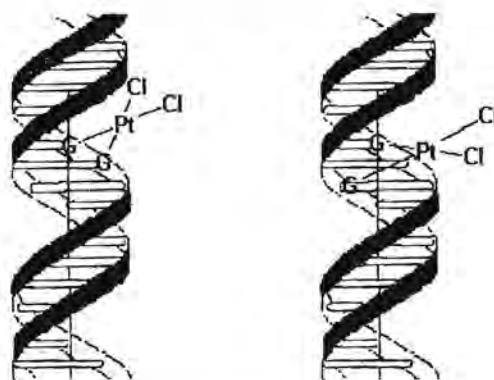


Figure 1.3. Interstrand- and intrastrand cross-linking of cisplatin to DNA.

The cisplatin-DNA adduct can be accommodated in the double helix, causing only small localized disruptions of the helix that cannot be recognized by repair enzymes¹⁵. The double helix can be unwound due to short-range intrastrand cross-links and shortening of the double helix can occur due to long range cross-links¹⁶. A crystal structure by Lippard and co-workers¹⁷ demonstrates that the one strand of DNA is slightly bent towards the major groove (Figure 1.4) This distortion of the DNA structure by cisplatin triggers a series of events responsible for its antitumor activity.

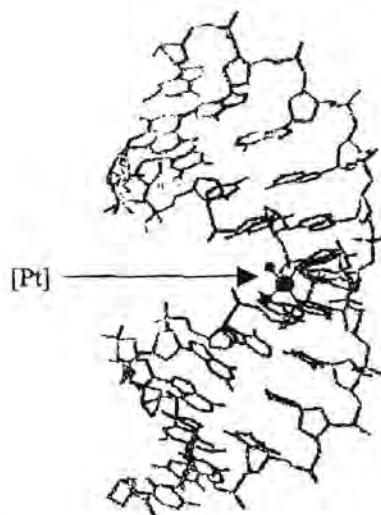


Figure 1.4. Damage done to the DNA structure due to cisplatin cross-links¹⁷.

15. R. B. Ciccarelli, M. J. Solomon, A. Varshavsky, S. J. Lippard, *Biochemistry*, **1985**, *24*, 7533.

16. S. J. Lippard, *Pure Appl. Chem.*, **1987**, *59*, 731 (and references therein).

17. P. M. Takahara, A. C. Rosenzweig, C. A. Frederick, S. J. Lippard, *Nature*, **1995**, *377*, 649.

The binding of high mobility group domain proteins (which specifically recognize cisplatin induced DNA 1,2-intrastrand cross-links) shields the adduct from repair¹⁸. The hydrophobic surface in the minor groove is the target for interaction of the high mobility group proteins. The major biochemical effect is inhibition of replication. Studies into the structure-activity relationships of cisplatin analogues lead to a set of empirical rules to ensure antitumor activity in second-generation platinum complexes^{19,20}. These rules concluded that active complexes should have:

- a *cis* configuration of labile ligands– The *cis* isomer is generally more active because of the chelating ability to biological molecules. Synthesis of new metal complexes that can act against cisplatin resistant tumors due to different mechanisms of action.
- two labile ligands – The labile groups must be readily replaced by water to be active. Too labile ligands lead to increased toxicity and too stable ligands lead to inactivity.
- two non-labile groups – The nature of the amine ligands has an influence on the antitumor activity and toxicity of the compound. The ligand must have at least one N-H bond.
- a specific oxidation state of platinum – Generally the Pt(II) complexes are more active than Pt(IV) analogues. Pt(0) complexes are too reactive and unstable.
- a neutral charge on complex – Neutral complexes allow for passive diffusion into cells.

The story of cisplatin shows that it is possible to design and develop new drugs from the field of inorganic chemistry capable of curing specific types of cancers. It has been of interest for inorganic chemists to search for new metal complexes with improved antitumor activity. Basic strategies in the development of new compounds are the following:

- Synthesis of cisplatin analogues was not very fruitful because of similar mechanism for their antitumor action. The major achievement of this exercise was to reduce toxic side effects.
- Linking tumor-inhibiting platinum complexes to other tumor inhibiting metal complexes with carrier systems to have selective accumulation in specific tissues.
- Using cisplatin in combination with other chemotherapeutic agents like intercalators, which is often referred to as a cocktail drug.
- Incorporating more than one platinum atom in a molecule.

18. B. A. Donahue, M. Augot, S. F. Bellon, D. K. Treiber, J. H. Toney, S. J. Lippard, J. M. Essigman, *Biochemistry*, **1990**, *29*, 5872.

19. M. J. Cleare, J. D. Hoeschele, *Plat. Met. Rev.*, **1973**, *17*, 3.

20. M. J. Cleare, J. D. Hoeschele, *Bioinorg. Chem.*, **1973**, *2*, 187.

- Using radiosensitizers as ligands. The drug is accumulated in the cancerous tissue and activated *in situ* by irradiation.
- Synthesis of new metal complexes that can act against cisplatin resistant tumors due to different mechanisms of action.

Eventually scientists realized that an alternative solution would be to find complexes that differ in their mechanisms of DNA attack compared to that of cisplatin (third generation drugs). Because of the success of cisplatin, the movement to include other transition metal antitumor agents has been exceptionally slow. Possible advantages of using non-platinum transition metal ions may involve the following:

- Additional coordination sites
- Different oxidation states
- Alterations in ligand and substituent affinities
- Photodynamic approaches to therapy
- Selective targeting

1.3 Metallocene compounds

The metallocene compounds are of interest in this study and they consist of compounds representing various structural types:

- Neutral metallocene diacido complexes $[M(C_5H_5)_2X_2]$ that contain early transition metals like Ti(IV) and V(IV). The acido ligands are favorably positioned and the cyclopentadienyl rings affords a pseudo tetrahedral geometry.
- Ionic metallocenium salts $[M(C_5H_5)_2]^+ X^-$ have improved water solubility and the cyclopentadienyl (Cp) ligands are arranged in a parallel sandwich geometry.
- Uncharged deca-substituted metallocenes $[M(C_5R_5)_2]$, which comprise the main group elements as central atoms, like Sn(II) and Ge(II). The cyclopentadienyl ligands are fully substituted and can be arranged in either sandwich or open sandwich geometry, depending on the substituents.

The titanium complexes were selected for this study, mainly because of titanium's lower toxicity to the body compared to platinum. The main representative of this class of active complexes is titanocene dichloride.

1.3.1. Titanocene dichloride

The titanocene dichloride complex belongs to the class of metallocenes illustrated in Figure 1.5. In 1979 Köpf and Köpf-Maier⁴ discovered the cytostatic properties of some metallocenes after it was tested *in vitro* and *in vivo*. Following the discovery of the antitumor properties of titanocene dichloride a series of complexes were synthesized, investigated and tested, but to date titanocene dichloride proved to be the superior compound of its derivatives. Apart from antitumor properties, titanocene dichloride exhibits antiviral²¹, antiarthritic and anti-inflammatory activities²².

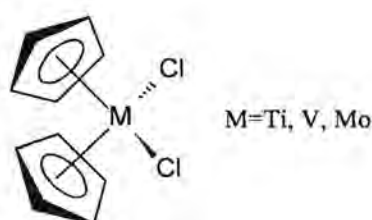


Figure 1.5. Bioactive metallocene dichlorides.

Köpf and Köpf-Maier^{23,24} studied the structure activity relationship of the metallocenes. Chemical variation was used to investigate modification at (a) the central atom, (b) the acido ligands and (c) the protons of the cyclopentadienyl rings.

(a) With variation of the central metal (Ti, V, Nb, Mo, Ta, W, Zr and Hf) high cure rates were observed for Ti, V, Nb and Mo at optimal doses. These four metals have almost similar atomic radii, resulting in quite similar intermolecular non-bonding Cl...Cl distances as illustrated in Figure 1.6. This inter-ligand distance of about 3.2Å corresponds approximately to the bite distance of *cisplatin* and to the distance between two adjacent DNA base pairs. In spite of this observation it is generally believed that this is coincidental and the mechanism of interaction of titanocene dichloride with DNA differs from that of *cisplatin*.

21. E. Tonew, M. Tonew, B. Heyn, H. P. Schroer, *Zentralb. Bakteriol. Parasitenskol. Infektionskr. Bakt. Hyg. Abt. Orig. Reihe A.*, **1981**, 250, 425; *Chem. Abstr.*, **1982**, 96, 82566.

22. D. P. Fairlie, M. W. Whitehouse, J. A. Broomhead, *Chem. Biol. Interact.*, **1987**, 61, 277.

23. H. Köpf, P. Köpf-Maier in *Platinum, Gold and Other Metal Chemotherapeutic Agents*, S. J. Lippard (ed.), ACS Symposium Series, **1983**, 315.

24. I. Haiduc, C. Silvestru, *Organometallics in Cancer Chemotherapy*, Vol II, CRC Press, **1990**, 36.

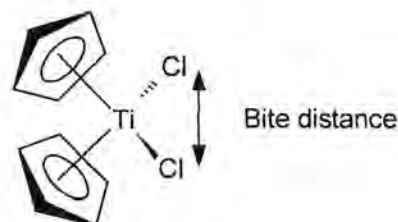


Figure 1.6. The intramolecular non-bonding Cl...Cl distance.

(b) Variation of the acido ligands with halides or pseudohalides (Cl, F, Br, I, NCS and N₃) had no effect on the level of antitumor activity²⁵. Titanocene derivatives with certain thiolate ligands, such as TiCp₂(SR)₂²⁶ and TiCp₂S₅²⁷ (Figure 1.7), have low activity against EhAT, which is ascribed to their hydrophobic character and the strength of the Ti-S bonds. This makes the dissociation of the sulfur donor atom ligands and subsequent coordination of the diorgano titanium moiety to biological molecules difficult.

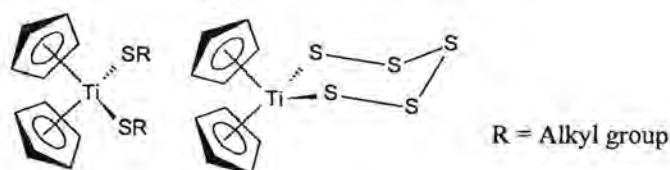


Figure 1.7. Biological inactive titanocene derivatives.

It is interesting to note however that compounds with thiolato and oxo ligands containing fluoro substituted aromatic rings (Figure 1.8) had a 100% cure rate against EhAT at optimal doses²⁸.

25. P. Köpf-Maier, B. Hesse, R. Voightländer, H. Köpf, *J. Cancer Res. Clin. Oncol.*, **1980**, *97*, 31.

26. H. Köpf, M. Schmidt, *Z. Anorg. Allg. Chem.*, **1965**, *340*, 139.

27. H. Köpf, B. Block, M. Schmidt, *Chem. Ber.*, **1968**, *101*, 272.

28. P. Köpf-Maier, H. Köpf, *J. Organomet. Chem.*, **1988**, *342*, 167.

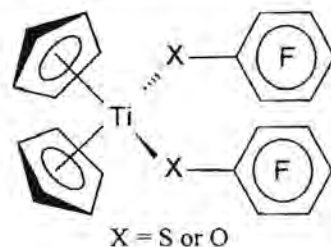


Figure 1.8. Tumor active titanocene derivatives fluorine substituents.

Complexes where one chloro ligand is replaced by an aromatic thiolato ligand displayed much weaker antitumor properties than the parent compound, titanocene dichloride²⁹. Note that the ligands in Figure 1.9 consist only of one benzene ring.

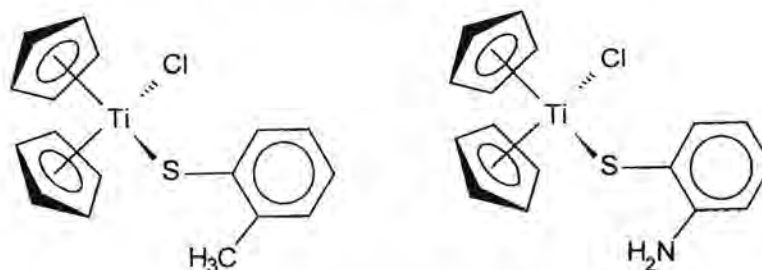


Figure 1.9. Titanocene derivatives with one anionic thioligand.

- (c) The modification of the cyclopentadienyl ligands showed that the activity on tumors is strongly influenced by substitution on one of the rings. As more substituents were introduced, the activity against the tumors decreased³⁰. When one of the rings was replaced by an acido ligand, a decrease in the antitumor activity was also observed. It was concluded that unsubstituted, small Cp-rings are necessary for antitumor activity because they act as carrier ligands to enable the transport of the active metal centre to intracellular target sites.

DNA is suspected to be the prime target for attack and studies done by Köpf and Köpf-Maier²³ indicated that titanocene dichloride attack the nucleic acids. The interactions of metallocenes with

29. P. Köpf-Maier, S. Grabowski, H. Köpf, *Eur. J. Med. Chem.*, **1984**, *19*, 347.

30. P. Köpf-Maier, W. Kahl, N. Klouras, G. Hermann, H. Köpf, *Eur. J. Med. Chem.*, **1981**, *16*, 275.

DNA have recently been reviewed³¹. Initial studies suggested a correlation between DNA binding and antitumor activity. Later studies show that metallocene dihalides do not bond strongly to DNA at neutral pH and do not suppress DNA processing enzymes so it is unlikely that their activity involves nucleic acids.

The cyclopentadienyl ligand can be cleaved to liberate free cyclopentadiene (Fig. 1.10)³². The antitumor activity of titanocene derivatives is not due to the cyclopentadienyl and dicyclopentadienyl released, but it should be assumed that the organometallic moiety is involved in the process in a supportive manner²⁸.



Figure 1.10. Cleavage of the cyclopentadienyl-titanium bond.

Sadler and co-workers³³ studied transferrin as metal ion mediator. The transferrins are a class of iron binding proteins, typified by serum transferrin, the iron transport protein in blood. The transferrin serum involves the specific recognition of Fe^{3+} along with an obligatory synergistic anion. There is potential for use in therapy, because transferrin can also bind strongly to a range of other metals and many metal-transferrin complexes are still recognized by the transferrin receptor. The uptake and release of the metal can be controlled thermodynamically and kinetically. Transferrin can also communicate with other proteins besides blood serum. In agreement with predictions based on metal ion acidity, Ti^{4+} or the hydrated titanium ion forms a strong complex with human apo-transferrin by binding to two specific Fe^{3+} binding sites under physiological conditions³⁴. The uptake of titanium by transferrin is slow and requires several hours for completion. Each transferrin molecule binds to two Ti^{4+} ions, one in each lobe. Such binding may be important for the antitumor activity of titanium if

31. L. Y. Kuo, H. Andrew, T. J. Marks in *Metal Ions in Biological Systems*, A. Sigel, H. Sigel (eds.), Marcel Dekker, Inc., New York, 1996, 33, 53.

32. J. H. Toney, T. J. Marks, *J. Am. Chem. Soc.*, **1985**, *107*, 947.

33. H. Sun, H. Li, P. J. Sadler, *Chem. Rev.*, **1999**, *99*, 2817.

34. M. Guo, H. Sun, H. J. McArdle, L. Gambling, P. J. Sadler, *Biochem.* **2000**, *39*, 10023.

transferrin delivers Ti^{4+} to the tumor cells³⁵. Ti^{4+} binding to transferrin is reversible and Ti is released at low pH. At pH 5.5 Ti^{4+} can bind to DNA. Serum function studies and ^{45}Ti radiolabelling experiments have shown that Ti^{4+} is associated only with transferrin both *in vivo* and *in vitro*³⁶. The strong interaction of titanocene dichloride with transferrin may be relevant to its low toxicity and high activity.

Sadler and co-workers³⁷ also investigated reactions between the anticancer drug titanocene dichloride and various nucleotides and their constituents in aqueous solution or *N,N*-dimethylformamide (DMF) by 1H and ^{31}P NMR spectroscopy and in the solid state by IR spectroscopy. For titanocene dichloride, complexation to nucleobases in water is weak and interactions to nucleobases at pH 2-4 happen with simultaneous binding to the base and the oxygen of the phosphate³⁸. At pH > 6, almost no complexation of aqueous titanocene dichloride to nucleotides or nucleobases was observed. In aqueous solution species containing titanocene bound to the phosphate group of deoxynucleoside guanine monophosphate (dGMP), adenine monophosphate (AMP), deoxynucleoside thiamine monophosphate (dTMP) and uracil monophosphate (UMP) are formed. Binding of titanocene dichloride to 5'-deoxynucleoside adenosine monophosphate (5'-dAMP) appears to involve an oxygen of phosphate and a nitrogen atom of the base (N7)³⁹. These reactions contrast markedly with those of the drug cisplatin, which binds predominantly to the base nitrogen atoms of nucleotides and only weakly to the phosphate groups. The high affinity of Ti(IV) for phosphate groups may be important for its biological activity.

Titanocene dichloride was considered as model complex, because it proved to be a successful antitumor agent against colon cancer as well as various other tumors *in vivo* and *in vitro*. It can easily be modified to form new complexes, for example, replacing the chloro ligands to accommodate new ligands. The toxic side effects of titanocene dichloride are different and far less than that produced by cisplatin. *In vivo* studies showed that titanocene dichloride is not selective and all treated cell lines are

35. M. Guo, H. Sun, P. J. Sadler, *J. Inorg. Biochem.* **1999**, *74*, 150.

36. K. Ishiwata, T. Ido, M. Monma, M. Murakami, H. Fukuda, M. Kameyama, K. Yamada, S. Endo, S. Yoshika, T. Sato, T. Matsuzwana, *Appl. Radiat. Isot.* **1991**, *42*, 707.

37. M. Guo, Z. Guo, P. J. Sadler, *J. Biol. Inorg. Chem.*, **2001**, *6*, 698.

38. J. H. Murray, M. M. Harding, *J. Med. Chem.*, **1994**, *37*, 1936.

39. G. Mokdsi, M. M. Harding, *J. Organomet. Chem.*, **1998**, *565*, 29.

similarly affected by exposure to this antitumor agent⁴⁰. The number of dead cells also increased with an increased concentration of the drug. Inhibition of all growth *in vitro* by titanocene dichloride seems to be due to the cytostatic effect of this compound^{23,41}. By modifying the parent compound it may be possible to increase the selectivity of these new complexes.

1.3.2 Budotitane

This complex belongs to the bis- β -diketonate metal complexes as illustrated in Figure 1.11. The antitumor activity of this type of complex was reported as early as 1982⁴². Budotitane shows a high degree of antitumor activity against colon tumors and the toxicity of the complex is less than for cisplatin. Phase I clinical investigations were started in 1986 and results were promising⁴³. Today it is the most advanced antitumor agent in the titanium field.

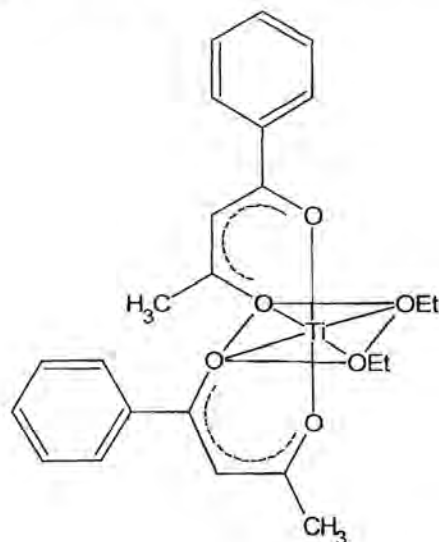


Figure 1.11. Budotitane.

40. P. Köpf-Maier, W. Wagner, H. Köpf, *Cancer Chemother. Pharmacol.*, **1981**, *5*, 237.

41. H. Köpf, P. Köpf-Maier, *Drugs of the Future*, **1986**, *11*, 297.

42. H. J. Keller, B. K. Keppler, D. Schmähl, *Arzneim.-Forsch./Drug Res.* **1982**, *32 (II)*, 806.

43. B. K. Keppler, H. Bischoff, M. R. Berger, M. E. Heim, G. Reznik, D. Schmähl, *Platinum and Other Metal Coordination Compounds in Cancer Chemotherapy*, M. Nicolini (Ed) Martinus, Nijhoff, Boston, **1988**, 313.

A large number of similar complexes with various β -diketonato ligands were screened and found to have antitumor properties⁴⁴. The structure-activity relation was investigated by variation of the complex at (a) the β -diketonato ligand, (b) central metal and (c) the leaving group.

- (a) High antitumor activity was observed when there was a phenyl ring on the β -diketonato ligand (Figure 1.12) in position R'1 or R'3, but decreased when phenyl rings occupied both these positions. Activity increased when a spacer between the diketonato ligand and the second phenyl group was incorporated, for example a benzyl group was more effective. Introduction of water-soluble groups did not increase the antitumor activity.

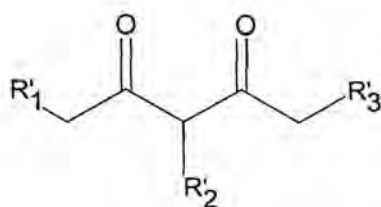


Figure 1.12. β -diketonato ligand.

Substituents on the phenyl group had different effects. When methyl was used, the activity was not altered, but methoxy, chloro or nitro groups decreased the activity. When one of the positions in Figure 1.12 contained a tert-butyl group, the activity decreased, thus supporting the fact that an unsubstituted aromatic ring in the periphery of the molecule is necessary.

- (b) Variation of the central metal (Ti, Zr, Hf, Mo, Sn and Ge) showed that the highest antitumor activity was obtained when Ti or Zr was used. The activity of the other metals decreased in the order given above in brackets.
- (c) The *cis* configured hydrolysable groups did not seem to play a major role in the antitumor activity. As with titanocene dichloride the leaving group is lost fairly rapidly. The leaving group is important for galenic formulation in the clinic. This galenic formulation is a coprecipitate with chromophor EL and propylene glycol. This is necessary to make the drug more soluble in water and to protect it from hydrolysis. Alkoxy groups proved to be more stable in water than the corresponding halides. Budotitane was chosen for further development, because it displayed the ethoxy group that had the slowest rate of hydrolysis.

44. W. Sun, Y. Ren, *Dalian Gongxueyuan Xuebao*, 1984, 23, 138; *Chem. Abstr.*, 1985, 102, 105001

Although the complex has a *cis* configuration, the mechanism of action is not yet understood, but believed to be completely different from that of cisplatin⁴⁵ as it displays a different structure activity relation. The activity of the complex depends on the β -diketonato ligand and it is believed that the planar phenyl group in the β -diketonato ligand is intercalating with DNA. Comparing the activity of a complex with acetyl acetone with a benzoyl acetone ligand, it was found that the acetyl acetonato complex is almost inactive while the benzoyl acetonato complex is highly active. This tendency is commonly observed with anticancer drugs where an intercalating mechanism is proposed. This result was also observed for certain titanocene complexes studied by Köpf and Köpf-Maier. Since intercalation is an important factor in the design of new complexes for this project, some background information will be presented.

1.4 Modes of action

1.4.1 Covalent bond formation of titanium(IV)

Further studies investigated the binding of metallocenes to the potential donor sites of 2'-deoxynucleoside 5'-monophosphates (Figure 1.13), such as the nitrogen atoms of the nucleobases and the oxygen atoms of the phosphate groups, as was observed for molybdenocene (Figure 1.14⁴⁶), where N—N is 5'-dMAP, 5'-dTMP, 5'-deoxynucleoside thiamine monophosphate (5'-dCMP) or Me(5'-dGMP).

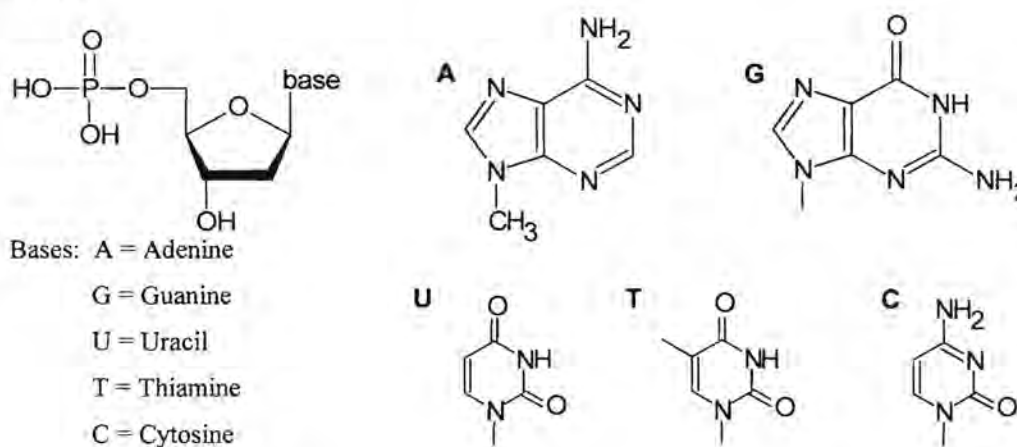


Figure 1.13. Structures of the 2'-deoxynucleoside 5'-monophosphates.

45. T. Pieper, K. Borsky, B. K. Keppler, *Top. Biol. Inorg. Chem.*, **1999**, *1*, 171.

46. B. Lippert in *Progress in Inorganic Chemistry*, S. J. Lippard (ed.), John Wiley and Sons, New York, **1989**, 1.

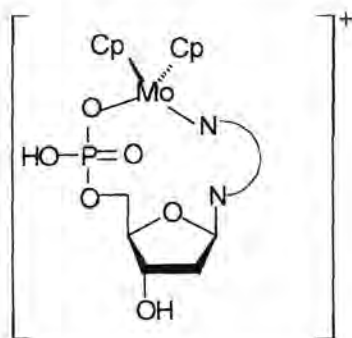


Figure 1.14. Coordination of $\text{Cp}_2\text{Mo}^{2+}$ to 2'-deoxynucleoside 5'-monophosphates.

Also studied was the direct interaction of titanocene dichloride with bases of nucleic acids by formation of covalent bonds. The synthesis of model complexes of the titanocene system with nucleic acid components as ligands has turned out to be difficult under physiological conditions. In literature there are a few examples of purine and uracil complexes that show that the titanocene moiety can be attached to purine and pyrimidine bases^{47,48,49,50}.

Two titanocene complexes bound to nucleobases were synthesised and characterised in nonaqueous media. In the $\text{Ti(IV)Cp}_2\text{Cl(purinato)}$ complex⁴⁹ (Figure 1.15) the TiCp_2Cl^+ moiety binds to the N9 position of the purinato ligand to form a monofunctional bond. In the $\text{Ti(III)Cp}_2(\text{theophyllinato})$ complex⁴⁷ (Figure 1.15) the Cp_2Ti^+ moiety simultaneously binds to the O6 and the N7 sites of the theophyllinato ligand to form a bifunctional chelate. In both complexes the nucleobase ligand planes are situated in the equatorial plane of the $\text{Cp}_2\text{Ti}^{2+}$ wedge.

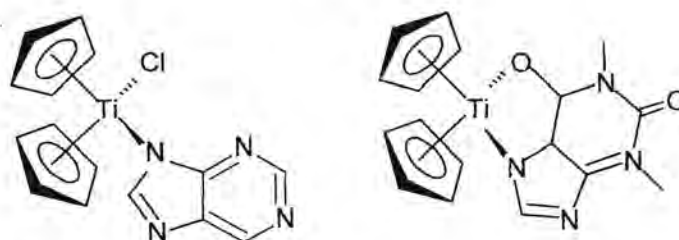


Figure 1.15. Chlorobis(η^5 -cyclopentadienyl)purinatotitanium(IV) and bis(η^5 -cyclopentadienyl)theophyllinatotitanium(III).

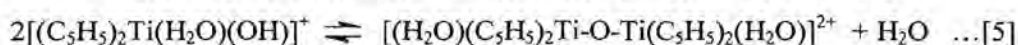
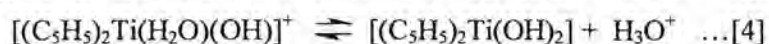
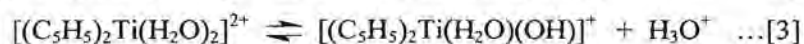
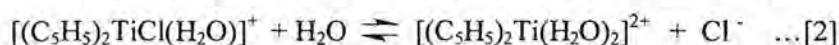
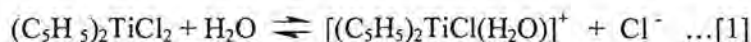
47. D. Cozac, A. Mardhy, A. Morneau, *Can. J. Chem.*, **1986**, *64*, 751.

48. A. L. Beauchamp, F. Bélanger-Garlépy, A. Mardhy, D. Cozac, *Inorg. Chim. Acta*, **1986**, *124*, 23.

49. A. L. Beauchamp, D. Cozac, A. Mardhy, *Inorg. Chim. Acta*, **1984**, *92*, 191.

50. D. Cozac, A. Mardhy, M. J. Olivier, A. L. Beauchamp, *Inorg. Chem.*, **1986**, *25*, 2600.

The mechanism of action is also determined by the behaviour of the complex in aqueous media. The antitumor activity of metallocene dichlorides probably depends on hydrolysis of the metal which for Ti, V, Zr and Mo proceeds much faster than for cisplatin⁵¹. In aqueous solution most metallocene complexes are not stable but undergo dissociation, aquation and hydrolysis reactions followed by condensation to oxobridged polynuclear species as seen in reactions [1] – [5]³². These oxobridged and aqua species have a higher affinity for phosphate oxygen atoms than the cisplatin hydrolysis products⁴²



It is known that titanocene dichloride is more stable in acidic or saline solutions than in pure water. The most acidic of the aquated metallocenes is $[TiCp_2(H_2O)_2]^{2+}$ so that it exists as neutral $[TiCp_2(OH)_2]$ at neutral pH. The difference in the aquated forms between the various metallocenes may influence their activity in that those forming neutral species under physiological conditions probably enter the cells easier⁵². The hydrolysed species of titanocene dichloride appear to have high affinity for plasma proteins.

1.4.2 Intercalation

The predominant mode of action of most cytostatic agents with coplanar (heterocyclic) chromophores is intercalation into human DNA. In this study intercalation is understood as the insertion of a chromophoric (planar) part of a molecule between two stacked base pairs as illustrated in Figure 1.16⁵³. This causes basically two changes in DNA. Firstly, the DNA tertiary structure (helix) is lengthened and somewhat unwound, while the primary and secondary structures remain intact. With intercalation, the average separation between two stacked base pairs increases from 3.4Å to ~7.0Å. At biochemical level a blockage of the matrix functions occurs. Secondly, there is a significant change in

51. L. Y. Kuo, A. H. Lui, T. J. Marks, *Met. Ion. Biol. Syst.*, **1996**, 33, 53.

52. M. S. Murthy, L. N. Rao, L. Y. Kuo, J. H. Toney, T. J. Marks, *Inorg. Chim. Acta*, **1988**, 152, 117.

53. U. Pindur, M. Haber, K. Sattler, *J. Chem. Ed.*, **1993**, 70, 263.

the torsion angles of the sugar phosphate skeleton. This causes reading errors in the replication process and cell proliferation comes to a standstill. The major contribution to intercalative binding in DNA arises from electrostatic, van der Waals and most importantly hydrophobic forces. Stabilisation is maintained through π,π -stacking and hydrogen bonds. For an optimal intercalation, the planar part of the molecule (the chromophore) should have a minimum surface of 28\AA^2 (optimum at three to four condensed five or six membered rings).

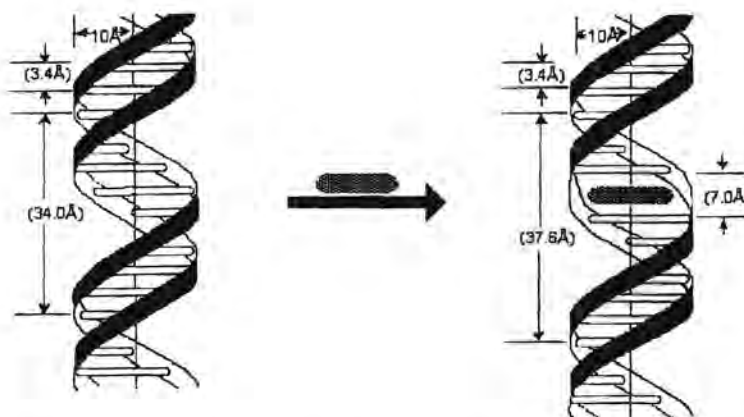


Figure 1.16. Schematic representation of intercalation between stacked base pairs of DNA

Transition metal complexes can also be used as intercalators when they form part of the planar ring system and are referred to as metallointercalators. Lippard *et al*⁵⁴ were the first to establish that square planar Pt(II) complexes containing an aromatic heterocyclic ligand bind to DNA by intercalation. Also, three-dimensional octahedral metallointercalators target specific DNA sites by matching the shape, symmetry and functionalities of the metal complex to the DNA target⁵⁵. Different intercalative ligands stack with different orientations in the double helix due to their shape and polarity. Metallointercalators are among few synthetic complexes that target the DNA major groove with specificity. Such site specific targeting can lead to selective inhibition of DNA binding proteins.

In 1988 Palmer⁵⁶ studied the chromophore structure-activity relationships for linear, tricyclic carboxamides and concluded that the best antitumor results were obtained when the ligand intercalated. The majority of DNA monointercalating antitumor drugs compose of a planar tri- or tetracyclic chromophore with one or two side chains added, especially on the 1-position. A

54. J. K. Barton, S. J. Lippard, *Biochemistry*, **1979**, *12*, 2661.

55. E. C. Long, J. K. Barton, *Acc. Chem. Res.*, **1990**, *23*, 271.

56. B. D. Palmer, G. W. Rewcastle, G. J. Atwell, B. C. Baguley, W. A. Denny, *J. Med. Chem.*, **1988**, *31*, 707.

heteroatom (preferably nitrogen or oxygen) peri to the side chain is a further prerequisite. It was decided to incorporate these findings in the design of new titanium antitumor complexes for this study.

1.5. Aim of Study

One of the most important problems in the development of new tumor inhibiting complexes and potentially chemotherapeutic drugs is of a strategic nature. The action of existing models must be adequately understood and evaluated in order to improve significantly on their performance. Unless totally unique and selective in its anticancer properties it is unlikely that an improved derivative of an existing compound will succeed to eventually become a drug. This is a result of the enormous costs involved in launching a compound through the clinical trails until it eventually becomes registered. By using titanocene dichloride as model complex and through careful design by incorporating specific ligands it was hoped to synthesize complexes with a different spectrum of antitumor properties. Evaluation of the activity of the new complexes *in vitro* and an understanding of the mechanism of action in the body will direct the design of improved analogous complexes.

In this study new titanium complexes were designed, synthesized, characterized and tested *in vitro*. Certain aspects of the mechanism of their interaction with DNA were investigated.

Design of Complexes

In the design of the complexes it was assumed that the new complex would attack DNA and in the process change the DNA structure. The objective was to incorporate ligands with different functionalities. One ligand should be labile and easily substituted to make available a vacant coordination site for covalent bond formation to DNA. A second, less labile ligand should consist of a planar condensed polycyclic ring system for possible intercalation. To achieve these goals the complexes had to meet certain geometrical requirements based on the metallocene dihalide model (Fig. 1.17).

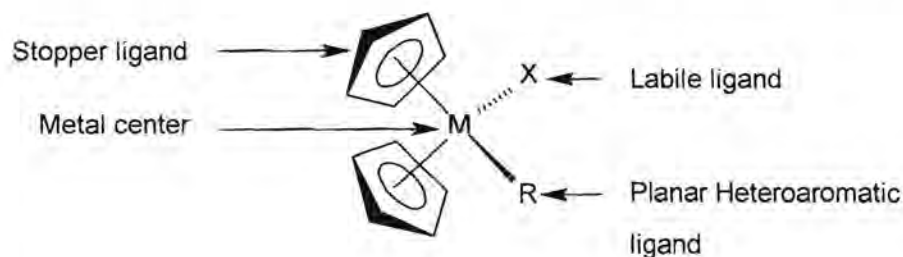


Figure 1.17. A designer model of the features of new antitumor complexes.

The new titanocene complexes have to meet the following requirements:

- The metal centre (**M**) must be in a high oxidation state to prevent oxidation in the body, hence Ti(IV).
- A labile ligand (**X**), which will dissociate readily to leave a vacant coordination site on the metal to allow for covalent bonding to DNA.
- A unique planar heteroaromatic ligand (**R**) with two to four rings to intercalate in the major groove of the DNA helix.
- Stable stopper ligands to direct and align the intercalation process.
- The orientation of the plane of the ring system with respect to the other ligands is important and special attention should be given to obtain the correct structural features, to achieve the above objectives.

Titanocene dichloride was chosen as the starting compound for a number of reasons. It is a very versatile precursor, which can be used to synthesize a large spectrum of derivatives. For this reason it would be possible to combine labile ligands with polycyclic condensed heteroaromatic rings. Alternatively, [TiCpCl₃] could have been used, but for this study [TiCp₂Cl₂] was selected because of its stability and proven success in the field of drug design.

The covalent binding affinities of titanocene dichloride (Ti⁴⁺ is a hard metal center) to hard heteroatoms are to be combined with the intercalation features of aromatic ring ligands, to synthesize a series of compounds, which could potentially display antitumor properties. The interaction of the complexes with DNA is expected to be different from that of titanocene dichloride, because only one labile ligand will be available for dissociation. Covalent bond formation between the metal and DNA is expected to occur at an oxygen of the phosphate backbone of DNA. No cross-links are expected as in the case of titanocene dichloride.

The unique ligand (**R**) was altered to investigate the effect on antitumor activity in two ways. Firstly, the feature of the intercalator was changed and secondly, the intercalator was positioned differently relative to the metal center to try and determine the ideal geometry for optimized intercalation.

The ligand supposed to intercalate was varied as illustrated in Figure 1.18 to determine the effect of:

- two versus three coplanar rings (**1, 4 vs. 2,5**)
- the type of heteroatom in the ring (**1-5**)
- one versus two heteroatoms in the ring (**2, 5 vs. 3**)
- a substituent on the ring (**6**)

116542678
615954419

The positioning of the intercalator was investigated by determining the effect of:

- inserting a linker atom between the ring and the metal (4, 5)

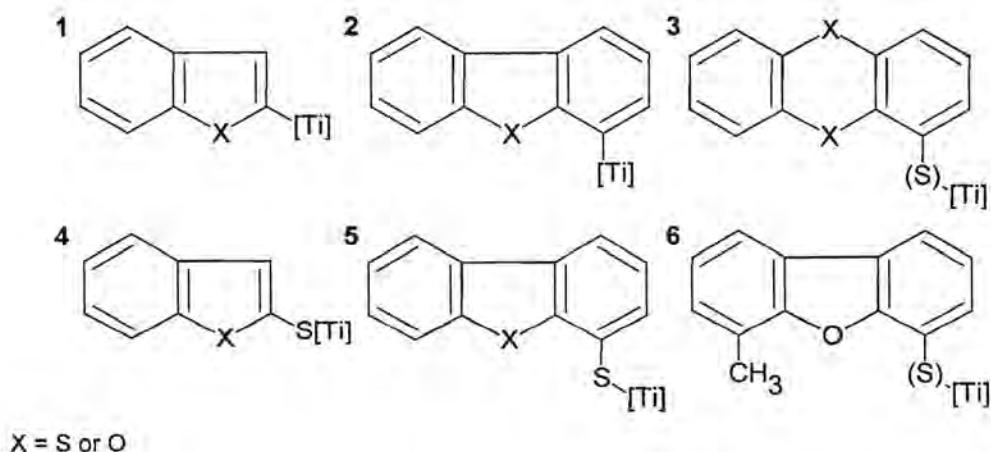


Figure 1.18. The metallated coplanar polycyclic heteroaromatic rings studied.

Synthesis

Titanocene dichloride will, after one chloro ligand (X) was displaced, display a unique heteroaryl ligand from a family of heteroaromatic substrates (R) illustrated in Figure 1.18. Some of the ligands in Figure 1.18 will be synthesized and others will be prepared from commercially available materials. The synthesis is based on a displacement reaction involving a lithiated heteroaromatic substrate and a chloro ligand of the titanocene dichloride. The site and effectiveness of lithiation of the heteroaromatic rings as well as their subsequent reactivity with titanocene dichloride will also be studied.

Characterization

The complexes will be characterized by using various standard methods. The degree by which the aromatic character of the rings in the new complexes will be affected, due to the metal-carbon or metal-sulphur bond, will be studied with NMR spectroscopy. Structural features and properties will be investigated, using NMR spectroscopy, mass spectrometry and as far as possible, X-ray crystallography.

In Vitro tests

A selection of complexes will be tested *in vitro* against human cervix epitherioid carcinoma (HeLa) and colorectal carcinoma (CoLo) cell cultures to determine possible antitumor activity. One aim will

be to determine whether variations in the heteroaromatic ring ligands have any effect on antitumor activity and if so to determine a pattern for use in future studies.

Aspects of the Mechanism

Tests to confirm or disprove the assumptions about covalent bonding and intercalation by the new complexes will be conducted. A selection of the best complexes will be studied for intercalation by an application of a flow cytometry technique. A further objective was, if intercalation was observed to be relevant, to try and find a correlation between the geometry of the complex and intercalation. The relative labilities of the ligands are to be tested in aqueous medium and monitored by NMR spectroscopy.

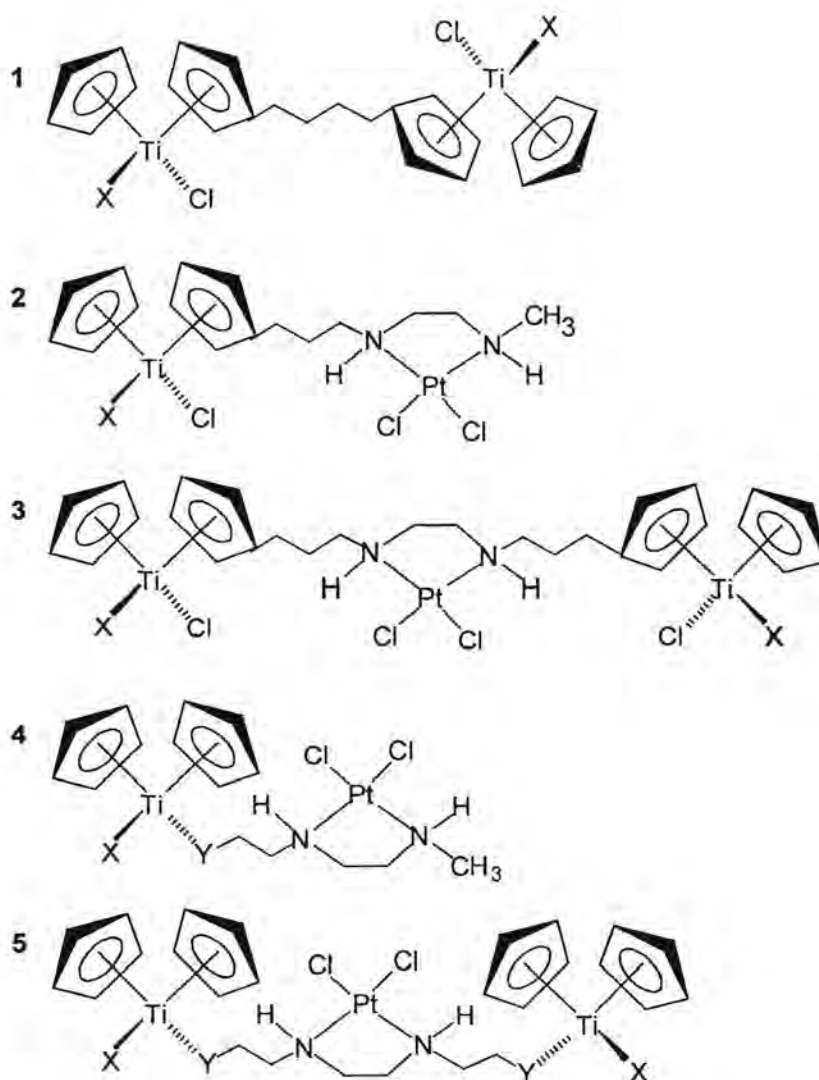
Extension to Bi- and Trinuclear Systems

The design of these complexes was based on the mononuclear metallocene model. A further point of interest was to design binuclear titanium complexes that still displayed the features of the parent compound, titanocene dichloride. Another aim was to study the synthesis of multinuclear complexes incorporating *cisplatin*-like platinum fragments into the titanocene complexes. These will include the following complexes (Figure 1.19):

- Titanocene – titanocene complexes (1)
- Titanocene – *cisplatin* complexes linked via the cyclopentadienyl ring (2, 3)
- Titanocene – *cisplatin* complexes linked via the titanium center (4, 5)

The aim was to use metal complexes that proved to be successful as antitumor agents (titanocene and *cisplatin*) and incorporate two or three of these metal centers into the same molecule. In the first case two titanocene dichloride fragments are to be linked by inserting a hydrocarbon chain between one of the cyclopentadienyl ligands on each metal fragment. This will lead to a complex that should display antitumor properties, but have a different mechanism of action compared to titanocene dichloride. Farrel⁵⁷ followed a similar approach in linking *cisplatin* units via a bridging amine ligand. The bi- and trinuclear complexes displayed antitumor properties very different from those of *cisplatin*.

57. H. Rauter, R. Di Domenico, E. Menta, A. Olivia, Y. Qu, N. Farrel, *Inorg. Chem.*, 1997, 36, 3919.



X = Cl or heteroaromatic ring ligand

Y = S or O

Figure 1.19 Bi- and trinuclear complexes.

Titanocene dichloride is to be combined with a platinum fragment that is analogous to *cis*platin. To accomplish this a linker need to be attached to one of the cyclopentadienyl rings of titanocene dichloride and the nitrogen of the amino group on the platinum fragment. The covalent bond properties of titanocene dichloride can now be combined with the cross-linking properties of the platinum fragment at different sites in the same molecule which could possibly lead to a broader spectrum of antitumor activity. It is also possible that competition between the two metal fragments of the molecule can facilitate a totally different mechanism of action compared to that of the two model

complexes. In this type of Ti-Pt complex there are two chloro ligands on the titanocene fragment available to dissociate and give vacant sites for covalent bonding. These complexes can also be used as starting compounds to incorporate polycyclic condensed heteroaromatic rings by replacing labile chloro ligands as was done with titanocene dichloride as precursor.

A variation of the Ti-Pt type of complexes can be achieved by inserting a linker between the nitrogen of the amino group of the platinum fragment and replacing a chloro ligand on the titanium fragment. The mechanism of this type of complex with DNA is expected to be different from that of the previous type of Ti-Pt complex. In this case only one labile ligand will be available on the titanocene fragment for dissociation to allow for covalent bond formation between the metal and DNA.

1.6 Construction of the thesis

In Chapters 2 - 4 the synthesis and characterisation of the new complexes will be discussed. A scheme of the planned route for the synthesis of the compounds will be given and the results discussed. The purity of the compounds will be determined by chemical analysis and mass spectrometry. Molecular composition and structural features of the products will be derived from techniques of NMR spectroscopy and where possible, single crystal X-ray determinations will be done to confirm the structure of new complexes. In Chapter 6 the experimental procedures for all new compounds are given.

Chapters 2 and 3 deal with titanocene complexes focussing on varying aspects associated with the intercalating ligand. Two classes of complexes will be discussed. Firstly, those where the metal centre is bound directly to the heteroatomic ring ligand and part of the intercalator (Chapter 2) and secondly, those where a sulfur atom is placed between the metal and the ring ligand to distance the metal from the intercalator (Chapter 3). Chapter 4 studies bi- and trinuclear complexes.

In Chapter 5 the antitumor properties of the complexes will be discussed in terms of their *in vitro* test results. Structure-activity correlations will be made. Investigation of the mechanism of bioactivity of these complexes, the results of the intercalation tests will be discussed and the aspect of covalent bonding to DNA will be investigated. The most important results of the ligand substitution studies will be listed and conclusions from this study summarized.

Chapter 2

Titanocene derivatives with a heteroaromatic ligand containing a direct metal-carbon σ -bond

2.1 Introduction

The properties of dibenzothiophene (**L2-01**) and benzo(b)thiophene (**L2-02**) derivatives have been studied extensively and a number of these compounds have shown biological activity¹. Some of these compounds are illustrated in Figure 2.1. One of the best known benzo(b)thiophene derivatives with anti-inflammatory properties is Tianafac (**a**), while 3-amino-2-aryl thiophene (**b**) is known as a hypolipidamic compound. The benzothiophene compound (**c**) with an isopropanol substituent has spasmolytic activity, whereas (**d**) is a hydroxytryptamin antagonist. Examples of **L2-01** derivatives with biological activity are RMA 11877 (**e**), a viristaticum agent and (**f**) is a hypolipidamic compound.

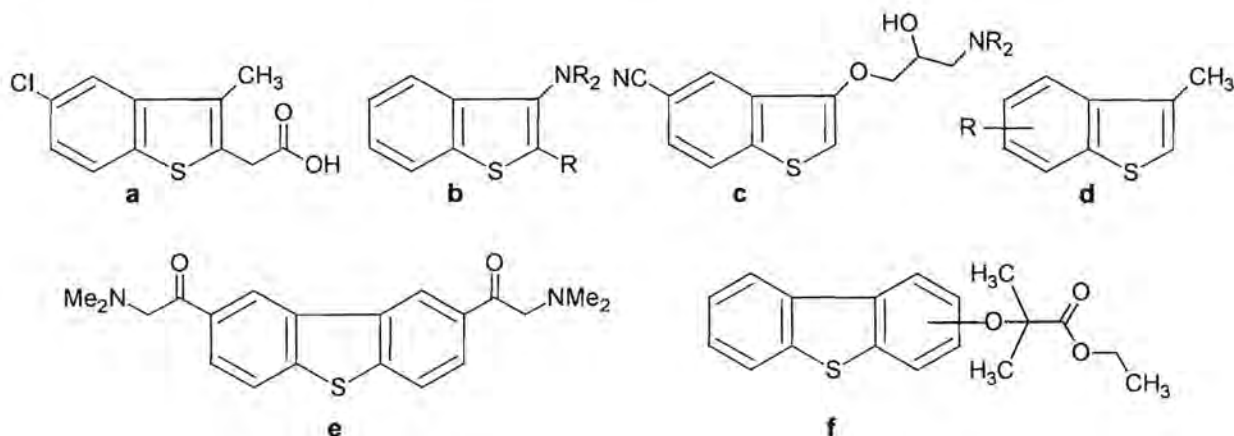


Figure 2.1 Biological active **L2-01** and **L2-02** derivatives: (a) anti-inflammatory, (b) and (f) hypolipidamic, (c) spasmolytic, (d) hydroxytryptamin and (e) viristaticum.

1. R. Pech, R. Böhm, *Pharmazie*, **1984**, *39*, 4.

Osborn and co-workers studied the biological activity of **L2-01** derivatives and they suggested that the activity of these complexes results from their absorption onto adenine-thymine or guanine-cytosine base pairs at the end of DNA strands². Recently McCowan and co-workers^{3,4} reported that dibasic benzothiophene derivatives have been discovered and optimised through structural modification to represent a new class of active site-directed thrombin inhibitors of which the complex in Figure 2.2 performed the best.

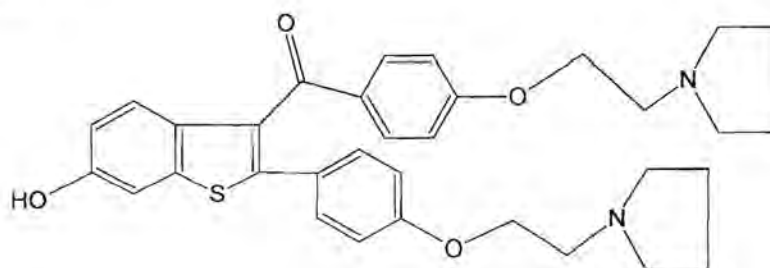


Figure 2.2 A dibasic **L2-02** derivative.

The value of **L2-01** and **L2-02** as ligands in biological active complexes was realized and introducing these ligands to titanocene complexes might lead to antitumor activity. Titanocene derivatives with the general formula $[\text{TiCp}_2(\text{R})\text{Cl}]$. R = Dbt (**2-08**); Bt; Dbz (**2-05**); Thr (**2-09**); Dbf (**2-01**) and Bf (**2-07**) are shown in Figure 2.3. (DbtH = dibenzothiophene, BtH = benzo(b)thiophene, DbzH = dibenzodioxin, ThrH = thianthrene, DbfH = dibenzofuran and BfH = benzo(b)furan). The heteroatom directs lithiation and ultimately complexation to the titanium in such a manner that the heteroatom is on the same side of the rings as titanium. **L2-01** is easily metallated by butyllithium on the 4-position and a reaction with titanocene dichloride gives $[\text{TiCp}_2(\text{Dbt})\text{Cl}]$ **2-08** (Figure 2.3). **L2-02** is metallated on the 2-position to produce the titanium complex $[\text{TiCp}_2(\text{Bt})\text{Cl}]$ which was too unstable for further use in antitumor studies⁵.

2. E. Champaigne, J. Ashby, S. W. Osborn, *J. Heterocycl. Chem.*, **1969**, *6*, 885.

3. D. J. Sall, J. A. Bastian, S. L. Briggs, J. A. Buben, N. Y. Chirgadze, D. K. Klawson, M. L. Denny, D. D. Giera, D. S. Gifford-Moore, R. W. Harper, K. L. Hauser, V. J. Klimkovski, T. J. Kohn, H-S. Lin, J. R. McCowan, A. R. Palkovitz, G. F. Smith, K. Takeuchi, K. J. Thrasher, J. M. Tinsley, B. G. Utterback, S-C. B. Yan, M. Zhang, *J. Med. Chem.* **1997**, *40*, 3489.

4. D. J. Sall, D. L. Bailey, J. A. Bastian, J. A. Buben, N. Y. Chirgadze, A. C. Clemmins-Smith, M. L. Denny, M. J. Fisher, D. D. Giera, D. S. Gifford-Moore, R. W. Harper, L. M. Johnson, V. J. Klimkovski, T. J. Kohn, H-S. Lin, J. R. McCowan, A. D. Palkowitz, M. E. Richett, G. F. Smith, D. W. Snyder, K. Takeuchi, J. E. Toth, M. Zhang, *J. Med. Chem.* **2000**, *43*, 649.

5. R. Meyer, *Titanium, Molybdenum and Platinum Complexes with Potential Antitumor Properties*, Ph. D. (Chemistry) Thesis, University of Pretoria, **1998**, 24.

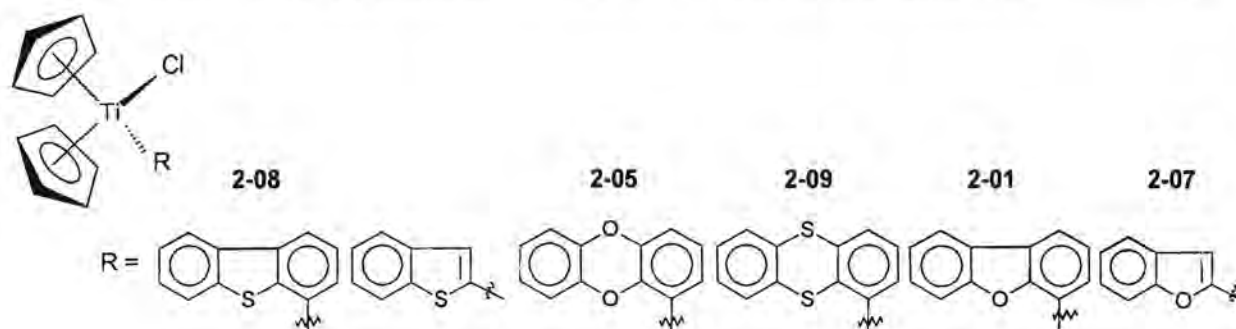


Figure 2.3 Titanocene derivatives with the general formula $[\text{TiCp}_2(\text{R})\text{Cl}]$.

For intercalation it could be advantageous to have a heteroatom on the ring on the opposite side of the metal in the complex. Hence, the next step was to introduce heteroaromatic ligands with two heteroatoms in the ring and dibenzodioxin (**L2-03**) and thianthrene (**L2-04**) were considered. Derivatives of **L2-03** were investigated before and found to be promising biological agents⁶. Palmer⁷ reported that the dibenzo[1,4]dioxin-1-carboxamide (Figure 2.4) has significant antitumor activity. Since the surface areas of **L2-03** and **L2-04** are larger than that of **L2-01** it is believed that they would perform better as potential intercalation agents. Metallation of **L2-03** and **L2-04** on the 1-position and subsequent reaction with titanocene dichloride afforded $[\text{TiCp}_2(\text{Dbz})\text{Cl}]$ (**2-05**) and $[\text{TiCp}_2(\text{Thr})\text{Cl}]$ (**2-09**).

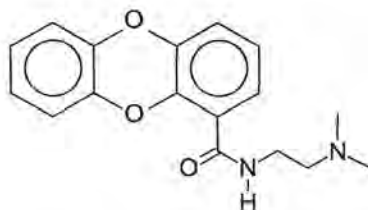


Figure 2.4. Dibenzo[1,4]dioxin-1-carboxamide.

Many substances with pharmacological, therapeutic or toxic properties are found among natural products with a benzofuran (**L2-05**) ring. Of the synthetic **L2-05** derivatives synthesized some are biologically active and their numbers are much larger than the **L2-02** series^{8,9}. Examples of these are

6. B. D. Palmer, M. Boyd, W. A. Denny, *J. Org. Chem.*, **1990**, *55*, 438.

7. B. D. Palmer, G. W. Rewcastle, G. J. Atwell, B. C. Baguley, W. A. Denny, *J. Med. Chem.* **1988**, *31*, 707.

8. J.P. Garnier, *Actualités de Chimie Thérapeutique*, Edifor, Paris, **1971**, 9.

9. P. N. Craig, H. C. Caldwell, W.G. Groves, *J. Med. Chem.* **1970**, *13*, 1079.

nitrobenzofurans, which are bactericidal, and in Figure 2.5 compounds are listed which are estrogenic (a), has anti-inflammatory properties (b) and anti-fertility properties in animals (c).

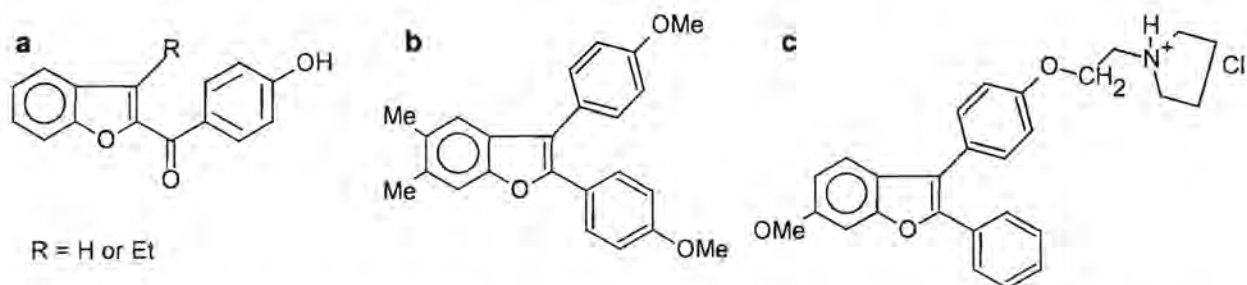


Figure 2.5 Biological active **L2-05** derivatives which display (a) estrogenic, (b) anti-inflammatory and (c) anti-fertility properties.

The ligand **L2-05** and dibenzofuran (**L2-06**) are metallated at slightly higher temperatures than their sulfur analogous and $[\text{TiCp}_2(\text{Dbf})\text{Cl}]$ (**2-01**) and $[\text{TiCp}_2(\text{Bf})\text{Cl}]$ (**2-07**) were isolated. The role of a methyl substituent was tested by introducing it at the 4-position of **L2-06** to give 4-methyl dibenzofuran (**L2-07**). In all of the above mentioned products the metal fragment was on the outside of the heteroaromatic ligand and not part of the rings. It was decided to investigate a complex where both chloro ligands are replaced by titanium to form a wedge-like complex with the ring oxygen opposite the titanium which is inserted into the central ring of three condensed rings (Figure 2.6).

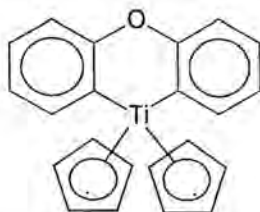
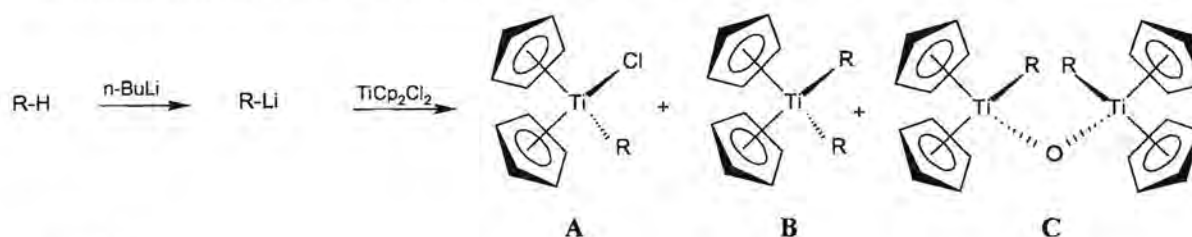


Figure 2.6 Titanocene complex with the metal inserted into the heteroaromatic ring.

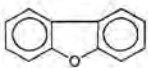
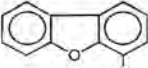
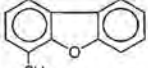
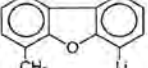
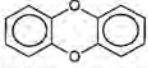
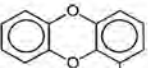
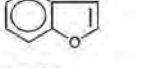
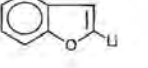
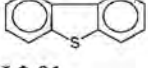
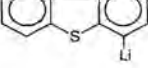
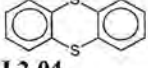
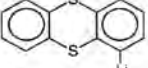
2.2 Synthesis

The complexes were synthesized using the same method for all. The heteroaromatic ring compound was lithiated and added to titanocene dichloride at low temperatures. Lithiation of **L2-01**, **L2-03**, **L2-04**, **L2-05**, **L2-06**, **L2-07** and diphenylether (**L2-08**) proceeded in high yields and complexes were isolated in moderate to high yields. The synthesis route afforded **A**, **B** and **C** type products as is illustrated in Scheme 2.1. Table 2.1 shows the identification numbers of the complexes.



Scheme 2.1

Table 2.1 Identification numbers of the complexes in Scheme 2.1.

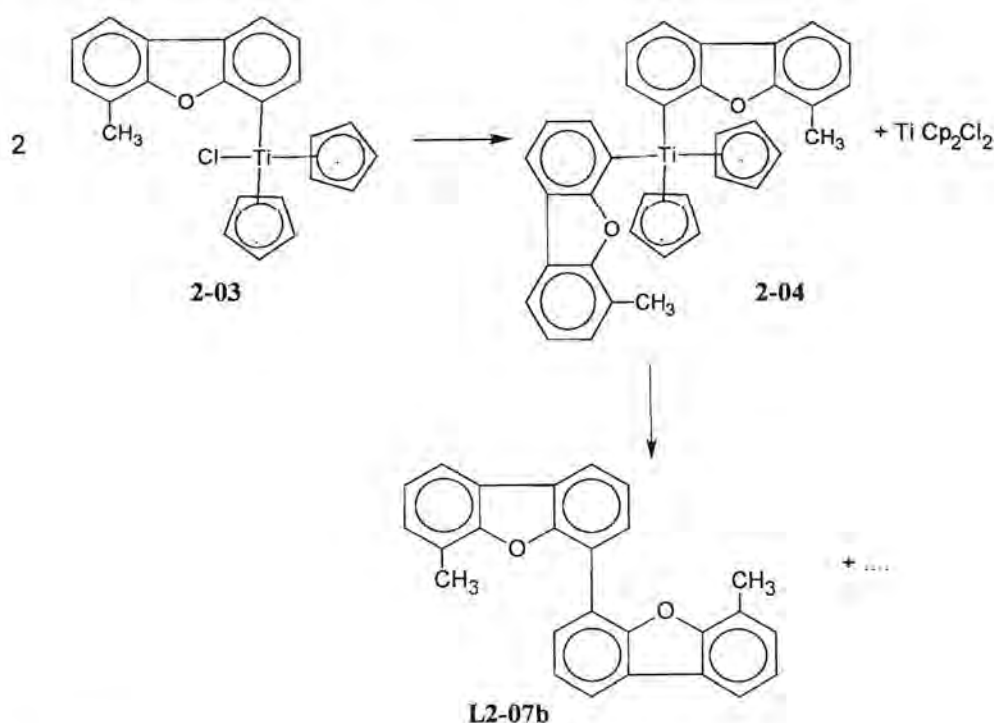
Heteroarene (R-H)	Reagent (R-Li)	Product A	Product B	Product C
 L2-06		2-01	2-02	-
 L2-07		2-03	2-04	-
 L2-03		2-05	-	2-06
 L2-05		2-07	-	-
 L2-01		2-08	-	-
 L2-04		2-09	-	2-10

Addition of titanocene dichloride to L2-06

L2-06 was metallated by *n*-BuLi at the 4-position and addition of titanocene dichloride caused a colour change from red to orange. Chromatography on aluminium oxide yielded bis(cyclopentadienyl)bis(dibenzofuran-4-yl)titanium(IV), [TiCp₂(Dbf)₂] (**2-02**) and chlorobis(cyclopentadienyl)(dibenzofuran-4-yl)titanium(IV), [TiCp₂(Dbf)Cl] (**2-01**). Product **2-02** was crystallized from a dichloromethane-hexane solution that yielded crystals suitable for a single crystal, X-ray diffraction study.

Addition of titanocene dichloride to L2-07

Addition of methyl iodide to lithiated **L2-06** afforded a yellow solid that was purified by column chromatography and characterized as **L2-07** after recrystallization from dichloromethane. Lithiation of **L2-07** with *n*-BuLi deprotonated the unsubstituted ring on the 4-position. On addition of titanocene dichloride the reaction colour turned from red to yellow-brown, which after column chromatography on silica gel, yielded bis(cyclopentadienyl)bis(6-methyl dibenzofuran-4-yl)titanium(IV), [TiCp₂(Dbf-Me)₂] (**2-04**) and chlorobis(cyclopentadienyl)(6-methyl dibenzofuran-4-yl)titanium(IV), [TiCp₂(Dbf-Me)Cl] (**2-03**). Complex **2-03** is unstable and converts rapidly to **2-04** and titanocene dichloride (Scheme 2.2). Complex **2-04** is also unstable, but more stable than **2-03** and converts slowly to a dimer of **L2-07**, [Me-Dbf-Dbf-Me] **L2-07b**.

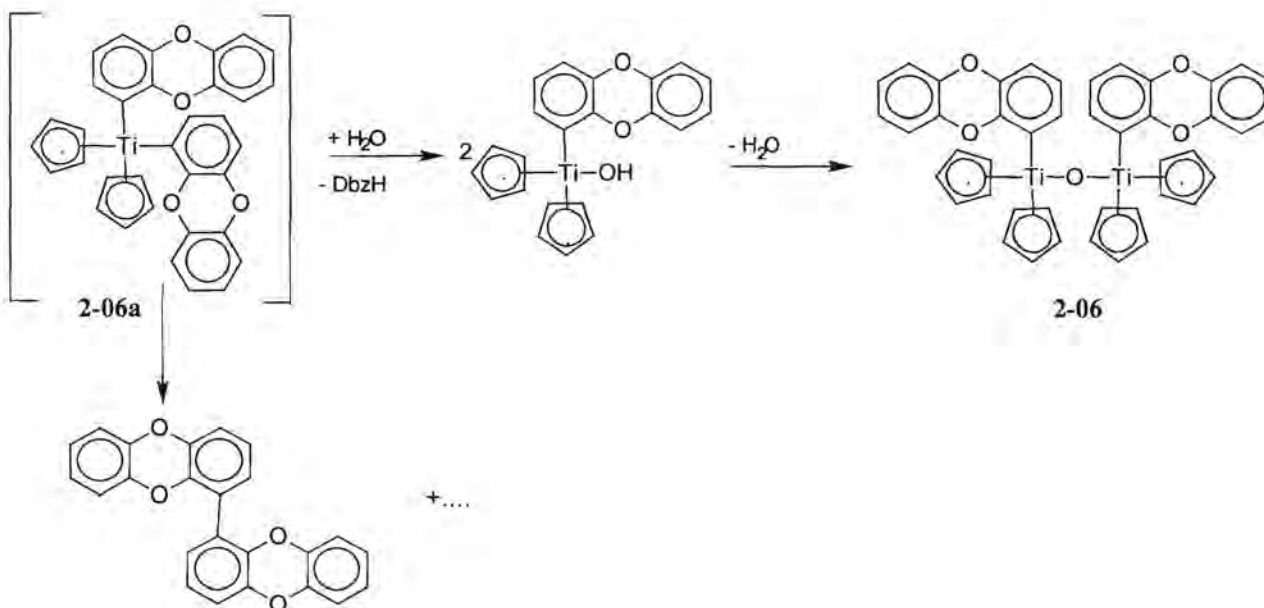


Scheme 2.2

Addition of titanocene dichloride to L2-03

L2-03 was metallated by a mixture of *n*-BuLi/TMEDA at the 1-position. Addition of titanocene dichloride caused a colour change from red to dark orange-brown. Chromatography on silica gel yielded the expected product, chlorobis(cyclopentadienyl)(dibenzodioxin-1-yl)titanium(IV) **2-05** [TiCp₂(Dbz)Cl]. Solvent mixtures such as dichloromethane-hexane or toluene-hexane did not produce crystals of a good enough quality for X-ray structural studies. After many attempts, the slow crystallisation from a THF-hexane mixture, afforded crystals suitable for a single crystal X-ray

diffraction study. A second yellow product is believed to be bis(cyclopentadienyl)bis(dibenzodioxin-1-yl)titanium(IV), $[\text{TiCp}_2(\text{Dbz})_2]$ (**2-06a**). This complex was very unstable and NMR studies revealed decomposition with regeneration of the free ligand. The solution slowly turned black every time the compound was dissolved in a chlorinated solvent. Finally **2-06a** was filtered successfully with benzene. The yellow product **2-06a** converted into a second yellow product, of which the composition was verified by NMR spectral data. The oxygen bridged binuclear complex, $(\mu\text{-oxo})\text{bis}[\text{bis}(\text{cyclopentadienyl})(\text{dibenzodioxin-1-yl})\text{titanium(IV)}]$, $[(\mu\text{-O})\{\text{TiCp}_2(\text{Dbz})\}_2]$ (**2-06**), is consistent with the NMR data obtained for this product. The titanocene bis(dibenzodioxin-1-yl) complex, **2-06a** is unstable and slowly reacts with water from the column material. As a result, the water protonates one of the Dbz ligands, leading to the release of **L-03** and the formation of a hydroxo complex (Scheme 2.3). Two hydroxo complexes combine by water elimination to give the oxobridged binuclear complex **2-06**. During the conversion water acts as reactant and catalyst. Complex **2-06a** also decomposes competitively by a reductive elimination reaction of the two heteroarene ligands to give a dimer Dbz-Dbz.



Scheme 2.3

A possible reason for the instability of **2-06a** may result from the presence of two bulky dibenzodioxin ligands. Furthermore, the formation of **2-06** is proof of the fact that in the reaction mixture, **2-05** has a reactive remaining chloro ligand, which in the presence of lithiated **L2-03** can lead to the displacement of the second chloro ligand.

Addition of titanocene dichloride to L2-05

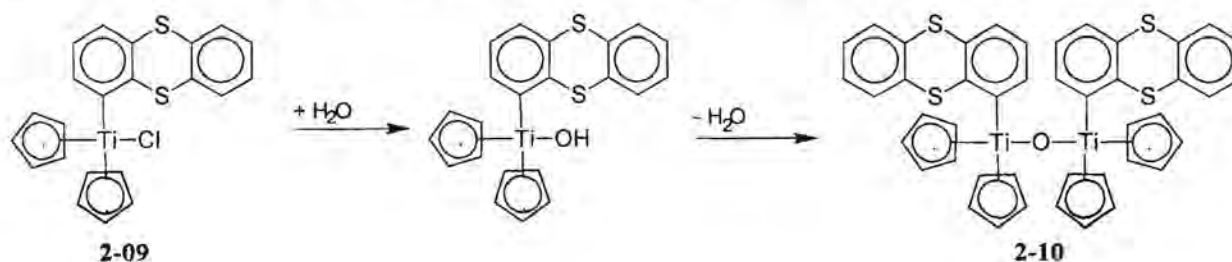
L2-05 was deprotonated on the 2-position using n-BuLi in a THF/hexane solution. Addition of titanocene dichloride to the lithiated product gave an immediate colour change from red to bright orange. Attempts to separate the product on silica gel led to immediate decomposition. Column chromatography on alumina yielded (benzofuran-2-yl)chlorobis(cyclopentadienyl)titanium(IV), [TiCp₂(Bf)Cl] **2-07**. This product was very sensitive to oxygen and was highly unstable at room temperature. It could be kept under argon at low temperatures for about one week. Due to the instability it was only possible to characterize **2-07** with ¹H NMR spectroscopy.

Addition of titanocene dichloride to L2-01

Metallation of **L2-01** with n-BuLi and addition of titanocene dichloride gave the expected product chlorobis(cyclopentadienyl)(dibenzothiophen-4-yl)titanium(IV), [TiCp₂(Dbt)Cl] (**2-08**) which was purified by column chromatography on silica gel.

Addition of titanocene dichloride to L2-04

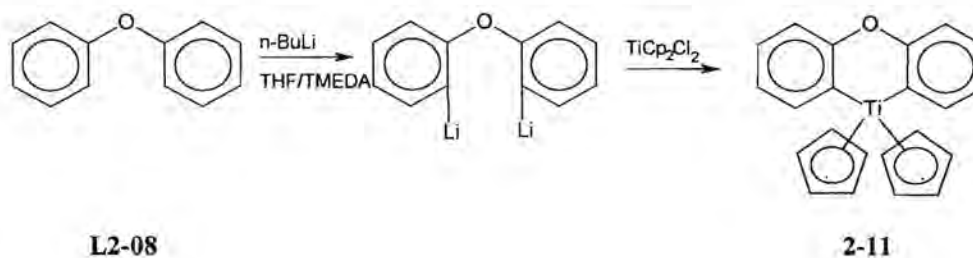
Lithiation of **L2-04** proceeded in a high yield and on addition of titanocene dichloride, the colour changed from red to orange-brown. From the silica gel column chlorobis(cyclopentadienyl)(thianthren-1-yl)titanium(IV), [TiCp₂(Thr)Cl] (**2-09**) was collected followed by a yellow fraction bis(cyclopentadienyl)bis(thianthren-1-yl)titanium(IV), [TiCp₂(Thr)₂] (**2-10a**), which was too unstable to purify. Complex **2-09** readily converted into a second yellow product, (μ -oxo)bis[bis(cyclopentadienyl)(thianthren-1-yl)titanium(IV)] [(μ -O){TiCp₂(Thr)}₂] (**2-10**). Due to the instability of **2-09** in solution, the only way to characterize the complex was through measuring the ¹H NMR spectrum as soon as possible. Attempts to obtain a ¹³C NMR spectrum failed, as the complex already started to decompose to **2-10** during measurement. In comparison with **2-05**, complex **2-09** is far less stable, indicating that the **L2-04** ligand has a stronger activation effect on the remaining chloro ligand, than was the case with the **L2-03** ligand. The yellow fraction in this case originated from **2-09**. The fact that **2-10a** was too unstable to isolate is ascribed to steric constraints of the two ring ligands. Comparing stabilities one could conclude that **2-05** > **2-09** and **2-06a** > **2-10a**. Although **2-10** and **2-06** originate from different precursors, the conversion in both cases is brought about by the presence of water on the column material. The desired complex **2-09** has a highly activated chloro ligand, which in the presence of traces of water converts into the corresponding hydroxo complex. In a subsequent reaction the hydroxo complex forms the dinuclear complex **2-10**, by the elimination of water between two intermediate hydroxo complexes or the elimination of hydrochloric acid between complex **2-09** and a hydroxo intermediate complex (Scheme 2.4).



Scheme 2.4

Addition of titanocene dichloride to L2-08

In Scheme 2.5 the ring ligand is bound directly to the metal center by replacing both chloro ligands. Diphenyl ether (L2-08) was double lithiated in high yield by a *n*-BuLi / TMEDA solution and a brown red precipitate settled out. The addition of titanocene dichloride caused an immediate colour change from red to orange affording {bis(cyclopentadienyl)}(diphen-2,2'-ylether)titanium(IV) [TiCp₂(Dpe)] (DpeH₂ = diphenyl ether) 2-11.



Scheme 2.5

2.3 Characterization

• Mass spectrometry

The mass spectral data for L2-01¹⁰, L2-03¹¹, L2-04¹¹, L2-05¹² and L2-06¹³ is reported in literature. The data for complexes L2-07, 2-01 – 2-06 and 2-08 – 2-11 is summarized in Table 2.2. It was not possible to record a spectrum for complex 2-07 due to instability.

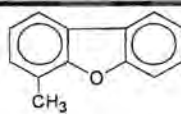
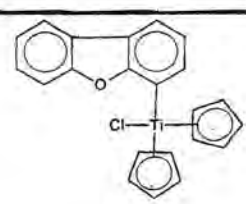
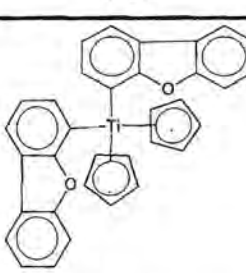
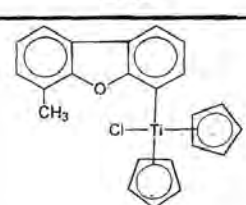
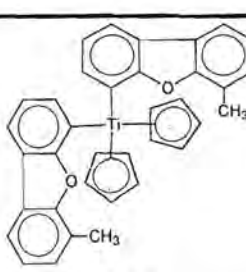
10. W Riepe, M. Zander, *Org. Mass Spectrom.*, **1979**, *14*, 455.

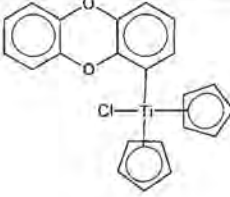
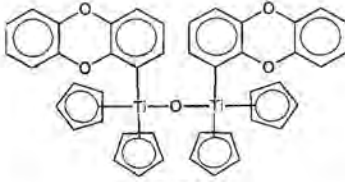
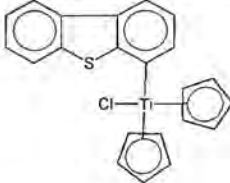
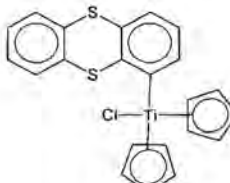
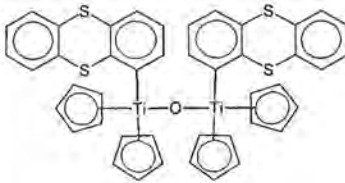

11. N. P. Buu-Hoi, G. Saint-Ruf, M. Mangane, *J. Heterocycl. Chem.*, **1972**, *9*, 691.

12. T. Kuster, H. Mändli, R. Robbiani, J. Seibl, *Helv. Chem. Acta*, **1978**, *61*, 1017.

13. B. G. Pring, N. E. Sjernstrom, *Acta Chem. Scand.*, **1968**, *22*, 549.

Table 2.2 Mass spectral data for ligand **2-07** and complexes **2-01** - **2-06** and **2-08** – **2-11**.

Mass Peaks, m/z(1%)		
 <p>L2-07</p>	182 (100) [M] ⁺	91 (4) [C ₇ H ₇] ⁺
	168 (20) [M - CH ₃] ⁺	76 (6) [C ₆ H ₄] ⁺
	140 (5) [M - CH ₃ CO] ⁺	63 (5) [C ₅ H ₃] ⁺
	127 (5) [C ₁₀ H ₇] ⁺	51 (3) [C ₄ H ₃] ⁺
	115 (3) [C ₉ H ₇] ⁺	39 (2) [C ₃ H ₃] ⁺
	103 (2) [C ₈ H ₇] ⁺	27 (1) [C ₂ H ₃] ⁺
	 <p>2-01</p>	381 (3) [M] ⁺
346 (100) [M ⁺ -Cl]		178 (5) [TiCp ₂] ⁺
315 (35) [TiCp(Dbf)Cl] ⁺		168 (100) [DbfH] ⁺
280 (28) [TiCp(Dbf)] ⁺		167 (100) [Dbf] ⁺
250 (5) [Ti(Dbf)Cl] ⁺		148 (48) [TiCpCl] ⁺
234 (55) [Ti(Dbf)O] ⁺		113 (15) [TiCp] ⁺
 <p>2-02</p>		513 (13) [M] ⁺
	463 (1) [TiCp(Dbf) ₂ O] ⁺	234 (20) [Ti(Dbf)O] ⁺
	447 (2) [TiCp(Dbf) ₂] ⁺	215 (13) [Ti(Dbf)] ⁺
	398 (2) [Ti(Dbf) ₂ O] ⁺	178 (12) [TiCp ₂] ⁺
	382 (3) [Ti(Dbf) ₂] ⁺	168 (100) [DbfH] ⁺
	346 (100) [M ⁺ -Dbf]	167 (48) [Dbf] ⁺
	296 (12) [TiCp(Dbf)O] ⁺	113 (8) [TiCp] ⁺
	 <p>2-03</p>	541 (5) [M] ⁺ (2-04)
493 (4) [TiCp(Dbf-Me)O] ⁺		213 (7) [TiCp ₂ Cl] ⁺
395 (4) [M] ⁺		181 (100) [Dbf-MeH] ⁺
359 (48) [TiCp ₂ (Dbf-Me)] ⁺		180 (100) [Dbf-Me] ⁺
330 (4) [TiCp(Dbf-Me)Cl] ⁺		178 (5) [TiCp ₂] ⁺
294 (11) [TiCp(Dbf-Me)] ⁺		148 (12) [TiCpCl] ⁺
264 (3) [Ti(Dbf-Me)Cl] ⁺		113 (5) [TiCp] ⁺
 <p>2-04</p>		573 (14) [M + 2O] ⁺
	557 (9) [M ⁺ + O] ⁺	294 (3) [TiCp(Dbf-Me)] ⁺
	541 (85) [M] ⁺	245 (4) [Ti(Dbf-Me)O] ⁺
	493 (50) [TiCp(Dbf-Me) ₂ O] ⁺	181 (100) [Dbf-MeH] ⁺
	475 (7) [TiCp(Dbf-Me) ₂] ⁺	180 (100) [Dbf-Me] ⁺
	410 (24) [Ti(Dbf-Me) ₂] ⁺	178 (5) [TiCp ₂] ⁺
	360 (39) [TiCp ₂ (Dbf-Me)] ⁺	113 (3) [TiCp] ⁺

 <p>2-05</p>	<p>396 (3) $[M]^+$ 361 (96) $[M^+-Cl]^+$ 366 (13) $[Dbz-Dbz]^+$ 331 (10) $[TiCp(Dbz)Cl]^+$ 295 (29) $[TiCp(Dbz)]^+$ 248 (23) $[TiCp_2Cl_2]^+$</p>	<p>230 (22) $[Ti(Dbz)]^+$ 213 (12) $[TiCp_2Cl]^+$ 184 (100) $[DbzH]^+$ 183 (100) $[Dbz]^+$ 178 (7) $[TiCp_2]^+$ 148 (32) $[TiCpCl]^+$</p>
 <p>2-06</p>	<p>738 $[M^+]$ not observed 430 (53) $[Ti(Dbz)_2O]^+$ 378 (1) $[TiCp_2(Dbz)O]^+$ 366 (3) $[Dbz-Dbz]^+$ 361 (3) $[TiCp_2(Dbz)]^+$</p>	<p>312 (3) $[TiCp(Dbz)O]^+$ 247 (6) $[Ti(Dbz)O]^+$ 184 (13) $[DbzH]^+$ 183 (13) $[Dbz]^+$</p>
 <p>2-08</p>	<p>396 (27) $[M]^+$ 366 (96) $[Dbt-Dbt]^+$ 331 (29) $[TiCp(Db)Cl]^+$</p>	<p>231 (6) $[Ti(Db)]^+$ 184 (100) $[Dbt]^+$ 148 (48) $[TiCpCl]^+$</p>
 <p>2-09</p>	<p>624 (11) $[TiCp_2(OThr)(Thr)]^+$ 608 (1) $[M^+]$ (2-10a) 559 (10) $[TiCp(OThr)(Thr)]^+$ 494 (18) $[Ti(OThr)(Thr)]^+$ 430 (2) $[Thr-Thr]^+$ 428 (3) $[M^+]$ 409 (28) $[TiCp_2(OThr)]^+$ 393 (11) $[TiCp_2(Thr)]^+$</p>	<p>344 (31) $[TiCp(OThr)]^+$ 280 (59) $[Ti(Thr)OH]^+$ 247 (27) $[TiCp_2Cl_2]$ 216 (21) $[ThrH]^+$ 215 (21) $[Thr]^+$ 178 (15) $[TiCp_2]^+$ 113 (6) $[TiCp]^+$ 64 (9) $[TiO]^+$</p>
 <p>2-10</p>	<p>802 $[M^+]$ not observed 624 (2) $[TiCp_2(OThr)(Thr)]^+$ 608 (1) $[M^+]$ (2-10a) 559 (1) $[TiCp(OThr)(Thr)]^+$ 543 (1) $[TiCp(Thr)_2]^+$ 494 (7) $[Ti(OThr)(Thr)]^+$ 430 (5) $[Thr-Thr]^+$ 409 (77) $[TiCp_2(OThr)]^+$ 393 (42) $[TiCp_2(Thr)]^+$</p>	<p>344 (60) $[TiCp(OThr)]^+$ 280 (100) $[Ti(Thr)OH]^+$ 232 (72) $[ThrOH]^+$ 216 (66) $[ThrH]^+$ 215 (66) $[Thr]^+$ 178 (51) $[TiCp_2]^+$ 113 (13) $[TiCp]^+$ 64 (11) $[TiO]^+$</p>
 <p>2-11</p>	<p>347 (73) $[M]^+$ 281 (100) $[TiCp(C_{12}H_8O)]^+$ 215 (20) $[Ti(C_{12}H_8O)]^+$ 178 (12) $[TiCp_2]^+$</p>	<p>170 (14) $[DpeH_2]^+$ 168 (10) $[Dpe]^+$ 113 (22) $[TiCp]^+$</p>

L2-07 has the expected fragmentation pattern. The molecular ion has a high intensity and the methyl substituent fragments first. A similar pattern was observed for **L2-06**.

Complexes **2-01** to **2-03** have low intensity signals for the molecular ion. For complex **2-01** two fragmentation pathways can be deduced from the fragment ions in the spectrum. In the first, major route, the chlorine ligand is lost giving the principle ion $[M^+-Cl]$, followed by the cleavage of a Cp or Dbf ligand. There is also a minor pathway where a Cp is fragmented first, followed by a Cp, Cl or ring ligand. For complex **2-02** the dominant pathway represents the fragmentation of the ring ligand to give the principle ion $[M^+-Dbf]$, followed by a Cp or other ring ligand. The major pathway for the fragmentation of complex **2-03** again comprises the cleavage of the chloro ligand (48%), followed by a Dbf or Cp ring. There is a minor route (4%) whereby the ring ligand is fragmented first. Two fragment ions were identified where an oxygen atom was included in the fragment ion. The molecular ion gives a high intensity signal for complex **2-04** and there are different fragmentation pathways whereby the ring ligands or Cp ligands fragments first. Like in the previous case there are some fragment ions with oxygen atoms.

The intensity of the molecular ion peak for **2-05** is low (3%), which means that the compound is relatively unstable under the experimental conditions during the measurement. The dominant pathway corresponds to the initial fragmentation of a chloro ligand from the molecular ion. According to other fragment ions, several possible pathways exist. One pathway shows the initial loss of a chloro ligand, followed by the loss of the ring ligand or one or both Cp ligands. In a second route a Cp ligand is lost first, followed by the ring ligand or the chloro ligand and then a Cp ligand. In another pathway the loss of a chloro or Cp ligand follows the loss of the ring ligand. The intensities of the fragment ions reveal that the importance of initial fragmentation decreases according to Cl > heteroaromatic ring ligand > Cp. Complex **2-06** cleaves into two fragments at the oxygen bridge. The molecular ion peak was not observed.

Although the intensity of the molecular ion peak for **2-08** is high (27%) no fragmentation pathway could be deduced from the spectrum. Fragmentation of the ligands seems to be random. The spectra for **2-09** and **2-10** are almost identical. This is ascribed to the fact that **2-09** readily converts to **2-10**. There is a weak signal for the $[M^+]$ in the spectrum of **2-09** (8%), which indicates the instability of this complex. A fragment indicating thianthrene with an oxygen atom bound to it (most probably an oxidation at a sulfur atom) was detected on many fragments for both **2-09** and **2-10**. The fragmentation pattern of **2-10** shows similarities to that of **2-06**. The molecule is cleaved into two parts and the

fragment ions $[\text{TiCp}_2(\text{Thr})\text{O}]^+$ and $[\text{TiCp}_2(\text{Thr})]^+$ are of highest intensity in the spectrum of **2-10**. A common feature in many of the spectra is the dimerization of the heteroaromatic ring.

Complex **2-11** gives a high intensity signal for the molecular ion and the fragmentation route follows the sequence of losing a Cp ligand first and then the biphenyl ring. Reductive elimination of the ring ligand is manifested in the presence of the fragment ion $[\text{DpeH}_2]^+$.

• *¹H NMR and ¹³C NMR spectroscopy*

The ¹H and ¹³C NMR spectra for **L2-01**¹⁴, **L2-03**^{15,16}, **L2-04**^{15,16}, **L2-05**^{17,18}, **L2-06**^{19,20} and **L2-08** were recorded and assignments agree with those reported in literature. A summary is given in Table 2.3 for purposes of comparison with those in the complexes. The ¹H and ¹³C NMR spectral data for **L2-07**, **L2-07b** and complexes **2-01** – **2-11** are summarized in Table 2.3 and Table 2.4. Due to the instability of **2-07** and **2-09** their ¹³C NMR spectra could not be obtained.

¹H NMR spectroscopy

The proton chemical shifts of the ring of the heteroaromatic ligand that is not attached to the metal were normally quite unaffected by coordination and compared well with the resonances of the heteroaromatic substrate. The greatest changes in shifts were recorded for the ring coordinated to titanium. The more electropositive titanium removes less electron density from the ring compared to a hydrogen of a ring carbon and an upfield shift was observed. The protons closest to the metal fragment were being influenced more (these resonances are shifted upfield).

14. K. D. Bartlet, D. W. Jones, R. S. Matthews, *Tetrahedron*, **1971**, *27*, 5177.

15. N. E. Sharpless, R.B. Bradley, *Org. Magn. Res.*, **1974**, *6*, 115.

16. V. Galasso, K. J. Irgolic, G.C. Pappalardo, *J. Organomet. Chem.*, **1979**, *181*, 329.

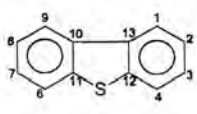
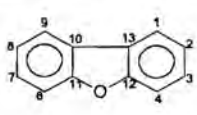
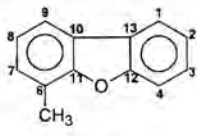
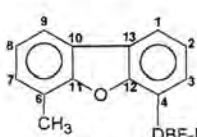
17. M. Audit, P. Demerseman, N. Goasdoue, N. Platzter, *Org. Magn. Reson.*, **1983**, *21*, 698.

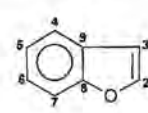
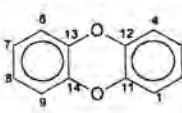
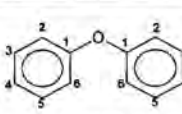
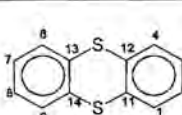
18. R. R. Fraser, T. S. Mansour, S. Savard, *Can. J. Chem.*, **1985**, *63*, 3505.

19. M. E. Amato, A. Grassi, K.J. Irolic, G.C. Pappalardo, L. Radics, *Organometallics*, **1993**, *12*, 775.

20. S. Florea, W. Kimpenhaus, V. Farsacan, *Org. Magn. Reson.*, **1977**, *9*, 133.

Table 2.3 ^1H and ^{13}C NMR spectroscopic data^a for L2-01 and L2-03 - L2-08.

Ligand	C	Chemical Shift (δ ppm)	H	Chemical Shift (δ ppm)	Splitting & Integration	Coupling Constant (J Hz)
 L2-01	1,9	122.4	1,9	8.15	d 2H	8.0/1.2
	2,8	124.0	2,8	7.46	t 2H	7.2/8.0/1.0
	3,7	127.1	3,7	7.46	t 2H	8.0/7.2/1.2
	4,6	123.3	4,6	7.87	d 2H	8.0/1.0
	10,13	136.1				
	11,12	139.1				
 L2-06	1,9	120.6	1,9	7.58	d 2H	8.0
	2,8	122.7	2,8	7.46	t 2H	7.2/8.0
	3,7	127.1	3,7	7.34	t 2H	7.8/7.2
	4,6	111.6	4,6	7.93	d 2H	7.8
	10,13	124.2				
	11,12	156.1				
 L2-07	1	120.6	1	7.58	d 1H	8.0/8.0
	2	122.7	2	7.46	t 1H	7.2
	3	127.1	3	7.34	t 1H	7.8
	4	111.6	4	7.93	d 1H	7.6
	6	120.8	7	7.14	dd 1H	7.2/1.1
	7	127.8	8	7.34	t 1H	7.2
	8	122.6	9	7.39	dd 1H	7.2/1.1
	9	117.6	Me	2.35	s 3H	
	10	134.6				
	11	162.1				
	12	150.9				
	13	114.7				
	Me	15.0				
	 L2-07b	1	120.7	1	7.75	dd 2H
2		122.6	2	7.56	dd 2H	8.0/8.3
3		126.9	3	7.90-7.93	m 2H	-
4		118.4	7	7.22	dd 2H	6.2/1.3
6		111.6	8	7.31	dd 2H	7.5/7.5
7		128.1	9	7.43	dd 2H	7.2/1.3
8		122.5	Me	2.59	s 6H	
9		117.9				
10/11/12/13		156.3/150.3 127.3/113.6				
Me		15.2				

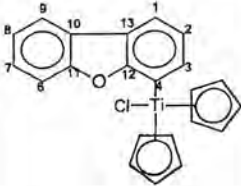
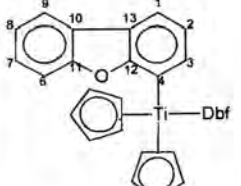
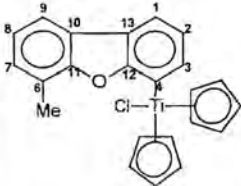
 L2-05	2	144.8	2	7.66	d	1H	2.3
	3	106.5	3	6.81	d	1H	2.3
	4	121.1	4	7.66	dd	1H	7.2
	5	122.7	5	7.36	td	1H	7.2
	6	124.1	6	7.30	td	1H	7.8/7.2
	7	111.4	7	7.58	d	1H	7.8
	8	154.9					
	9	127.4					
	 L2-03	1,9,4,6	116.2	1,4,6,9	6.81	d	4H
2,8,3,7		123.6	2,3,7,8	6.85	t	4H	7.5
11,14,12,13		142.1					
 L2-08	1	157.3	2,6	7.03	d	4H	7.5
	2,6	118.9	3,5	7.35	t	4H	7.4/7.5
	3,5	123.2	4	7.13	d	2H	7.4
	4	129.8					
 L2-04	1,9,4,6	128.7	1,9,4,6	7.48	d	4H	7.7/1.5
	2,8,3,7	127.7	2,8,3,7	7.23	t	4H	7.5/7.7/1.5
	11,14,12,13	135.5					

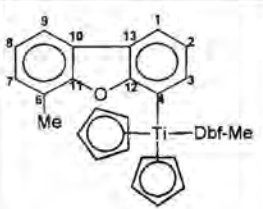
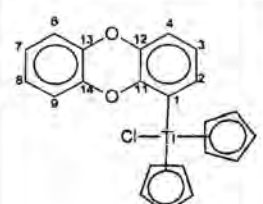
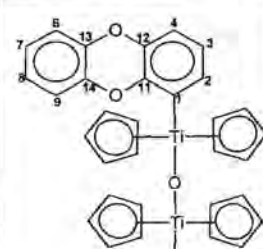
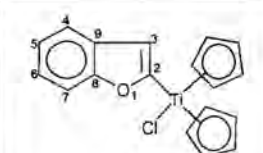
^a Recorded in CDCl₃

The reason for this shift of electron density can be explained by using different models. Firstly, as a result of an σ -inductive effect whereby the Ti, being the more electropositive element, is part of a polar covalent bond with the carbon the negative pole. This results in the electron density shifting more towards the carbon atom, leaving the metal partially electropositive and the carbon partially electronegative. Secondly, a similar end result is achieved by assuming that the Ti-C bond is an ionic bond; the titanium fragment acts as the cation and the ring carbon as the anion.

The presence of a methyl substituent on a benzene ring, will as a result of the inductive effect of the methyl, shift all the resonances of that particular ring upfield, whereas, the resonances of the unsubstituted ring remain the same and are unaffected. According to Amato, *et al*¹⁹ there are upfield shifts for the H1, H4, H6 and H9 protons in **L2-03**, when compared with the other chalcanthrenes (S, Se, Te), due to the modification of the paramagnetic term by oxygen.

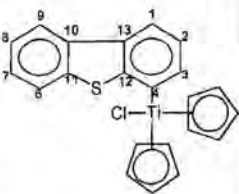
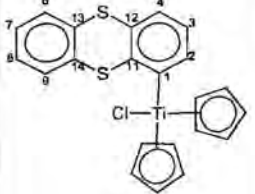
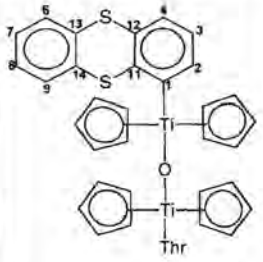
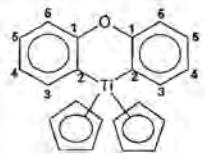
Table 2.4 ^1H and ^{13}C NMR spectroscopic data^a for 2-01 – 2-11.

Complex	C	Chemical Shift ^b (δ ppm)	H	Chemical Shift (δ ppm)	Splitting & Integration	Coupling Constant (J Hz)
 <p>2-01</p>	1	116.9	1	7.56	dd 1H	7.5/1.3
	2	123.8	2	6.98	t 1H	7.2/7.5
	3	136.5	3	7.18	dd 1H	7.2/1.3
	4	182.5	6	7.94	dd 1H	7.5/1.3
	6	111.7	7	7.28	td 1H	7.2/7.5/1.3
	7	127.1	8	7.38	td 1H	8.0/7.2/1.3
	8	122.3	9	7.43	tt 1H	8.0/1.3
	9	120.7	Cp	6.46	s 10H	
	10	112.7				
	11	157.9				
	12	161.8				
	13	120.6				
	Cp	117.2				
 <p>2-02</p>	1	111.7	1	7.57/7.61	dd 2H	8.3/6.7/1.8
	2	122.0	2	7.09/7.11	t 2H	7.2/6.7/8.3
	3	132.4	3	7.13	dd 2H	7.2/1.8
	4	169.1	6	7.92-7.97	m 2H	-
	6	120.6	7	7.31/7.33	td 2H	7.2/7.8/8.5
	7	122.5	8	7.42/7.45	td 2H	8.3/7.2/8.0
	8	127.1	9	7.52	dd 2H	8.3
	9	111.0	Cp	6.34/6.47	s 10H	
	10	124.2				
	11	155.5				
	12	159.9				
	13	125.1				
	Cp	115.7				
 <p>2-03</p>	1	118.2	1	7.74-7.76	m 1H	-
	2	125.9	2	7.56	t 1H	8.3
	3	120.7	3	7.91	dd 1H	7.8/1.5
	4	169.6	7	7.21-7.23	m 1H	-
	6	111.6	8	7.32	dt 1H	8.3/1.3
	7	136.5	9	7.44	dd 1H	7.3/1.3
	8	127.1	Me	2.59	s 3H	
	9	122.6	Cp	6.44	s 10H	
	10/11/12/13	155.1/156.1/159.8/154.3				
	Me	15.4				
Cp	117.0					

 <p style="text-align: center;">2-04</p>	<p>1 117.9 2 126.0 3 120.6 4 169.4 6 110.9 7 136.4 8 128.1 9 122.7 10/11/12/13 154.9/156.0/159.6/153.6 Me 15.2 Cp 117.2</p>	<p>1 7.73-7.75 m 2H - 2 7.55 td 2H 8.3 3 7.93 dd 2H 7.8/1.5 7 7.18-7.20 m 2H - 8 7.31 dt 2H 8.3/1.3 9 7.43 dd 2H 7.3/1.33 Me 2.58 s 6H Cp 6.44 s 10H</p>
 <p style="text-align: center;">2-05</p>	<p>1 175.1 2 133.0 3 120.1 4 113.4 6 116.3 7/8 124.0/123.2 9 115.1 11 150.2 12/13/14 142.6/143.0/143.1 Cp 117.1</p>	<p>2 6.74 dd 1H 7.4/1.6 3 6.55 dd 1H 7.7/7.4 4 6.48 dd 1H 7.7/1.6 6/7/8/9 6.67-6.70 m 4H - Cp 6.43 s 10H</p>
 <p style="text-align: center;">2-06</p>	<p>1 176.0/178.7 2 132.2/132.4 3 120.8/122.7 4 113.1/113.5 6 116.3/116.5 7/8 123.1/123.5/123.6/123.8 9 115.4/116.1 11 150.1 12/13/14 142.0-145.0 Cp 112.6/114.4/114.6</p>	<p>2 6.34/7.05 dd 2H 8.2/7.5/ 1.5/1.6 3 6.72/6.69 t 2H 8.2/7.5 4 6.29/6.62 dd 2H 8.2/7.5/ 1.5/1.6 6/7/8/9 6.80-6.95 m 8H - Cp 6.05/6.08/ 6.27 s 20H</p>
 <p style="text-align: center;">2-07</p>	<p>Not recorded -</p>	<p>3 7.15 d 1H 1.0 4 7.62 dd 1H 7.1/1.0 5 7.34 td 1H 7.1/7.2 6 7.23 dd 1H 7.2/7.2 7 7.53 d 1H 7.2 Cp 6.50 s 10H</p>

2. Titanocene derivatives with a heteroaromatic ligand containing a direct metal-carbon σ -bond

43

 <p>2-08</p>	<p>1 117.7 2 124.8 3 134.5 4 185.5 6 121.9 7 125.9 8 124.2 9 121.5 10 136.2 11 138.5 12 147.3 13 133.2 Cp 117.2</p>	<p>1 7.75 dd 1H 7.7/1.1 2 7.07 t 1H 7.6/7.4 3 7.35 dd 1H 7.4/1.1 6/9 7.77-8.09 m 2H - 7/8 7.38-7.45 m 2H - Cp 6.49 s 10H</p>
 <p>2-09</p>	<p>Not recorded -</p>	<p>2 7.14 dd 1H 7.4/1.1 3 6.86 t 1H 7.5/7.4 4 6.77 dd 1H 7.5/1.1 6/9 7.45-7.57 m 2H - 7/8 7.20-7.27 m 2H - Cp 6.41 s 10H</p>
 <p>2-10</p>	<p>1 207.1/200.9 2 137.5/139.7 3 125.7/126.6 4 114.8/116.8 6/9 128.1/128.3/128.6/128.7 7/8 127.4/127.5/127.7/127.7 11 150.2/150.2 12/13/14 135.0-136.0 Cp 115.4</p>	<p>2 6.98/7.68 dd 2H 7.5/1.3 3 6.93/7.06 t 2H 7.6/7.5 4 6.38/6.59 dd 2H 7.6/1.3 6/9 7.46-7.55 m 4H - 7/8 7.22-7.27 m 4H - Cp 6.38 s 20H</p>
 <p>2-11</p>	<p>1 no 2 no 3 137.2 4 127.9 5 124.5 6 119.9 Cp 115.6</p>	<p>3 6.45 dd 2H 7.8 4 7.01 td 2H 8.5/7.8 5 6.89 td 2H 8.0/8.5 6 7.69 dd 2H 8.0 Cp 6.06 s 10H</p>

^a Recorded in CDCl₃ ^b no = not observed

Titanium is a d^0 species and has 16 valence electrons in its coordination sphere in **2-05**, which leaves one available coordination site on the metal. This site can be occupied by an interaction between the lone pair of an oxygen and the metal centre, which in turn could deshield the adjacent protons. Examples of this effect are known in literature and was shown by a crystal structure of

$[\text{TiCp}_2(\text{CH}_2\text{OCH}_3)\text{Cl}]^{21}$. However for the complexes in this study, the carbon bonded to titanium is sp^2 -hybridised and as a result of the orientation of the heteroatom it is less likely to interact with the metal.

The chemical shifts for H6-H9 were difficult to assign in **2-05**, **2-06**, **2-08** and **2-09** due to their overlapping signals, but were not strongly affected. The reason for the high downfield shifts for H3 in **L2-07b** and **2-03** is not easily explainable. A possible option is to ascribe it to an intramolecular hydrogen bond interaction as seen in Figure 2.7. The similar tendency in **2-04** cannot be explained by hydrogen bonding (compare the solid state structure, *vide infra*).

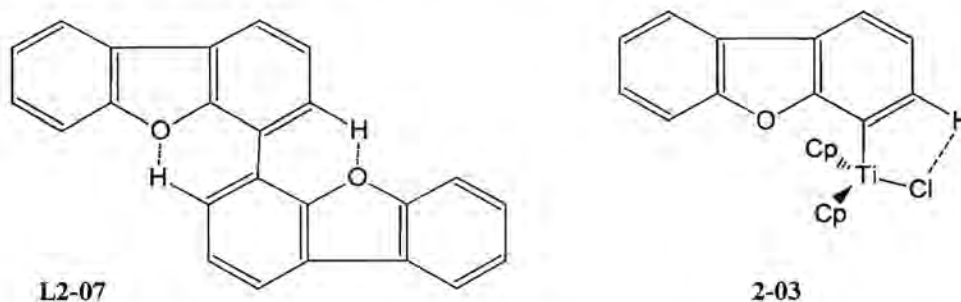


Figure 2.7 Possible explanations for the high downfield shift of H3 in **L2-07b** and **2-03**.

The spectra for **2-06** and **2-10** are complex. There are two sets of signals for the heteroaromatic rings. A possible explanation is that the two heteroaromatic rings are caught in two different chemical environments, because of the bulkiness of the heteroaromatic ligands and resulting restriction in rotation. In complexes **2-06** and **2-10** one of the two resonances of H2 displays a significant downfield shift, while the other is shifted upfield, which can only be due to ring current effects.

The singlet observed at 7.15 ppm in the ^1H NMR spectrum of **2-07** proves that the titanium fragment is bound to the 2-position of **L2-05**. Since the H3 proton is the closest proton to the coordination site, it is expected that this proton is influenced most as is manifested in a 0.34 ppm upfield shift.

In most complexes the two Cp rings resonate as a singlet due to similar chemical environments. The Cp values are shifted upfield in all the cases compared to titanocene dichloride, which has a Cp value of 6.57 ppm. This is due to the replacement of the electronegative chloro ligand by a carbon atom of the ring in titanocene dichloride and a resulting increase in electron density on the metal fragment. Hence less electron density is transferred from the Cp ligands to the titanium. In most cases the shift is

21. G. Erker, R. Schlund, C. J. Krüger, *J. Organomet. Chem.*, 1988, 338, C4.

around 0.10 to 0.50 ppm. The replacement of both chloro ligands caused even more electron density to reside on the metal fragment and the chemical shifts of the Cp rings were observed even further upfield.

There are two different signals for the four Cp rings in **2-06**. One signal displays a strong singlet indicating two Cp rings that are free to rotate while the other two Cp rings afforded two singlets displaying an intensity ratio of 4:1, about 0.2ppm upfield from the first signal. This means that one of the five protons on these Cp rings is in a different electronic environment. The most likely explanation for this shift is that the two oxygen atoms of the heteroaromatic ring ligands caused it. A second possibility is the presence of ring currents of the heteroaromatic rings as a result of two of the Cp ligands being very close to the aromatic rings. Whereas **2-06** displayed two Cp signals, the spectrum of **2-10** revealed only one Cp signal. This means that the Cp rings are all in the same chemical environment in **2-10**, but that the heteroaromatic ligands are in different chemical environments.

Two-dimensional homonuclear shift correlation spectroscopy (COSY) was used to aid in the unambiguous assignment of the different protons in **2-01**, **2-02**, **2-03** and **2-05**.

¹³C NMR spectroscopy

In the ¹³C NMR spectra of the complexes the chemical shift for the carbon bound directly to the titanium is shifted far downfield in all the complexes due to attaching a very electropositive metal to the carbon atom. The average is around 30 to 80 ppm compared to the heteroaromatic substrates. The direct neighbouring carbons also have downfield shifts, but much less than that of the *ipso* carbon. The average shift for the neighbouring carbon is about +10 ppm. The rest of the chemical shifts are similar to those of the uncoordinated ligand. The signals for the quaternary carbons C10-C14 were difficult to assign in most of the spectra.

The ¹³C NMR spectra of complexes **2-05**, **2-06** and **2-10** displayed a duplication of peaks for the two heteroaromatic ligands resulting from different chemical environments for the rings, supporting the ¹H NMR spectral data.

In most cases the Cp protons resonate upfield (about 3 - 8 ppm) due to increased electron density on the metal fragment, when compared to titanocene dichloride. The ¹³C NMR spectrum of **2-06** again displays a 4:1 ratio of Cp ring carbons supporting the ¹H NMR data.

HETCOR spectra of **2-02**, **2-03**, **2-05** and **2-08** were used to assign and correlate the specific proton resonances to their corresponding carbons.

• *X-ray crystallography*

Structure of complex 2-02

Final confirmation of the structure of 2-02 was obtained from a single crystal X-ray diffraction study. The complex crystallised from a 1:1 dichloromethane:hexane solution by layering the solvents. This method gave bright orange crystals of good quality. In Figure 2.8 the structure of the molecule is given as a ball and stick representation, which also indicates the atom numbering scheme that was used for the structural data. Each unit cell contains two independent molecules with the metal centres labelled Ti(A) and Ti(B) respectively. Only the case for the A molecule is represented in the figure. The most important bond lengths and angles are listed in Table 2.5 and Table 2.6 respectively. Other structural information is given in Chapter 6 and in Appendix A.

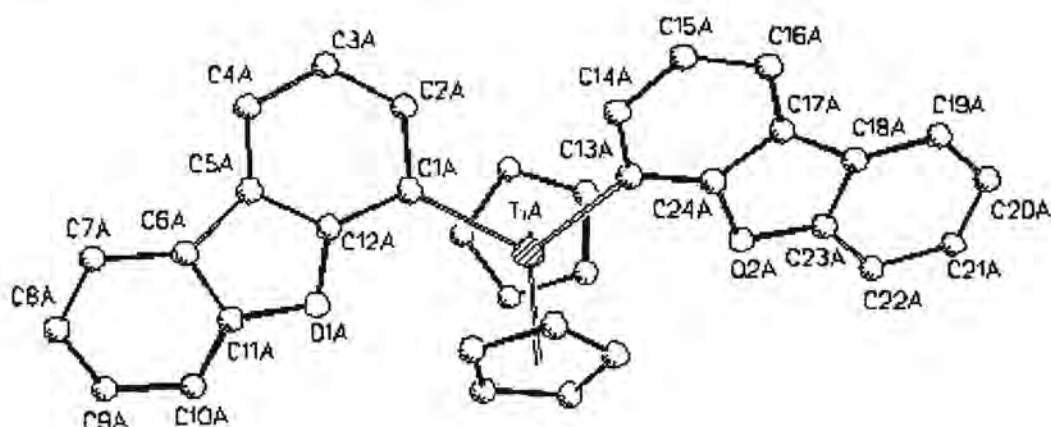


Figure 2.8 Ball and stick representation of the molecular structure A of 2-02.

Table 2.5. Selected bond lengths for 2-02.

	Bond length [Å]		Bond length [Å]
TiA-C(13A)	2.210(4)	C(5A)-C(12A)	1.410(6)
TiA-C(1A)	2.218(5)	C(5A)-C(6A)	1.450(7)
O(1A)-C(11A)	1.398(5)	C(6A)-C(11A)	1.395(6)
O(1A)-C(12A)	1.405(5)	C(6A)-C(7A)	1.422(7)
C(1A)-C(12A)	1.410(6)	C(7A)-C(8A)	1.372(8)
C(1A)-C(2A)	1.415(6)	C(8A)-C(9A)	1.363(8)
C(2A)-C(3A)	1.422(6)	C(9A)-C(10A)	1.400(7)
C(3A)-C(4A)	1.382(7)	C(10A)-C(11A)	1.375(7)
C(4A)-C(5A)	1.393(7)		

Table 2.6. Selected bond angles for **2-02**.

	Bond angle [°]		Bond angle [°]
C(13A)-TiA-C(1A)	105.0(2)	C(11A)-C(6A)-C(5A)	106.6(4)
C(11A)-O(1A)-C(12A)	106.3(4)	C(7A)-C(6A)-C(5A)	135.9(5)
C(12A)-C(1A)-C(2A)	110.3(4)	C(8A)-C(7A)-C(6A)	117.8(6)
C(12A)-C(1A)-TiA	126.3(3)	C(9A)-C(8A)-C(7A)	123.2(6)
C(2A)-C(1A)-TiA	123.3(4)	C(8A)-C(9A)-C(10A)	120.7(6)
C(1A)-C(2A)-C(3A)	123.9(5)	C(11A)-C(10A)-C(9A)	116.2(5)
C(4A)-C(3A)-C(2A)	121.5(5)	C(10A)-C(11A)-O(1A)	124.9(5)
C(3A)-C(4A)-C(5A)	118.1(5)	C(10A)-C(11A)-C(6A)	124.4(5)
C(4A)-C(5A)-C(12A)	117.9(5)	O(1A)-C(11A)-C(6A)	110.7(5)
C(4A)-C(5A)-C(6A)	135.6(5)	C(5A)-C(12A)-O(1A)	110.1(4)
C(12A)-C(5A)-C(6A)	106.2(4)	C(5A)-C(12A)-C(1A)	127.9(4)
C(11A)-C(6A)-C(7A)	117.4(5)	O(1A)-C(12A)-C(1A)	122.0(4)

Four ligands surround the titanium centre in a distorted tetrahedral arrangement, with positions defined by the centra of the Cp rings and the carbon connecting the metal to the dibenzofuran ring. The Cp rings and titanium belong to the open clamshell class of Cp-compounds. The bulky ring ligands cause an enlargement of the angle between the two non-Cp ligands. In titanocene dichloride this Cl-Ti-Cl angle²² is 94.6°, which is smaller than the 105.0° of C(13A)-TiA-C(1A) of **2-02**. This angle in **2-02** is also larger than the values of 96.7 and 98.4° recorded for the two molecules in the unit cell recorded for C-Ti-Cl of [TiCp₂(Dbt)Cl]²³ (Dbt = Dibenzothienyl)

The dihedral angle of C(11A)-O(1A)-C(12A)-C(1A) is 2.5(0)° and C(11B)-O(1B)-C(12B)-C(1B) is -0.9(0)°, which shows that the dibenzofuran ring is almost planar. The titanium atom is also in the plane of the furan ligand. If we compare the bond lengths of the dibenzofuran^{24,25} to those of **2-02**, we can see that they differ very little and that coordination to titanium has very little effect on the bond distances.

22. A. Clearfield, D. K. Warner, C. H. Salderiaga-Molina, R. Ropal, J. Bernal, *Can. J. Chem.*, **1975**, *53*, 1622.

23. S. Lotz, H. Görls, R. Meyer, unpublished results.

24. O. Dideberg, L. Dupont, J. M. Andre, *Acta Cryst., Sect B*, **1972**, *B28*, 1002.

25. A. Banerjee, *Acta Cryst., Sect B*, **1972**, *B29*, 2070.

The Ti-C(1A) and Ti(C13A) bond distances of 2.210 Å and 2.218 Å, respectively is significantly shorter than the observed Ti-C (sp^2 , phenyl) bond distance of 2.27(1) Å for $TiCp_2Ph_2$ ²⁶ and is comparable with the Ti-C(Ph) distance of 2.193(3) Å recorded for the titanacycle $[TiCp_2(C_6H_4-C_6H_4S)]$ ²⁷ and the average value of 2.188(5) Å for $[TiCp_2(C_6H_4-C_6H_4)]$ ²⁸. Complexes displaying significant π -interaction between titanium and a sp^2 -bonded carbon atom, should have Ti-C bond distances of about 2.00-2.10 Å^{29,30,31,32}, which is a little shorter than the corresponding distance in **2-05**.

The shorter Ti-C distance in **2-02** suggests that some multiple bonding interaction exists between the titanium and the dibenzofuran carbon atom. Titanium(IV) has no electrons in the d-orbitals and will therefore, only be able to act like a Lewis acid and accept electron density from the π -cloud of the ring ligand. The σ -bonded ring ligand exhibits some carbene character, which supports observations of the ¹³C NMR data that the relevant carbon resonances are shifted downfield into the carbene region²⁸. If applicable, one would expect that the adjacent bonds of the phenyl bonded to the titanium should be lengthened. Although not significant, these are the longest C-C distances in the ring. The average C-C bond distance for the benzene ring bearing Ti is 1.405 Å compared to 1.378 Å for the other benzene ring. The O-C bond length 1.148 Å in **L2-06**^{24,25} is shorter than these bond distances in **2-02** which are 1.398(5) Å and 1.405 Å for O(1A)-C(11A) and O(1A)-C(12A), respectively, and 1.388(5) Å and 1.418(4) Å for O(2A)-C(11A) and O(2A)-C(12A), respectively. The bond angle of 104.4° for **L2-06** is slightly smaller than that of these angles in **2-02**, which are 106.3(4)° and 105.9(3)° for C(11A)-O(1A)-C(12A) and C(23A)-O(2A)-C(24A), respectively.

26. V. Kocman, J. C. Rucklidge, R. J. O'Brien, W. Santo, *J. Chem. Soc., Chem. Commun.*, **1976**, 1340.

27. P. R. Stafford, T. B. Rauchfuss, A. K. Verma, S. R. Wilson, *J. Organomet. Chem.*, **1996**, 526, 203.

28. C. A. Mike, T. Nelson, J. Graham, A. W. Cordes, N. T. Allison, *Organometallics*, **1988**, 7, 2573.

29. P. Binger, P. Müller, P. Phillips, P. Gabor, R. Mynott, A. T. Herrmann, F. Langhauser, C. Krüger, *Chem. Ber.*, **1992**, 125, 2209.

30. M. M. Francl, W. J. Hehre, *Organometallics*, **1983**, 2, 457.

31. R. Beckhaus, S. Flatiu, S. Trojanov, P. Hofmann, *Chem. Ber.*, **1992**, 125, 291.

32. A. K. Rappe, *Organometallics*, **1987**, 6, 354.

Structure of complex **2-05**

The final confirmation of **2-05** was obtained from a single crystal X-ray diffraction study. The complex crystallised from a 1:1 THF:hexane solution by using the layering technique and gave bright orange crystals. Figure 2.9 gives the structure of the molecule as an ORTEP drawing, which also indicates the atom-labelling scheme that was used. The most important bond lengths and angles are listed in Table 2.7 and Table 2.8, respectively. Other structural information is given in Chapter 6 and in Appendix B. In the unit cell of the structure there is also a highly distorted THF molecule and a hexane. Bearing in mind the numerous unsuccessful attempts to obtain crystals of **2-05**, it is believed that the solvent molecules were essential in the packing process of the crystal. High thermal motions in the molecule necessitated low temperature data collections.

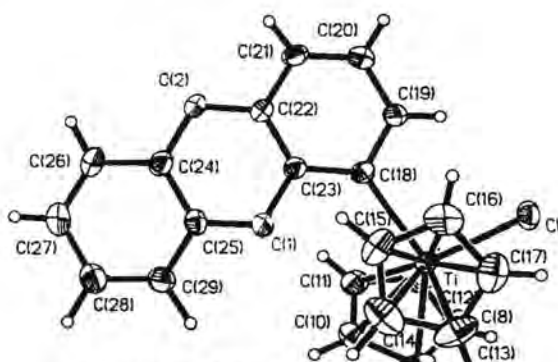


Figure 2.9 ORTEP diagram of **2-05**.

Table 2.7. Selected bond lengths of **2-05**.

	Bond Length [Å]		Bond Length [Å]
Ti-Cl	2.3684(7)	O(2)-C(22)	1.389(3)
Ti-C(18)	2.208(2)	O(2)-C(24)	1.378(3)
C(18)-C(19)	1.397(4)	C(24)-C(25)	1.397(4)
C(19)-C(20)	1.403(4)	C(24)-C(26)	1.387(4)
C(20)-C(21)	1.376(4)	C(26)-C(27)	1.388(4)
C(21)-C(22)	1.383(4)	C(27)-C(28)	1.398(4)
C(22)-C(23)	1.392(3)	C(28)-C(29)	1.383(4)
C(18)-C(23)	1.404(3)	C(29)-C(25)	1.387(4)
O(1)-C(23)	1.389(3)	H(19)-Cl	2.699
O(1)-C(25)	1.379(3)	H(27)-Cl	2.885

Table 2.8. Selected bond angles of **2-05**.

	Bond Angle [°]		Bond Angle [°]
Cl-Ti-C(18)	97.42(7)	C(23)-O(1)-C(25)	116.3(2)
Ti-C(18)-C(19)	118.5(2)	O(1)-C(25)-C(24)	121.5(2)
Ti-C(18)-C(23)	126.2(2)	O(1)-C(25)-C(29)	118.7(2)
C(18)-C(19)-C(20)	122.4(2)	C(21)-C(22)-O(2)	117.1(2)
C(19)-C(20)-C(21)	120.7(2)	C(23)-C(22)-O(2)	122.2(2)
C(20)-C(21)-C(22)	118.4(2)	C(22)-O(2)-C(24)	115.7(2)
C(21)-C(22)-C(23)	120.7(2)	O(2)-C(24)-C(25)	121.3(2)
C(22)-C(23)-C(18)	122.6(2)	O(2)-C(24)-C(26)	118.3(2)
C(23)-C(18)-C(19)	115.2(2)	C(24)-C(26)-C(27)	119.6(3)
C(18)-C(23)-O(1)	117.1(2)	C(26)-C(27)-C(28)	119.6(3)
C(22)-C(23)-O(1)	120.4(2)		

The arrangement of the ligands is like discussed in complex **2-02**. Because only one bulky ring ligand is present a decrease of the angle between the two non-Cp ligands (97.42°) compared to **2-02** (104.96°) with two bulky ligands was observed. The dihedral angle, Cl-Ti-C(18)-C(19) of $-6.6(2)^\circ$ reveals that the chloro ligand is approximately in the plane of the ring ligand. Furthermore, the chloro ligand and oxygen of the ring ligand are on opposite sides of the Ti-C bond. The dihedral angle of C(25)-O(1)-C(23)-C(22) is $12.2(4)^\circ$, which shows that the dibenzodioxin ring is not planar. The titanium atom is also in the plane of the dioxin ligand

As a result of the orientation of the ring, the hydrogen on C(19) is forced close to the chloro ligand. In fact, the H(19)...Cl non bonding intramolecular distance is only 2.699\AA , which is very short. Comparing the bond lengths of the **L2-03**³³ to those of **2-05**, we can see that they differ very little and that coordination to titanium has very small effect on the bond lengths. Thus the large downfield chemical shift of H2 observed in the NMR spectra is ascribed to the hydrogen bonding. There is also an interatomic hydrogen bond interaction between a Cl of one molecule and the H(27) of the other molecule, which measured 2.885\AA .

The Ti-C(18) bond distance of 2.208\AA is slightly shorter than the observed Ti-C(1A) and Ti(C13A) bond distances of **2-02** which are 2.210\AA and 2.218\AA , respectively. This value is comparable with

33. P. Singh, J. D. McKinney, *Acta Cryst.*, **1978**, B34, 2956.

similar complexes in literature as discussed for **2-06** and again suggests that some multiple bonding interactions exists between the titanium and the dibenzodioxin carbon atom.

2.4 Conclusions

The aim was to synthesize a series of titanocene complexes where the heteroaromatic ligand is linked directly to the metal fragment. This was done by lithiation of the heteroaromatic ligand, followed by addition of titanocene dichloride and [TiCp₂(Dbf)Cl] **2-01**, [TiCp₂(Dbf)₂] **2-02**, [TiCp₂(Dbf-Me)Cl] **2-03**, [TiCp₂(Dbf-Me)₂] **2-04**, [TiCp₂(Dbz)Cl] **2-05**, [TiCp₂(Bf)Cl] **2-07**, [TiCp₂(Dbt)Cl] **2-08** and [TiCp₂(Thr)Cl] **2-09** were isolated. Due to instability, **2-09** decomposed to yellow [(μ -O){TiCp₂(Thr)}₂] **2-10** and [TiCp₂(Dbz)₂]**2-06a** decomposed to [(μ -O){TiCp₂(Dbz)}₂] **2-06**. Most complexes were fully characterized using mass spectrometry and NMR spectroscopy, but **2-07** and **2-09** were only characterized by ¹H NMR spectroscopy. The structures of complexes **2-02** and **2-05** were confirmed by X-ray crystallography. To investigate the effect of a heteroaromatic ligand bonding bidentately to the metal center, [TiCp₂(Dpe)] **2-11** was synthesized and characterized.

Complexes **2-05** and **2-08** were compared with titanocene dichloride **S-01** for antitumor activity *in vitro* and complexes **2-01**, **2-03**, **2-05**, **2-08** and **2-11** were compared with **S-01** and **3-05** in cell inhibition tests for antitumor activity. It was clear that serious handling problems would eliminate **2-07** and **2-09** as possible candidates for further testing in biological systems. The antitumor properties of these complexes will be investigated in Chapter 5.

Chapter 3

Titanocene derivatives with heteroaromatic thiolate ligands

3.1 Introduction

Metallo-intercalators, such as the complexes in Chapter 2, are designed to either intercalate or bond covalently, but not both and their antitumor activities are ascribed to a particular type of interaction with DNA. This was not the objective of the present study as the combined effects of intercalation and covalent bonding were to be investigated. The insertion of a spacer atom between the titanium fragment and the ring ligand will change the geometry of the molecule and allow the heteroaromatic ligand to be more flexible. Thus, both covalent bonding and intercalation are a possibility. This can readily be achieved by introducing a sulfur atom between the heteroaromatic rings and metal. Titanocene derivatives with the general formula $[\text{TiCp}_2(\text{SR})\text{Cl}]$ were synthesized ($\text{R} = \text{Dbt}, \text{Bt}, \text{Dbz}, \text{Thr}, \text{Dbf}$ and Bf) and are shown in Figure 3.1.

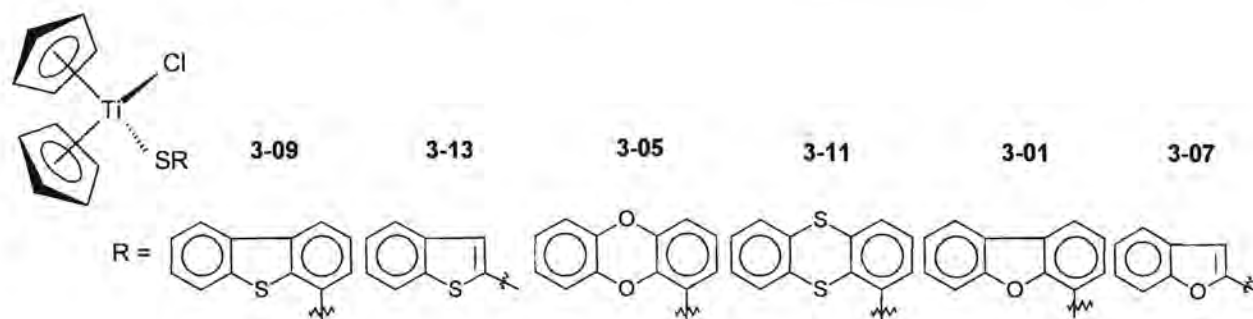
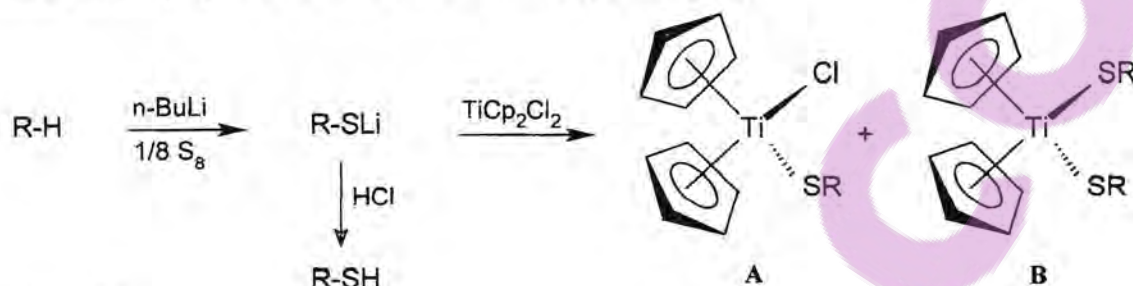


Figure 3.1 Titanocene thiolate complexes, $[\text{TiCp}_2(\text{SR})\text{Cl}]$.

The same heteroaromatic ligands used in Chapter 2 were investigated and their structure-antitumor activity relationships will be compared with that of the corresponding complexes where the ligand was bound directly to the metal.

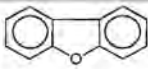
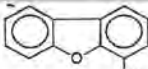
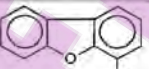
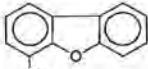
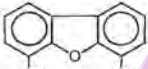
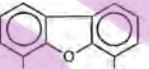
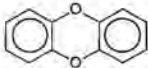
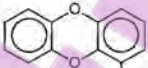
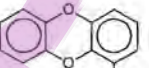
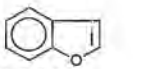
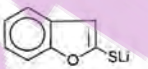
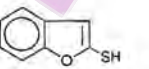
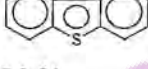
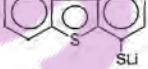
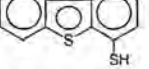
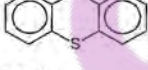
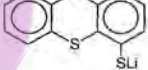
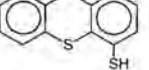
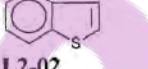
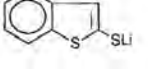
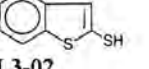
3.2 Synthesis

The synthesis of the complexes is given in Scheme 3.1 and the identification numbers of the compounds are listed in Table 3.1. Flowers of sulfur was added to the lithiated heteroaromatic ligand before reaction with titanocene dichloride. Lithiation and subsequent addition of sulfur afforded thiolates in high yields for all of the heteroarenes, **L2-01-L2-07**.



Scheme 3.1

Table 3.1 Identification numbers of the complexes in Scheme 3.1.

Heteroarene (R-H)	Thiolates(R-SLi)	Thiol(R-SH)	Product A	Product B
 L2-06		 L3-06	3-01	3-02
 L2-07		 L3-07	3-03	3-04
 L2-03		 L3-03	3-05	3-06
 L2-05		 L3-05	3-07	3-08
 L2-01		 L3-01	3-09	3-10
 L2-04		 L3-04	3-11	3-12
 L2-02		 L3-02	3-13	3-14

Reaction of L2-06 with butyllithium/sulfur and titanocene dichloride

Addition of sulfur to lithiated L2-06 at low temperature caused a colour change from yellow to orange due to the formation of lithiated dibenzofuran-4-thiolate. Protonation of the thiolate, by bubbling HCl gas through the solution, formed dibenzofuran-4-thiol, [HSDbf] L3-06. Addition of titanocene dichloride to the thiolate resulted in a colour change of the reaction mixture from red to purple. Chromatography yielded chlorobis(cyclopentadienyl)(dibenzofuran-4-ylsulfanyl)titanium(IV), [TiCp₂(SDBf)Cl] 3-01 and bis(cyclopentadienyl)bis(dibenzofuran-4-ylsulfanyl)titanium(IV), [TiCp₂(SDBf)₂] 3-02.

Reaction of L2-07 with butyllithium/sulfur and titanocene dichloride

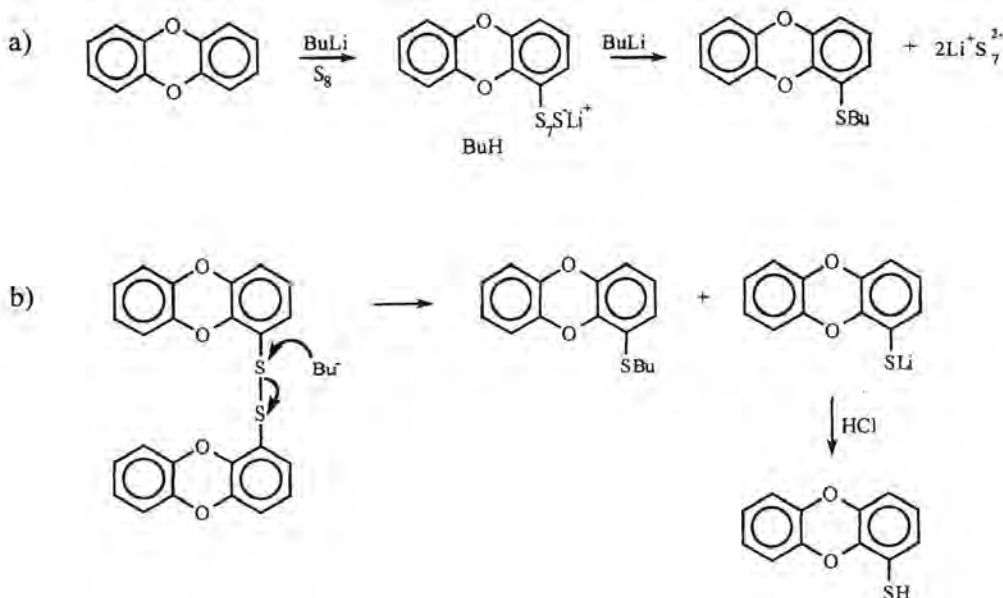
The ligand L2-07 was deprotonated at the 6-position. On addition of sulfur the reaction colour turned from yellow to orange and protonation of the lithiated 6-methyl dibenzofuran-4-thiolate formed 6-methyl dibenzofuran-4-thiol, [HSDbf-Me] L3-07. Addition of titanocene dichloride to the thiolate changed the colour of the reaction mixture from red to dark red. Purification by column chromatography gave chlorobis(cyclopentadienyl)(6-methyl dibenzofuran-4-ylsulfanyl)titanium(IV), [TiCp₂(SDBf-Me)Cl] 3-03 and bis(cyclopentadienyl)bis(6-methyl dibenzofuran-4-ylsulfanyl)titanium(IV), [TiCp₂(SDBf-Me)₂] 3-04.

Reaction of L2-03 with butyllithium/sulfur and titanocene dichloride

Addition of sulfur to the lithiated L2-03 at low temperature caused a colour change from yellow to orange-brown due to the formation of lithiated dibenzodioxin-1-thiolate. Protonation yielded dibenzodioxin-1-thiol, [HSDbz] L3-03. The formation of 1-butylsulfanyl dibenzodioxin, [BuSDBz] L3-03b during the reaction is difficult to explain, but a possible explanation for the formation is shown in Scheme 3.2. Initial attack of lithiated L2-03 on S₈ is followed by an attack of a second molecule BuLi resulting in the release of a S₇²⁻ molecule in (a). A second, more likely explanation takes a different route and involves the prior formation of bis(dibenzodioxin)disulfide. Interestingly, the disulfide is a fragment ion in the mass spectrometer of the complexes, [TiCp₂(SR)₂] (*vide infra*), and may have resulted from an elimination reaction of the two thiolate ligands. The disulfide is cleaved by BuLi resulting in the formation of the thioether and thiol according to (b).

The reaction of DbzSLi and titanocene dichloride was accompanied by a colour change from red to dark red-brown for the reaction mixture. On the silica gel column chlorobis(cyclopentadienyl)(dibenzodioxin-1-ylsulfanyl)titanium(IV), [TiCp₂(SDBz)Cl] 3-05 and bis(cyclopentadienyl)bis(dibenzodioxin-1-ylsulfanyl)titanium(IV), [TiCp₂(SDBz)₂] 3-06 were separated and collected. The

complexes were light sensitive and lost colour within a few hours after being exposed to normal daylight.



Scheme 3.2

Reaction of **L2-05** with butyllithium/sulfur and titanocene dichloride

Addition of sulfur to lithiated benzofuran gave a colour change from yellow to light pink to yellow and the lithiated benzofuran-2-thiolate was protonated to form benzofuran-2-thiol [HSBf] **L3-05**. Addition of titanocene dichloride to the thiolate resulted in an immediate colour change from red to purple. The solvent was removed and separation and purification by column chromatography gave bis(cyclopentadienyl)bis(benzofuran-2-ylsulfanyl)titanium(IV), $[\text{TiCp}_2(\text{SBf})_2]$ **3-08** and (benzofuran-2-ylsulfanyl)chlorobis(cyclopentadienyl)titanium(IV), $[\text{TiCp}_2(\text{SBf})\text{Cl}]$ **3-07**.

Reaction of **L2-01** with butyllithium/sulfur and titanocene dichloride

Addition of sulfur to DbtLi resulted in a colour change from green to yellow and protonation of lithiated dibenzothiophene-4-thiolate formed dibenzothiophene-4-thiol, [HSDbt] **L3-01**. The addition of titanocene dichloride to DbtSLi resulted in an immediate colour change from red to dark red. Purification by column chromatography gave bis(cyclopentadienyl) bis(cyclopentadienyl)bis(dibenzothien-4-ylsulfanyl)titanium(IV), $[\text{TiCp}_2(\text{SDbt})_2]$ **3-10** and chlorobis(cyclopentadienyl) (dibenzothien-4-ylsulfanyl)titanium(IV), $[\text{TiCp}_2(\text{SDbt})\text{Cl}]$ **3-09**. Complex **3-09** was crystallized from a dichloromethane-hexane solution and this yielded crystals suitable for a single crystal structure determination.

Reaction of L2-04 with butyllithium/sulfur and titanocene dichloride

The reaction of ThrLi with flowers of sulfur yielded thianthrene-1-thiolate, that was converted to thianthrene-1-thiol [HSThr] L3-04, when protonated with HCl gas. No information of this product could be found in literature and it was fully characterized. Unlike L2-03, the compound L2-04 did not react with butyllithium to give the corresponding thioether. The reaction of ThrLi with flowers of sulfur caused a colour change from yellow to orange-brown. The reaction of the thiolate and titanocene dichloride was accompanied by a colour change from red to dark red for the reaction mixture. The complexes chlorobis(cyclopentadienyl)(thianthren-1-ylsulfanyl)titanium(IV), [TiCp₂(SThr)Cl] 3-11 and bis(cyclopentadienyl)bis(thianthrenyl-1-ylsulfanyl)titanium(IV), [TiCp₂(SThr)₂] 3-12 were separated and collected by column chromatography. 3-12 is a light sensitive complex, which lost colour within a few hours after being exposed to light. 3-11 was very unstable and the ¹H NMR spectrum showed that it decomposed to L2-04 and the oxygen bridged dimer (μ-oxo)bis(chlorobis(cyclopentadienyl)titanium(IV))¹.

Reaction of L2-02 with butyllithium/sulfur and titanocene dichloride

Addition of sulfur to BtLi gave a colour change from yellow to orange and protonation of the lithiated benzothiophene-2-thiolate BtSLi yielded benzothiophene-2-thiol, [HSBt] L3-02. Addition of titanocene dichloride to the thiolate resulted in an immediate colour change from red to dark red. Column chromatography on silica gel afforded bis(cyclopentadienyl)bis(benzothien-2-ylsulfanyl)titanium(IV), [TiCp₂(SBt)₂] 3-14 and (benzothien-2-ylsulfanyl)chlorobis(cyclopentadienyl)titanium(IV), [TiCp₂(SBt)Cl] 3-13.

3.3 Characterization

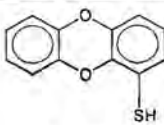
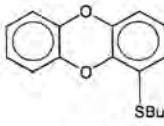
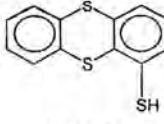
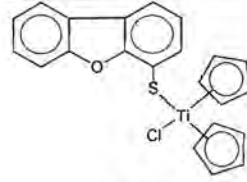
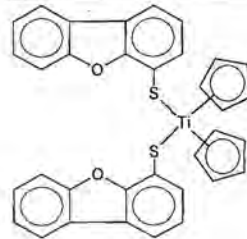
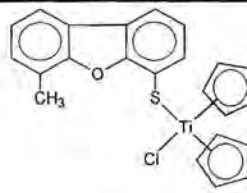
- *Mass spectrometry*

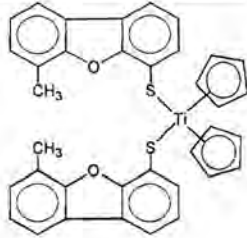
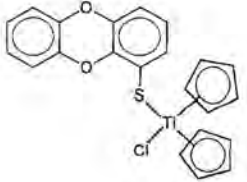
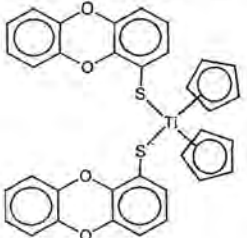
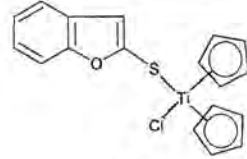
The mass spectral data for L3-01² was reported in literature. The data for the ligands L3-03, L3-04, L3-03b and the complexes 3-01 – 3-10 as well as for 3-12 – 3-14 are summarized in Table 3.2. Due to the instability of 3-11 a representative mass spectrum could not be obtained for the complex.

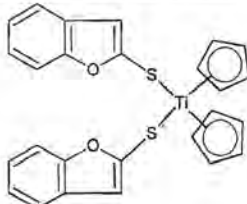
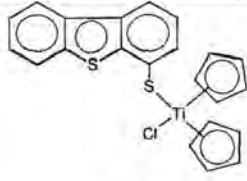
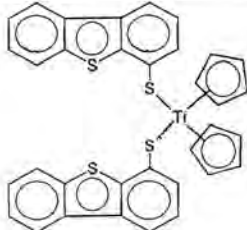
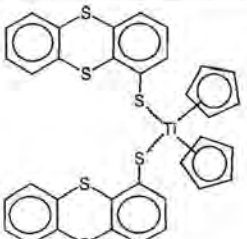
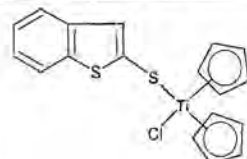
1. D. Nath, R. K. Sharma, A. N. Bhat, *Inorg. Chim. Acta*, **1976**, *20*, 109; S. A. Giddings, *Inorg. Chem.*, **1964**, *3*, 684.

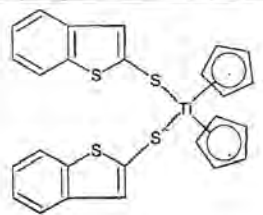
2. T. Kuster, H. Mändli, R. Robbani, J. Seibl, *Helv. Chem. Acta*, **1978**, *61*, 1017.

Table 3.2 Mass spectral data for complexes **L3-03**, **L3-03b**, **L3-04**, **3-01** – **3-10** and **3-12** – **3-14**.

Mass Peaks, m/z(I, %)		
 <p>L3-03</p>	216 (100) [M] ⁺ 184 (26) [DbzH] ⁺	183 (20) [Dbz] ⁺
 <p>L3-03b</p>	272 (2) [M] ⁺ 216 (5) [M-Bu] ⁺ 184 (5) [DbzH] ⁺	183 (5) [Dbz] ⁺ 57 (5) [Bu] ⁺
 <p>L3-04</p>	248 (100) [M] ⁺ 217 (13) [ThrH ₂] ⁺ 216 (11) [ThrH] ⁺ 184 (53) [ThrH-S] ⁺	171 (38) [Thr-CSH] ⁺ 152 (1) [Thr-2S] ⁺
 <p>3-01</p>	No [M] ⁺ 378 (3) [M-Cl] ⁺ 347 (2) [M-Cp] ⁺ 328 (1) [TiCp(SDbf)O] ⁺ 312 (1) [TiCp(SDbf)] ⁺ 282 (1) [Ti(SDbf)Cl] ⁺ 263 (1) [Ti(SDbf)O] ⁺ 247 (1) [Ti(SDbf)] ⁺	214 (4) [M-SDbf] ⁺ 200 (2) [HSDbf] ⁺ 199 (2) [SDbf] ⁺ 178 (72) [TiCp ₂] ⁺ 148 (9) [TiCpCl] ⁺ 113 (18) [TiCp] ⁺
 <p>3-02</p>	577 (100) [M] ⁺ 511 (38) [M-Cp] ⁺ 446 (10) [Ti(Dbff) ₂] ⁺ 398 (32) [Dbf S- SDbf] ⁺ 378 (95) [M-SDbf] ⁺ 312 (20) [TiCp(SDbf)] ⁺	280 (13) [TiCp(Dbff)] ⁺ 200 (100) [HSDbf] ⁺ 199 (100) [SDbf] ⁺ 178 (100) [TiCp ₂] ⁺ 113 (15) [TiCp] ⁺
 <p>3-03</p>	539 (1) [TiCp ₂ (SDbf-Me) ₂] ⁺ (3-04) 426 (5) [M] ⁺ or [Me-DbfS-SDbf-Me] ⁺ 391 (1) [TiCp ₂ (SDbf-Me)] ⁺ 361 (4) [TiCp(SDbf)Cl] ⁺ 326 (2) [TiCp(SDbf-Me)] ⁺ 296 (2) [Ti(SDbf-Me)Cl] ⁺ 261 (4) [Ti(SDbf-Me)] ⁺	214 (100) [TiCp ₂ Cl] ⁺ or [SDbf-Me] ⁺ 200 (52) [HSDbf] ⁺ 199 (52) [SDbf] ⁺ 181 (96) [Dbf-Me] ⁺ 178 (9) [TiCp ₂] ⁺ 148 (20) [TiCpCl] ⁺ 113 (12) [TiCp] ⁺

 <p>3-04</p>	<p>539 (1) [M]⁺ 426 (14) [Me-DbfS- SDbf-Me]⁺ 326 (4) [TiCp(SDbf-Me)]⁺ 277 (7) [Ti(SDbf-Me)O]⁺ 261 (2) [Ti(SDbf-Me)]⁺ 245 (9) [Ti(Db f -Me)O]⁺</p>	<p>214 (52) [HSDbf-Me]⁺ 213 (52) [SDbf-Me]⁺ 181 (100) [Dbf -Me]⁺ 178 (5) [TiCp₂]⁺ 113 (14) [TiCp]⁺</p>
 <p>3-05</p>	<p>428 (60) [M]⁺ 396 (11) [TiCp₂(Dbz)Cl]⁺ 393 (4) [M-Cl]⁺ 361 (4) [TiCp₂(Dbz)]⁺ 360 (6) [M-Cp]⁺ 328 (8) [TiCp(SDbz)]⁺ 298 (1) [Ti(SDbz)Cl]⁺</p>	<p>296 (1) [TiCp(Dbz)]⁺ 263 (1) [Ti(SDbz)]⁺ 231 (1) [Ti(Dbz)]⁺ 216 (13) [HSDbz]⁺ 215 (13) [SDbz]⁺ 184 (5) [DbzH]⁺ 183 (4) [Dbz]⁺ 178 (100) [TiCp₂]⁺</p>
 <p>3-06</p>	<p>610 (66) [M]⁺ 545 (1) [M-Cp]⁺ 426 (5) [DbzS-SDbz]⁺ 425 (5) [TiCp₂(SDbz)S]⁺ 393 (12) [M-SDbz]⁺ 360 (73) [TiCp(SDbz)S]⁺ 328 (27) [TiCp(SDbz)]⁺</p>	<p>295 (5) [Ti(SDbz)S]⁺ 263 (10) [Ti(SDbz)]⁺ 214 (100) [HSDbz]⁺ 213 (100) [SDbz]⁺ 184 (37) [DbzH]⁺ 183 (37) [Dbz]⁺ 178 (36) [TiCp₂]⁺</p>
 <p>3-07</p>	<p>477 (36) [TiCp₂(SBf)₂]⁺ (3-08) 411 (61) [TiCp(SBf)₂]⁺ 363 (4) [M]⁺ 360 (8) [TiCp₂(SBf)S]⁺ 328 (7) [M-Cl]⁺ 297 (56) [M-Cp]⁺ 265 (33) [TiCp(Bf)Cl]⁺ 262 (5) [TiCp(SBf)]⁺</p>	<p>236 (30) [TiCp₂(Bf)]⁺ 232 (6) [Ti(SBf)Cl]⁺ 210 (25) [TiSCp₂]⁺ 197 (12) [Ti(SBf)]⁺ 178 (27) [TiCp₂]⁺ 150 (94) [HSBf]⁺ 149 (94) [SBf]⁺ 113 (12) [TiCp]⁺</p>

 <p>3-08</p>	<p>477 (55) [M]⁺ 445 (4) [TiCp₂(SBf)(Bf)]⁺ 413 (13) [TiCp₂(Bf)₂]⁺ 411 (52) [M-Cp]⁺ 379 (5) [TiCp(SBf)(Bf)]⁺ 360 (8) [TiCp₂(SBf)S]⁺ 347 (6) [TiCp(Bf)₂]⁺ 346 (8) [Ti(SBf)₂]⁺ 328 (65) [M-SBf]⁺ 314 (4) [TiCp(SBf)(Bf)]⁺</p>	<p>300 (13) [BfS-SBf]⁺ 296 (20) [TiCp₂(Bf)]⁺ 262 (10) [TiCp(SBf)]⁺ 210 (11) [TiSCp₂]⁺ 197 (7) [Ti(SBf)]⁺ 178 (100) [TiCp₂]⁺ 150 (36) [HSBf]⁺ 149 (94) [SBf]⁺ 113 (19) [TiCp]⁺</p>
 <p>3-09</p>	<p>430 (36) [DbtS-SDbt]⁺ 428 (30) [M]⁺ 393 (36) [M-Cl]⁺ 363 (49) [M-Cp]⁺ 328 (17) [TiCp(SDbt)]⁺</p>	<p>263 (1) [Ti(SDbt)]⁺ 213 (100) [M-SDbt]⁺ 178 (10) [TiCp₂]⁺ 152 (7) [C₁₂H₈]⁺</p>
 <p>3-10</p>	<p>608 (48) [M]⁺ 543 (2) [M-Cp]⁺ 430 (9) [DbtS-SDbt]⁺ 393 (100) [M-SDbt]⁺ 366 (3) [Dbt-Dbt]⁺ 328 (20) [TiCp(SDbt)]⁺ 295 (2) [Ti(SDbt)S]⁺</p>	<p>263 (2) [Ti(SDbt)]⁺ 215 (13) [HSDbt]⁺ 214 (13) [SDbt]⁺ 178 (11) [TiCp₂]⁺ 152 (7) [C₁₂H₈]⁺ 113 (1) [TiCp]⁺</p>
 <p>3-12</p>	<p>674 (6) [M]⁺ 609 (66) [M-Cp]⁺ 544 (47) [Ti(SThr)₂]⁺ 496 (23) [ThrS-SThr] 457 (6) [TiCp₂(SThr)S]⁺ 425 (4) [M-Cl]⁺ 392 (100) [TiCp(SThr)S]⁺ 360 (5) [Ti(SThr)S]⁺</p>	<p>327 (6) [Ti(SThr)S]⁺ 295 (6) [Ti(SThr)]⁺ 263 (9) [Ti(Thr)]⁺ 248 (2) [HSThr]⁺ 247 (2) [SThr]⁺ 216 (22) [ThrH]⁺ 216 (22) [Thr]⁺ 178 (81) [TiCp₂]⁺ 113 (4) [TiCp]⁺</p>
 <p>3-13</p>	<p>378 (5) [M]⁺ 343 (52) [M-Cl]⁺ 213 (22) [M-SBt]⁺</p>	<p>166 (24) [HSBt]⁺ 165 (24) [SBt]⁺</p>

 <p style="text-align: center;">3-14</p>	508 (10) [M] ⁺	178 (100) [TiCp ₂] ⁺
	378 (5) [Ti(SBt) ₂] ⁺	166 (22) [HSBt] ⁺
	343 (52) [M-SBt] ⁺	165 (24) [SBt] ⁺
	330 (2) [BtS-SBt] ⁺	

The mass spectra of **L3-03** and **L3-04** show the molecular ion and fragments that correspond to the elimination of the thiol sulfur. In the spectrum of **L3-03b** additional fragment ions are observed due to a butyl group.

Although three different fragmentation routes look possible from the observed fragment ions of complex **3-01** the high intensity of the [TiCp₂]⁺ fragment is noteworthy. This indicates that either DbfS or the Cl ligand fragments first. The intensities of [TiCp₂(SDBf)]⁺ and [TiCp₂Cl]⁺ are almost the same which makes suggestions of a preferred fragmentation route risky. The fragment ions of highest intensities for **3-02** are again [TiCp₂]⁺ and [TiCp₂(SDBf)]⁺ which indicates that the fragmentation of the thiolato ligands dominates again and also explains the formation of (DbfS-SDBf)⁺ in the mass spectrometer. Noteworthy for complexes **3-03** and **3-07** are the formation of the bithiolato complexes **3-04** and **3-08**, respectively, which implies that the fragment ion [TiCp₂(SDBf)]⁺ or [TiCp₂(SBf)]⁺ exists for a long enough period of time to attached to a free thiolate from the environment in the mass spectrometer. This result represents the initial fragmentation of a chloro ligand. Unlike **3-04** and **3-06**, the complexes **3-02**, **3-08** and **3-14** again showed [TiCp₂]⁺ to be the principle fragment ion indicating initial fragmentation of the thiolate ligands. By contrast, the former compounds revealed irregular patterns of fragmentation representative of routes whereby any of the four ligands are fragmented. The intensities of the fragment ions however are very low. Many complexes display the fragment ion M⁺-Cp, sometimes of reasonably high intensity for bis-thiolato complexes which is not easy to explain in the light of very strong bonding between Cp-ligands and transition metals. Complex **3-10** gives a principle peak corresponding to the fragment ion [TiCp₂(SDBt)]⁺ which represents the initial fragmentation of a thiolate ligand. Thereafter fragmentation is again irregular. Generally it was found that the monothiolato or chloro containing complexes are very unstable under the conditions employed to measure the mass spectra. This is evident from the absence of molecular ion peaks in some instances and the many fragment ions observed in the spectra of which many are formed in the mass spectrometer. Some of the assignments for fragment ions may be incorrect, for example, in complex **3-05** the fragment ion of second highest m/z-value represents a loss of 32 units which could

be either the elimination of a sulfur of the thiolato ligand or the elimination of a molecule oxygen from the dibenzodioxim rings.

- *¹H NMR and ¹³C NMR spectroscopy*

The ¹H NMR chemical shifts and peak assignments for **L3-01**³, **L3-02**⁴ and **L3-05**⁴ agree with those reported in literature and a summary of the shift values (ppm) for **L3-03**, **L3-03b** and **L3-04** is given in Table 3.3. The ¹H NMR and ¹³C NMR spectral data for complexes **3-01** – **3-10** and **3-12** – **3-14** is summarized in Table 3.4. Due to instability of **3-11** in solution no useful spectrum was obtained and for **L3-01** and **L3-05** no useful ¹³C NMR spectral data could be recorded.

¹H NMR spectroscopy

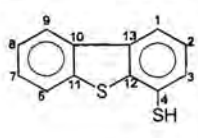
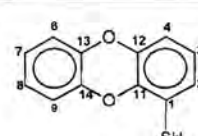
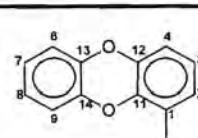
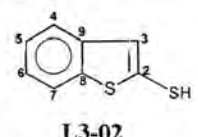
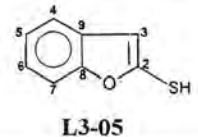
When comparing the chemical shifts of **L3-03**, with **L2-03** (Chapter 2), it is clear that the addition of the sulfur atom did not, with the exception of H2, influence the chemical shifts much. The same was observed for **L3-04** compared to **L2-04**. The chemical shifts of the protons of the ring without the thiol group are roughly the same as the corresponding resonances for the protons of **L2-06** or **L2-01**, but due to their overlapping signals the specific chemical shifts could not be assigned for H6-H9. The ring with the thiolate sulfur as substituent has a downfield shift of 0.34ppm (**L3-03**) and 0.24ppm (**L3-04**) for H2 compared to **L2-03** and **L2-04**, respectively, whereas the resonances of H3 and H4 are little affected. The proton closest to the substituent is shifted downfield because of the electron withdrawing effect of the sulfur atom. In the spectrum of **L3-03b** the presence of the butyl group is seen in resonances at ppm-values of 2.90, 1.44, and 0.89. The triplet at 2.9ppm is indicative of protons on a carbon attached to a sulfur atom and adjacent to a methylene carbon. This observation supports **L3-03b** being a thioether rather than a butyl substituent on the thiophenol ring of the dioxin molecule.

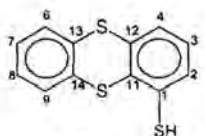
Sulfur atoms in **L2-04** tend to affect the chemical shifts of its adjacent protons in such a way that they are shifted further downfield compared to the same protons of an oxygen molecule such as **L2-03**. In the case of the thiolato complexes the proton closest to the substituent is downfield because of the electron withdrawing effect of the sulfur atom. Coordination of the thiolate to titanium results in a more shielded proton on C2, which indicates that the phenyl ring is shielded and not really affected by the coordination of the sulfur atom. The upfield shift of this proton can only be ascribed to π -resonance effects of the sulfur lone pair to the substituted phenyl ring. This will compete with π -

3. L. V. Dunkerton, B. C. Barot, A. Nigam, *J. Heterocycl. Chem.*, **1987**, *24*, 749.

4. P. C. Montevacchi, M. L. Navacchia, *J. Org. Chem.*, **1995**, *60*, 6455.

Table 3.3 ^1H and ^{13}C NMR spectroscopic data^a for L3-01 – L3-04.

Ligand	C	Chemical Shift (δ ppm)	H	Chemical Shift (δ ppm)	Splitting & Integration	Coupling Constant (J Hz)	
 <p>L3-01</p>	Not recorded	-	1/9 2/7/8 3/6 SH	8.04-8.14 7.36-7.48 7.75-7.83 2.14	m m m s	2H 3H 2H 1H	- - - -
 <p>L3-03</p>	1 2 3 4 6/9 7/8 11 12/13/14	141.7 124.7 123.5 116.6 115.9/116.2 124.1/124.3 167.7 141.7/141.8 /142.4	2 3 4 6/7/8/9 SH	7.19 6.83 6.73 6.76-6.91 -	dd t dd m	1H 1H 1H 4H	7.9/1.6 8.1/7.9 8.1/1.6 -
 <p>L3-03b</p>	1 2 3 4 6/9 7/8 11 12/13/14 SBu	141.5 124.4 123.3 116.8 114.3/114.3 123.8/124.1 150.1 141.5-143.0 13.6/22.0/ 31.1/32.4	2 3 4 6/7/8/9 SBu	7.13 6.83 6.68 6.76-6.91 2.90 1.44 0.89	dd t dd m t m m	1H 1H 1H 4H 2H 4H 3H	7.1/1.9 7.7/7.1 7.7/1.9 - 5.6 - -
 <p>L3-02</p>	2 3 4 5 6 7 8 9	142.8 130.9 122.7 125.4 123.9 122.1 141.6 139.9	3 4/7 5/6 SH	7.29 7.64/7.69 7.31/7.27 3.67	s m m s	1H 2H 2H 1H	- - -
 <p>L3-05</p>	Not recorded	-	3 4/5/6/7 SH	6.80 7.17-7.50 3.70	s m s	1H 4H 1H	- - -

 <p>L3-04</p>	1	136.9	2	7.48	dd	1H	7.8/1.4
	2	129.2	3	7.13	t	1H	7.7/7.8
	3	128.7	4	7.33	dd	1H	7.7/1.4
	4	123.5	6/9	7.18-7.29	m	2H	-
	6/9	126.2/127.7	7/8	7.43-7.57	m	2H	-
	7/8	127.8/128.2	SH	-			
	11	176.0					
	12/13/14	134.2/135.7					
		/136.2					

^a Recorded in CDCl₃

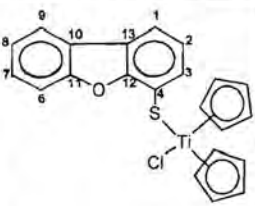
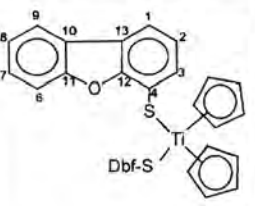
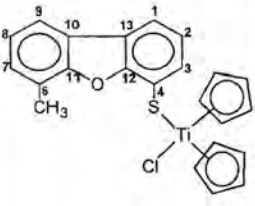
donation from the sulfur to the titanium. Notable is a significant downfield shift for H2 of 0.89ppm for **3-06** compared to **3-05**. A similar trend but smaller effect was observed for H3 of **3-10** and **3-09**. The chemical shifts of H3 and H4 are about the same for **L3-03**, **3-05** (shifted a little more upfield) and **3-06**.

In the cases where there is a methyl substituent on the ring we have all the protons influenced. In the case of **3-03** and **3-04** there is also a big upfield shift for H2 and H5, while H3 is shifted upfield compared to **L2-07**. An explanation can be that the methyl substituents have interaction with other parts of the molecule. The rest of the protons are also downfield but only moderately. The methyl protons in both cases are very much upfield.

The singlet observed in **3-07** and **3-08** shows that the titanium fragment is bound to the sulfur in the 2-position of **L3-05**. Since the H3 protons are the closest protons to the coordination site, it is expected that these protons be influenced most and in the case of **3-07** and **3-08** it is -0.4 and -0.03ppm, respectively. In the case of **3-07** and **3-08**, the protons in the substituted ring were shifted upfield and the H3 resonances were further downfield than expected. The H4 protons were most influenced, which is the opposite of the trend discussed Chapter 2.

In **3-09** and **3-10** the protons of the unsubstituted ring of the heteroaromatic ligand were shifted upfield by -0.01 on average. These shifts for the rest of the complexes were normally around -0.10. The greatest shifts were recorded for the ring coordinated to titanium. In **3-05**, **3-06** and **3-12** the unsubstituted ring's protons are assigned as a multiplet and the general tendency of the chemical shifts are slightly downfield.

Table 3.4 ¹H and ¹³C NMR spectroscopic data^a for 3-01 – 3-10 and 3-12 – 3-14.

Complex	C	Chemical Shift ^b (δ ppm)	H	Chemical Shift (δ ppm)	Splitting & Integration	Coupling Constant (J Hz)	
 <p>3-01</p>	1	115.3	1	7.48	Dd	1H	7.8/1.3
	2	120.4	2	7.35	t	1H	7.7/7.8
	3	139.0	3	7.83	dd	1H	7.7/1.3
	4	no	6	7.97	ddd	1H	7.8/7.5/0.8
	6	112.1	7	7.35	t	1H	7.5/7.8
	7	125.8	8	7.45	td	1H	8.3/7.5/0.8
	8	122.5	9	7.65	dd	1H	8.3
	9	119.8	Cp	6.31	s	10H	
	10/13	122.3					
	11	156.5					
	12	161.5					
	Cp	112.0/113.0					
 <p>3-02</p>	1	118.3	1	7.97	dd	2H	7.6/1.1
	2	123.3	2	7.34	t	2H	7.6
	3	132.1	3	7.80	dd	2H	7.6/1.1
	4	154.0	6	7.96	dd	2H	7.8/1.3
	6	112.1	7	7.27	t	2H	7.4/7.8
	7	127.0	8	7.44	td	2H	8.2/7.4/1.3
	8	122.8	9	7.64	dt	2H	8.2/0.8
	9	120.8	Cp	6.47	s	10H	
	10	123.6					
	11/12	no					
	13	123.0					
	Cp	113.1					
 <p>3-03</p>	1	118.2	1	7.73	dd	1H	7.1/1.1
	2	122.3	2	7.35	t	1H	7.1/6.7
	3	137.0	3	7.92	dd	1H	6.7/1.1
	4	147.2	7	7.34	m	1H	-
	6	116.0	8	7.45	td	1H	7.0/7.7
	7	127.0	9	7.54	dd	1H	7.7/1.0
	8	123.0	Me	1.53	s	3H	
	9	120.7	Cp	6.46	s	10H	
	10/13	123.8					
	11/12	no					
	Me	29.7					
	Cp	117.2					

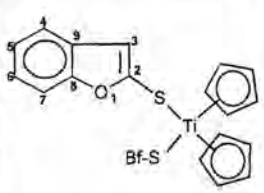
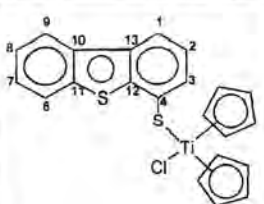
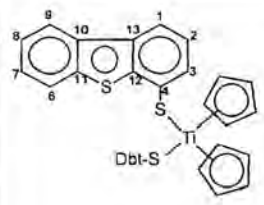
3. Titanocene derivatives with heteroaromatic thiolate ligands

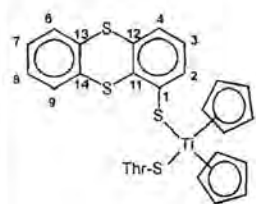
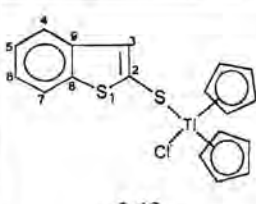
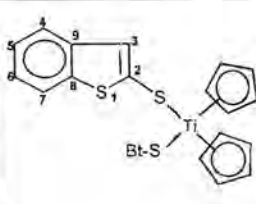
65

<p style="text-align: center;">3-04</p>	<p>1 118.1</p> <p>2 123.0</p> <p>3 132.2</p> <p>4 145.0</p> <p>6 112.1</p> <p>7 128.1</p> <p>8 122.7</p> <p>9 118.3</p> <p>10 123.0</p> <p>11/12 no</p> <p>13 120.8</p> <p>Me 15.6</p> <p>Cp 113.0</p>	<p>1 7.77 dd 2H 7.5/1.0</p> <p>2 7.31 t 2H 7.5/7.8</p> <p>3 7.92 dd 2H 7.8/1.0</p> <p>7 7.33 m 2H -</p> <p>8 7.45 td 2H 7.5/7.2</p> <p>9 7.97 dd 2H 7.2/0.8</p> <p>Me 1.54 s 6H</p> <p>Cp 6.12 s 5H</p> <p>6.13 s 5H</p>
<p style="text-align: center;">3-05</p>	<p>1 136.1</p> <p>2 124.3</p> <p>3 111.0</p> <p>4 108.0</p> <p>6 116.3</p> <p>7 123.2</p> <p>8 123.8</p> <p>9 116.7</p> <p>11 158.0</p> <p>12/13/14 139.8/143.0</p> <p>Cp 112.0/113.0</p>	<p>2 6.42 dd 1H 8.3/1.3</p> <p>3 6.76 t 1H 8.3</p> <p>4 6.57 dd 1H 8.3/1.3</p> <p>6/7/8/9 6.83-6.96 m 4H -</p> <p>Cp 6.05 s 5H</p> <p>6.33 s 5H</p>
<p style="text-align: center;">3-06</p>	<p>1 138.7</p> <p>2 129.5</p> <p>3 123.0</p> <p>4 116.9</p> <p>6/9 114.4/116.1</p> <p>7/8 123.6/123.7</p> <p>11 150.2</p> <p>12/13/14 142.2/142.2/142.5</p> <p>Cp 112.8</p>	<p>2 7.31 dd 1H 7.9/1.6</p> <p>3 6.84 t 1H 8.0/7.9</p> <p>4 6.69 dd 1H 8.0/1.6</p> <p>6/7/8/9 6.71-6.94 m 4H -</p> <p>Cp 6.11 s 10H</p>
<p style="text-align: center;">3-07</p>	<p>2 137.0</p> <p>3 110.6</p> <p>4 120.5</p> <p>5 123.0</p> <p>6 123.8</p> <p>7 111.0</p> <p>8 no</p> <p>9 131.0</p> <p>Cp 114.1</p>	<p>3 6.77 s 1H</p> <p>4 7.46 dd 1H 7.2/0.8</p> <p>5 7.20 t 1H 7.2</p> <p>6 7.19 td 1H 5.2/0.8</p> <p>7 7.43 dd 1H 5.2/1.3</p> <p>Cp 6.21 s 10H</p>

3. Titanocene derivatives with heteroaromatic thiolate ligands

66

 <p>3-08</p>	2	no	3	6.78	s	1H	
	3	110.8	4	7.43	dd	1H	6.3/1.0
	4	119.9	5	7.18	t	1H	6.2/6.3
	5	122.8	6	7.15	td	1H	7.5/1.0
	6	123.4	7	7.33	d	1H	7.5
	7	110.6	Cp	6.14	s	5H	
	8	156.0		6.21	s	5H	
	9	129.9					
	Cp	114.6					
	 <p>3-09</p>	1	119.5	1	8.00	dd	1H
2		124.9	2	7.46	t	1H	8.3
3		131.2	3	7.53	dd	1H	7.2/1.3
4		143.1	6	7.85	m	1H	-
6		122.7	7	7.45	m	1H	-
7		126.6	8	7.45	m	1H	-
8		124.4	9	8.14	m	1H	-
9		121.9	Cp	6.27	s	10H	
10		136.4					
11		139.8					
12		142.0					
13		134.7					
Cp		115.9					
 <p>3-10</p>		1	118.9	1	7.99	dd	2H
	2	125.0	2	7.48	t	2H	7.6
	3	130.7	3	7.96	dd	2H	6.4/1.0
	4	142.5	6	7.86	m	2H	-
	6	122.8	7	7.45	m	2H	-
	7	126.5	8	7.45	m	2H	-
	8	124.3	9	8.16	m	2H	-
	9	122.0	Cp	6.09	s	10H	
	10	136.6					
	11	139.7					
	12	142.3					
	13	134.5					
	Cp	112.8					

 <p>3-12</p>	1	148.0/148.0	2	7.72	dd	1H	7.8/1.4
	2	132.5/133.2	3	7.13	dd	1H	7.6/7.8
	3	128.7	4	7.27	dd	1H	7.6/1.4
	4	128.3	6/9	7.18-7.24	m	2H	-
	6/9	126.9/126.4	7/8	7.43-7.50	m	2H	-
	7/8	127.5/127.7	Cp	6.31	s	10H	
	11	no					
	12/13/14	135.7/135.9/137.4					
	Cp	112.8/113.4					
 <p>3-13</p>	2	149.6	3	7.16	s	1H	
	3	127.7	4	7.69	d	1H	7.5
	4	122.8	5	7.32	td	1H	7.5/1.2
	5	124.2	6	7.24	td	1H	7.5/1.2
	6	123.7	7	7.74	d	1H	8.8
	7	121.5	Cp	6.35	s	10H	
	8	141.9					
	9	140.4					
	Cp	116.3					
 <p>3-14</p>	2	149.9	3	7.34	s	2H	
	3	126.8	4	7.66	dd	2H	7.4/0.8
	4	122.5	5	7.39	td	2H	7.5/1.1
	5	124.1	6	7.22	td	2H	7.5/1.3
	6	123.5	7	7.72	d	2H	7.9
	7	121.5	Cp	6.19	s	10H	
	8	141.6					
	9	140.6					
	Cp	113.6					

^a Recorded in CDCl₃ ^b no = not observed

The two Cp rings resonate as a singlet due to similar chemical environments for the protons on the rings. The resonances are shifted upfield in all instances compared to titanocene dichloride, which has a chemical shift value of 6.57ppm for its Cp ligands. This can be ascribed to the replacement of the chloro ligand in titanocene dichloride and a resulting increase in the electron density on the metal fragment. In most cases the shift is around -0.10 to -0.50ppm. It is interesting to note that there is a tendency for the Cp to split up in two singlets in the bis-thiolato complexes. The replacement of both chloro ligands caused even more electron density to reside on the metal fragment and the chemical shift of the Cp rings was even further upfield.

Two-dimensional homonuclear shift correlation spectroscopy (COSY) was used to aid in the unambiguous assignment of the different protons in **3-01** - **3-03**, **L3-03** and **L3-04**. In spite of this, it was still difficult to assign protons in the multiplets of **L3-03** and **L3-04**.

¹³C NMR spectroscopy

In **L3-03**, **L3-03b** and **L3-04** the chemical shift of C1 is observed downfield due to the electron withdrawing effect of the thiol/thioether substituent. The other carbons are little affected and have about the same chemical shifts compared to the corresponding carbons in the unsubstituted heteroaromatic compounds. The carbons C2 and C3 are downfield and this correlates with the results from the ¹H NMR spectrum.

The resonances of the *ipso* carbons of C1(C4) (*ca* 140ppm) of the thiolato complexes are shifted downfield but not as far as was observed for the complexes where this carbon was directly bonded to the titanium centre (*ca* 180 ppm). The values fall between those of the uncoordinated thiols and the titanium-C(heteroarene) complexes. This observation is supported by the ¹H NMR data. The neighbouring carbons, C2 (C3) and C12 (C11), also display resonances that represent downfield shifts, but much less than C1. Resonances of carbons, C11 and C12, are further downfield because of the effects of the neighbouring oxygen atoms. The rest of the chemical shifts are quite similar to those of the uncoordinated heteroaromatic molecules. The Cp signal is upfield (about 3 - 8 ppm) due to increased electron density on the metal fragment, when compared to titanocene dichloride. In **3-12** the Cp signals appear as two single peaks in a ratio of 3:1. This ratio is repeated for the rest of the spectrum and can be ascribed to two different isomers in solution.

The HETCOR spectra of **L3-03** and **3-04** were used to assign and correlate the specific proton resonances to the corresponding carbons resonances. Again it was impossible to assign the protons in the unsubstituted ring of **L3-03**.

• *X-ray crystallography*

Structure of complex 3-09

The final confirmation of **3-09** was obtained from a single crystal X-ray diffraction study. The complex was recrystallised from a 1:1 dichloromethane:hexane solution by using the layering technique. It gave dark red crystals suitable for data collection on the diffractometer. In Figure 3.2 the structure of the molecule is given as a ball and stick representation, which also indicates the atom-labelling scheme that was used. The most important bond lengths and angles are listed in Table 3.5 and Table 3.6 respectively. Other structural information is given in Chapter 6 and in Appendix C.

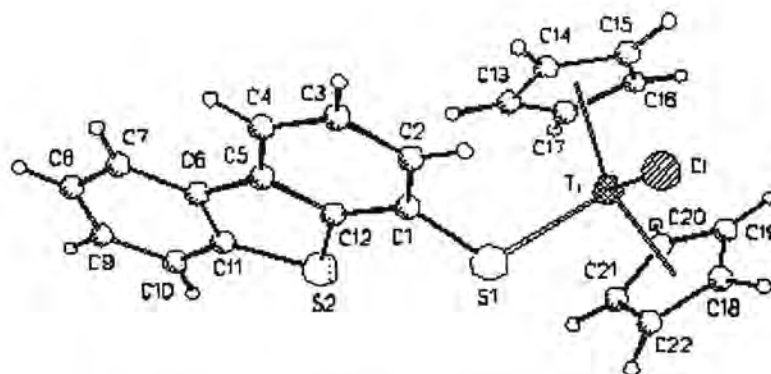


Figure 3.2. Ball and stick picture of the structure of **3-09**.

Table 3.5. Selected bond lengths of **3-09**.

	Bond length [Å]		Bond length [Å]
Ti-Cl	2.3948(7)	C(5)-C(12)	1.408(3)
Ti-S(1)	2.4068(7)	C(5)-C(6)	1.460(3)
S(1)-C(1)	1.782(2)	C(6)-C(7)	1.408(3)
S(2)-C(12)	1.757(2)	C(6)-C(11)	1.411(3)
S(2)-C(11)	1.762(2)	C(7)-C(8)	1.379(4)
C(1)-C(2)	1.394(3)	C(8)-C(9)	1.400(4)
C(1)-C(12)	1.400(3)	C(9)-C(10)	1.388(4)
C(2)-C(3)	1.404(4)	C(10)-C(11)	1.396(4)
C(3)-C(4)	1.389(4)	C(21)-C(22)	1.415(4)
C(4)-C(5)	1.403(3)		

Table 3.6. Selected bond angles of **3-09**.

	Bond angle [°]		Bond angle [°]
Cl-Ti-S(1)	96.13(3)	C(7)-C(6)-C(11)	118.2(2)
Cl-Ti-C(18)	77.39(7)	C(7)-C(6)-C(5)	129.7(2)
C(1)-S(1)-Ti	114.89(8)	C(11)-C(6)-C(5)	112.0(2)
C(12)-S(2)-C(11)	91.06(12)	C(8)-C(7)-C(6)	120.0(2)
C(2)-C(1)-C(12)	117.6(2)	C(7)-C(8)-C(9)	120.8(3)
C(2)-C(1)-S(1)	124.4(2)	C(10)-C(9)-C(8)	120.7(3)
C(12)-C(1)-S(1)	117.8(2)	C(9)-C(10)-C(11)	118.3(3)
C(1)-C(2)-C(3)	120.7(2)	C(10)-C(11)-C(6)	122.0(2)
C(4)-C(3)-C(2)	120.9(2)	C(10)-C(11)-S(2)	125.7(2)
C(3)-C(4)-C(5)	119.7(2)	C(6)-C(11)-S(2)	112.4(2)
C(4)-C(5)-C(12)	118.3(2)	C(1)-C(12)-C(5)	122.7(2)
C(4)-C(5)-C(6)	130.0(2)	C(1)-C(12)-S(2)	124.5(2)
C(12)-C(5)-C(6)	111.7(2)	C(5)-C(12)-S(2)	112.8(2)

The arrangement of the ligands is similar to complexes **2-02**, **2-05** (Chapter 2) and **2-08**⁵ displays a pseudo tetrahedral environment of ligands around titanium. The insertion of a sulfur atom between the bulky ring ligand and the metal center causes almost no change of the angle between the two non-Cp ligands Cl-Ti-S(1) of **3-09** (96.1°) compared to the Cl-Ti-Cl angle in titanocene dichloride⁶ which is 94.6°. This angle was significantly larger in **2-02** (105.0°), **2-05** (97.4°) and **2-08** (96.7°) with the bulky ligands directly bound to the metal. The dihedral angle, Cl-Ti-S(1)-C(1) of 73.16(9)° reveals that the chloro ligand is not in the plane of the rings. The dihedral angle of C(11)-S(2)-C(12)-C(1) is -179.2(2)°, which shows that the dibenzothiophene ring is planar.

If we compare the bond lengths of dibenzothiophene⁷ to those of **3-09**, we can see that they differ very little and that coordination to titanium has very little effect on the bond lengths. The average C-S bond distance 1.74(8)Å in the free ligand is similar to the bond distances for S(2)-C(11) 1.757(2)Å and S(2)-C(12) 1.76(2)Å in **3-09**. The C-S-C bond angle in the free ligand is 91.5(4)° is also similar to the

5. R. Meyer, *Titanium, Molybdenum and Platinum Complexes with Potential Antitumor Properties*, Ph. D. (Chemistry) Thesis, University of Pretoria, 1998, 73.

6. A. Clearfield, D. K. Warner, C. H. Salderiaga-Molina, R. Ropal, J. Bernal, *Can. J. Chem.*, 1975, 53, 1622.

7. R. M. Schaffrin, J. Trotter, *J. Chem. Soc. (A)*, 1970, 651.

C(12)-S(2)-C(11) angle of $91.1(1)^\circ$ in **3-09**. The structure reveals that the chloro and dibenzothiophene ligands does not share the same plane, unlike that found for **2-05**. In **3-09** the ring is more flexible to rotate and chances of covalent bond formation at the chloro site as well as intercalation by the dibenzothiophene ring ligand is greatly enhanced for this improved ligand orientations.

3.4 Conclusions

The aim was to synthesize a series of titanocene complexes where the heteroaromatic ligand is linked via a sulfur atom to the metal fragment. This was done by lithiation of the heteroaromatic ligand (compare Chapter 2), followed by the addition of a stoichiometric amount of sulfur to obtain the corresponding thiolates. The thiolates were then added to titanocene dichloride at low temperatures to give mono- and bis-thiolato complexes of titanium. The desired mono-thiolate complexes [TiCp₂(SDBf)Cl] **3-01**, [TiCp₂(SDBf-Me)Cl] **3-03**, [TiCp₂(SDBz)Cl] **3-05**, [TiCp₂(SBf)Cl] **3-07**, [TiCp₂(SDBt)Cl] **3-09**, [TiCp₂(SThr)Cl] **3-11** and [TiCp₂(SBt)Cl] **3-13** were isolated in high yields. In addition, the untargetted bis-thiolato complexes were obtained as by-products of the reaction and are [TiCp₂(SDBf)₂] **3-02**, [TiCp₂(SDBf-Me)₂] **3-04**, [TiCp₂(SDBz)₂] **3-06**, [TiCp₂(SBf)₂] **3-08**, [TiCp₂(SDBt)₂] **3-10**, [TiCp₂(SThr)₂] **3-12**, [TiCp₂(SBt)₂] **3-14**. The structure of complex **3-09** was confirmed by X-ray crystallography. The introduction of a linking sulfur atom greatly affects the electronic properties and geometric features of the complexes compared to the previously described titanium complexes with a direct bond between the metal and a carbon atom of the heteroaromatic ring ligand.

Thiolato complexes were selected for preclinical testing based on their stability, solubility and most importantly their structural features. Complexes **3-05**, **3-09** and **3-10** were selected for initial testing and complexes **3-01**, **3-02**, **3-03**, **3-05**, **3-06**, **3-07**, **3-09** and **3-13** were tested against antitumor activity in a later test series. Serious handling problems eliminated **3-11** and **3-12** as possible candidates for further testing in biological systems. Based on the assumptions of this study, the geometry of complexes **3-02**, **3-04**, **3-06**, **3-08**, **3-10** and **3-14** were not desirable for intercalation and covalent bonding. In hindsight, the lability of the thiolate ligands were much higher than generally expected and could in some instances be comparable with the very labile chloro ligands. This observation makes the requirement of a chloro ligand in the molecular design of these compounds for fast displacement and covalent bonding to DNA less important and also has consequences for intercalation. The antitumor properties of the selected complexes will be further investigated in Chapter 5.

Chapter 4

Bi- and trinuclear complexes of titanium(IV) and platinum(II)

4.1 Introduction

Recently some of the interest in the *cisplatin* area of research shifted towards complexes containing more than one Pt(II) center for various reasons, but also because they tend to display activity against some *cisplatin* resistant tumors¹. Figure 4.1 illustrates two examples of bifunctional binuclear platinum complexes with linear coordinating spermidine and spermine. Both these complexes exhibit high antitumor activity against *cisplatin* sensitive as well as *cisplatin* resistant cell lines. It is believed that complexes with more than one Pt(II) coordination center may take part in different intra- and interstrand interactions on each strand of the DNA double helix.

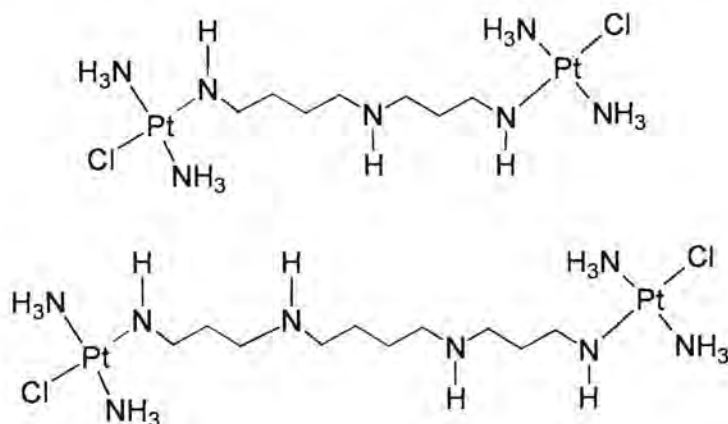


Figure 4.1 Bifunctional binuclear platinum complexes exhibiting antitumor activity.

Another approach is to combine non-platinum antitumor complexes into the framework of the *cisplatin* molecule to produce heteronuclear bimetallic complexes. Since NN donor ligands have been used in complexation with many transition metals, it is reasonably easy to synthesize such complexes.

1. H. Rauter, R. Di Domenico, E. Menta, A. Olivia, Y. Qu, N. Farrell, *Inorg. Chem.*, **1997**, *36*, 3919.

The example in Figure 4.2 combines ferrocenyl groups with *cis*-platin and the resulting complex was identified as a possible anticancer agent².

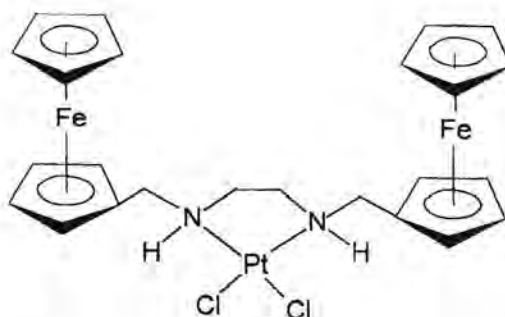


Figure 4.2 Platinum complex tested as a positive anticancer agent.

Figure 4.3 show examples of ferrocenyl and platinum fragments combined in one molecule and one or two platinum fragments were incorporated, producing bi- or trinuclear ferrocenyl complexes³.

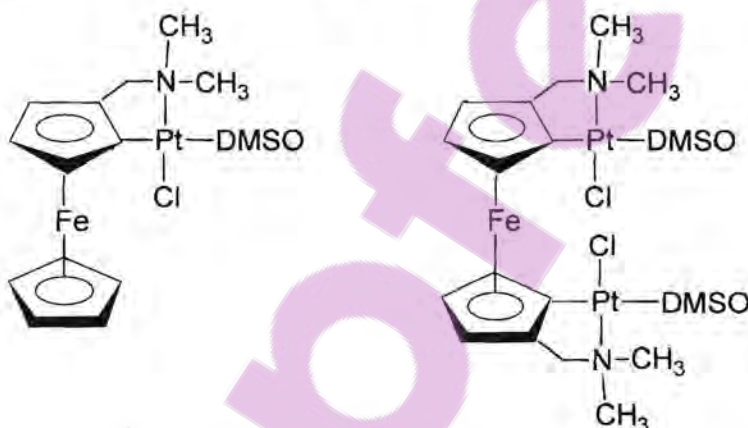


Figure 4.3 Platinum complexes tested as positive anticancer agents.

The antitumor active titanocene complexes are mainly mononuclear. Although binuclear titanocene complexes are mentioned in literature, they have mostly application as catalysts. So far no titanocene binuclear complexes were identified as antitumor agents. The product of the reaction in Figure 4.4 has attractive structural features that make it worthwhile to investigate the antitumor properties. This complex was mentioned in literature as the product of a ligand exchange process in a photochemical

2. E. N. Neuse, M. G. Meirim, N. F. Bolm, *Organometallics*, **1988**, *7*, 2562.

3. P. Ramani, R. Ranatunge-Bandarage, N. W. Duffy, S. M. Johnston, B. H. Robinson, J. Simpson, *Organometallics*, **1994**, *13*, 511.

reaction⁴. However, the yield for this reaction was very low and it was decided to use a different route for synthesizing the complex.

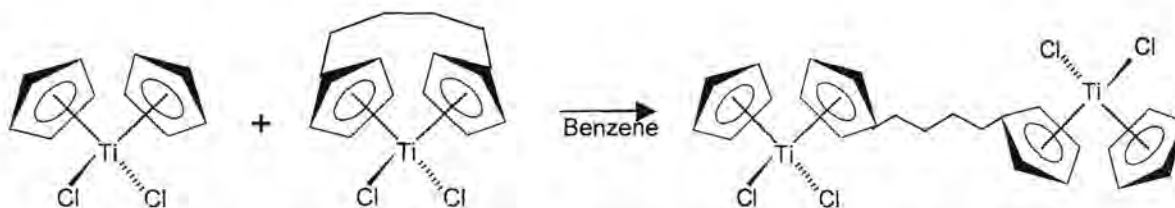


Figure 4.4 Photochemical reaction affording a binuclear titanocene complex.

In the context of this study it was decided to try and combine the best of the *cisplatin* and titanocene dichloride to synthesize new binuclear complexes with antitumor properties. The above examples demonstrated that a carefully chosen chain of atoms could act as a bridge between two metal centres.

In this chapter the focus is on combining ligand donor functions with linking atoms which will ultimately act as a bridge to incorporate titanocene and platinum in one molecule, as seen in Figure 4.5. On one end of the common ligand donor atoms are needed that could coordinate effectively to platinum such as amines and on the other end of the ligand a moiety that could be attached to titanium. For the latter, a heteroatom (class 1) or a cyclopentadiene that is readily convertible into a cyclopentadienyl ligand (class 2) was chosen. For the first class the reaction would mean the substitution of a chloro ligand in titanocene dichloride by a heteroatom whereas for the second class the substrate will be reacted with TiCpCl_3 to give a titanocene derivative.

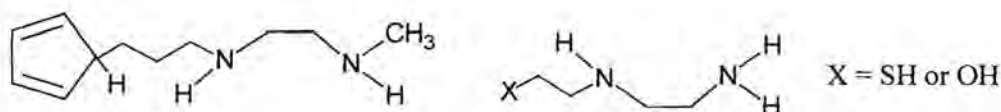


Figure 4.5 Typical substrates designed to be used as bridging ligands for binuclear complexes.

In this chapter the synthesis of two main types of Pt(II) complexes will be investigated. The first structure (Figure 4.6) represents a binuclear heterometallic complex with an early (Ti) and late (Pt) transition metal. In the first approach only one chloro ligand remain on the titanium and is available for further manipulation. In another method the two metals are bridged by an ethylene diamine on one end of the chain to coordinate to platinum and a cyclopentadienyl ring on the other end to coordinate to titanium. In the latter case two chloro ligands are available for manipulation or covalent bonding.

4. E. Vitz, C. H. Brubaker, *J. Organomet. Chem.*, 1976, 104, C33.

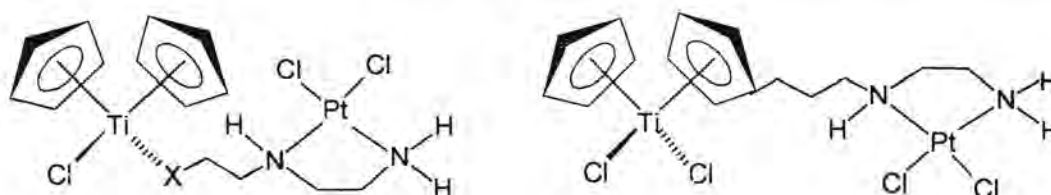


Figure 4.6 Binuclear heterometallic complexes of Ti(IV) and Pt(II).

The structures in Figure 4.7 represent binuclear complexes with two titanium metal moieties linked by donor atoms on the two ends of a chain of methylene fragments. The bridge can run between a cyclopentadienyl ligand of each fragment or directly between the metal centers by replacing a chloro ligand in each titanocene fragment by another donor atom.

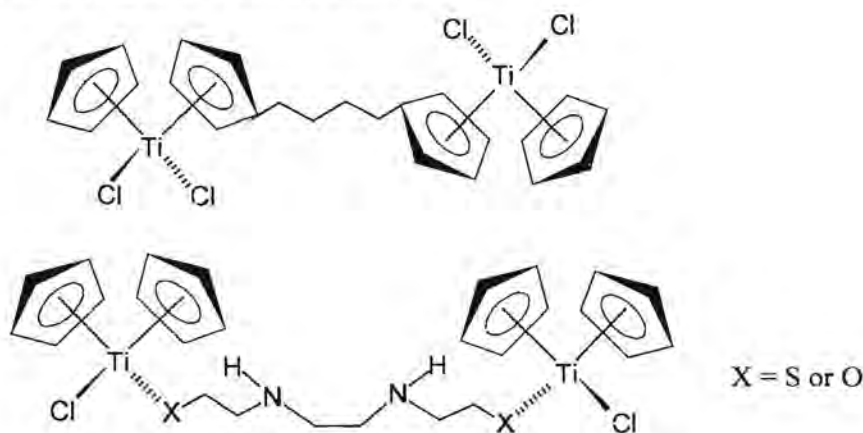
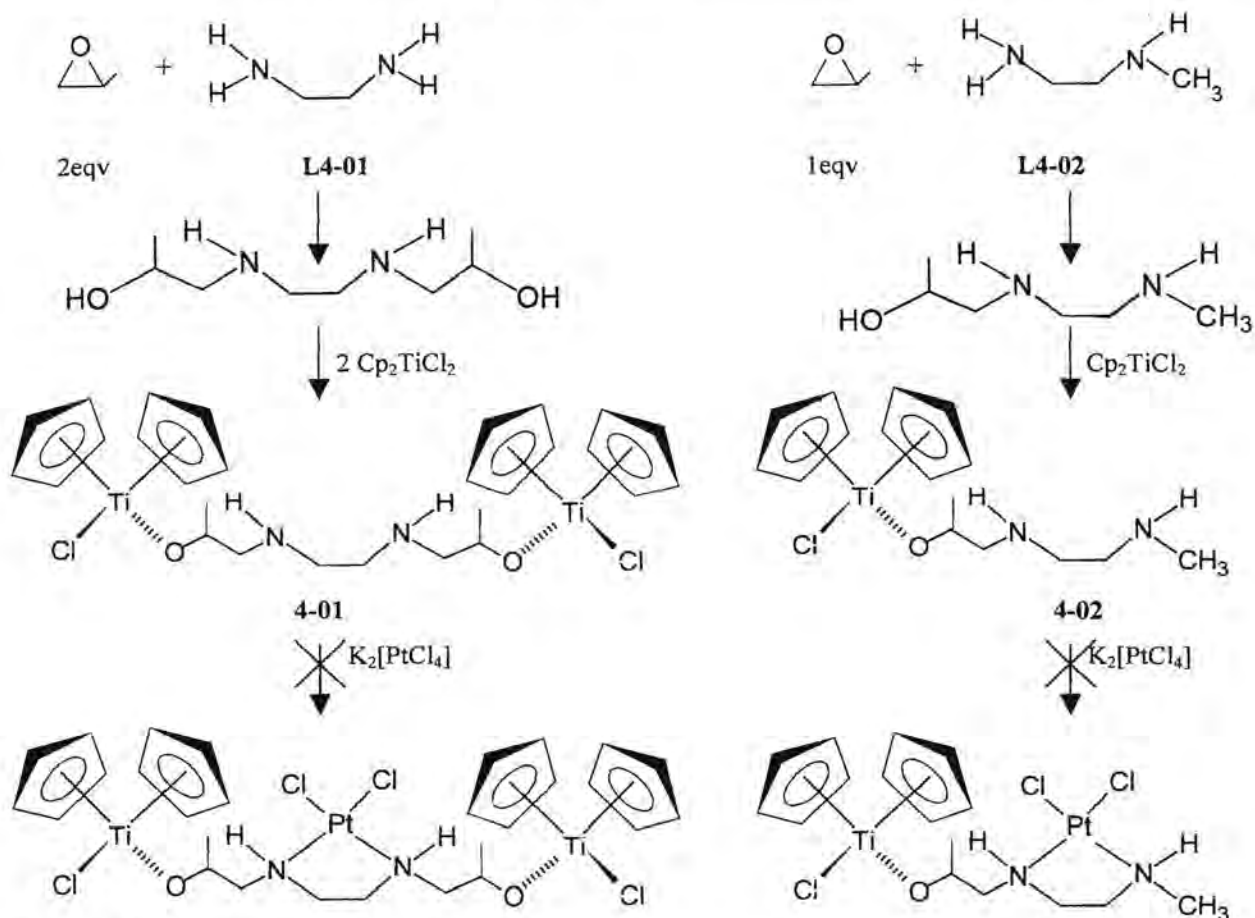


Figure 4.7 Binuclear homometallic complexes of Ti(IV).

4.2 Synthesis

Schemes 4.1 and 4.2 represent the planned syntheses of complexes where a heteroatom is used to replace a chloro ligand in the coordination sphere of titanium. Titanium has a strong affinity for sulfur and oxygen ligands and the introduction of thiolate and oxolate donor atoms were considered. The bridging ligands were to be constructed by either adding one or two equivalents of epoxide to ethylene diamine. When two equivalents of epoxide were added, two titanocene chloride fragments are found at the ends of the bridging ligand with the possibility to afterwards introduce a platinum fragment. For one equivalent epoxide the result would lead to a binuclear Ti-Pt complex. To enable the addition of only one equivalent of epoxide methyl ethylene diamine was chosen as starting substrate as the methyl group would effectively block one side of the molecule.

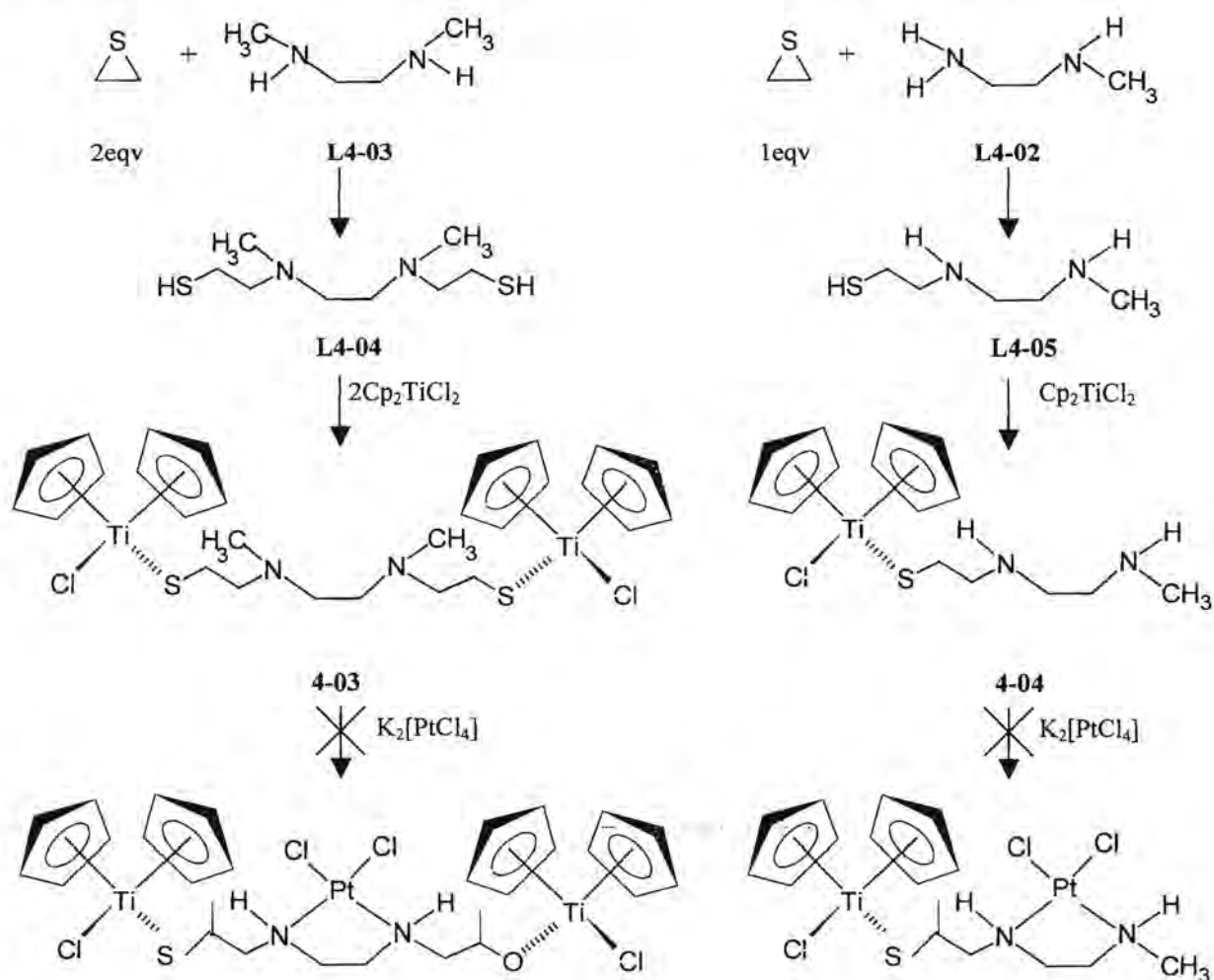


Scheme 4.1

In the first case of Scheme 4.1 methyl epoxide was added to ethylene diamine **L4-01** and to this colourless solution were added two equivalents of titanocene dichloride and the colour changed from red-orange to yellow. The product was extracted with hot toluene and precipitated with hexane to give a yellow product identified by mass spectrometry and ^1H NMR spectroscopy as $[\{\mu\text{-C}_8\text{H}_{18}\text{N}_2\text{O}_2\}\text{Ti}_2\text{Cp}_2\text{Cl}_2]$ **4-01**. Addition of **4-01** to $\text{K}_2[\text{PtCl}_4]$ in an aqueous acetonitrile solution afforded unreacted **4-01** as well as titanocene decomposition products. One of these being the oxygen bridged bis titanocene chloride dimer, $[(\mu\text{-O})\{\text{TiCp}_2\text{Cl}\}_2]$.

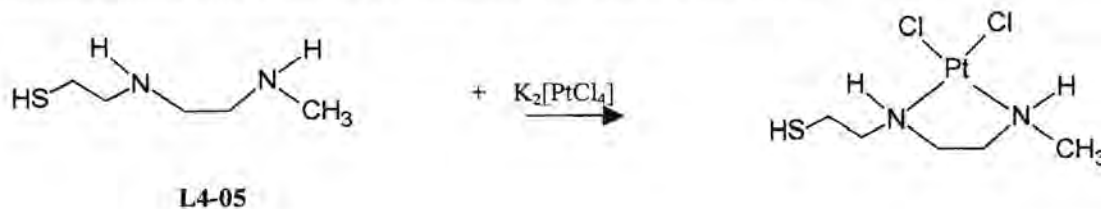
The same procedure was repeated with methyl epoxide and N-methyl ethylene diamine **L4-02** (Scheme 4.1) and adding titanocene dichloride changed the colour from red to orange. Extraction and precipitation gave a yellow product identified by mass spectrometry and ^1H NMR spectroscopy as $[\text{TiCp}_2(\text{OC}_6\text{H}_{15}\text{N}_2)\text{Cl}]$ **4-02**. Addition of **4-02** to $\text{K}_2[\text{PtCl}_4]$ in aqueous solution again did not lead to the desired product but afforded similar decomposition products.

The same basic procedure was followed for thiiran, as shown in Scheme 4.1 for epoxides, but in this case the bridge was built by adding two equivalents of thiiran to *N,N'*-dimethyl ethylene diamine **L4-03** and reacting at high temperature and pressure (Scheme 4.2). The product was purified by filtration and distillation to yield a colourless oil [$C_8H_{20}N_2S$] **L4-04**. The addition of this new ligand to two equivalents of titanocene caused a colour change from red to orange-red. The product was extracted with dichloromethane and addition of hexane precipitated [$\{\mu-C_8H_{18}N_2S_2\}Ti_2Cp_4Cl_2$] **4-03** as a red-orange product. The binuclear complex was characterized by 1H NMR spectroscopy. The addition of one equivalent of thiiran to **L4-02** and reaction at high pressure and temperature yielded an oily substance that was purified by filtration and distillation. The resulting colourless oil was identified as [$C_5H_{14}N_2S$] **L4-05**. Reaction of this substrate with titanocene dichloride changed the colour of the mixture from red to red-orange. Extraction with dichloromethane and precipitation with hexane yielded an orange product [$TiCp_2(SC_6H_{15}N_2)Cl$] **4-04**. Subsequent reactions of **4-03** and **4-04** with $K_2[PtCl_4]$ again did not afford the desired bi- and trinuclear complexes of platinum and titanium.



Scheme 4.2

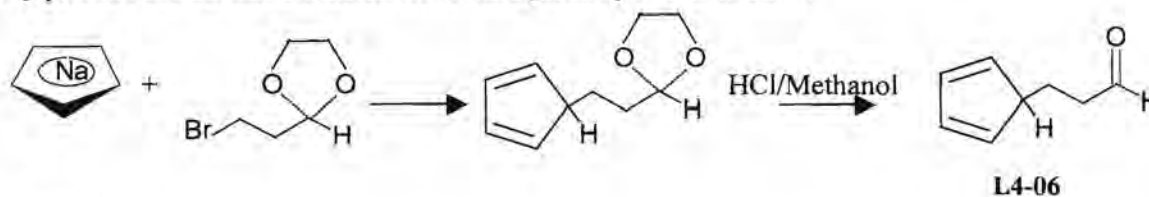
Scheme 4.3 represents an alternative approach where the order in which the metal fragments are introduced are being reversed. However, this was not a very good idea as a number of platinum complexes formed with different combinations of N and S donor atoms.



Scheme 4.3

A better method would undoubtedly be to start with a different platinum precursor. The most likely contender would be to use [Pt(COD)Cl₂] instead of [PtCl₄²⁻] as this compound has available a readily displaceable COD ligand. In the light of the instability of especially **4-01** and **4-03** in solution it was apparent that pursuing this line of research would defy the objectives of the study. Preparing useful compounds that displayed superior antitumor activities had to be supported by easy to handle, unambiguously characterizable compounds. The weakness of this approach was found in the relatively weak Ti-O/S bond in solution in bi- and trinuclear Pt-Ti complexes. To solve this problem it was decided to make use of a much stronger bonded ligand such as cyclopentadienyl.

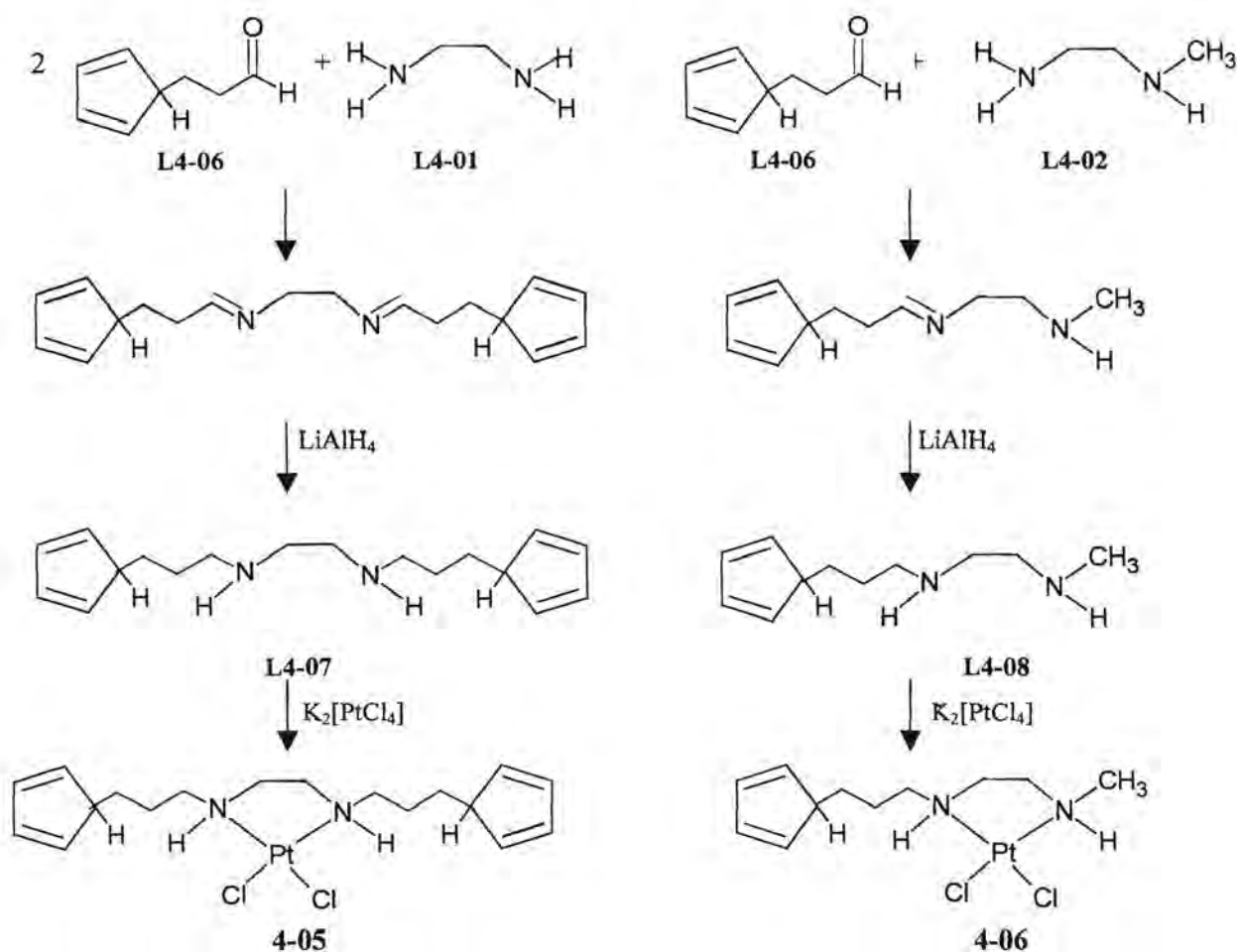
Scheme 4.4 shows the synthesis of 3-cyclopenta-2,4-dienyl propionaldehyde **L4-06**. 2-(2-Bromoethyl)-[1,3]dioxolan was added to NaCp (freshly prepared) and the colour of the mixture changed from purple to brown. The residue was treated with HCl to deprotect the acetal and a brown oily product **L4-06** was extracted from the aqueous phase with ether.



Scheme 4.4

Scheme 4.5 shows the synthesis of two ligands that were designed to bridge two heterobimetallic fragments. In the first example two equivalents of **L4-06** was refluxed overnight with **L4-01** in a Schiff Base reaction to give the unsaturated product. The product was subsequently reduced to give the desired bisdiene precursor. Purification by extraction and precipitation with a dichloromethane-hexane mixture yielded N,N'-bis-(3-cyclopenta-2,4-dienyl propyl) ethylene diamine **L4-07** as a yellow-brown oil. Addition of **L4-07** to K₂[PtCl₄] in an aqueous acetonitrile solution resulted in a

colour change of the reaction mixture from red to brown to yellow-brown. The product $[\text{Pt}(\mu\text{-N}_2\text{N}'\text{C}_{18}\text{H}_{28}\text{N}_2)\text{Cl}_2]$ **4-05** precipitated from the brown solution.

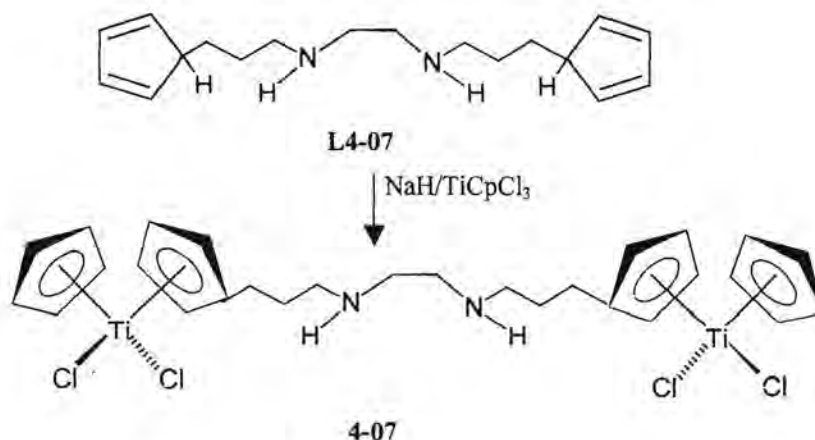


Scheme 4.5

Addition of one equivalent of **L4-06** to **L4-02** in refluxing benzene yielded a Schiff Base, which was subsequently reduced. Extraction with dichloromethane yielded *N*-(3-cyclopenta-2,4)dienyl propyl)-*N'*-methyl ethylene diamine **L4-08** as a yellow-brown oil. Treatment of **L4-08** with $\text{K}_2[\text{PtCl}_4]$ in an aqueous acetonitrile solution gave a brown product $[\text{Pt}(\mu\text{-N}_2\text{N}'\text{-C}_{11}\text{H}_{20}\text{N}_2)\text{Cl}_2]$ **4-06** after precipitation.

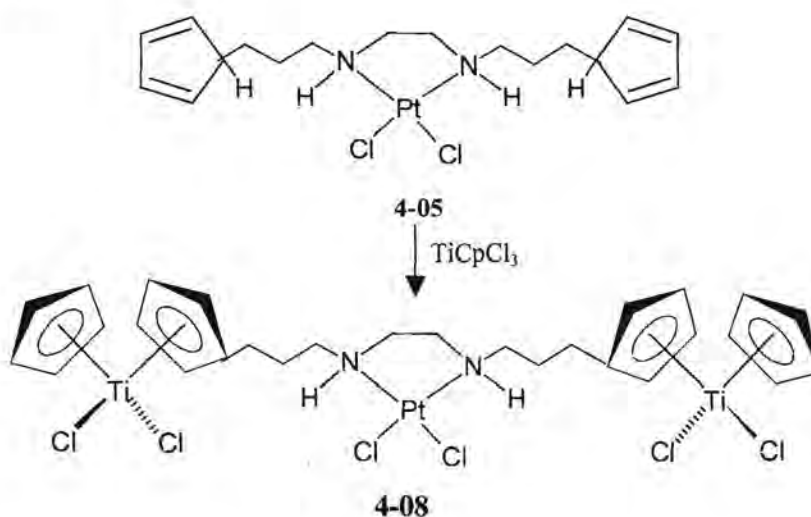
In Scheme 4.6 the cyclopentadiene rings on ligand **L4-07** was deprotonated with NaH and trichloro cyclopentadienyl titanium (IV) was added. The colour of the reaction mixture changed to dark brown and the product was extracted with toluene, concentrated and mixed with hexane causing unreacted $[\text{TiCpCl}_3]$ to precipitate. The yellow filtrate was evaporated and extracted into dichloromethane. Addition of hexane precipitated a black solid, which was insoluble and removed by filtration. The

filtrate was evaporated to give the desired product $[\{\mu\text{-}\eta^5,\eta^5\text{-C}_{18}\text{H}_{26}\text{N}_2\}\text{Ti}_2\text{Cp}_2\text{Cl}_4]$ **4-07**. This is an example of binuclear complexes displaying two titanocene fragments joined by a chain of methylene units and a central ethylene diamine moiety.



Scheme 4.6

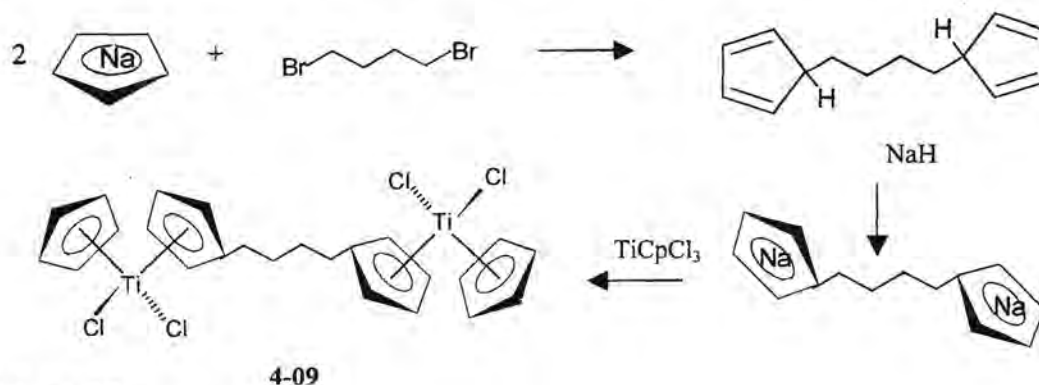
In Scheme 4.7 the synthesis of a mixed trinuclear complex is illustrated. The titanocene fragments are joined by a chain containing ethylene diamine which in turn is coordinated to a dichloro platinum fragment. The cyclopentadiene rings on product **4-05** were deprotonated (NaH) and two equivalents of trichloro cyclopentadienyl titanium (IV) were added in THF. The brown solution turned yellow and a cream-pink precipitate was isolated and identified as the trinuclear product $[\text{Ti}_2\{\mu\text{-}\eta^5,\eta^5\text{-}(\text{Pt}(\text{N},\text{N}'\text{-C}_{18}\text{H}_{26}\text{N}_2)\text{Cl}_2)\}\text{Cp}_2\text{Cl}_4]$ **4-08**.



Scheme 4.7

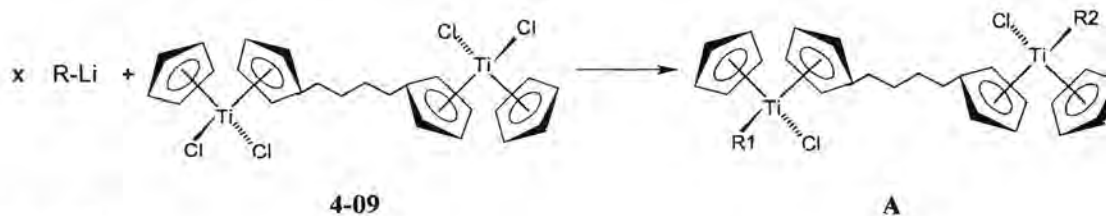
The method shown in Scheme 4.8 was used to synthesize a binuclear bistitanocene complex where the two metal fragments are coordinated to two cyclopentadienyl ligands connected by a butane chain.

Reacting NaCp and 1,4-dibromobutane accomplished this goal. After deprotonation the resulting brown solution was added to trichloro cyclopentadienyl titanium (IV) and evaporated to dryness. The residue gave a dark green product which was identified as $[\{\mu-\eta^5, \eta^5-C_{14}H_{16}\}Ti_2Cp_2Cl_4]$ **4-09**.



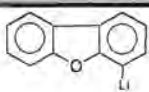
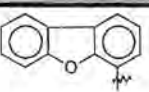
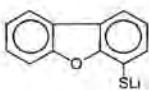
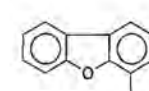
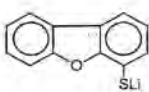
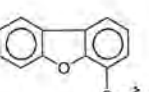
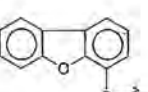
Scheme 4.8

Product **4-09** was treated with lithiated dibenzofuran precursors in ratios of 1:1 and 1:2 as shown in Scheme 4.9. The identification numbers of the isolated complexes are shown in Table 4.1



Scheme 4.9

Table 4.1

x	R-Li	R1	R2	Complex A
1			Cl	4-10
1			Cl	4-11
2				4-12

Addition of one equivalent of **4-09** to one equivalent [Dbf-Li] caused a colour change from dark green to green-yellow. Extraction with ether yielded a green product which was isolated and characterized to be $[\{\mu\text{-}\eta^5, \eta^5\text{-C}_{14}\text{H}_{16}\}\text{Ti}_2(\text{Dbf})\text{Cp}_2\text{Cl}_3]$ **4-10**. Similarly, the addition of one equivalent of **4-09** to one equivalent [DBF-SLi] yielded an orange-yellow product, $[\{\mu\text{-}\eta^5, \eta^5\text{-C}_{14}\text{H}_{16}\}\text{Ti}_2(\text{Dbf-S})\text{Cp}_2\text{Cl}_3]$ **4-11**. Addition of one equivalent of **4-09** to two equivalents lithiated dibenzofuranylthiolate caused a colour change from dark green to red. The red-purple residue was subjected to column chromatography and a purple fraction was collected and contained the product $[\{\mu\text{-}\eta^5, \eta^5\text{-C}_{14}\text{H}_{16}\}\{\text{Ti}(\text{Dbf-S})\text{CpCl}\}_2]$ **4-12**.

4.3 Characterization

- *Mass spectrometry*

The mass spectral data for thiiran⁵, methyl epoxide⁶, **L4-02**⁷ and **L4-03**⁸ are given in literature and the mass spectral data for **L4-07** and **L4-08** and complexes **4-01**, **4-02**, **4-05**, **4-09**, **4-10**, **4-11** and **4-12** are summarized in Table 4.2. The most prominent peaks for **L4-07** correspond to *m/z*-values that belong to fragments that result from C-N bond cleavage in the molecule. In **L4-08** the $[\text{M}^+]$ ion was observed and the principle ion corresponds to a fragment whereby the methyl on the nitrogen was fragmented first.

The molecular ions of **4-01** and **4-02** were observed and they fragmented in a similar way. Most fragmentation ions represent fragmentation patterns due to C-N bond cleavage. No molecular ion was observed for **4-05** and the peak of highest *m/z*-value corresponds to the fragment $\text{M}^+\text{-Cl}$. It is clear from the fragment ions that the chlorine and biscyclopentadiene ethylene diamine ligands were bonded to the platinum. Again the molecular ion was not observed for **4-09** in the spectrum and the peak of highest intensity at *m/z*=268 for a binuclear species is one that corresponds to a fragment ion where the two titanium metals are bridged only by the biscyclopentadienyl ligand, $[\text{Ti}_2(\text{Cp}_2\text{C}_4\text{H}_8)^+]$.

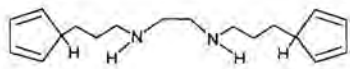
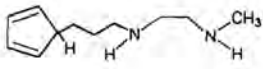
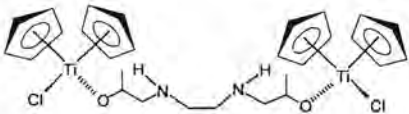
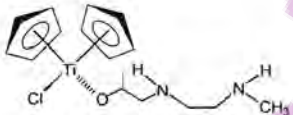
5. G. N. Merrill, U. Zoller, D. R. Reed, S. R. Kass, *J. Org. Chem.*, **1999**, *64*, 7395.

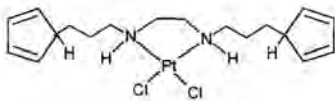
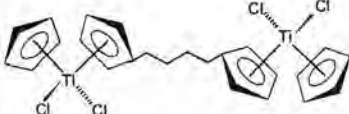
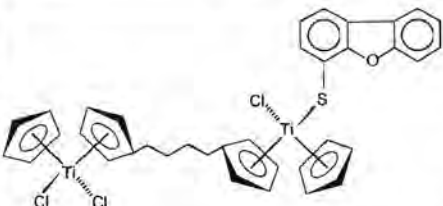
6. W. J. Van de Guchte, W. J. Van der Hart, *Org. Mass Spectrom.*, **1990**, *25*, 309.

7. M. Pykaelainen, A. Vianiotalo, T. A. Pakkenen, P. Vianiotalo, *J. Mass Spectrom.*, **1996**, *31*, 716.

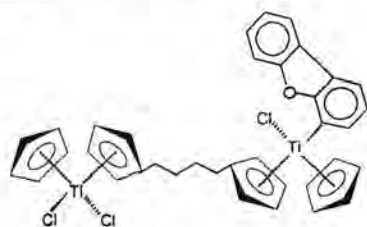
8. P. C. Parikh, P. K. Bhattacharya, *Bull. Acad. Pol. Sci. Ser. Sci. Chim.*, **1975**, *23*, 289.

Table 4.2 Mass spectral data for L4-07, L4-08, 4-01, 4-02, 4-05 and 4-09 - 4-12.

Mass Peaks, m/z (I, %)	
 <p>L4-07</p>	<p>272 (30) [M⁺], 207 (7) [M⁺-Cp], 165 (51), 142 (9) [M⁺-2Cp], 120 (7), 107 (58), 100 (65)</p> <p>71 (100) [(C₄H₉N)⁺], 66 (3) [CpH⁺], 58 (26), 57 (15), 42 (25), 42 (25), 28 (5)</p>
 <p>L4-08</p>	<p>180 (7) [M⁺], 165 (100) [M⁺-CH₃], 120 (1), 107 (18), 100 (9), 71 (11),</p> <p>66 (3) [CpH⁺], 58 (17), 57 (15), 42 (14), 28 (7)</p>
 <p>4-01</p>	<p>352 (5) [TiCp₂(OC₃H₆)₂(C₂H₆N₂)⁺], 340 (9) [M⁺-4Cp], 335 (1) [M⁺-3Cp-2Cl], 322 (2) [TiCpCl(OC₃H₆)₂(C₂H₆N₂)⁺], 305 (1) [M⁺-4Cp-Cl], 294 (5) [TiCp₂(OC₃H₆)(C₂H₆N₂)⁺], 287 (6) [TiCp(OC₃H₆)₂(C₂H₆N₂)⁺], 271 (1) [TiCp₂Cl(OC₃H₆)⁺], 270 (1) [M⁺-4Cp-2Cl], 257 (6) [TiCl(OC₃H₆)₂(C₂H₆N₂)⁺], 246 (8) [TiCpCl(OC₃H₆)(C₂H₆N₂)⁺], 236 (25) [TiCp₂(OC₃H₆)⁺], 229 (2) [TiCp(OC₃H₆)(C₂H₆N₂)⁺], 222 (3) [Ti(OC₃H₆)₂(C₂H₆N₂)⁺],</p> <p>213 (4) [TiCp₂Cl⁺], 206 (3) [TiCpCl(OC₃H₆)⁺], 178 (8) [TiCp₂⁺], 174 (2) [(OC₃H₆)₂(C₂H₆N₂)⁺], 171 (3) [TiCp(OC₃H₆)⁺], 164 (2) [Ti(OC₃H₆)(C₂H₆N₂)⁺], 148 (7) [TiCpCl⁺], 141 (5) [TiCl(OC₃H₆)⁺], 116 (1) [(OC₃H₆)(C₂H₆N₂)⁺], 113 (8) [TiCp⁺], 106 (5) [Ti(OC₃H₆)⁺], 58 (60) [C₂H₆N₂⁺], 42 (60) [C₂H₆N⁺], 28 (100) [C₂H₄⁺</p>
 <p>4-02</p>	<p>264 (1) [M⁺-Cp-Me], 243 (1) [M⁺-Cp-Cl], 236 (2) [TiCp₂(OC₃H₆)⁺], 229 (2) [M⁺-Cp-Cl-Me], 213 (17) [M⁺-2Cp], 213 (17) [TiCp₂Cl⁺], 206 (1) [TiCpCl(OC₃H₆)⁺], 199 (1) [M⁺-2Cp-Me], 178 (2) [M⁺-2Cp-Cl], 178 (2) [TiCp₂⁺], 171 (1) [TiCp(OC₃H₆)⁺],</p> <p>164 (1) [M⁺-2Cp-Cl-Me], 148 (7) [TiCpCl⁺], 141 (1) [TiCl(OC₃H₆)⁺], 131 (1) [(OC₃H₆)(C₃H₉N₂)⁺], 116 (2) [(OC₃H₆)(C₂H₆N₂)⁺], 113 (5) [TiCp⁺], 106 (2) [Ti(OC₃H₆)⁺], 74 (7) [(C₃H₉N₂)⁺], 58 (16) [C₂H₆N₂⁺], 42 (100) [C₂H₆N⁺], 28 (20) [C₂H₄⁺</p>
<p>601 (5) [M⁺], 565 (6) [M⁺-Cl], 536 (4) [M⁺-Cp], 530 (1) [M⁺-2Cl], 435 (1) [M⁺-2Cp-Cl], 400 (1) [M⁺-2Cp-2Cl], 405 (4) [M⁺-3Cp],</p>	
<p>343 (1) [M⁺], 294 (2) [M⁺-Cl-Me], 271 (1) [TiCp₂Cl(OC₃H₆)⁺],</p>	

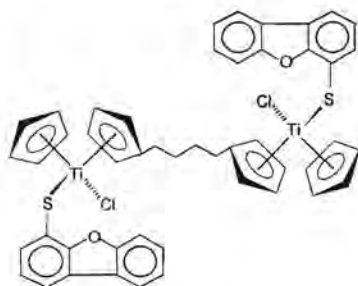
	<p>537 not observed $[M^+]$ 502 (1) $[M^+-Cl]$, 467 (1) $[M^+-2Cl]$, 428 (2), 408 (2), 395 (1), 372 (1), 366 (2), 360 (1), 337 (1), 330 (5), 323 (5), 295 (1), 288 (2),</p>	<p>272 (4) $[(CpC_3H_6)_2(C_2H_6N_2)^+]$ 266 (2), 253 (5), 230 (15), 195 (10) $[Pt^+]$, 165 (4), 142 (6), 107 (8), 100 (2), 65 (15), 58 (100), 42 (94),</p>
	<p>552 not observed $[M^+]$ 345 (5) $[M^+-4Cl-Cp]$, 280 (54) $[Ti_2(Cp_2C_4H_8)^+]$, 268 (3) $[TiCl(Cp_2C_4H_8)^+]$, 238 (50), 203 (5),</p>	<p>184 (80) $[Cp_2C_4H_8]^+$, 183 (100) $[TiCpCl_2]^+$, 178 (12) $[TiCp_2]^+$, 168 (31), 148 (7), 120 (43), 113 (7) $[TiCp^+]$, 70 (10), 57 (35)</p>
	<p>480 (18) $[Ti_2Cp_2Cl_2(Cp_2C_4H_8)^+]$, $[Ti_2(Dbfs)(Cp_2C_4H_8)^+]$, 479 (36) $[Ti(Dbfs)Cl(Cp_2C_4H_8)^+]$, 445 (5) $[Ti_2Cp_2Cl(Cp_2C_4H_8)^+]$, 432 (14) $[Ti(Dbfs)(Cp_2C_4H_8)^+]$, 415 (14) $[Ti_2CpCl_2(Cp_2C_4H_8)^+]$, 412 (4) $[TiCp_2(Dbfs)Cl]^+$, 402 (17) $[Ti(Dbfs)Cl(CpC_4H_8)^+]$, 399 (2) $[Ti(Dbfs)(Cp_2C_4H_8)^+]$, 385 (1) $[Ti_2Cl_3(Cp_2C_4H_8)^+]$, 380 (1) $[Ti_2CpCl(Cp_2C_4H_8)^+]$, 377 (1) $[TiCp_2(Dbfs)^+]$, 370 (1) $[Ti(Dbfs)Cl(CpC_4H_8)^+]$, 367 (15) $[TiCpCl_2(Cp_2C_4H_8)^+]$, 350 (2) $[TiCl_2(Cp_2C_4H_8)^+]$, 347 (4) $[TiCp(Dbfs)Cl]^+$, 346 (5) $[Ti_2Cp(Cp_2C_4H_8)^+]$, 335 (1) $[Ti(Dbfs)(Cp_2C_4H_8)^+]$, 332 (32) $[TiCpCl(Cp_2C_4H_8)^+]$, 315 (2) $[Ti_2Cl(Cp_2C_4H_8)^+]$,</p>	<p>312 (2) $[TiCp(Dbfs)^+]$, 302 (2) $[TiCl_2(Cp_2C_4H_8)^+]$, 299 (1) $[TiCp(Cp_2C_4H_8)^+]$, 280 (1) $[Ti_2(Cp_2C_4H_8)^+]$, 267 (3) $[TiCl(Cp_2C_4H_8)^+]$, 248 (2) $[TiCp_2Cl_2]^+$, 238 (8) $[TiCl_2(CpC_4H_8)^+]$, 232 (12) $[Ti(Cp_2C_4H_8)^+]$, 213 (8) $[TiCp_2Cl]^+$, 203 (4) $[TiCl(CpC_4H_8)^+]$, 200 (100) $[Dbfs-SH]^+$, 186 (1) $[CpH-C_4H_8-CpH]$ 184 (12) $[Cp_2C_4H_8]^+$, 183 (12) $[TiCpCl_2]^+$, 178 (3) $[TiCp_2]^+$, 168 (55) $[Dbfs-H]^+$, $[Ti(CpC_4H_8)^+]$, 148 (5) $[TiCpCl]^+$, 120 (3) $[CpC_4H_8]^+$, 113 (6), 70 (10), 57 (3)</p>

716 (2) $[M^+]$,
680 (1) $[M^+-Cl]$
615 (7) $[M^+-Cp-Cl]$,
579 (4) $[M^+-Cp-2Cl]$,
550 (8) $[M^+-2Cp-Cl]$,
545 (3) $[M^+-Cp-3Cl]$,
544 (8) $[Ti_2Cp(Dbfs)(Cp_2C_4H_8)^+]$,
531 (8) $[TiCp(Dbfs)Cl(Cp_2C_4H_8)^+]$,
516 (8) $[M^+-DbfsSH]$,
514 (8) $[Ti_2(Dbfs)Cl(Cp_2C_4H_8)^+]$,
496 (4) $[TiCp(Dbfs)(Cp_2C_4H_8)^+]$,



4-10

683 not observed $[M^+]$	267 (2) $[\text{TiCl}(\text{Cp}_2\text{C}_4\text{H}_8)^+]$,
399 (2) $[\text{Ti}(\text{Dbf})(\text{Cp}_2\text{C}_4\text{H}_8)^+]$,	248 (1) $[\text{TiCp}_2\text{Cl}_2^+]$,
380 (1) $[\text{Ti}_2\text{CpCl}(\text{Cp}_2\text{C}_4\text{H}_8)^+]$,	232 (1) $[\text{Ti}(\text{Cp}_2\text{C}_4\text{H}_8)^+]$, $[\text{Dbf-Cp}^+]$
370 (1) $[\text{Ti}(\text{Dbf})\text{Cl}(\text{Cp}_2\text{C}_4\text{H}_8)^+]$,	213 (3) $[\text{TiCp}_2\text{Cl}^+]$,
367 (1) $[\text{TiCpCl}_2(\text{Cp}_2\text{C}_4\text{H}_8)^+]$,	186 (1) $[\text{CpH-C}_4\text{H}_8\text{-CpH}]$
346 (1) $[\text{Ti}_2\text{Cp}(\text{Cp}_2\text{C}_4\text{H}_8)^+]$,	184 (5) $[\text{Cp}_2\text{C}_4\text{H}_8]^+$,
345 (1) $[\text{TiCp}_2(\text{Dbf})^+]$,	183 (17), $[\text{TiCpCl}_2^+]$,
332 (1) $[\text{TiCpCl}(\text{Cp}_2\text{C}_4\text{H}_8)^+]$,	168 (100) $[\text{Dbf-H}^+]$,
315 (1) $[\text{TiCp}(\text{Dbf})\text{Cl}^+]$,	148 (1) $[\text{TiCpCl}^+]$,
$[\text{Ti}_2(\text{Cp}_2\text{C}_4\text{H}_8)\text{Cl}^+]$,	120 (1) $[\text{CpC}_4\text{H}_8]^+$,
302 (2) $[\text{TiCl}_2(\text{Cp}_2\text{C}_4\text{H}_8)^+]$,	113 (5) $[\text{TiCp}^+]$,
280 (1) $[\text{TiCp}(\text{Dbf})^+]$, $[\text{Ti}_2(\text{Cp}_2\text{C}_4\text{H}_8)^+]$,	70 (3), 57 (2)



4-12

610 (45) $[\text{Ti}_2\text{Cp}_2(\text{DbfS})(\text{Cp}_2\text{C}_4\text{H}_8)^+]$,	346 (75) $[\text{Ti}_2\text{Cp}(\text{Cp}_2\text{C}_4\text{H}_8)^+]$,
579 (4) $[\text{Ti}_2\text{CpCl}(\text{DbfS})(\text{Cp}_2\text{C}_4\text{H}_8)^+]$,	332 (14) $[\text{TiCpCl}(\text{Cp}_2\text{C}_4\text{H}_8)^+]$,
576 (14) $[\text{TiCp}_2(\text{DbfS})_2^+]$,	315 (44) $[\text{Ti}_2\text{Cl}(\text{Cp}_2\text{C}_4\text{H}_8)^+]$,
550 (12) $[\text{Ti}_2\text{Cl}_2(\text{DbfS})(\text{Cp}_2\text{C}_4\text{H}_8)^+]$,	313 (25) $[\text{TiCp}(\text{DbfS})^+]$,
545 (17) $[\text{Ti}_2\text{Cp}(\text{DbfS})(\text{Cp}_2\text{C}_4\text{H}_8)^+]$,	303 (12) $[\text{TiCl}_2(\text{Cp}_2\text{C}_4\text{H}_8)^+]$,
544 (17) $[\text{Ti}_2\text{Cp}(\text{DbfS})(\text{Cp}_2\text{C}_4\text{H}_8)^+]$,	299 (10) $[\text{Ti}(\text{Cp}_2\text{C}_4\text{H}_8)^+]$,
531 (12) $[\text{TiCp}(\text{DbfS})\text{Cl}(\text{Cp}_2\text{C}_4\text{H}_8)^+]$,	280 (20) $[\text{Ti}_2(\text{Cp}_2\text{C}_4\text{H}_8)^+]$,
514 (90) $[\text{Ti}_2\text{Cl}(\text{DbfS})(\text{Cp}_2\text{C}_4\text{H}_8)^+]$,	268 (18) $[\text{TiCl}(\text{Cp}_2\text{C}_4\text{H}_8)^+]$,
513 (85) $[\text{TiCp}(\text{DbfS})_2^+]$,	248 (14) $[\text{TiCp}_2\text{Cl}_2^+]$,
496 (15) $[\text{TiCp}(\text{DbfS})(\text{Cp}_2\text{C}_4\text{H}_8)^+]$,	238 (20) $[\text{TiCl}_2(\text{Cp}_2\text{C}_4\text{H}_8)^+]$,
480 (10) $[\text{Ti}_2\text{Cp}_2\text{Cl}_2(\text{Cp}_2\text{C}_4\text{H}_8)^+]$,	233 (14) $[\text{Ti}(\text{Cp}_2\text{C}_4\text{H}_8)^+]$,
479 (17) $[\text{Ti}_2(\text{DbfS})(\text{Cp}_2\text{C}_4\text{H}_8)^+]$,	213 (32) $[\text{TiCp}_2\text{Cl}^+]$,
467 (13) $[\text{Ti}(\text{DbfS})\text{Cl}(\text{Cp}_2\text{C}_4\text{H}_8)^+]$,	203 (8) $[\text{TiCl}(\text{Cp}_2\text{C}_4\text{H}_8)^+]$,
466 (10) $[\text{Ti}(\text{DbfS})\text{Cl}(\text{Cp}_2\text{C}_4\text{H}_8)^+]$,	200 (100) $[\text{Dbf-SH}^+]$,
445 (6) $[\text{Ti}_2\text{Cp}_2\text{Cl}(\text{Cp}_2\text{C}_4\text{H}_8)^+]$,	186 (1) $[\text{CpH-C}_4\text{H}_8\text{-CpH}]$
432 (13) $[\text{Ti}(\text{DbfS})(\text{Cp}_2\text{C}_4\text{H}_8)^+]$,	184 (4) $[\text{Cp}_2\text{C}_4\text{H}_8]^+$,
415 (8) $[\text{Ti}_2\text{CpCl}_2(\text{Cp}_2\text{C}_4\text{H}_8)^+]$,	183 (4) $[\text{TiCpCl}_2^+]$,
413 (9) $[\text{TiCp}_2\text{Cl}(\text{DbfS})^+]$,	178 (10) $[\text{TiCp}_2^+]$,
410 (15) $[\text{Ti}_2\text{Cp}_2(\text{Cp}_2\text{C}_4\text{H}_8)^+]$,	168 (17) $[\text{Dbf-H}^+]$,
402 (12) $[\text{Ti}(\text{DbfS})\text{Cl}(\text{Cp}_2\text{C}_4\text{H}_8)^+]$,	168 (17) $[\text{Ti}(\text{Cp}_2\text{C}_4\text{H}_8)^+]$,
380 (13) $[\text{Ti}_2\text{CpCl}(\text{Cp}_2\text{C}_4\text{H}_8)^+]$,	148 (5) $[\text{TiCpCl}^+]$,
378 (96) $[\text{TiCp}_2(\text{DbfS})^+]$,	120 (13) $[\text{CpC}_4\text{H}_8]^+$,
367 (45) $[\text{TiCpCl}_2(\text{Cp}_2\text{C}_4\text{H}_8)^+]$,	113 (8) $[\text{TiCp}^+]$,
350 (11) $[\text{TiCl}_2(\text{Cp}_2\text{C}_4\text{H}_8)^+]$,	70 (18) $[\text{TiS}^+]$,
348 (75) $[\text{TiCpCl}(\text{DbfS})^+]$,	57 (23)
881 (13) $[M^+]$,	
845 (28) $[M^+\text{-Cl}]$,	
815 (20) $[M^+\text{-CpH}]$,	
810 (6) $[M^+\text{-2Cl}]$,	
780 (23) $[M^+\text{-Cl-CpH}]$,	
750 (14) $[M^+\text{-2Cp}]$,	
745 (10) $[M^+\text{-2Cl-Cp}]$,	
715 (14) $[M^+\text{-Cl-2Cp}]$,	
696 (13) $[\text{TiCp}(\text{DbfS})_2(\text{Cp}_2\text{C}_4\text{H}_8)^+]$,	
680 (8) $[\text{MH}^+\text{-2Cl-2Cp}]$,	
$[M^+\text{-DbfSH}]$,	
679 (8) $[\text{Ti}_2(\text{DbfS})_2(\text{Cp}_2\text{C}_4\text{H}_8)^+]$,	
645 (42) $[\text{Ti}_2\text{Cp}_2\text{Cl}(\text{DbfS})(\text{Cp}_2\text{C}_4\text{H}_8)^+]$,	
631 (3) $[\text{Ti}(\text{DbfS})_2(\text{Cp}_2\text{C}_4\text{H}_8)^+]$,	
615 (18) $[\text{Ti}_2\text{CpCl}_2(\text{DbfS})(\text{Cp}_2\text{C}_4\text{H}_8)^+]$,	

The molecular ions of **4-11** and **4-12** were observed but in the case of **4-10** the peak of highest m/z -value was assigned to a mononuclear titanium fragment. Peaks of fragments containing two titaniums as well as the bridging biscyclopentadienyl ligand were observed but all of them without the Dbf ligand. The spectrum is of poor quality and this is ascribed to the instability of the complex. The dinuclear thiolate compounds are of higher stability and gave spectra of higher quality. There are two pathways for the fragmentation of the complexes **4-10** to **4-12**. In the first instance the two titanium atoms remain bonded to the bridging ligand and other ligands are fragmented randomly. Ultimately all ligands are lost except for the bridging biscyclopentadienyl ligand to give the fragment ion ($m/z=280$) which is present on all the spectra, all though not observed as a peak of high intensity. The second route represents the fragmentation of a titanium fragment by decomplexation from a cyclopentadienyl ligand. This leaves the bridging ligand in tact, but replaces the metal by a hydrogen atom to give a diene at the open end of the ligand. As a result, it is difficult to distinguish between the fragments DbfSH and $2Cp + 2Cl$ as they have very similar mass contributions. Whereas the intensity of fractions with the Dbf ligand is very low for **4-10**, higher intensities peaks assigned to fractions containing DbfS were observed in the spectra of **4-11** and **4-12**. It is not possible to write a general fragmentation sequence for the ligands

• *¹H NMR and ¹³C NMR spectroscopy*

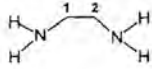
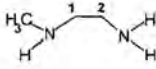
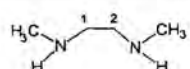
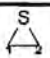
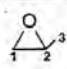
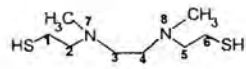
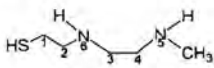
A summary of the ¹H NMR and ¹³C NMR data for thiiran^{9,10}, methyl epoxide^{11,12} **L4-01**^{13,14}, **L4-02**¹⁵, **L4-03**¹⁶ and **L4-04** - **L4-08** is given in Table 4.3. The values of the commercially available compounds were confirmed with the literature values. The ¹H NMR and ¹³C NMR spectral data for complexes **4-01**, **4-02**, **4-03**, **4-07** and **4-09** - **4-12** are summarized in Table 4.4.

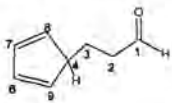
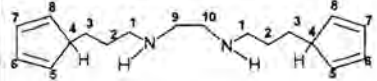
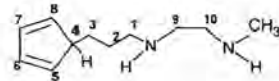
Table 4.3 ¹H and ¹³C NMR spectral data^a for the diamines, thiiran and methyl oxiran, **L4-01** - **L4-08**.

9. V. N. Drozd, V. N. Knyazev, N. L. Nam, V. P. Lezina, T. Y. Mozhaeva, V. L. Savelev, *Russ. J. Org. Chem.*, **1993**, *29*, 653.
10. J. C. Facelli, A. M. Orendt, A. J. Beeler, M. S. Solum, G. Depke, *J. Am. Chem. Soc.*, **1985**, *107*, 6749.
11. Y. Xiang, S. C. Larsen, V. H. Grassian, *J. Am. Chem. Soc.*, **1999**, *121*, 5063.
12. B. Riegel, W. Kiefer, S. Hofacker, G. Schottner, *Appl. Spectrosc.*, **2000**, *54*, 1384.
13. Y. Nakano, E. Yamazaki, H. Hanahata, K. Okajima, Y. Kitahama, *Bull. Chem. Soc. Jpn.*, **1997**, *70*, 1185.
14. M. V. Kulikova, K. P. Balashev, P. -I. Kvam, J. Songstad, *Russ. J. Gen. Chem.*, **2000**, *70*, 163.
15. V. Barone, F. Leij, O. Nicolaus, G. Abbate, R. Barucci, *Gazz. Chim. Ital.*, **1984**, *114*, 249.
16. S. Cortes, H. Kohn, *J. Org. Chem.*, **1983**, *48*, 2246.



4. Bi- and trinuclear complexes of titanium(IV) and platinum(II)

Ligand	C	Chemical Shift (δ ppm)	H	Chem. Shift (δ ppm)	Splitting/ Integration	Coupling Constant (J Hz)	
 L4-01	1,2	44.7	1,2 NH	2.66 1.17	s s	4H 4H	
 L4-02	1 2 N-Me	54.5 41.2 36.1	1 2 N-Me NH	2.49 2.66 2.30 1.29	t t s s	2H 2H 3H 3H	5.4/5.9 5.9/5.4
 L4-03	1,2 N-Me	51.5 36.2	1,2 N-Me NH	2.54 2.29 1.14	s s s	4H 6H 2H	
 L4-04	1,2	18.9	1,2	2.30	s	4H	
 L4-05	1 2 3	46.3 46.6 16.8	1/2 3	2.46-3.00 1.32	m br	3H 1H	-
 L4-06	1,6 2,5 3,4 N-Me	22.3 41.8 60.3 36.3/	1,6 2,5 3,4 N-Me SH	2.40 2.46-2.50 2.53 2.13 1.70	d m d s br	4H 4H 4H 6H 2H	5.7 - 5.9
 L4-07	1 2 3 4 N-Me	23.0 42.2 60.6 60.8 39.9	1 2/3 4 N-Me NH/SH	2.36 2.47-2.54 2.58-2.61 2.16/2.17 1.46/1.47	d m m s/s s/s	2H 4H 2H 3H 2H	5.43 - -

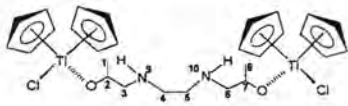
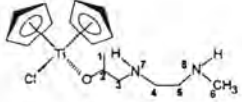
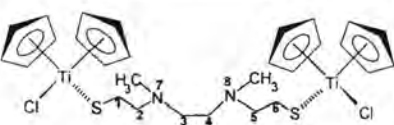
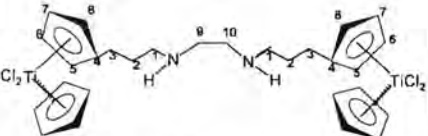
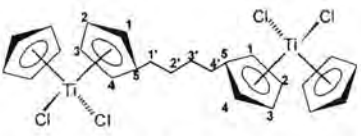
 <p>L4-06</p>	<p>1 199.1 2 35.8 3 28.5 4 45.9/50.8 5,8 102.9 6,7 102.9</p>	<p>1 9.71 s 1H 2 3.40 t 2H 6.7 3 2.10-2.12 m 2H - 4 2.59-2.61 m 1H - 5,8 3.05 t 2H 6.6 6,7 4.51-4.54 m 2H -</p>
 <p>L4-07</p>	<p>1 32.7 2 30.0 3 49.3 4 45.3 5,8 103.0 6,7 103.5 9,10 49.2</p>	<p>1 1.77-1.78 m 4H - 2 1.70-1.72 m 4H - 3 2.44 t 4H 6.7/7.2 4 2.60-2.63 m 2H - 5,8 4.38-4.40 m 4H - 6,7 4.34-4.35 m 4H - 9,10 2.68 s 4H NH 2.11 s 2H</p>
 <p>L4-08</p>	<p>1 32.9 2 30.4 3 49.2 4 45.4 5,8 103.1 6,7 104.2 9 51.5 10 42.16 N-Me 36.4</p>	<p>1 2.14 t 2H 5.9/5.9 2 1.59-1.61 m 2H - 3 1.69-1.70 m 2H - 4 2.58-2.60 m 1H - 5,8 4.30 d 2H 5.7 6,7 4.39 t 2H 5.7/5.7 9 2.58 d 2H 6.7 10 2.32 d 2H 6.7 N-Me 2.35 s 3H NH 1.18 s 2H</p>

^a Recorded in CDCl₃

¹H NMR spectroscopy

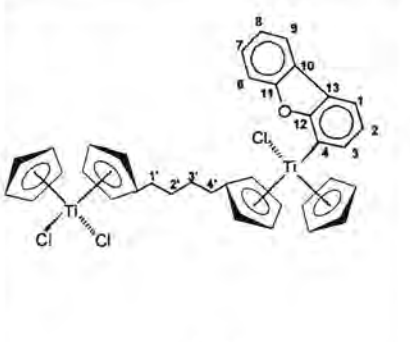
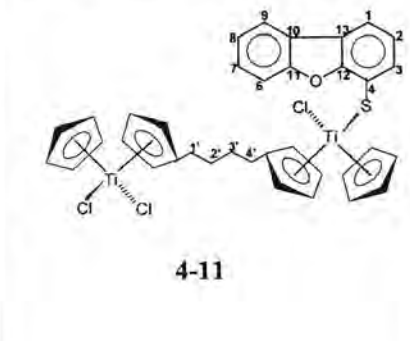
The NH signal of **L4-05** was broadened to such an extent that it coincided with the baseline and no meaningful assignment could be made. The characteristic -C(O)H peak for the aldehyde is observed at 9.71 ppm. Due to poor resolution of resonances it was difficult to get all the coupling constants for **L4-07** and **L4-08**.

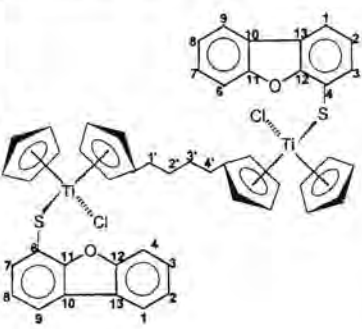
Table 4.4 ¹H and ¹³C NMR spectral data^a for 4-01, 4-02, 4-03, 4-07 and 4-09 - 4-12.

Complex	C	Chem. Shift ^b (δ ppm)	H	Chem. Shift (δ ppm)	Splitting/Integration	Coupling Constant (J Hz)	
 <p>4-01</p>	1/8 2/7 3/6 4/5 Cp	20.1 67.7 50.0 51.6 116.8	1/8 2/7 3/6 4/5 NH Cp	1.25 3.99-4.00 3.57-3.59 3.41/3.45 1.57 6.28	d m m d/d s s	6H 2H 4H 4H 2H 20H	6.4 - - 7.2/7.2 - -
 <p>4-02</p>	Not recorded	-	1 2 3 4/5 N-Me NH Cp	1.25 3.98-3.99 3.57-3.59 3.41/3.45 3.47 1.68 6.28/6.31	d m m d/d s br s,s	3H 1H 2H 4H 3H 2H 10H	6.2 - - 7.2/7.2 - -
 <p>4-03</p>	Not recorded	-	1,6 2,5 3,4 N-Me Cp	3.71 4.32-4.33 3.25 2.76 6.41/6.42	t m s s s/s	4H 4H 4H 6H 20H	6.2 - - -
 <p>4-07</p>	Not recorded	-	1 2 3 5-8 9/10 NH Cp	2.29 2.20-2.21 3.33-3.35 6.57-7.04 3.47 1.22 6.60	d m m m s s s	2H 2H 2H 8H 4H 2H 10H	6.0 - - -
 <p>4-09</p>	1/4 2/3 5 1'/4' 2'/3' Cp	119.5 119.7 122.2 23.9 41.0 115.8	1/4 2/3 5 1'/2'/3'/4' Cp	6.34-6.36 6.27-6.28 6.43 2.68-2.70 6.48	m m s m s	4H 4H 2H 8H 20H	- - - -



4. Bi- and trinuclear complexes of titanium(IV) and platinum(II)

 <p style="text-align: center;">4-10</p>	1	116.6	1	7.50	d	1H	7.5
	2	123.0	2	7.21	t	1H	7.5/8.0
	3	129.1	3	7.00	d	1H	8.0
	4	no	6	7.94	d	1H	7.5
	6	111.7	7	7.33	t	1H	7.5/7.2
	7	127.1	8	7.44	t	1H	7.2/7.2
	8	122.7	9	7.56	t	1H	7.2
	9	120.6	1'/4'	3.64	t	4H	6.5
	10/12/13	no	2'/3'	3.72-3.73	m	4H	-
	11	159.5	Cp	6.61/6.63	s/s	10H	
	1'/4'	23.7	Cp*	6.44/6.57	s/s	8H	
	2'/3'	39.0		6.62/6.65	s/s		
	Cp	119.2					
		119.4					
Cp*	119.2						
	119.3						
	119.5						
	119.7						
 <p style="text-align: center;">4-11</p>	1	120.2	1	7.67/7.73	d	1H	7.8
	2	123.3	2	7.23/7.24	t	1H	7.8
	3	129.5	3	7.87/7.87	d	1H	7.8
	4	no	6	7.92/7.94	d	1H	7.5
	6	112.0	7	7.33/7.34	t	1H	7.5
	7	127.5	8	7.44/7.47	t	1H	7.5
	8	123.0	9	7.56/7.60	d	1H	7.5
	9	121.3	1'/4'	3.09	t	4H	7.5
	10-13	no	2'/3'	1.62-1.64	m	4H	-
	1'/4'	25.9	Cp	6.61	s	10H	
	2'/3'	38.9	Cp*	6.48/6.52	s/s	8H	
	Cp	120.8		6.56/6.64	s/s		
	Cp*	120.7					
		120.8					
	120.9						
	120.9						

 <p style="text-align: center;">4-12</p>	<p>Not recorded</p>	<table border="1"> <tbody> <tr><td>1</td><td>7.77</td><td>d</td><td>2H</td><td>7.5</td></tr> <tr><td>2</td><td>7.31</td><td>t</td><td>2H</td><td>7.5</td></tr> <tr><td>3</td><td>7.93</td><td>d</td><td>2H</td><td>7.5</td></tr> <tr><td>6</td><td>7.94</td><td>d</td><td>2H</td><td>7.5</td></tr> <tr><td>7</td><td>7.32</td><td>t</td><td>2H</td><td>7.5/6.2</td></tr> <tr><td>8</td><td>7.39</td><td>t</td><td>2H</td><td>6.2/8.0</td></tr> <tr><td>9</td><td>7.59</td><td>d</td><td>2H</td><td>8.0</td></tr> <tr><td>1'/4'</td><td>3.73</td><td>t</td><td>4H</td><td>7.5</td></tr> <tr><td>2'/3'</td><td>1.82-1.84</td><td>m</td><td>4H</td><td>-</td></tr> <tr><td>Cp</td><td>6.01/6.08</td><td>s</td><td>10H</td><td></td></tr> <tr><td>Cp*</td><td>5.87/5.87</td><td>s/s</td><td>8H</td><td></td></tr> <tr><td></td><td>5.88/6.07</td><td>s/s</td><td></td><td></td></tr> </tbody> </table>	1	7.77	d	2H	7.5	2	7.31	t	2H	7.5	3	7.93	d	2H	7.5	6	7.94	d	2H	7.5	7	7.32	t	2H	7.5/6.2	8	7.39	t	2H	6.2/8.0	9	7.59	d	2H	8.0	1'/4'	3.73	t	4H	7.5	2'/3'	1.82-1.84	m	4H	-	Cp	6.01/6.08	s	10H		Cp*	5.87/5.87	s/s	8H			5.88/6.07	s/s		
1	7.77	d	2H	7.5																																																										
2	7.31	t	2H	7.5																																																										
3	7.93	d	2H	7.5																																																										
6	7.94	d	2H	7.5																																																										
7	7.32	t	2H	7.5/6.2																																																										
8	7.39	t	2H	6.2/8.0																																																										
9	7.59	d	2H	8.0																																																										
1'/4'	3.73	t	4H	7.5																																																										
2'/3'	1.82-1.84	m	4H	-																																																										
Cp	6.01/6.08	s	10H																																																											
Cp*	5.87/5.87	s/s	8H																																																											
	5.88/6.07	s/s																																																												

^a Recorded in CDCl₃ ^b no = not observed

A 2D-COSY experiment was used to confirm the assignments of the peaks for **4-01**. In complexes **4-02** and **4-03** two Cp peaks were observed. The ¹H NMR spectrum for **4-04** had very poor resolution and no definite assignments could be made. Overlapping of resonances in the ¹H NMR spectrum of **4-05** complicated assignments (all the peaks are stacked around 4.49 ppm) and unambiguous assignments could not be made. The data was omitted from Table 4.4, as well as the spectral data of **4-06** and **4-08** as no spectrum could be recorded due to very poor solubility. In **4-07** the unsubstituted cyclopentadienyl rings are seen as singlets and the substituted Cp's as multiplets. The intensity ratios between the unsubstituted Cp and substituted Cp's are, as expected, 1:1. The chemical shift values of the C₃H₆-link between the Cp and amine portions of the bridging ligand are downfield compared to **L4-07**. This is ascribed to the electron withdrawing effect of the titanium atoms once they are coordinated to the Cp rings.

In complex **4-09** all the chemical shifts for the substituted Cp ring were resolved, but the CH₂ protons overlap. In **4-10** the cyclopentadienyl rings of the bridging ligand are electronically not equivalent due to the presence of the dibenzofuranyl ligand on one of the titanium centres. In Table 4.4 the substituted cyclopentadienyl rings are indicated as Cp*. Complexes **4-11** and **4-12** also display electronically non-equivalent Cp rings, the latter being ascribed to restricted rotation because of the bulkiness of two dibenzofuranyl ligands in **4-12**. Assignments of resonances for complex **4-12** were achieved by performing a 2D-COSY experiment.

¹³C NMR spectroscopy

A 2D-HETCOR experiment was used to confirm assignments to chemical shift values of the peaks for **L4-07**. In **L4-06** two peaks are observed where H4 is expected and it is not clear which one is correct,

so both values were listed. No ^{13}C NMR was obtained for **4-02** - **4-08** due to poor solubility in deuterated solvents.

The substituted rings in complex **4-09** display, as expected, two resonances. In **4-10** the peaks for most of the quaternary carbons are not observed. In **4-11** the quaternary peaks were not observed. Excessive decomposition of **4-12** during the recording of the spectrum gave spectral data that was not useful due to the bad resolution of the spectrum. Complex **4-11** displayed the expected multiple signals for the Cp rings.

4.4 Conclusions

The screening and preclinical testing of the complexes in this chapter was not included in the study at this point of time. The first priority was to establish sound methods of synthesis of binuclear compounds with specific features that will have properties suitable for handling during preclinical testing. These properties include high stability in solution, fixed compositions, favorable geometrical features and high solubility. Many problems were identified with regard to the synthesis of binuclear complexes and the foundations have now been laid for sound and successful syntheses of bi- and trinuclear complexes of platinum and titanium. The binuclear complexes of choice are shown in Figure 4.8 and represent an example of a titanium-platinum and a titanium-titanium combination. Whereas a method is available to synthesize complexes of the second type, this problem has not yet been solved for the mixed Ti-Pt dinuclear complex. Deprotonation of **L4-08** and subsequent reactions, first with TiCpCl_3 , and thereafter with $[\text{Pt}(\text{COD})\text{Cl}_2]$ seems like the correct approach. A further aspect to be considered before testing the products is the appropriate length of the connecting carbon chains between the two ligating functions. This will also have implications on the procedures during the synthesis. Binuclear complexes are more stable in solution compared to trinuclear complexes which makes the use of **4-07** as an ideal precursor questionable.

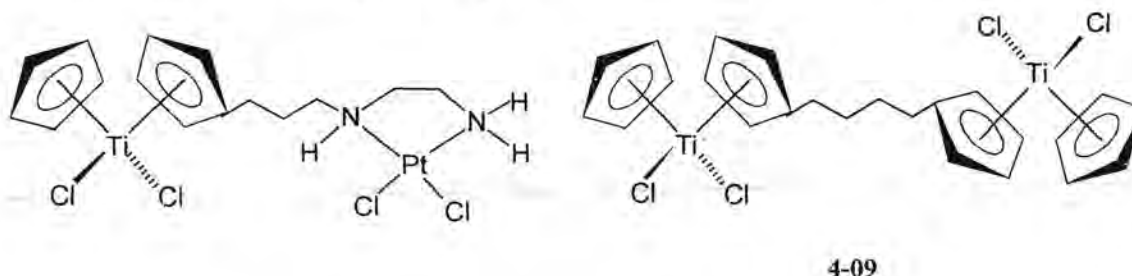


Figure 4.8 Model binuclear complexes chosen for future investigation.

Chapter 5

Antitumor properties, DNA interaction and ligand substitutions

5.1 Introduction

The complexes in this study were designed to exhibit antitumor activity and therefore it was important to test the complexes *in vitro* and study the structure activity relationships. It was apparent that the new titanocene derivatives should display antitumor activities as they were derived from titanocene dichloride for which the antitumor activities have been established. The candidates were selected based on their stability and composition. Two cell lines were selected for the *in vitro* tests. They are HeLa cells, a human cervix epithelioid carcinoma, and CoLo cells, a colorectal carcinoma. Titanocene dichloride was very successful in inhibiting colorectal carcinomas. One use of the test results will be for screening purposes and another to optimize the composition of the complexes. With this information available, by refining the structural features and studying their mode of antitumor action, new improved drugs could be designed. The results will also be discussed with respect to the structural features of the complexes and evaluated against the proposed mechanism of action and possible interaction with DNA.

In the design of the complexes the assumption was made that DNA will be targeted. This assumption is not necessarily correct. Covalent bond formation of the complexes should occur, after displacement of a labile ligand from the coordination sphere of titanium, at oxygen of the phosphate backbone of DNA. Titanium(IV) represents a hard metal center and oxygen is the hardest of the available heteroatoms with bonding properties in DNA. The introduction of condensed heteroaromatic rings in one of the ligands of titanocene derivatives could lead to intercalation or π -stacking into grooves formed by the double stranded DNA helix. For the latter, the number of rings, the size of the plane of the condensed rings and their orientation will be important. It is assumed that if both modes of action could be incorporated in one carefully designed compound their combined effects should

greatly enhanced the antitumor properties of the compound. Recently, Osella and co-workers¹ proposed that the mechanism of antitumor action for ferrocenyl compounds involves an electron transfer process by redox active enzymes in particular body compartments. The ferricinium species interact with water and oxygen to generate a hydroxyl radical (OH^{\bullet}) which cleaves the DNA strands and results in cell death. A similar mechanism could also apply for the titanium(IV) species.

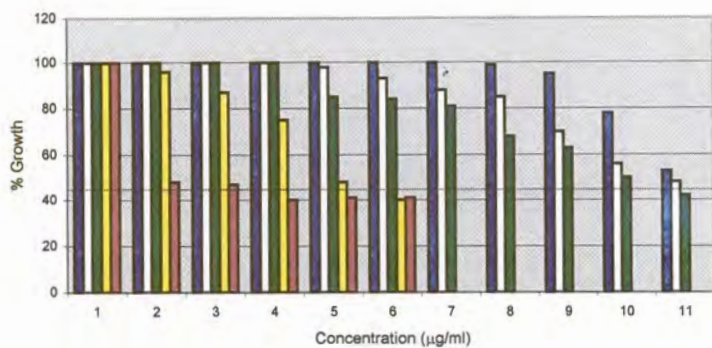
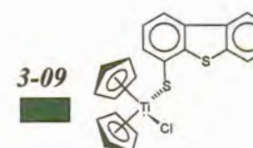
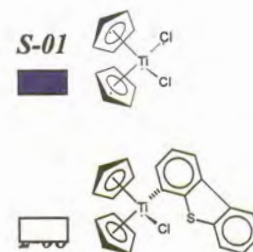
5.2 Antitumor activity

Comparison of the test results of the complexes will give some insight of geometric and electronic factors required to improve their antitumor activity. The first set of tests was devised to screen complexes and thereafter the best candidates were selected and compared against the assumptions made with regard to DNA interactions. Titanocene dichloride (**S-01**) was selected as a primary standard and included in a group of compounds for which both CoLo and HeLa cell lines were cultivated to test their antitumor activities. The free ligands dibenzothiophene (**L2-01**), dibenzodioxin (**L2-03**) and dibenzodioxinthiol (**L3-03**) as well as the complexes **2-05**, **2-08**, **3-05**, **3-09** and **3-10** were selected for testing. The complexes **3-05** and **3-09** have oxygen and sulfur heteroatoms in the rings, respectively and both are thiolato ligands. Complex **2-05** has oxygen atoms in the ring and a direct bond between the metal and a carbon atom of the ring. The antitumor results are shown in Figure 5.1.

In the presentations, 100% growth was taken as the concentration of untreated cells after three days (duration of experiment) and should be seen relative to the number of cells at the start of the experiment (day 0), which was about 43%. A line indicated the data at day 0 is given in the graphs. The results of the complexes that represent a decrease in cell growth compared to day 0, was ignored and not indicated on the graphs. These compounds were taken as not inhibiting cell growth, but to be toxic at these concentrations.

1. D. Osella, M. Ferrali, P. Zanello, F. Laschi, M. Fontani, C. Nervi, G. Cavigliolo, *Inorg. Chim. Acta*, **2000**, *306*, 42.

HeLa cells

Day 0
No Growth

CoLo Cells

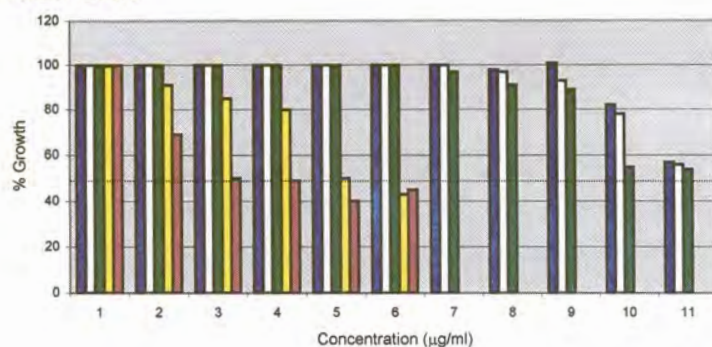
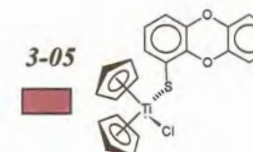
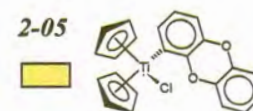
Day 0
No Growth

Figure 5.1. Inhibition of HeLa and CoLo cell growth by S-01, 2-05, 2-08, 3-05 and 3-09.

It is clear that all the complexes exhibited a concentration dependent suppression of cell growth towards HeLa and CoLo cells. They only differ in the tempo of inhibiting cell growth. The introduction of a heteroaromatic condensed ring ligand improved the activity significantly compared to that of the standard S-01 and it was further noted that by incorporating the harder oxygen atoms in the rings, cell growth was greatly inhibited. Also the insertion of a spacer atom between the metal and the rings produced improved suppression of cell growth. The free ligands L2-01, L2-03 and L3-03 were not very active inhibiting cell growth; even at maximum concentrations used, and to simplify the graphs their data are not included. The bis-substituted titanocene dichloride complex, the bithiolato derivative, 3-10 showed very little activity and was also not included in the graph.

From Figure 5.1 it was clear that the results for the CoLo and HeLa cell lines are very similar and it was decided to continue the rest of the tests only on CoLo cell lines. All growth data of the complexes were compared with the data of the standard S-01 and the complex that displayed the greatest cell growth inhibition was 3-05. Due to the large amount of data it was not wise to try and show all the

results on one graph. Instead the data was grouped together according to the objectives of the study mentioned in Chapter 1, and will be discussed accordingly.

Cell growth inhibition results of the model complexes and free ligands

Figure 5.2 displays the test results for the suppression of cell growth of the standards from Figure 5.1, **S-01** and **3-05**, the ligands dibenzofuran (**L2-06**) and dibenzofuranthiol (**L3-06**) and the complexes **2-01** and **3-01**.

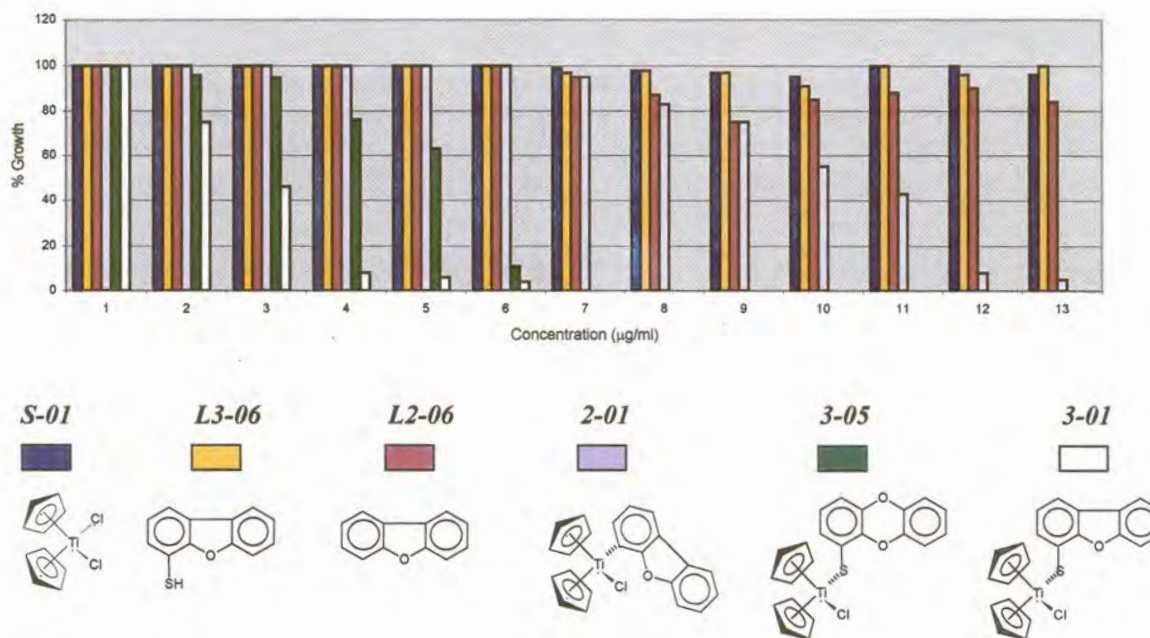


Figure 5.2. Inhibition of CoLo cell growth by **S-01**, **L2-06**, **L3-06**, **2-01**, **3-01** and **3-05**.

The uncoordinated heteroaromatic substrates exhibited very little antitumor effects in this concentration range and it was assumed that the liberation of the ligands played an insignificant role in contributing to the overall antitumor activity. The large inhibition of cell growth by **3-01** and **3-05** is demonstrated in the concentration range 2-7 µg Ti per ml solution. Complex **3-01** tested better than complex **3-05** especially in the 3-5 µg Ti per ml solution region.

(i) The role of the number of condensed rings in the ligand

In Figure 5.3 the cell growth suppression of **S-01** and **3-05** and the thiolato complexes **3-01**, **3-07**, **3-09** and **3-13** are represented against increasing concentrations of the compounds. In all cases inhibition of cell growth were always better by three rings than for two rings in the heteroaromatic ring ligand. This is demonstrated by comparing the test data of the thiolato complexes of benzothiophene (**3-13**) with that of the dibenzothiophene analogue (**3-09**). The former displays only

75% suppression at 14 μg Ti per ml solution compared to complete inhibition of cell growth at this concentration by **3-09**. Complexes **3-01** and **3-05** show complete inhibition of cell growth at a concentration level of 6-7 μg Ti per ml solution, whereas this level of suppression by **3-09** is only reached at 14 μg Ti per ml solution. Complete suppression of cell growth by titanocene dichloride (**S-01**) is only achieved at 460 μg Ti per ml solution which relate to **3-01** being twice as potent as **3-09** which in turn is 33 times more effective than **S-01**.

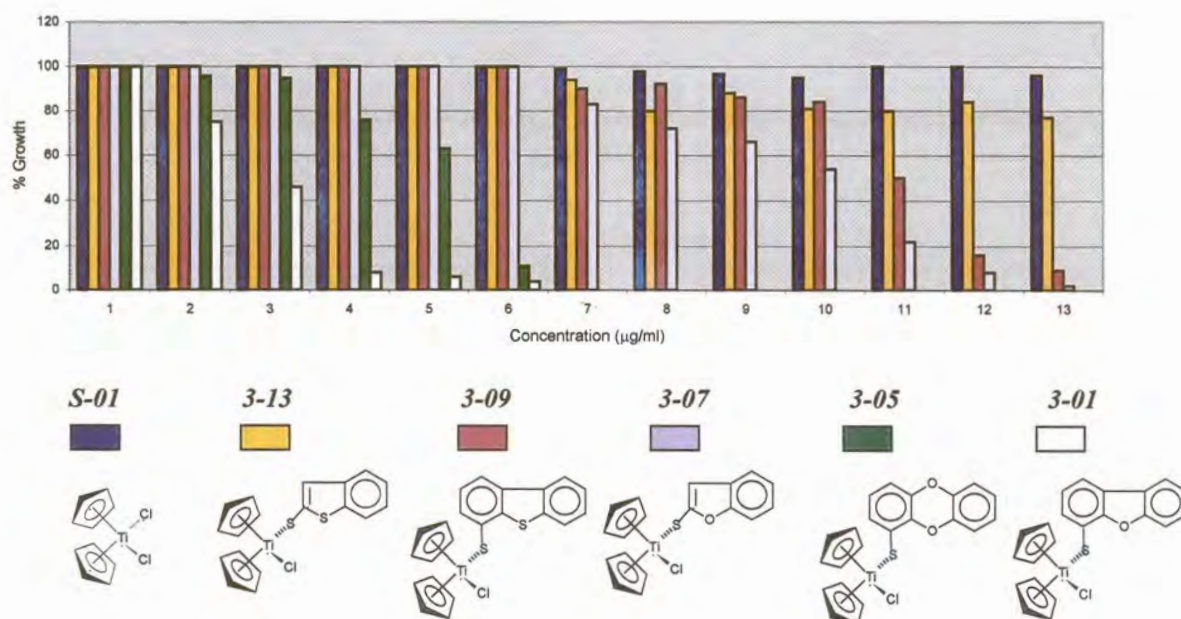


Figure 5.3. Inhibition of CoLo cells by **S-01**, **3-01**, **3-05**, **3-07**, **3-09** and **3-13**.

(ii) The role of the heteroatom(s) in the condensed rings of the ligand

In Figures 5.3 and 5.4 the role of different heteroatoms in the rings of the condensed heteroaromatic ligand is also demonstrated. It is clear that the ligands with oxygen as heteroatom achieved better inhibition results than their sulfur analogues.

(iii) The number of heteroatoms in the ligand

In Figure 5.4 the cell inhibition data of the two standards, **S-01** and **3-05** and the complexes **2-01**, **2-05** and **3-01** are given. It follows that the complexes with one oxygen heteroatom in the condensed ring was more effective in suppressing cell growth than the complexes with two oxygen atoms.

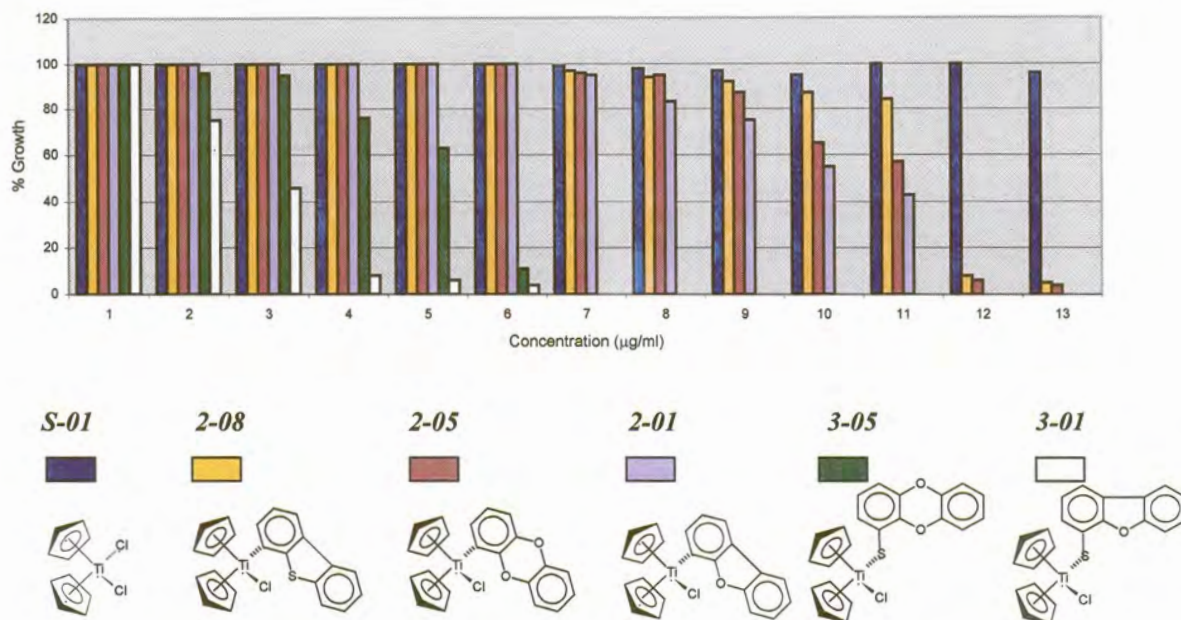


Figure 5.4. Inhibition of CoLo cells by S-01, 2-01, 2-05, 2-08, 3-01 and 3-05.

(iv) The role of substituents on the ring ligand

Figure 5.5 shows the results of the two standards, S-01 and 3-05 and the complexes 2-01, 2-03, 3-01 and 3-03. The substituent on the heteroaromatic ring ligand does not seem to have much of an effect on antitumor activity of the complex. This is evident in comparing 2-01 with 2-03 or 3-05 with 3-03. It was expected that a methyl group on the ring ligand would have an effect on intercalation.

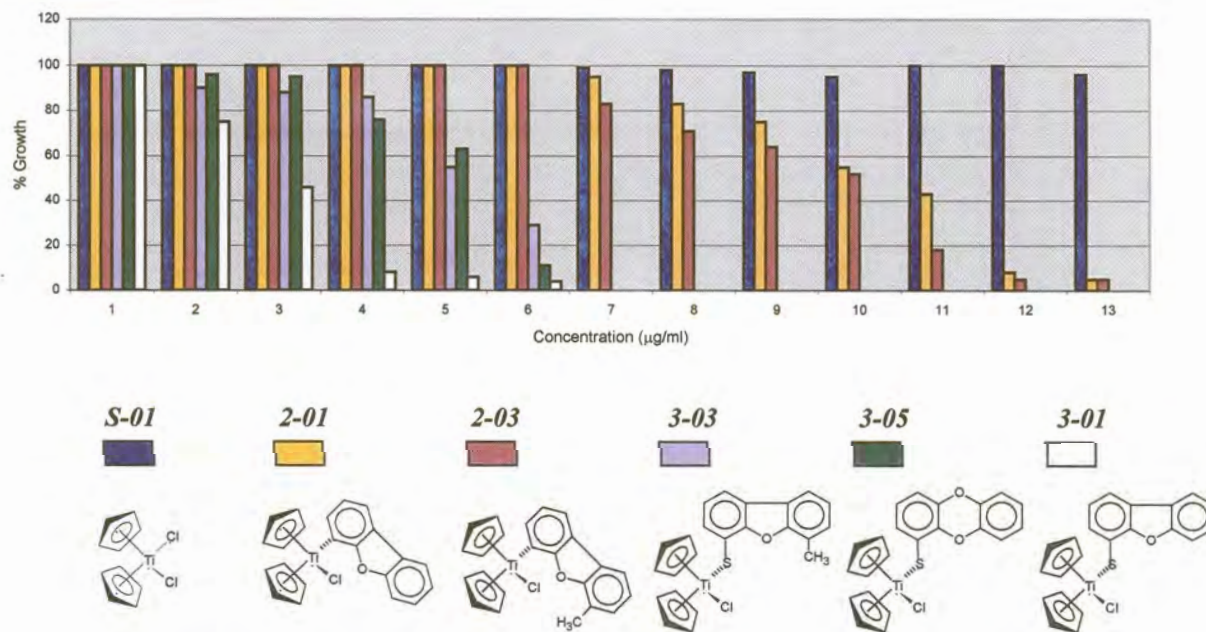


Figure 5.5. Inhibition of CoLo cells by S-01, 2-01, 2-03, 3-01, 3-03 and 3-05.

(v) The role of a spacer inserted between the metal and the rings

Figures 5.4 and 5.5 verify the observation made from Figure 5.1 that the insertion of a spacer atom between the metal and the heteroaromatic rings improve suppression of cell growth.

(vi) The role of the non-cyclopentadienyl ligands

In Figure 5.6 the results of the suppression of cell growth of the two standards, **S-01** and **3-05** and the complexes **3-01**, **3-02**, **3-06** and **2-11** are given. The complexes with one chloro ligand replaced by a thiolato ligand tested much better than the complexes where none or both chloro ligands were replaced by thiolato ligands. Thus, the order of activity of inhibiting cell growth is $[\text{TiCp}_2\text{Cl}_2] < [\text{TiCp}_2(\text{SR})_2] < [\text{TiCp}_2(\text{SR})\text{Cl}]$. Also the complex with a bidentate metallacyclic ring ligand had less activity than the complexes with one thiolato ligand.

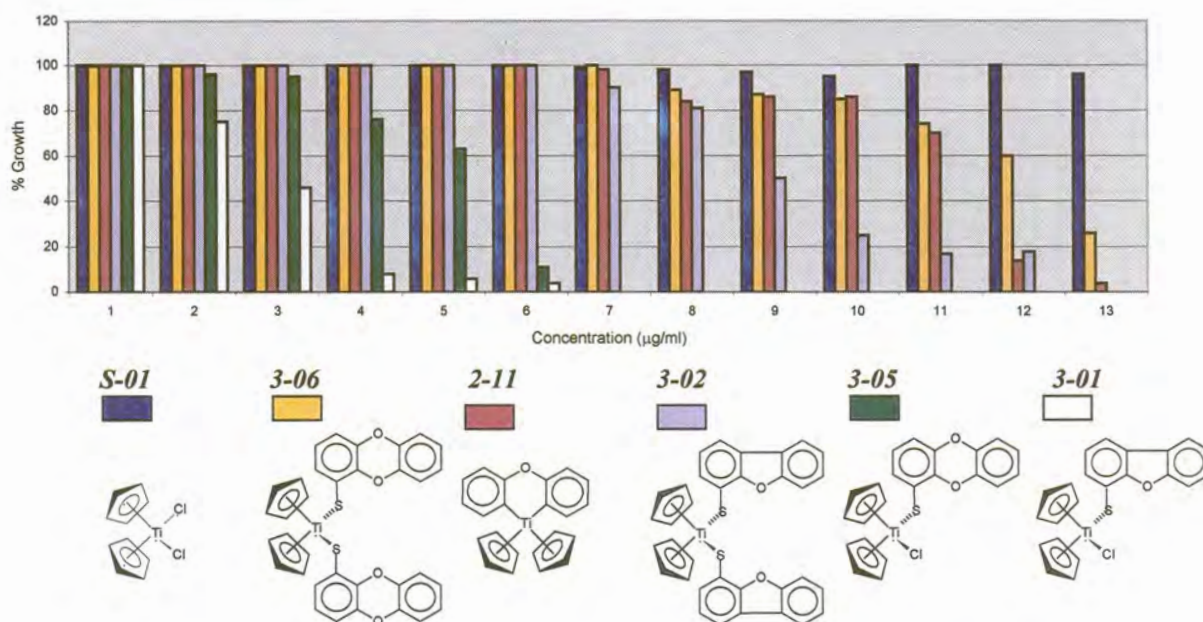


Figure 5.6. Inhibition of CoLo cells by **S-01**, **2-11**, **3-01**, **3-02**, **3-05** and **3-06**.

5.2.1 Conclusions

Of all the complexes tested for inhibiting cell growth, complex **3-01** gave the best results. This compound meets all the requirements of design implicated by the assumptions made for interacting with DNA. It has (i) a labile chloro ligand to afford a vacant coordination site for covalent bonding and (ii) display a condensed heteroaromatic ligand of favorable size for intercalation. The question remains whether the orientation of the different ligands in the complexes are such that they could participate in the above interactions effectively.

5.3 Structural features vs. antitumor activities

Correlation of activity with structure were studied by determining the solid state structures of **2-02**, **2-05**, **2-08** and **3-09** and comparing the structural features with cell growth suppression data. The structural requirements for effective covalent bond formation as well as intercalation into the major groove of DNA were compared with the molecular geometries of the complexes. The relative orientations of the two non-cyclopentadienyl ligands with respect to the two cyclopentadienyl ligands are important.

Figure 5.7 shows the structures of **2-05** and **2-08** that display the condensed ring ligand bound directly to the metal fragment. The metal, chloro and condensed heteroaromatic ring ligand are all part of the plane and these complexes are examples of metallointercalators. Hence only one of the modes of interaction, i.e. either covalent bonding or intercalation could be possible. The structures clearly show that this geometry would not be ideal for covalent bonding as well as intercalation into the major groove.

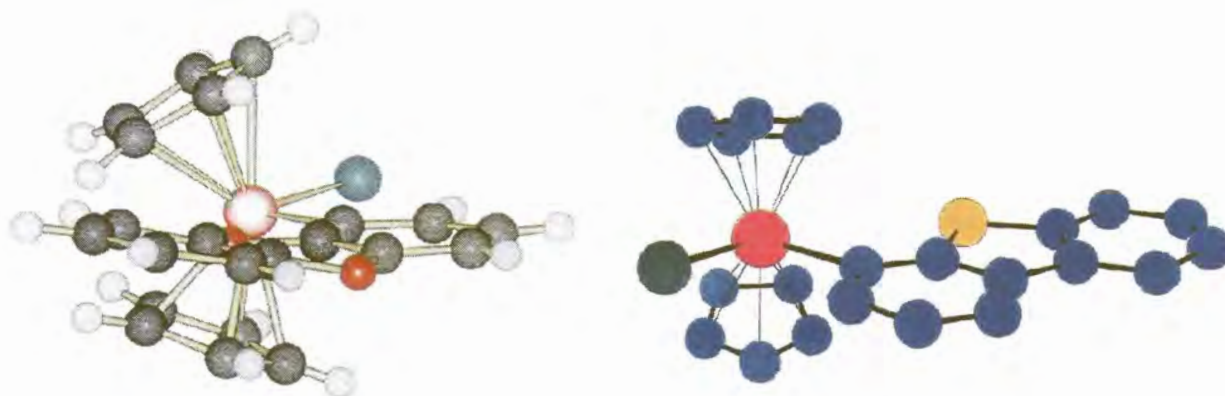


Figure 5.7. Molecular structures of **2-05** and **2-08**.

Figure 5.8 represents the molecular structure of a thiolato complex **3-09** with a sulfur atom as a spacer atom between the metal and the rings. This geometry is better suited for both intercalation and covalent bond formation, because the ligand is more flexible.

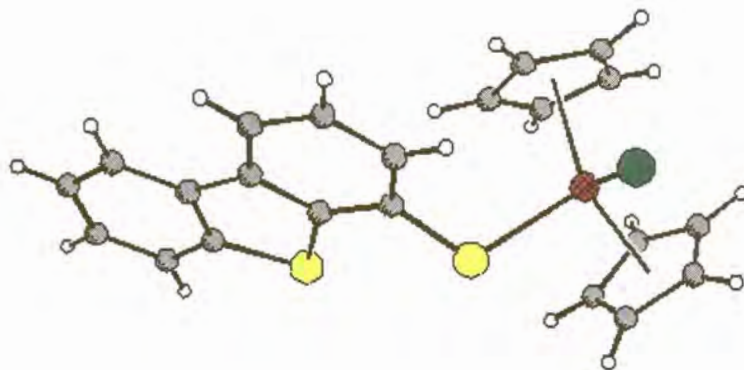


Figure 5.8. Molecular structure of 3-09.

Figure 5.9 shows the complex with two heteroaromatic ring ligands. This complex lacks an easily replaceable chloro ligand for covalent bond formation with DNA. Furthermore, the two rings are not configured ideally for intercalation.

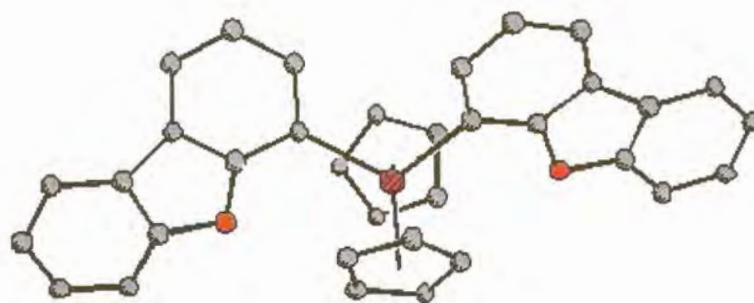


Figure 5.9. Molecular structure of 2-02.

A mechanism, based on the assumptions that the metal will covalently bond to an oxygen of the phosphate backbone of DNA and in addition be able to intercalate into the major groove of DNA, was tested by modeling the orientation of three rings bonded (i) directly and (ii) via a spacer atom to the metal within a fragment of DNA. In the first diagram (Figure 5.10) on the left side, the complex is shown being bonded covalently to the DNA backbone, but due to the geometry is not able to intercalate effectively. In the second diagram the complex is shown with a spacer atom between the metal and the intercalating rings. This allows for far greater flexibility making intercalation and simultaneous covalent bonding a reasonable assumption.

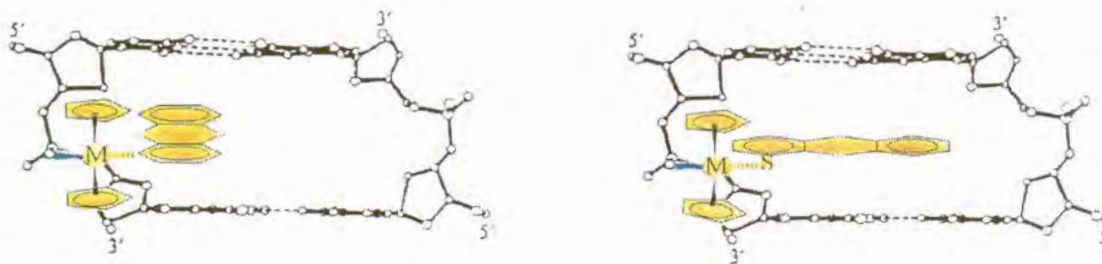


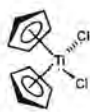
Figure 5.10. Geometrical constraints of complexes interacting with a double stranded DNA fragment.

5.3.1 Conclusions

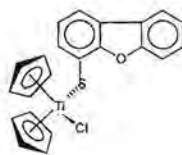
Good correlation was found between antitumor activity and the geometrical features of the compounds according to the requirements of the assumptions for both covalent bond formation and intercalation. The complex **3-09**, that are structurally best suited to participate in both modes of interaction with DNA of the compounds studied structurally, tested the best in inhibiting cell growth.

5.4 Ligand substitution in aqueous medium

To study the replacement of the ligands in the thiolato complexes, titanocene dichloride **S-01** was compared to **3-01** (the complex that showed the greatest cell growth inhibition) and the bithiolato complex **3-02**. A 0.25M solution of each complex in d^6 -DMSO was diluted in a saline (D_2O) solution in a 3:1 ratio. The solutions were kept at 37°C. The reaction was followed spectroscopically with 1H NMR and the chemical shifts recorded in the cyclopentadienyl and heteroaromatic regions as functions of time, as shown in Figures 5.11, 5.12, 5.13 and Appendix F. The results of **S-01**, **3-01** and **3-02** are compared.



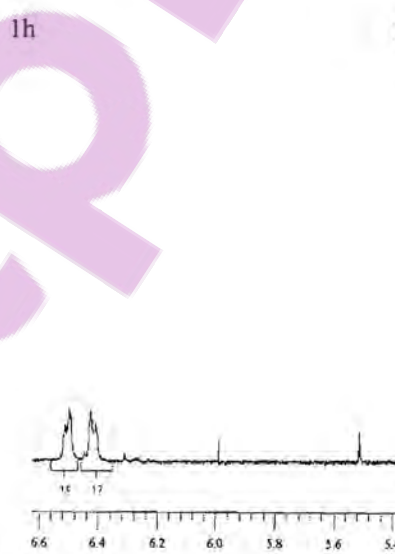
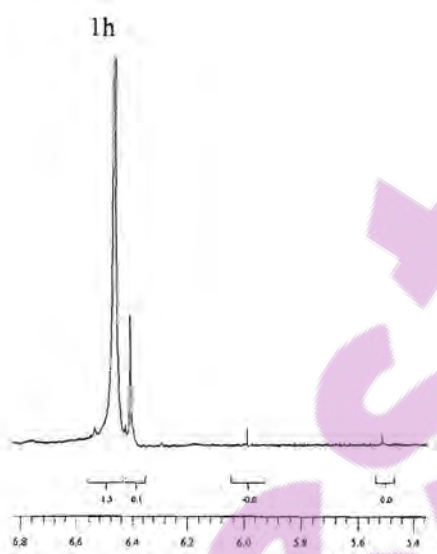
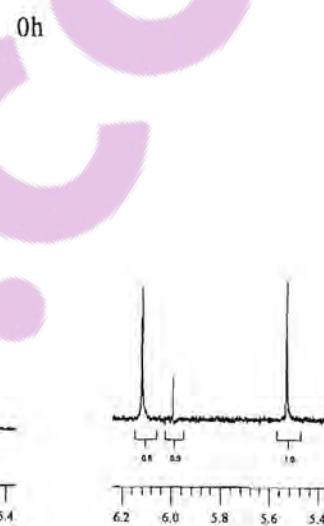
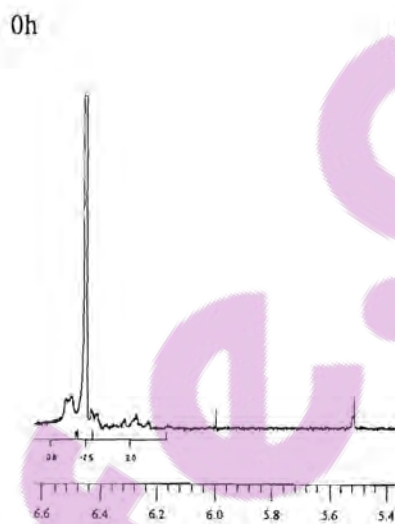
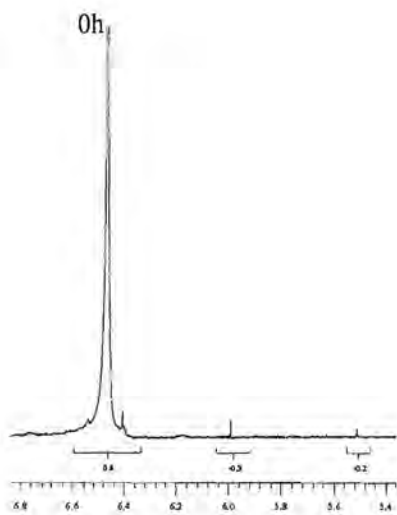
S-01



3-01



3-02



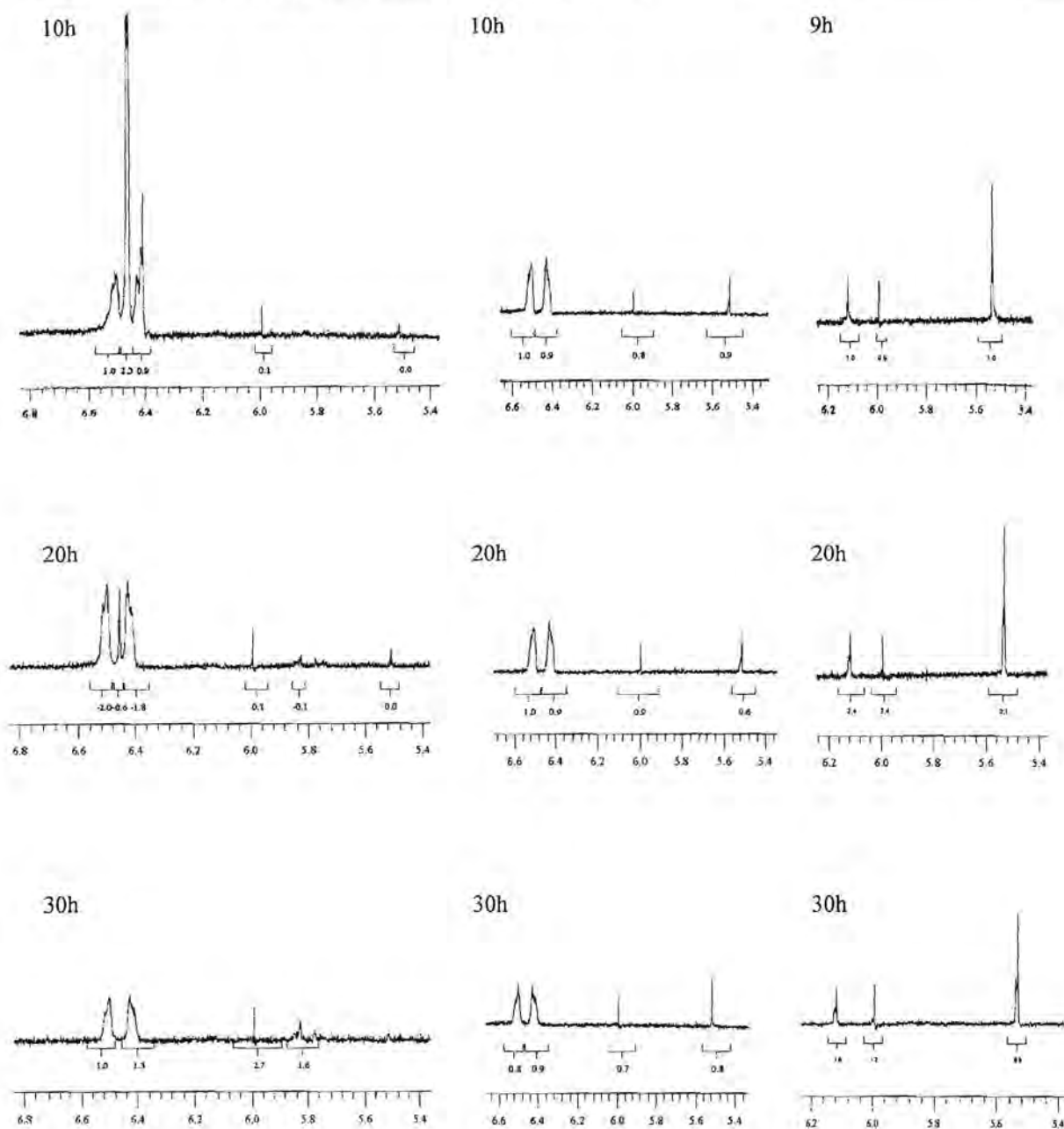
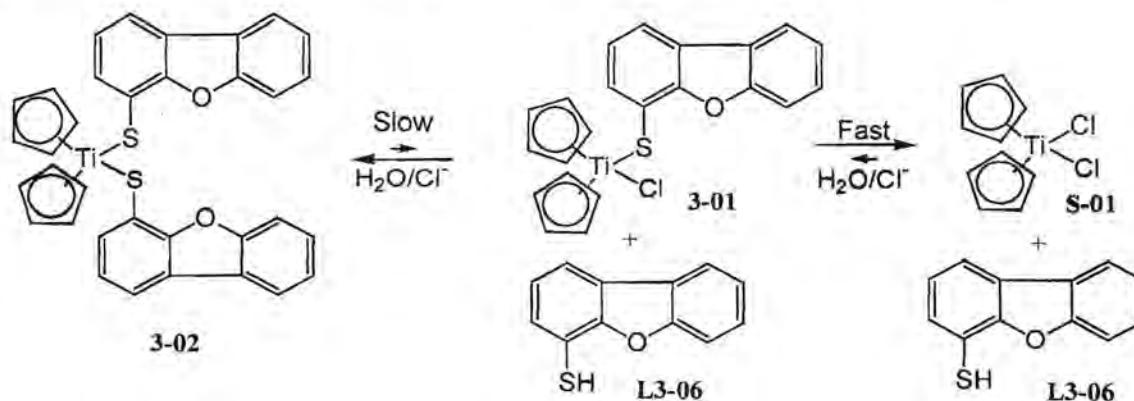


Figure 5.11. Comparison of Cp resonances in the ¹H NMR spectra of S-01, 3-01 and 3-02.

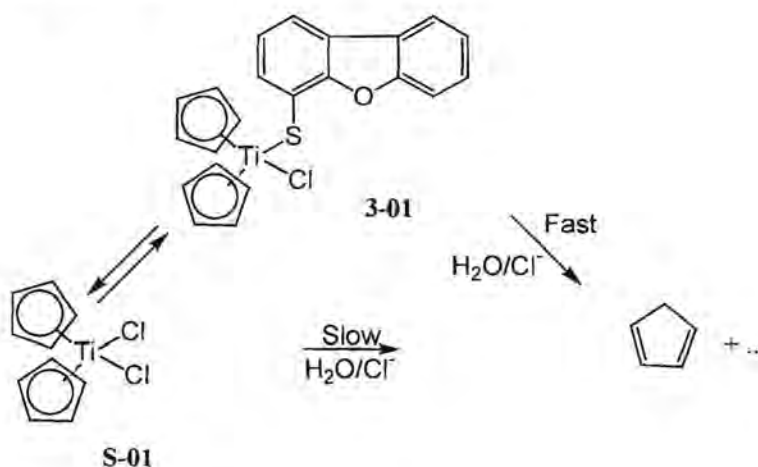
The hydrolysis of the Cp rings of S-01 started after 1h, were only significant after 10h and complete after 30h. For complex 3-01 hydrolysis started immediately and was complete after 1h. In fact, on mixing with the saline mixture the thiolate ligand was quickly replaced by Cl to give titanocene dichloride and dibenzofuranylthiol as products. Hence, after a short period of time the spectra are identical to the final spectrum of S-01. The fast disappearance of titanocene dichloride is ascribed to the presence of the thiolato ligand in solution. See Scheme 5.1. In complex 3-02 there was no visible

hydrolysis as compared to **S-01** and **3-01**, and the ratio of the peaks changed very little over time. Although **3-01** converts to **3-02**, the opposite is not true, not even in a saline mixture. From this information it was concluded that the dominant process for **3-01** in saline solution is equilibrated between titanocene dichloride and itself, whereas **3-02** is inert towards substitution reactions.

Displacement kinetics of the thiolato ligands



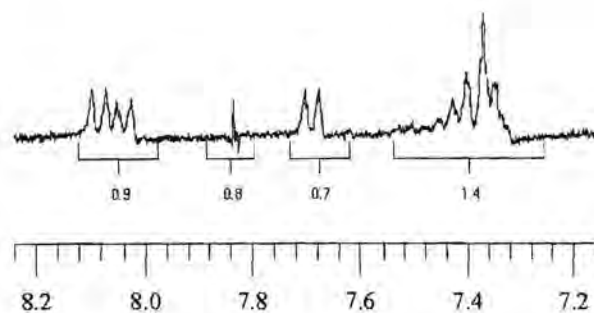
Cp-Hydrolysis of S-01 and 3-01



Scheme 5.1

The chemical shifts of the ^1H NMR spectra of **3-01** and **3-02** were also studied in the aromatic region to obtain information of the substitution of the thiolato ligands. Figure 5.12 displays the spectra for **3-01** at the start of the experiment and at the end after 30h. The chemical shifts of **3-01** in the aromatic region were assigned to those of dibenzofuranylthiol and did not change at all between the start of the experiment and after 30h. This result supports the hydrolysis data of the cyclopentadienyl rings and confirms rapid displacement of the thiolato ligand.

0h



30h

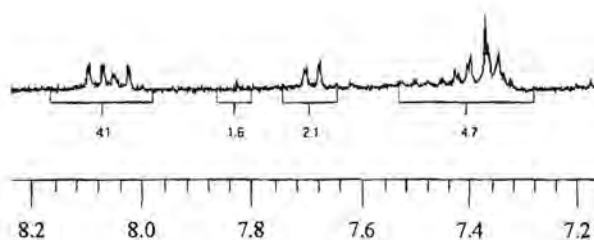
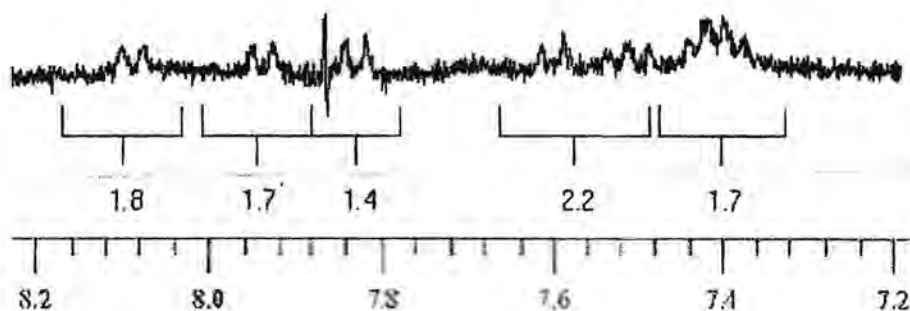


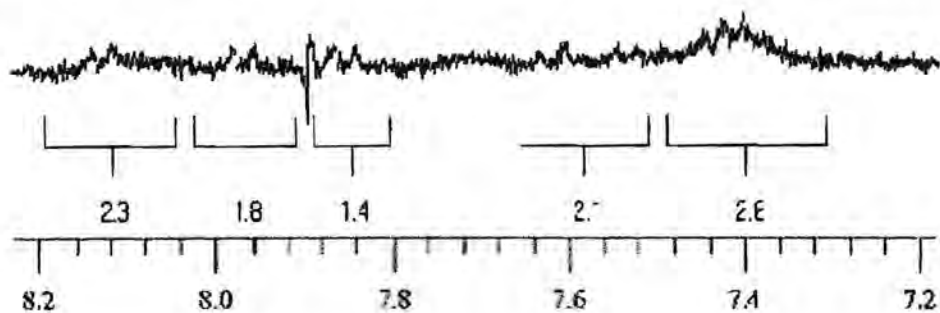
Figure 5.12. ^1H NMR resonances in the aromatic region of **3-01**.

By contrast, the resonances assigned to the thiolato ligand of **3-02** changed slowly over time. Figure 5.13 display patterns for the chemical shifts that changes gradually. In the time frame 0-3h, resonances of the bithiolato complex **3-02** dominates, whereas, a similar pattern is found for **S-01**, i.e. uncoordinated dibenzofuranylthiol, after 30h. In the intermittent time (6-9h) the pattern belongs to a solution containing both **3-02** and the thiol of **3-01**. The inertness of the thiolato ligands in solution of **3-02** and the high rate of displacement of the thiolate ligand of **3-01** is again demonstrated by these results.

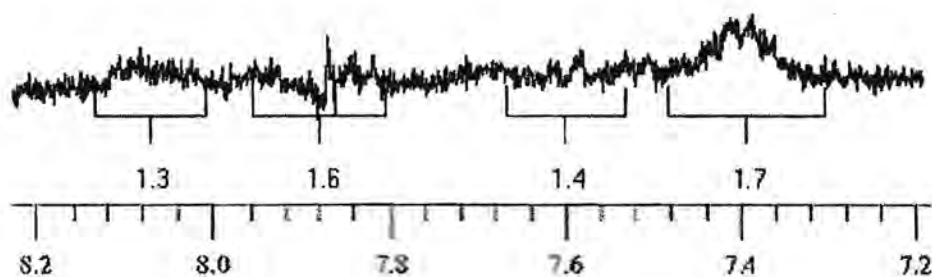
0h



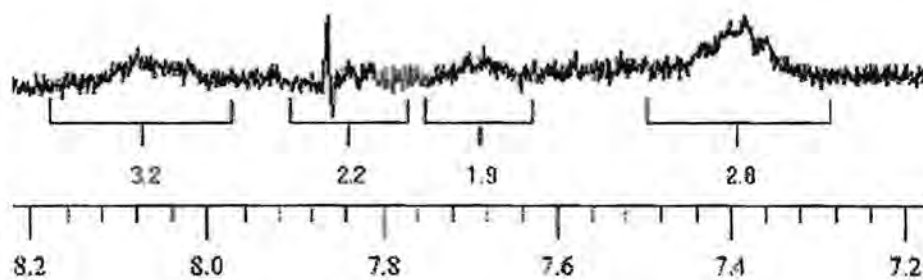
3h



7h



20h



30h

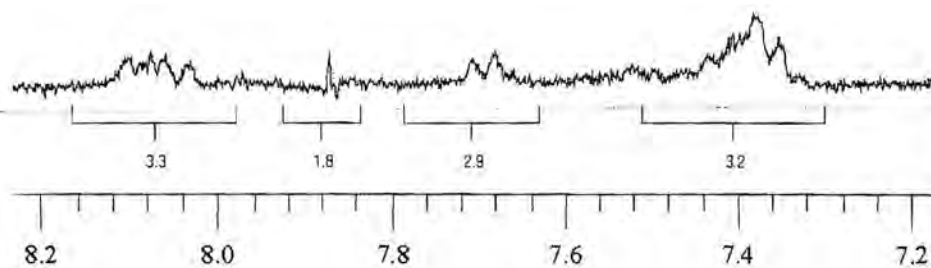


Figure 5.13. Substitution of the thiolato ligand of complex 3-02.

5.4.1 Conclusions

The data support substitution of ligands in the order SR, Cl > Cp and rates the stability against substitution of the complexes in the order $[\text{TiCp}_2(\text{SR})_2] > [\text{TiCp}_2\text{Cl}_2] > [\text{TiCp}_2(\text{SR})\text{Cl}]$ under the conditions of a DMSO/saline solution. The kinetic data does not support the initial assumptions pertaining to interactions with DNA. It does however show that **3-01**, which is the strongest inhibitor of cell growth, is also the least stable compound under the conditions applied.

5.5 Intercalation studies

The complexes were designed to intercalate with DNA and it was decided to perform some DNA intercalation tests using a technique based on flow cytometry. This was done to see if there was a correlation between antitumor activity and intercalation. Flow cytometry gives scattering information which could be applied to measure the winding characteristics of nucleoids. This is done by comparing the forward and side scattering of laser light through the substrate under regulated conditions. Figure 5.14 shows a model of the super coiled DNA that was used in the experiments. Intercalation will cause the DNA to unwind and then further intercalation will cause the DNA to wind up in the opposite direction. It is these phases of winding and unwinding that cause the scattering of the laser light to vary. The more complex and compact (dense) the structure of the substrate the greater the side scattering. By comparing the forward and side scattering as a function of concentration it should be possible to determine whether the complex will intercalate or not.

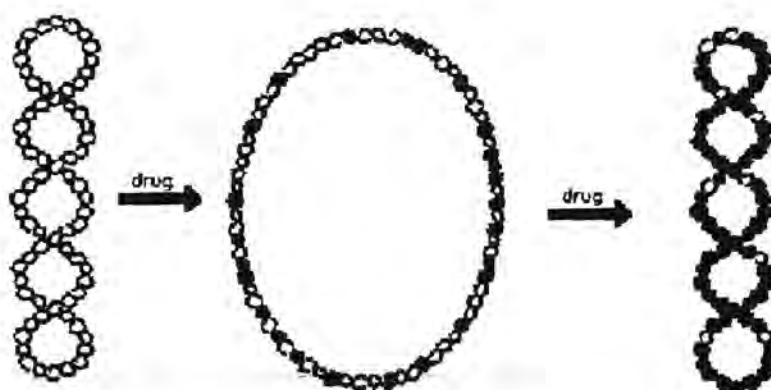


Figure 5.14. The unwinding and winding of super coiled DNA due to intercalation.

The intercalating abilities, as derived from the flow cytometry results of the complexes, were compared against similar data obtained for the known intercalators ethidium bromide (Figure 5.15),

doxorubicin (Figure 5.16) and propidium iodide (Figure 5.17)². At low concentration, where intercalation takes place, the nucleoids are unwound leading to a less dense substrate and an increase in forward scattering (FS) of the laser light and a comparably smaller increase in side scattering (SS). This is seen in the concentration range of 0.2-30.0 μg intercalator/mL. Intercalation will however lead to rewinding of the DNA at higher concentration and the difference between forward scattering and side scattering will decrease again to give a characteristic curve as seen in Figures 5.16 – 5.17. The sharp increase in side scattering at very high concentrations is ascribed to a much denser substrate resulting from an increase in the number of covalent bond formations of the complexes with DNA.

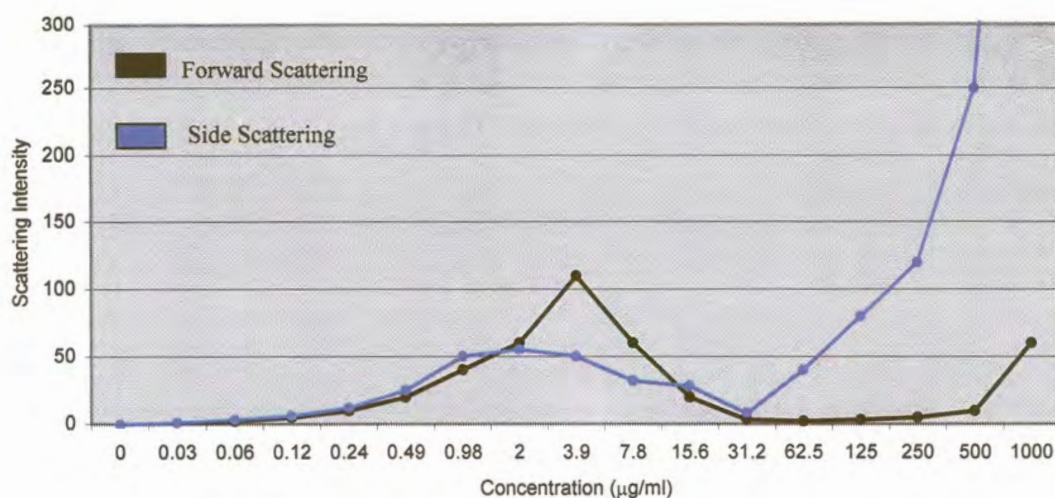


Figure 5.15. Intercalation of ethidium bromide with DNA.

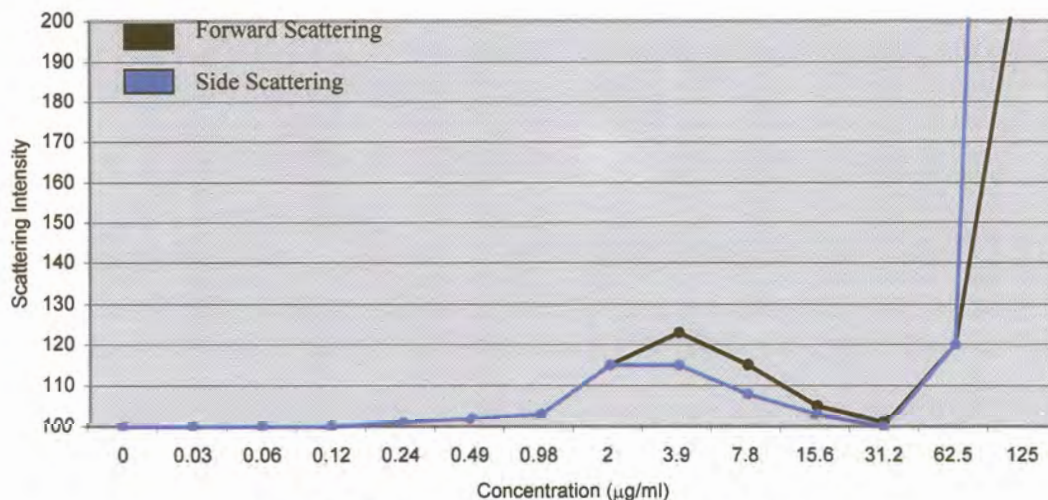


Figure 5.16. Intercalation of doxorubicin with DNA.

2. S. J. Lippard, *Acc. Chem. Res.*, 1978, 11, 211.

Figure 5.18 shows that very little unwinding of DNA occurred for **S-01** and therefore did not intercalate as the amount of forward scattering and side scattering are approximately constant at all concentrations. The results are in agreement with what was expected because the titanocene dichloride has no planar heteroaromatic ligands required for intercalation.

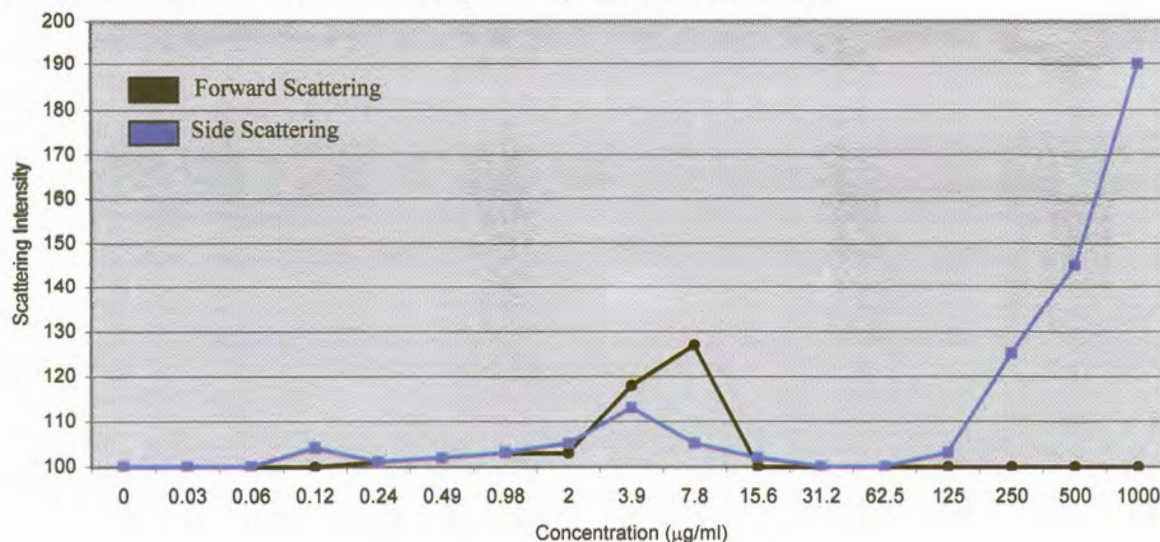


Figure 5.17. Intercalation of propidium iodide with DNA.

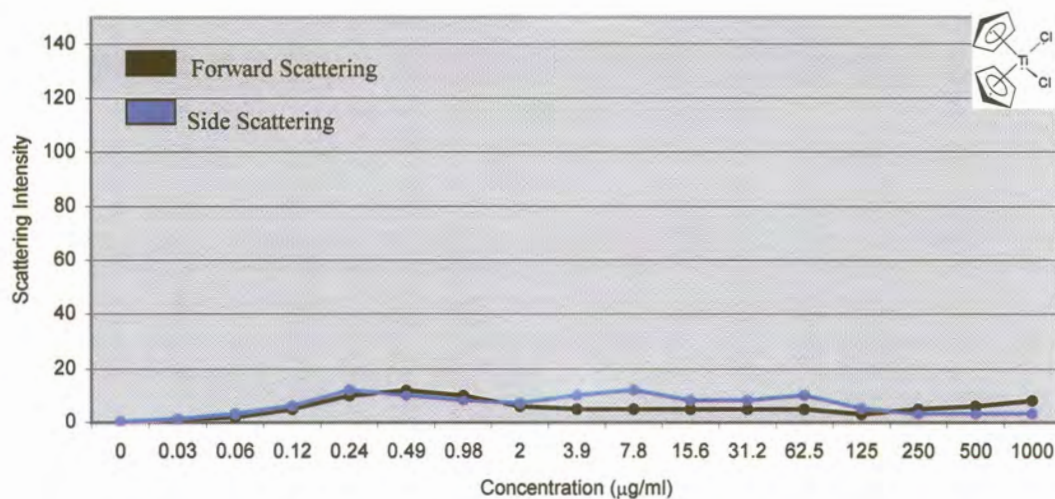


Figure 5.18. Intercalation studies of **S-01** with DNA.

Figure 5.19 shows the profile for **3-01** and it was concluded that no intercalation took place. At 2.4µg/ml the small difference between forward vs. side scattering was considered insignificant. The increase of side scattering is only observed at higher concentrations. This was ascribed to bond formation of **3-01** and an oxygen atom of the phosphate groups of DNA and as a result leading to a denser structure. This could also be interpreted that the mechanism of action of the new complexes is different from that of **S-01**.

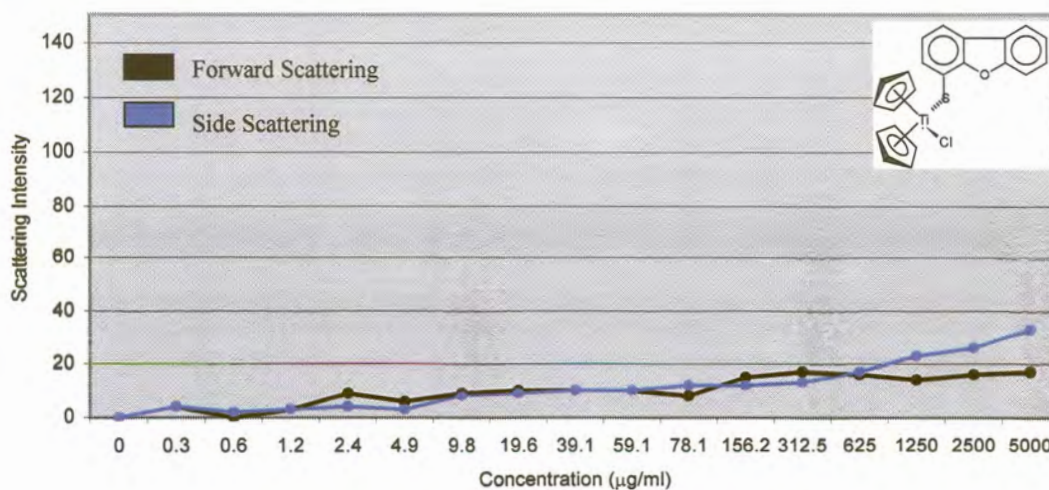


Figure 5.19. Intercalation studies of **3-01** with DNA.

Figure 5.20 shows the graph of one of the uncoordinated heteroaromatic substrates **L2-06** that displayed the same profile typical of that of an intercalator. No further interaction with DNA was observed at high concentrations.

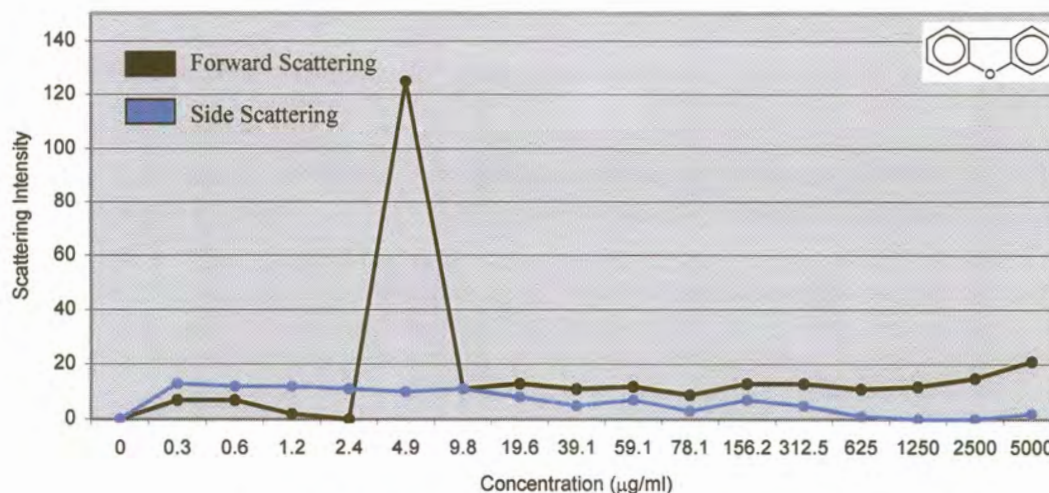


Figure 5.20. Intercalation studies of **L2-06** with DNA.

In Figure 5.21 no intercalation of the complexes with DNA was observed at lower concentrations, but at very high concentrations there was a sudden increase in side scattering. A possible explanation is that the complexes are sticking to the DNA strand and this causes increased scattering of the laser light. As observed in Figure 5.18, complex **S-01** showed no increase in side scattering at high concentrations. The complexes with thiolato ligands (**3-01** and **3-09**) showed significant increase in side scattering at higher concentrations.

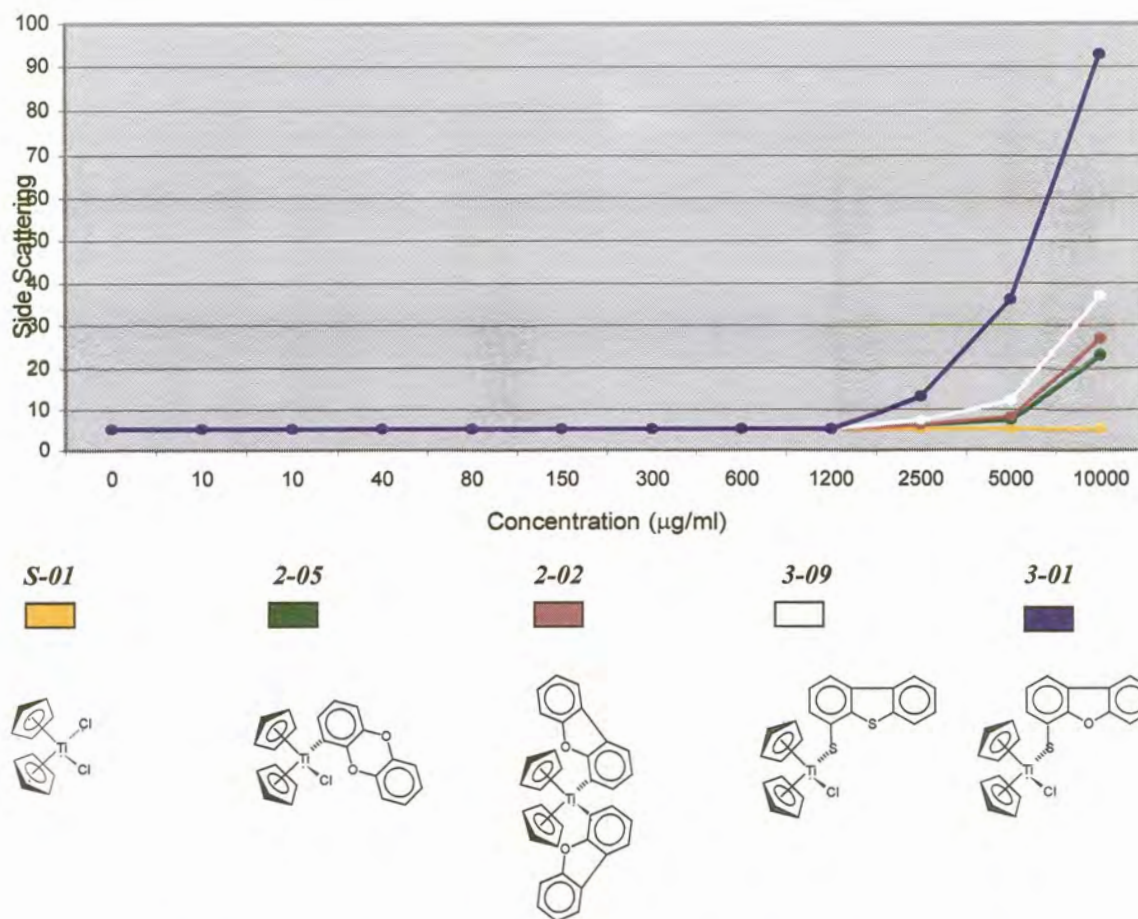


Figure 5.21. DNA bond formation of some complexes based on side scattering data.

5.5.1 Conclusions

The flow cytometry results confirmed that the species did indeed interact with DNA, but not by means of intercalation. When comparing the side scattering of the different compounds (Figure 5.21) the complexes that were expected to intercalate least caused less side scattering. This is not a contradiction but could mean that they have lower activities because their covalent binding ability to DNA was also weaker or slower. The two complexes that performed best in the antitumor tests caused *increased side scattering at higher concentrations*. It was concluded that the antitumor activity of the new titanocene derivatives with a heteroaromatic ring ligand could be ascribed to covalent bond formation with DNA, but not because of intercalation into the DNA grooves.

5.6 Summary of test results and DNA interaction

From these studies it was concluded that the increased antitumor properties of the titanocene derivatives result from covalent bond formation to DNA, most likely the phosphonate backbone of DNA. This observation is supported by studies of Sadler and co-workers who recently showed that the Ti(IV) hydrated ion would bind preferentially at an oxygen atom of the phosphate backbone of DNA³. The cytometry results do not, however, explain the increased activity of the complexes containing heteroaromatic ring ligands compared to titanocene dichloride. The thiolato ligands must play an important role to increase the activities. At first it was thought that the combined effect of titanium ion and the heteroaromatic substrate could account for the higher activities, but it was shown that for most heteroaromatic rings which were tested separately, very little antitumor activity was detected. The complexes with the highest antitumor activities were those that were the least stable in aqueous solution as was shown with the ligand substitution studies. The heteroatom in the mono thiolate complex could facilitate favourable substitution of the remaining chloro ligand in these complexes. This could also account for the fact that oxygen tested better than sulfur, as titanium is a hard metal centre.

At this point of time with the data generated from cell growth inhibition experiments, structural features and compositions of complexes, stability in saline solution against ligand substitution and intercalation studies, other mechanisms of interaction that differ from the pre-proposed modes of interaction with DNA, need to be considered. The inclination is to more seriously investigate the possibility that the antitumor activity of the titanium complexes of this study may arise from the ability of the titanium ion to take part in charge transfer processes as was proposed by Osella¹ for ferrocenyl species. It was not possible to determine the composition of the titanium species that bind to DNA. This implies that titanium is delivered at a rate determined by the thiolato ligands in the cells, leading to the formation of highly active radicals (OH^{\bullet} and O_2^{\bullet}) which could cleave DNA strands and cause cell deaths. This could explain the concentration dependence of the antitumor activities of the complexes. However, unlike Fe(II)/Fe(III) the titanium couple Ti(III)/Ti(IV) is unstable in aqueous medium and without further studies the Osella radical mechanism seems a less likely explanation for the titanocene derivatives.

3. M. Quo, Z. Quo, P. J. Sadler, *J. Biol. Inorg. Chem.*, 2001, 7, 698.

Chapter 6

Experimental

6.1 General

The following conditions applied throughout the synthesis of new complexes, unless stated otherwise in the method. Standard Schlenk methods were used as described by Shriver¹. All the solvents were distilled under inert reflux conditions and stored under dry nitrogen gas². THF was used immediately after distillation. Column chromatography was performed by circulation of cooled *iso*-propanol through the column jacket. Products were stored at 5°C under dry argon or nitrogen gas.

Characterization of complexes was done in an inert atmosphere, where possible. Melting points were determined on a Gallenkamp Melting Point Apparatus and are uncorrected. Nuclear magnetic resonance spectra were recorded on a Bruker AC-300 spectrometer. The ¹H and ¹³C NMR spectra were measured at 300.135 and 75.469MHz, respectively. Chemical shifts are reported as δ -values in parts per million (ppm) using the deuterated solvent signal as the internal reference. Deuterated chloroform (calibrated at δ H = 7.2400 ppm) was used as the routine solvent to record spectra and where not appropriate, deuterated DMSO (calibrated at δ H = 2.4900 ppm) was used. Microanalysis was obtained from the analytical section of the Division for Energy Technology of the Council of Scientific Research (CSIR) in Pretoria. High-resolution mass spectra were recorded on a Finnegan 8200 spectrometer.

Silica gel plates, silica gel 60 (0.200 – 0.063mm) and all other chemicals used are commercially available, except dibenzo[1,4]dioxin, which was synthesized according to methods described in literature³. All solid reagents were used without prior purification, while the liquid reagents were distilled. Deprotonations were carried out with *n*-BuLi, which was a 1.6mol/dm³ solution in hexane.

1. D. F. Shriver, M. A. Drezdson in *The Manipulation of Air-Sensitive Compounds*, 2nd edition, John Wiley and Sons, New York, 1986.

2. D. D. Perrin, W. L. F. Armarego, D. R. Perrin in *Purification of Laboratory Chemicals*, 2nd edition, Pergamon, New York, 1980.

3. H. H. Lee, W. A. Denny, *J. Chem. Soc. Perkin Trans. 1*, 1990, 1071-1074.

6.2 Lithiation and synthesis of heteroaromatic compounds

The lithiation procedures of the heteroaromatic molecules are summarized in Table 6.1 and the synthesis of heteroaromatic compounds are found in Table 6.2.

General lithiation methods using n-butyl lithium

Method A: At -30 °C n-butyl lithium (7.0ml, 11mmol) was added to a stirred solution of the heteroarene in 20ml THF. After stirring for the indicated time, the mixture was cooled to -50°C for subsequent reactions.

Method B: At -30 °C TMEDA (3.4ml, 11mmol) was added to a stirred solution of the heteroaromatic substrate in 20ml THF. n-Butyl lithium (7.0ml, 11mmol) was added and the solution stirred for the required time at -30 °C. The mixture was cooled to -50°C for subsequent reactions.

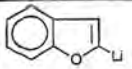
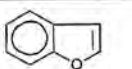
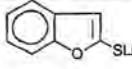
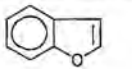
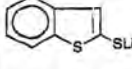
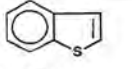
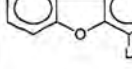
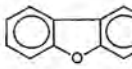
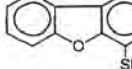
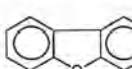
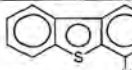


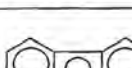
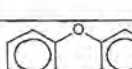
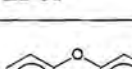
Method C: At 0°C 20ml THF was added to a stirred solution of n-butyl lithium (7.0ml, 11 mmol) in 20ml hexane. The solution was cooled to -50°C and the heteroarene added slowly (over 1 minute). After heating to -20 °C, the mixture was stirred for the indicated time and cooled to -50°C for subsequent reactions.

Method D: At room temperature (RT) 150ml hexane, 100ml diethyl ether and the heteroarene was mixed. TMEDA (15.0ml, 20.0mmol) and n-butyl lithium (14.0ml, 20.0mmol) was added subsequently. The solution was allowed to stand for the indicated time period at RT and a precipitate settled out. The suspension was cooled to -50°C for subsequent reactions.

Method E: At -30 °C n-butyl lithium (7.0ml, 11mmol) was added to a stirred solution of the heteroaromatic substrate in 20ml THF. After stirring for the indicated time, the temperature was raised to 0°C and stirring continued for another 2h. The mixture was cooled to -50°C for subsequent reactions.

Method F: At -30 °C n-butyl lithium (7.0ml, 11mmol) was added to a stirred solution of the heteroarene in 20ml THF. The temperature was raised to 0°C and stirred for the required time. The solution was cooled to -50°C for subsequent reactions

Table 6.1 Lithiation procedures of the heteroaromatic substrates used in this study.

Lithiated Precursor	Starting Compound	Method	Amount of starting material (mmol, g)	Reaction time (h)	Colour of lithiated product	Reference
	 L2-05	C	10.0; 1.1ml	30min.	Pink turns yellow	4
	 L2-05	C + G	10.0; 1.1ml	30min. + 20min.	Bright yellow	4
	 L2-02	A + G	10.0; 1.34	30min. + 20 min.	Orange-yellow	4, 5
	 L2-06	A	10.0; 1.68	5	Bright yellow	4, 6
	 L2-06	A + G	10.0; 1.68	5 + 2	Orange	4, 7
	 L2-01	F	10.0; 1.84	5	Deep orange	4, 7
	 L2-01	F + H	10.0; 1.84	5 + 1	Deep orange turns green, then yellow	4, 7
	 L2-03	B	10.0; 1.84	1	Bright yellow	4, 8

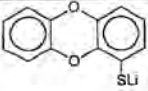
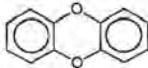
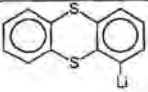
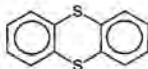
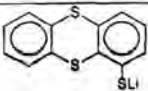
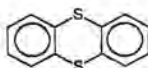
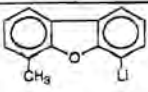
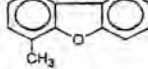
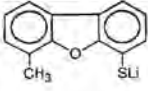
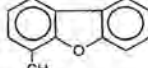
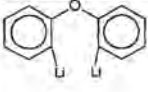
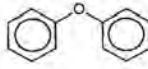
4. L. Brandsma, H. Verkruysse, *Preparative Polar Organometallic Chemistry I*, Springer-Verlag (Berlin, Heidelberg) 1987, 215-235

5. H. E. Gschwend, H. R. Rodriguez, *Org. React.*, 1979, 26, 1.

6. H. Gilman, S. Gray, *J. Org. Chem.*, 1958, 23, 1476.

7. C. Cuehm-Caubere, S. Adach-Becker, Y. Fort, P. Caubere, *Tetrahedron*, 1996, 52, 9087.

8. B. D. Palmer, M. Boyd, W. A. Denny, *J. Org. Chem.*, 1990, 55, 438.

	 L2-03	B + G	10.0; 1.84	1 + 15min.	Orange-brown	4, 8
	 L2-04	B	10.0; 2.16	2	Bright yellow	4, 10
	 L2-04	B + G	10.0; 2.16	2 + 15min.	Orange-brown	4, 10
	 L2-07	E	10.0; 1.82	1.5	Brown yellow turns yellow	4, 8
	 L2-07	E + G	10.0; 1.82	2 + 15min	Orange	4, 8
	 L2-08	D	10.0; 1.70	3	Brown red precipitate	4

General method to prepare lithiated thiolates

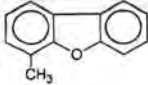
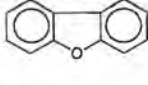
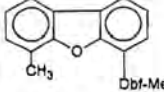
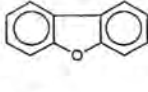

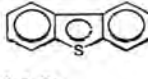
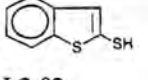
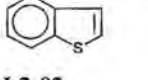
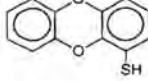
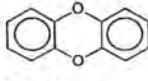
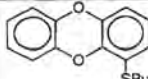
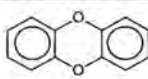
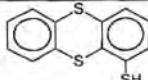
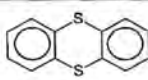
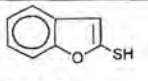
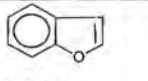
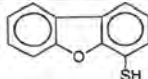
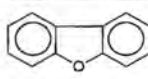
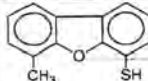
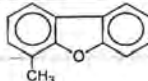
Method G: After lithiation of the substrate, flowers of sulfur (0.32g, 10mmol) was added in one portion, stirred for the indicated time at -50°C or until all of the sulfur reacted. The solution was ready for subsequent reactions.

Method H: After lithiation of the substrate, flowers of sulfur (0.32g, 10mmol) was added in one portion at -10°C. After stirring for the indicated time at RT, the solution was ready for subsequent reactions.

Addition of a methyl substituent (L2-07)

Method I: After lithiation of the substrate, MeI (0.65ml, 10mmol) was added and stirred for 30 minutes at -30°C. The mixture was removed from the cold and allowed to raise room temperature and stirring was continued for another 12h. The yellow-white solution was poured into water and extracted with ether. The ether layers were dried over MgSO₄ and evaporated to give a yellow oil. Column chromatography on silica gel with 1:1 hexane:dichloromethane as eluent gave 1-methyldibenzofuran (first fraction), a yellow waxy compound (1.46g, 80.22%). Recrystallization

Table 6.2 Synthesis of heteroaromatic precursors used in this study.

Heteroaromatic Precursor/Product	Starting Compound	Method	Amount of starting material (mmol; g)	Reaction time (h)	Colour and yield of product (g; %)	Reference
 L2-07	 L2-06	A + I	10.0; 1.68	5 + 12	White waxy solid 1.46; 80.2	4, 8
 L2-07b	 L2-06	A + I	10.0; 1.68	5 + 12	White waxy solid 1.46; 80.2	4, 8
 L3-01	 L2-01	F + H + J	10.0; 1.84	5 + 1	White-yellow solid 1.58; 73.2	4, 5, 8
 L3-02	 L2-02	A + G + J	10.0; 1.34	30min. + 20 min.	White-yellow solid 1.20; 72.5	4, 6
 L3-03	 L2-03	B + G + J	10.0; 1.84	1 + 15min.	White-yellow solid 1.60; 74.1	4, 9
 L3-03b	 L2-03	B + G + J	10.0; 1.84	1 + 15min.	White-yellow solid 1.60; 74.1	4, 9
 L3-04	 L2-04	B + G + J	10.0; 2.16	2 + 15min.	Pale yellow solid 1.78; 71.6	4, 10
 L3-05	 L2-05	C + G + J	10.0; 1.1ml	30min. + 20min.	White-yellow solid 1.06; 70.6	4, 5
 L3-06	 L2-06	A + G + J	10.0; 1.68	5 + 2	Pale yellow solid 1.52; 76.1	4, 7
 L3-07	 L2-07	E + G + J	10.0; 1.82	2 + 15min	Pale yellow solid 1.58; 73.8	4, 8

from dichloromethane yielded white crystals. *Anal.* Calc. for $C_{13}H_{10}O$: C, 85.68%; H, 5.54%. Found: C, 86.29%; H, 5.02%.

Protonation of lithiated heteroaromatic thiolates

Method J: To protonate the thiolates, HCl gas was bubbled through the solution for about 5 minutes. The solution turned into a pale yellow, milky colour and the solvent was evaporated under reduced pressure. The pale yellow residue was filtered through silica gel with dichloromethane and the resulting residue was again filtered with hexane to wash away the unreacted dibenzodioxin. Chromatography with dichloromethane:hexane (1:1) as eluent, gave a white-yellow product, which precipitated as soon as the solvent started evaporating. *Anal.* Calc. for **L3-01** $C_{12}H_8S_2$: C, 66.62%; H, 3.74%. Found: C, 66.86%; H, 3.49%. *Anal.* Calc. for **L3-02** $C_8H_6S_2$: C, 57.83%; H, 3.65%. Found: C, 58.27%; H, 3.98%. *Anal.* Calc. for **L3-03** $C_{12}H_8O_2S$: C, 66.35%; H, 6.31%. Found: C, 66.66%; H, 6.49%. *Anal.* Calc. for **L3-04** $C_{12}H_8S_3$: C, 57.83%; H, 3.65%. Found: C, 57.97%; H, 3.78%. *Anal.* Calc. for **L3-05** C_8H_6OS : C, 63.99%; H, 4.04%. Found: C, 64.37%; H, 4.39%. *Anal.* Calc. for **L3-06** $C_{12}H_8SO$: C, 71.99%; H, 4.04%. Found: C, 72.44%; H, 4.48%. *Anal.* Calc. for **L3-07** $C_{13}H_{10}OS$: C, 72.94%; H, 4.67%. Found: C, 73.56%; H, 4.89%.

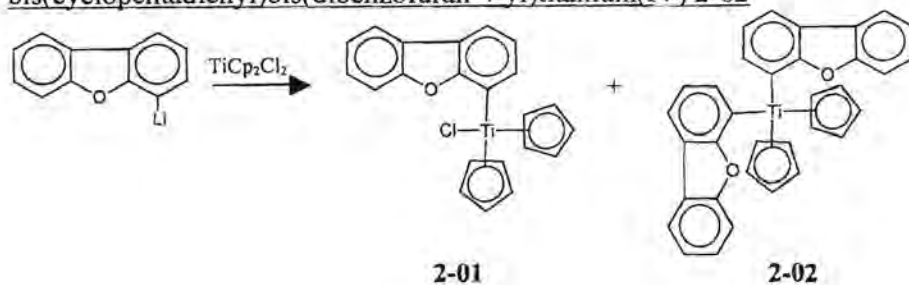
6.3 Synthesis of titanocene derivatives

The synthesis of new titanocene derivatives follows a general method, but the resulting complexes and the purification of the complexes are very different. A general procedure is given in the shaded area and thereafter follows the remaining details for each reaction.

General method for synthesis of titanocene derivatives (unless indicated otherwise)

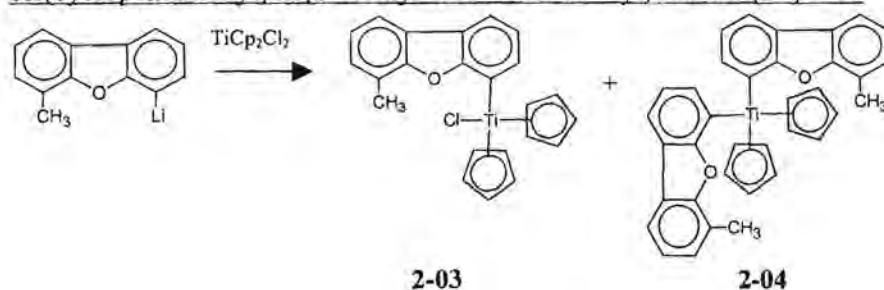
At -50°C the lithiated ligand mixture (Table 6.1) was added to a solution of titanocene dichloride (2.49g, 10.0mmol) in THF. A colour change of the reaction mixture was observed almost immediately and stirring was continued at -50°C for 30 minutes. The mixture was allowed to warm to room temperature and it was stirred for another 90 minutes. The solvent was evaporated and the residue was dissolved in dichloromethane and filtered through silica gel. The products were evaporated to dryness and the residue was stored under nitrogen at 5°C until it was subjected to purification. In all cases where column chromatography was used, the first fraction was colourless and was identified as unreacted heteroarene.

Synthesis of chlorobis(cyclopentadienyl)(dibenzofuran-4-yl)titanium(IV) 2-01 and bis(cyclopentadienyl)bis(dibenzofuran-4-yl)titanium(IV) 2-02



The general method described above was followed for lithiated dibenzofuran. The mixture was stirred for 10h at -30°C during which the colour of the reaction mixture changed from bright red to orange. After filtering, an orange residue remained which was subjected to column chromatography with aluminium oxide and with a 1:1 THF:hexane mixture as eluent. The first fraction was unreacted dibenzofuran and the second yellow band that followed was isolated and characterized, yielding bis(cyclopentadienyl)bis(dibenzofuran-4-yl)titanium(IV) **2-02** (1.79g, 34.9%) *Anal. Calc.* for $\text{C}_{34}\text{H}_{24}\text{O}_2\text{Ti}$: C, 79.66%; H, 4.73%. Found: C, 79.04%; H, 4.26%. The desired product, chlorobis(cyclopentadienyl)(dibenzofuran-4-yl)titanium(IV) **2-01** (0.39g, 10.2%), was collected as an orange band. *Anal. Calc.* for $\text{C}_{22}\text{H}_{17}\text{ClOTi}$: C, 69.38%; H, 4.51%. Found: C, 69.45%; H, 4.67%. Recrystallization of **2-02** in hexane:dichloromethane yielded orange crystals suitable for single crystal X-ray diffraction studies.

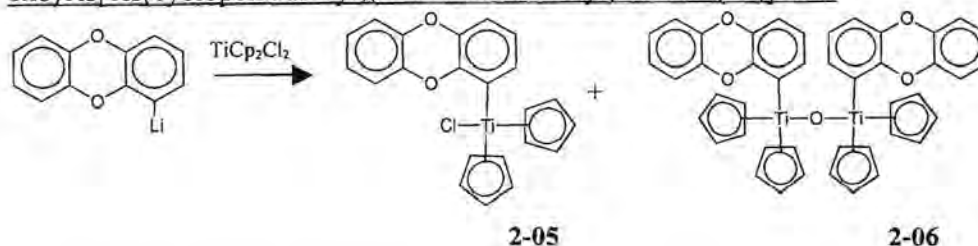
Synthesis of chlorobis(cyclopentadienyl)(6-methyl dibenzofuran-4-yl)titanium(IV) 2-03 and bis(cyclopentadienyl)bis(6-methyl dibenzofuran-4-yl)titanium(IV) 2-04



In this case the colour of the reaction mixture changed from bright red to yellow-brown. After filtering, an orange-brown residue was obtained which was subjected to column chromatography on silica gel and with a 7:1 hexane:THF mixture as eluent. The first fraction was a yellow band, identified as bis(cyclopentadienyl)bis(6-methyl dibenzofuran-4-yl)titanium(IV) **2-04** (2.27g, 42.0%). *Anal. Calc.* for $\text{C}_{36}\text{H}_{28}\text{O}_2\text{Ti}$: C, 79.97%; H, 5.23%. Found: C, 80.32%; H, 5.72%. An orange band followed, which was identified as the desired product chlorobis(cyclopentadienyl)(6-methyl

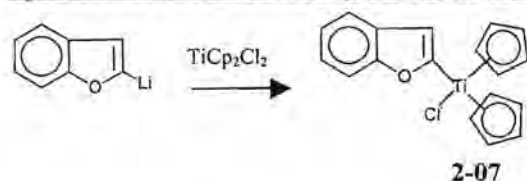
dibenzofuran-4-yl)titanium(IV) **2-03** (1.22g, 30.9%). *Anal.* Calc. for $C_{23}H_{19}ClO_2Ti$: C, 69.95%; H, 4.86%. Found: C, 69.65%; H, 4.43%.

Synthesis of chlorobis(cyclopentadienyl)(dibenzodioxin-1-yl)titanium(IV) **2-05** and (μ -oxo)bis[bis(cyclopentadienyl)(dibenzodioxin-1-yl)titanium(IV)] **2-06**



Following the general method with lithiated **L2-03** the colour of the reaction mixture changed from bright red to clear orange-brown and then to dark orange-brown. After filtering, the remaining orange residue was subjected to column chromatography on silica gel and with a 6:4 hexane:dichloromethane mixture as eluent. The desired product was obtained from an orange fraction, chlorobis(cyclopentadienyl)(dibenzodioxin-1-yl)titanium(IV) **2-05**. (Yield: 1.47g, 37.1%). Recrystallization from hexane/THF (1:1) gave bright orange, diamond shaped crystals with the solvents co-precipitating (mp.: 92°C). *Anal.* Calc. for $C_{22}H_{17}ClO_2Ti \cdot C_6H_{14} \cdot C_4H_8O$: C, 69.24%; H, 7.10%. Found: C, 69.45%; H, 7.22%. A yellow fraction was collected before the major product, but turned black on attempts to filter it with dichloromethane. Finally, a yellow product, (μ -oxo)bis[bis(cyclopentadienyl)(dibenzodioxin-1-yl)titanium(IV)] **2-06**, was collected by extracting and filtrating the black residue with benzene. (Yield: 2.07g, 28.0%). *Anal.* Calc. for $C_{44}H_{34}O_5Ti_2$: C, 71.53%; H, 4.65%. Found: C, 71.95%; H, 4.82%.

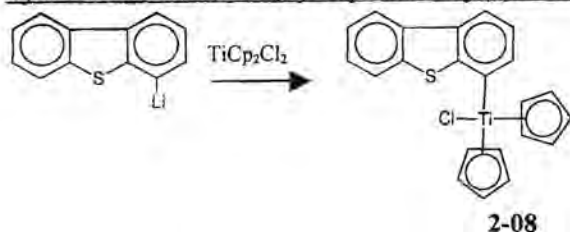
Synthesis of (benzofuran-2-yl)chlorobis(cyclopentadienyl)titanium(IV) **2-07**



Following the general method with lithiated **L2-05** the colour of the reaction mixture changed from bright red to bright orange. Due to decomposition on silica gel, an aluminium oxide filter was used instead and a bright red orange residue was obtained. The residue was subjected to column chromatography with aluminium oxide and with a 2:1 hexane:dichloromethane mixture as eluent. The first fraction was unreacted benzothiophene. The desired product, (benzofuran-2-yl)chlorobis(cyclopentadienyl)titanium(IV) **2-07** (1.49g, 45.0%), followed as a red-orange band. The

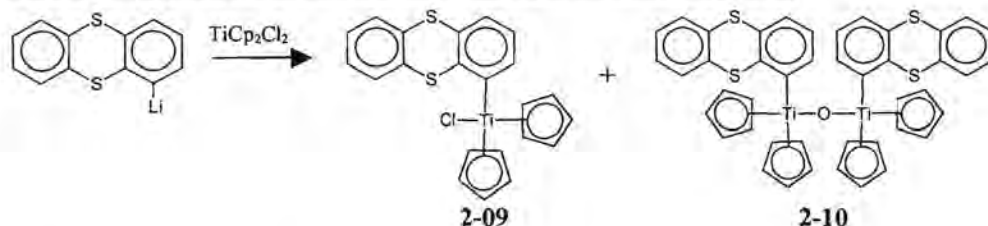
product was highly unstable and decomposed in air and at room temperature. It could be retained for only one week under argon at 5°C.

Synthesis of chlorobis(cyclopentadienyl)(dibenzothiophen-4-yl)titanium(IV) **2-08**

**2-08**

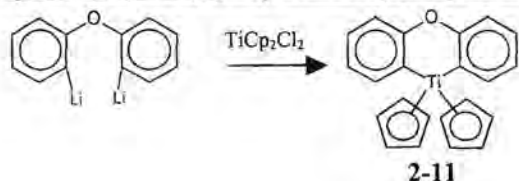
The general method was followed using lithiated **L2-01**. The mixture was stirred at -60°C during which time the colour of the reaction mixture changed from bright red to orange. After filtering, an orange residue remained which was subjected to column chromatography on silica gel with a 2:1 dichloromethane:hexane mixture as eluent. The desired product was isolated from an orange band, chlorobis(cyclopentadienyl)(dibenzothiophen-4-yl)titanium(IV) **2-08** (2.07g, 52.2%). *Anal. Calc.* for $\text{C}_{22}\text{H}_{17}\text{ClTi}$: C, 66.60%; H, 4.33%. Found: C, 67.02%; H, 4.67%.

Synthesis of chlorobis(cyclopentadienyl)(thianthren-1-yl)titanium(IV) **2-09** and (μ -oxo)bis[bis(cyclopentadienyl)(thianthren-1-yl)titanium(IV)] **2-10**.

**2-09****2-10**

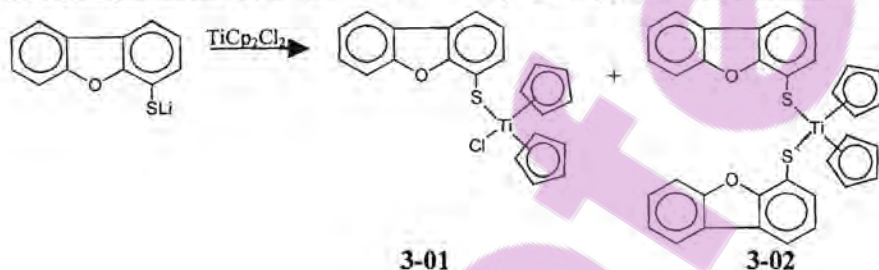
Using lithiated **L2-04** the mixture was stirred at RT for 2h. The colour of the reaction mixture changed from bright red to clear red-brown. After filtering an orange residue was left which was subjected to column chromatography on silica gel and with a 6:4 hexane:dichloromethane mixture as eluent. The desired product was isolated and characterized from an orange fraction to give, chlorobis(cyclopentadienyl)(thianthren-1-yl)titanium(IV) **2-09**. (Yield: 1.59g, 37.1%). Product **2-09** quickly converted to (μ -oxo)bis[bis(cyclopentadienyl)(thianthren-1-yl)titanium(IV)] **2-10**, a yellow band. (Yield: 2.51g, 31.3%). *Anal. Calc.* for $\text{C}_{44}\text{H}_{34}\text{S}_4\text{OTi}_2$: C, 65.83%; H, 4.28%. Found: C, 66.15%; H, 4.52%.

Synthesis of bis(cyclopentadienyl)(diphen-2,2'-yl ether)titanium(IV) 2-11



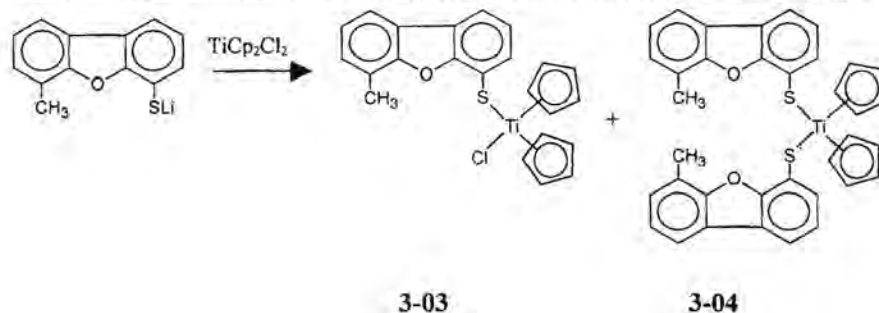
Following the general method with lithiated **L2-08** the colour of the reaction mixture changed from bright red to orange. After filtering an orange residue was subjected to column chromatography on silica gel and with a 1:1 hexane:dichloromethane mixture as eluent. The first yellow band was discarded and an orange band gave the expected product, bis(cyclopentadienyl)(diphen-2,2'-yl ether)titanium(IV) **2-11** (1.32g, 38.1%). *Anal. Calc.* for $C_{22}H_{18}OTi$: C, 76.30%; H, 5.25%. Found: C, 76.95%; H, 5.72%. The product was an oily residue.

Synthesis of chlorobis(cyclopentadienyl)(dibenzofuran-4-ylsulfanyl)titanium(IV) 3-01 and bis(cyclopentadienyl)bis(dibenzofuran-4-ylsulfanyl)titanium(IV) 3-02



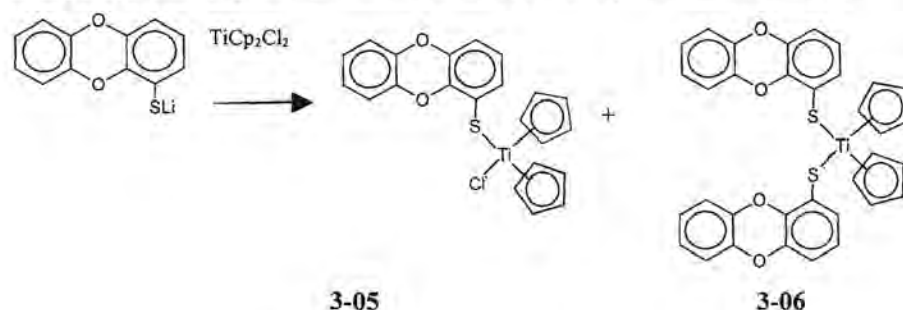
Following the general method with lithiated **L3-06** the colour of the reaction mixture changed from bright red to purple. After filtering, a purple residue was subjected to column chromatography with silica gel and with a 3:2 hexane:dichloromethane mixture as eluent. The first fraction gave the expected red-orange product, chlorobis(cyclopentadienyl)(dibenzofuran-4-ylsulfanyl)titanium(IV) **3-01** (1.21g, 29.3%). *Anal. Calc.* for $C_{22}H_{17}ClOSTi$: C, 64.00%; H, 4.16%. Found: C, 64.85%; H, 4.22%. An unidentified pink fraction was followed by a purple band, bis(cyclopentadienyl)bis(dibenzofuran-4-ylsulfanyl)titanium(IV) **3-02** (2.33g, 40.4%). *Anal. Calc.* for $C_{34}H_{24}O_2S_2Ti$: C, 70.22%; H, 4.20%. Found: C, 69.35%; H, 3.72%.

Synthesis of chlorobis(cyclopentadienyl)(6-methyl dibenzofuran-4-ylsulfanyl)titanium(IV) 3-03 and bis(cyclopentadienyl)bis(6-methyl dibenzofuran-4-ylsulfanyl)titanium(IV) 3-04



Following the general method for lithiated **L3-07** the colour of the reaction mixture changed from bright red to dark red. After filtering a dark red residue was obtained which was subjected to column chromatography on silica gel and with a 1:1 hexane:dichloromethane mixture as eluent. The first band contained very little of an unidentified purple product and the next fraction gave the expected product which was isolated from a red band, chlorobis(cyclopentadienyl)(6-methyl dibenzofuran-4-ylsulfanyl)titanium(IV) **3-03** (1.29g, 30.2%) *Anal. Calc.* for $C_{23}H_{19}ClOSti$: C, 64.71%; H, 4.30%. Found: C, 65.02%; H, 4.52%. A purple product followed yielding bis(cyclopentadienyl)bis(6-methyl dibenzofuran-4-ylsulfanyl)titanium(IV) **3-04** (2.11g, 34.9%) *Anal. Calc.* for $C_{36}H_{28}O_2S_2Ti$: C, 71.51%; H, 4.68%. Found: C, 71.95%; H, 5.02%.

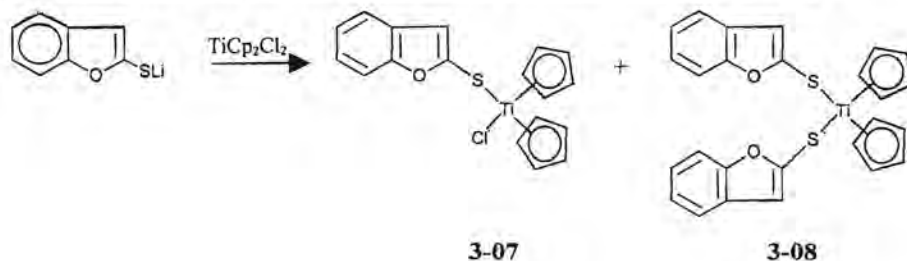
Synthesis of chlorobis(cyclopentadienyl)(dibenzodioxin-1-ylsulfanyl)titanium(IV) 3-05 and bis(cyclopentadienyl)bis(dibenzodioxin-1-ylsulfanyl)titanium(IV) 3-06



By using lithiated **L3-03** the colour of the reaction mixture changed from red to dark red. After filtering a red-purple residue remained which was subjected to column chromatography on silica gel and with a 1:1 hexane:dichloromethane mixture as eluent. First a red-purple band was collected and gave bis(cyclopentadienyl)bis(dibenzodioxin-1-ylsulfanyl)titanium(IV) **3-06** (1.27 g, 22.0%; mp. = 189°C). *Anal. Calc.* for $C_{34}H_{24}O_4STi$: C, 67.11%; H, 3.98%. Found: C, 67.39%; H, 4.11%. The last fraction afforded chlorobis(cyclopentadienyl)(dibenzodioxin-1-ylsulfanyl)titanium(IV) **3-05** (0.77 g,

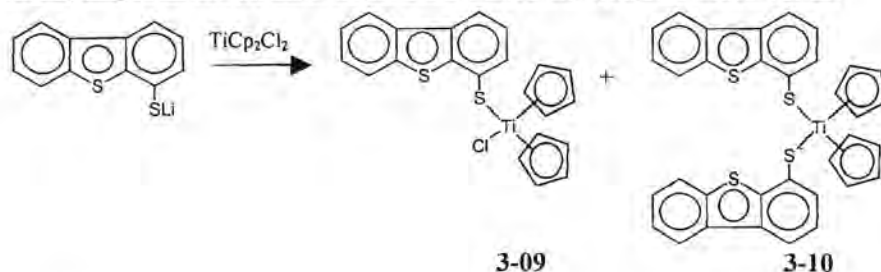
17.9%) from a red zone on the column. *Anal.* Calc. for $C_{22}H_{17}ClO_2STi$: C, 61.63%; H, 4.00%. Found: C, 62.09%; H, 4.23%.

Synthesis of (benzofuran-2-ylsulfanyl)chlorobis(cyclopentadienyl)titanium(IV) 3-07 and bis(cyclopentadienyl)bis(benzofuran-2-ylsulfanyl)titanium(IV) 3-08



Following the general method with lithiated **L3-05** the colour of the reaction mixture changed from bright red to purple. After filtering a purple residue was subjected to column chromatography on silica gel and with a 2:3 hexane:dichloromethane mixture as eluent. The first fraction gave unreacted benzofuran and the second fraction afforded the blue-purple product, bis(cyclopentadienyl)bis(benzofuran-2-ylsulfanyl)titanium(IV) **3-08** (1.95g, 41.0%). *Anal.* Calc. for $C_{26}H_{20}O_2S_2Ti$: C, 65.54%; H, 4.24%. Found: C, 66.05%; H, 4.52%. The desired product was obtained next from a red-purple band on the column (benzofuran-2-ylsulfanyl)chlorobis(cyclopentadienyl) titanium(IV) **3-07** (1.07g, 29.5%). *Anal.* Calc. for $C_{18}H_{15}ClO_2STi$: C, 59.59%; H, 4.18%. Found: C, 60.75%; H, 4.42%. Recrystallization of **3-08** from a hexane:dichloromethane mixture yielded dark purple crystals suitable for single crystal X-ray diffraction studies.

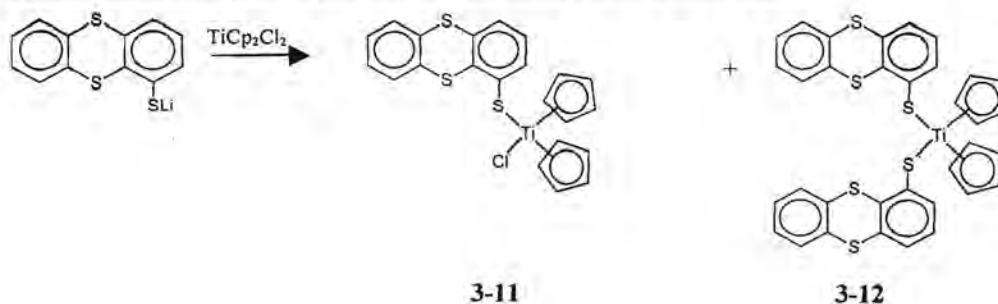
Synthesis of chlorobis(cyclopentadienyl)(dibenzothien-4-ylsulfanyl)titanium(IV) 3-09 and bis(cyclopentadienyl)bis(dibenzothien-4-ylsulfanyl)titanium(IV) 3-10



By using lithiated **L3-01** the colour of the reaction mixture changed from bright red to deep red. After filtering a red residue was obtained which was subjected to column chromatography on silica gel and with a 2:1 hexane:dichloromethane mixture as eluent. The first fraction collected was a purple band yielding bis(cyclopentadienyl)bis(dibenzothien-4-ylsulfanyl)titanium(IV) **3-10** (2.48g, 40.7%). *Anal.*

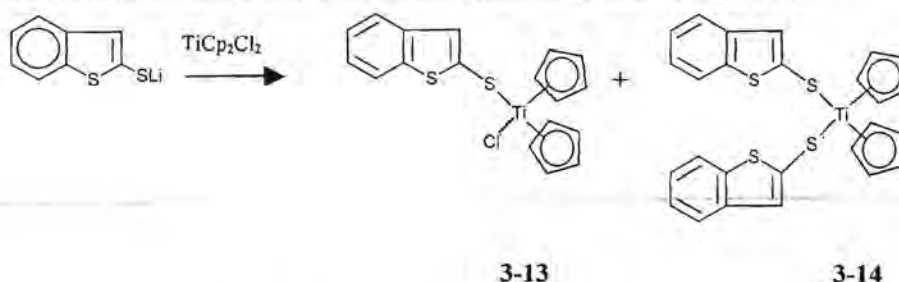
Calc. for $C_{34}H_{24}S_4Ti$: C, 67.10%; H, 3.98%. Found: C, 65.55%; H, 3.67%. The desired product was purified from a red band to give chlorobis(cyclopentadienyl)(dibenzothien-4-ylsulfanyl)titanium(IV) **3-09** (1.20g, 28.0%). *Anal.* Calc. for $C_{22}H_{17}ClS_2Ti$: C, 61.61%; H, 4.00%. Found: C, 61.85%; H, 4.42%. Recrystallization of **3-09** from a hexane:dichloromethane mixture yielded deep red crystals suitable for single crystal X-ray diffraction studies.

Synthesis of chlorobis(cyclopentadienyl)(thianthren-1-ylsulfanyl)titanium(IV) **3-11** and bis(cyclopentadienyl)bis(thianthren-1-ylsulfanyl)titanium(IV) **3-12**



Following the general method with lithiated **L3-03** the colour of the reaction mixture changed from red to dark red. After filtering a red-purple residue was obtained which was subjected to column chromatography on silica gel and with a 6:4 hexane:dichloromethane mixture as eluent. First a red-purple band was collected, affording bis(cyclopentadienyl)bis(thianthren-1-ylsulfanyl)titanium(IV) **3-12** (1.41 g, 21.0%). *Anal.* Calc. for $C_{34}H_{24}S_6Ti$: C, 60.63%; H, 3.60%. Found: C, 60.89%; H, 3.91%. A later fraction yielded chlorobis(cyclopentadienyl)(thianthren-1-ylsulfanyl)titanium(IV) **3-11** (0.83 g, 18%) from a red band on the column. *Anal.* Calc. for $C_{22}H_{17}ClS_3Ti$: C, 57.34%; H, 3.73%. Found: C, 57.69%; H, 3.93%.

Synthesis of (benzothien-2-ylsulfanyl)chlorobis(cyclopentadienyl)titanium(IV) **3-13** and bis(cyclopentadienyl)bis(benzothien-2-ylsulfanyl)titanium(IV) **3-14**



Following the general method with lithiated **L3-06** the colour of the reaction mixture changed from bright red to dark red. After filtering, a dark red residue was obtained which was subjected to column

chromatography on silica gel and with a 1:1 petroleum ether:dichloromethane mixture as eluent. The first fraction, a purple band, gave bis(cyclopentadienyl)bis(benzothien-2-ylsulfanyl)titanium(IV) **3-14** delete formula (2.48g, 48.8%). *Anal.* Calc. for $C_{26}H_{20}S_4Ti$: C, 61.41%; H, 3.97%. Found: C, 61.75%; H, 4.12%. The desired product was isolated from a red band (benzothien-2-ylsulfanyl)chlorobis(cyclopentadienyl)titanium(IV) **3-13** (1.33g, 35.1%). *Anal.* Calc. for $C_{18}H_{15}ClS_2Ti$: C, 57.07%; H, 4.00%. Found: C, 57.25%; H, 4.22%.

6.4 Synthesis of bi- and trinuclear complexes

The synthesis of homobinuclear and heterotrinnuclear complexes require (i) the synthesis of a suitable connecting molecule with appropriate metal bonding functions to act as a bridging ligand between the metal centra and (ii) the introduction of metal substrates designed to preferably coordinate to fixed positions on this ligand.

Synthesis of bridging ligands

Synthesis of 2-({2-[(2-mercaptoethyl)methylamino]ethyl}methylamino)ethanethiol [$C_8H_{20}N_2S$] **L4-04**



This synthesis was based on a method in literature, which was slightly modified⁹. N,N-dimethyl ethylene diamine **L4-03** (2.40g, 27.3mmol) was dissolved in dry toluene and thiiran (5.00ml, 83.0mmol), dissolved in dry toluene, was added dropwise at 50°C. It was immediately sealed in a pressure tube and heated to 110°C. After 5h the tube was cooled to RT and the solution was filtered to remove the polymer. The toluene was evaporated to give a pale yellow oil and distillation (110 - 120°C) under reduced pressure gave product **L4-04** (2.69g, 47.4%) as a colourless oil. *Anal.* Calc. for $C_8H_{20}N_2S_2$: C, 46.13%; H, 9.70%; N, 13.44%. Found: C, 49.01%; H, 9.43%; N, 13.85%.

Synthesis of 2-(2-methylamino ethylamino)ethanethiol [$C_5H_{14}N_2S$] **L4-05**

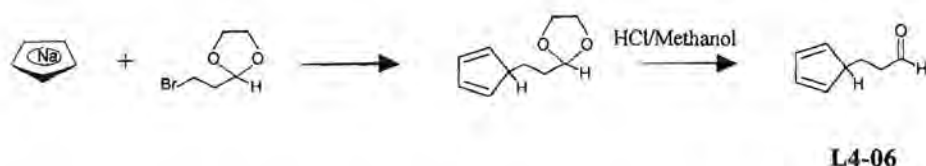


9. C. Marabella, J. Enemark, A. Miller, A. Bruce, N. Pariyadath, J. Corbin, E. Stiefel, *J. Org. Chem.*, **1983**, 22, 3456.

The method for **L4-04** was followed with N-methyl ethylene diamine **L4-02** (2.80g, 40.0mmol) and thiiran (2.80ml, 46.7mmol). The crude pale yellow oil was distilled (97 - 105°C) and gave product **L4-05** (2.75g, 51.3%) as a colourless oil. *Anal.* Calc. for C₅H₁₄N₂S: C, 44.75%; H, 10.54%; N, 20.87%. Found: C, 47.55%; H, 9.96%; N, 20.32%.

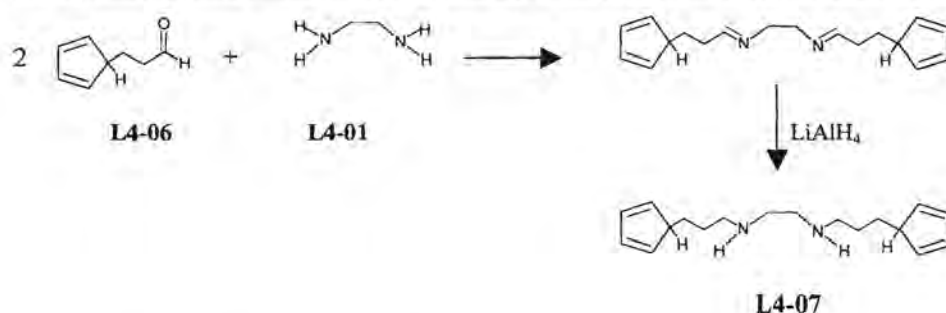
Synthesis of N,N'-bis-(3-cyclopenta-2,4-dienyl propyl) ethylene diamine **L4-07**

(a) Synthesis of 3-cyclopenta-2,4-dienyl propionaldehyde **L4-06**



NaCp (4.40g, 50.0mmol) was dissolved in THF and 2-(2-bromoethyl)-[1,3]-dioxolan (9.05g, 50.0mmol) was added and stirred for 4h at RT. The colour of the reaction mixture changed from purple to brown. The THF was evaporated and the residue was treated with a mixture of diluted HCl (1 part HCl in 3 parts distilled water) and methanol in a 1:1 ratio. The mixture was stirred for 1h at RT and the product was extracted from the water with diethyl ether. After evaporation a brown oil 3-cyclopenta-2,4-dienyl propionaldehyde **L4-06** (1.32g, 54.1%) remained and this product was used without further purification. *Anal.* Calc. for C₈H₁₀O: C, 78.64%; H, 8.27%. Found: C, 78.97%; H, 8.53%.

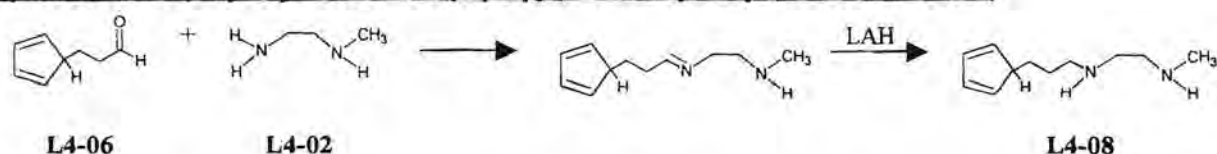
(b) Synthesis of N,N'-bis-(3-cyclopenta-2,4-dienyl propyl) ethylene diamine **L4-07**



L4-06 (2.40g, 20.0mmol) was dissolved in benzene and **L4-01** (0.78g, 10mmol) was added. The mixture was refluxed overnight under argon in a Dean-Stark apparatus. The water that formed during the first two hours of reflux was removed. After the reaction was completed the benzene was removed to leave a dark brown residue, which was dissolved in THF at RT. Lithium aluminium hydride (0.82g, 20mmol) was added in small portions and the mixture was stirred for 1h. The grey sticky mixture was

treated with 1ml of distilled water, then with 1ml 15% KOH solution and finally with 3ml distilled water. The mixture was filtered and evaporated to leave a brown residue. The residue was dissolved in the minimum dichloromethane whereafter hexane was added. The solution was filtered and the filtrate was evaporated to dryness to yield a yellow-brown oil that was identified as the product N,N'-bis-(3-cyclopenta-2,4-dienyl propyl) ethylene diamine **L4-07** (1.49g, 51.5%). *Anal.* Calc. for $C_{18}H_{28}N_2$: C, 46.31%; H, 10.38%; N, 10.28%. Found: C, 44.56%; H, 10.98%; N, 9.72%.

Synthesis of N-(3-cyclopenta-2,4-dienyl propyl)-N'-methyl ethylene diamine **L4-08**



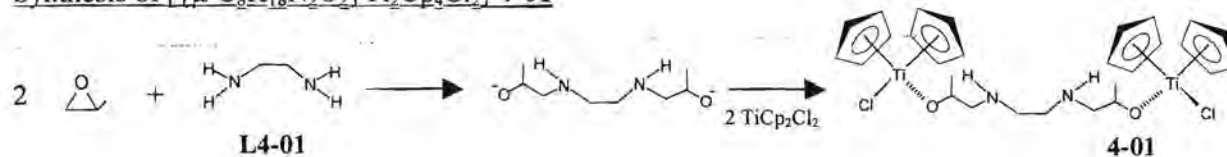
The procedure for **L4-07** was repeated with **L4-06** (2.03g, 17.0mmol) and **L4-02** (0.70g, 17mmol) instead. The reduction was done with $LiAlH_4$ (0.70g, 17mmol) and after extraction and filtration a yellow-brown oil was isolated and identified as the product N-(3-cyclopenta-2,4-dienyl propyl)-N'-methyl ethylene diamine **L4-08** (1.62g, 53.5%). *Anal.* Calc. for $C_{11}H_{18}N_2$: C, 74.10%; H, 10.20%; N, 15.70%. Found: C, 74.46%; H, 10.38%; N, 15.92%.

Synthesis of metal complexes

The general procedure for the addition of $K_2[PtCl_4]$ is given below in the shaded area. The introduction of the titanium fragment was achieved by using titanocene dichloride or trichloro cyclopentadienyl titanium (IV).

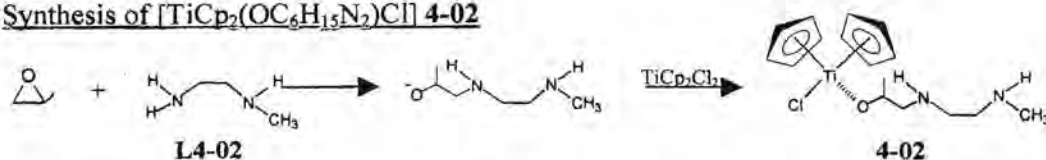
$K_2[PtCl_4]$ (0.42g, 1.0 mmol) was dissolved in the minimum of hot distilled water and the ligand was dissolved in acetonitrile. The latter was added to the platinum solution at RT. A colour change of the solution was observed and the mixture was stirred for 24 h at RT. The precipitate that formed was collected and dried.

Synthesis of $[\{\mu-C_8H_{18}N_2O_2\}Ti_2Cp_4Cl_2]$ **4-01**



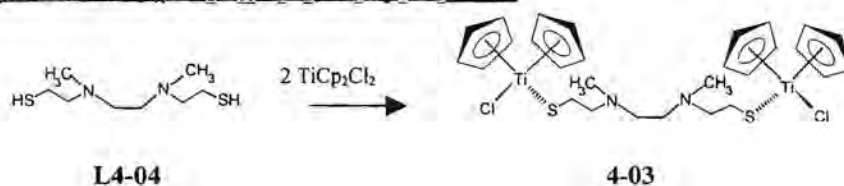
L4-01 (0.78g, 10mmol) was dissolved in THF and methyl epoxide (1.4ml, 20mmol) was added dropwise at RT while stirring. After stirring for 24h at RT the solution remained colourless. At -50°C titanocene dichloride (4.98g, 20.0mmol) was added and the solution was stirred for 30 minutes. After heating to RT the solution was stirred for 4 days. The colour changed from red-orange to yellow. The THF was evaporated and the residue was dissolved in hot toluene and filtered. The filtrate was concentrated and mixed with hexane causing a yellow precipitate to form, which was identified as $[\{\mu\text{-C}_8\text{H}_{18}\text{N}_2\text{O}_2\}\text{Ti}_2\text{Cp}_4\text{Cl}_2]$ **4-01** (1.51g, 25.1%). *Anal.* Calc. for $\text{C}_{28}\text{H}_{38}\text{Cl}_2\text{N}_2\text{O}_2\text{Ti}_2$: C, 55.89%; H, 6.38%; N, 4.65%. Found: C, 59.45%; H, 6.12%; N, 4.12%.

Synthesis of $[\text{TiCp}_2(\text{OC}_6\text{H}_{15}\text{N}_2)\text{Cl}]$ **4-02**



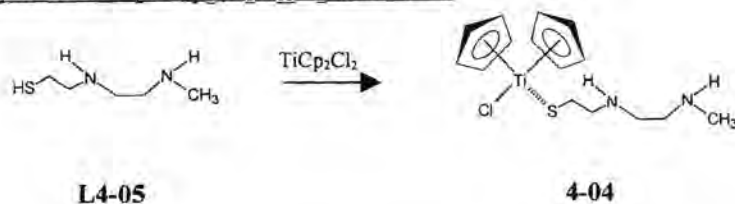
The procedure for **4-01** was repeated with **L4-02** (0.74g, 10mmol) and methyl oxiran (0.70ml, 10mmol). Addition of titanocene dichloride (2.49g, 10.0mmol) changed the colour from red to orange. The yellow precipitate was identified as $[\text{TiCp}_2(\text{OC}_6\text{H}_{15}\text{N}_2)\text{Cl}]$ **4-02** (1.00g, 29.2%). *Anal.* Calc. for $\text{C}_{16}\text{H}_{23}\text{ClN}_2\text{OTi}$: C, 56.12%; H, 6.78%; N, 8.17%. Found: C, 60.42%; H, 6.22%; N, 7.82%.

Synthesis of $[\{\mu\text{-C}_8\text{H}_{18}\text{N}_2\text{S}_2\}\text{Ti}_2\text{Cp}_4\text{Cl}_2]$ **4-03**



Titanocene dichloride (2.49g, 10.0mmol) was dissolved in THF and added to a solution of **L4-03** (1.04g, 5.00mmol) in THF at -50°C. The solution was stirred for 30 minutes at -50°C and after heating to RT stirring was continued for 24h. The colour changed from bright to red-orange. The THF was evaporated and the residue was dissolved in dichloromethane and filtered. The filtrate was concentrated and mixed with hexane causing an orange-red precipitate to form, which was identified as $[\{\mu\text{-C}_8\text{H}_{18}\text{N}_2\text{S}_2\}\text{Ti}_2\text{Cp}_4\text{Cl}_2]$ **4-03** (1.56g, 24.6%). *Anal.* Calc. for $\text{C}_{28}\text{H}_{38}\text{Cl}_2\text{N}_2\text{S}_2\text{Ti}_2$: C, 53.07%; H, 6.06%; N, 4.42%. Found: C, 55.65%; H, 6.29%; N, 4.02%.

Synthesis of [TiCp₂(C₆H₁₅N₂S)Cl] **4-04**



The same procedure was followed as for **4-03**, but with titanocene dichloride (0.75g, 3.0mmol) and **L4-05** (0.40g, 3.0mmol). The colour changed from bright to red-orange. From the filtrate an orange-red precipitate was collected, which was identified as [TiCp₂(SC₆H₁₅N₂)Cl] **4-04** (0.31g, 29.7%). *Anal. Calc.* for C₁₅H₂₃ClN₂STi: C, 52.01%; H, 6.71%; N, 8.08%. Found: C, 57.56%; H, 6.85%; N, 7.72%.

Synthesis of [Pt(N,N'-C₁₈H₂₈N₂)Cl₂] **4-05**

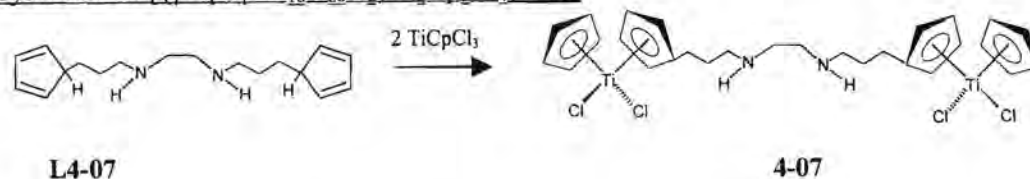


The general method for addition of K₂[PtCl₄] to **L4-07** (1.00g, 4.00mmol) was followed whereby the colour changed from red via brown to yellow-brown. After the reaction was completed a pink precipitate separated from the brown solution. The pink precipitate was identified as [Pt(N,N'-C₁₈H₂₈N₂)Cl₂] **4-05** (0.83g, 39.7%). *Anal. Calc.* for C₁₈H₂₈Cl₂N₂Pt: C, 23.43%; H, 5.25%; N, 5.20%. Found: C, 21.58%; H, 4.96%; N, 4.97%.

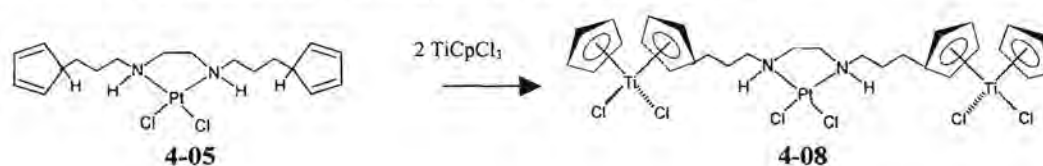
Synthesis of [Pt(N,N'-C₁₁H₂₀N₂)Cl₂] **4-06**



Following the general method for addition of K₂[PtCl₄] (1.25g, 3.00mmol) to **L4-08** (0.54g, 3.00mmol) the colour of the reaction mixture changed from red to brown to pale brown. After the reaction was completed a pale pink-brown precipitate was separated from the brown solution. The pink-brown precipitate was identified as the product [Pt(μ-N,N'-C₁₁H₂₀N₂)Cl₂] **4-06** (2.87g, 42.5%). *Anal. Calc.* for C₁₁H₂₀Cl₂N₂Pt: C, 29.74%; H, 4.09%; N, 6.30%. Found: C, 30.04%; H, 4.29%; N, 6.52%.

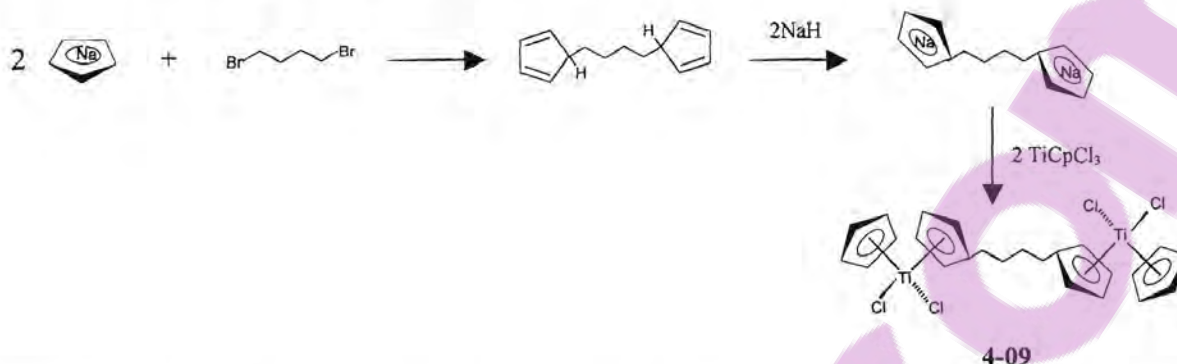
Synthesis of [$\{\mu\text{-}\eta^5\text{-}\eta^5\text{-C}_{18}\text{H}_{26}\text{N}_2\}\text{Ti}_2\text{Cp}_2\text{Cl}_4$] **4-07**


L4-07 (1.38g, 5.00mmol) was dissolved in THF and added to NaH (0.24g, 10mmol) at RT. After stirring overnight the colour of the reaction mixture changed from yellow to brown. At -50°C trichlorocyclopentadienyltitanium (IV) (2.19g, 10.0mmol) was added and the solution was stirred for 30 minutes. After heating to RT the solution was stirred for 5h. The colour of the solution changed to dark brown. The THF was evaporated and the residue was dissolved in hot toluene and filtered. The volume of toluene was reduced and hexane was added until precipitation was completed. After filtration the yellow filtrate was collected and the solvent removed under reduced pressure. The residue was dissolved in dichloromethane. Addition of hexane precipitated a yellow product that was identified as [$\{\mu\text{-}\eta^5\text{-}\eta^5\text{-C}_{18}\text{H}_{26}\text{N}_2\}\text{Ti}_2\text{Cp}_2\text{Cl}_4$] **4-07** (2.30g, 29.4%). *Anal.* Calc. for $\text{C}_{28}\text{H}_{36}\text{Cl}_4\text{N}_2\text{Ti}_2$: C, 52.66%; H, 5.69%; N, 4.38%. Found: C, 53.05%; H, 5.92%; N, 4.67%.

Synthesis of [$\text{Ti}_2\{\mu\text{-}\eta^5\text{-}\eta^5\text{-(Pt(N,N'-C}_{18}\text{H}_{26}\text{N}_2)\text{Cl}_2)\}\text{Cp}_2\text{Cl}_4$] **4-08**


4-05 (0.13g, 0.25mmol) was dissolved in THF and added to NaH (0.01g, 0.5mmol) at RT. After stirring overnight at RT the colour of the reaction mixture changed from pink to brown-pink. At -50°C trichloro cyclopentadienyl titanium(IV) (0.10g, 0.50mmol) was added and the solution was stirred for 30 minutes. After heating to RT the solution was stirred for 24h. The colour of the solution changed to yellow and a cream-pink precipitate formed. The cream-pink product was identified as [$\text{Ti}_2\{\mu\text{-}\eta^5\text{-}\eta^5\text{-(Pt(N,N'-C}_{18}\text{H}_{26}\text{N}_2)\text{Cl}_2)\}\text{Cp}_2\text{Cl}_4$] **4-08** (0.07g, 31.0%). *Anal.* Calc. for $\text{C}_{28}\text{H}_{36}\text{Cl}_6\text{N}_2\text{Ti}_2\text{Pt}$: C, 37.17%; H, 4.02%; N, 3.10%. Found: C, 37.45%; H, 4.42%; N, 3.41%. Attempts to synthesize this product by adding the metal substrates in the reverse order, i.e. the addition of $\text{K}_2[\text{PtCl}_4]$ to **4-07**, was unsuccessful.

Synthesis of [$\{\mu\text{-}\eta^5, \eta^5\text{-C}_{14}\text{H}_{16}\}\text{Ti}_2\text{Cp}_2\text{Cl}_4$] 4-09



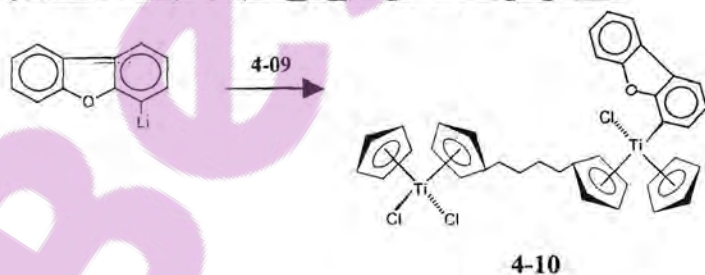
NaCp (4.40g, 50.0mmol) was dissolved in THF and added to 1,4-dibromobutane (5.40g, 25.0mmol) at RT. After stirring for 2h the pink-brown mixture was treated with NaH (1.20g for 60 % pure mixture, 50.0mmol) and stirred overnight. The resulting brown solution was then added to trichloro cyclopentadienyl titanium (IV) (10.95g, 50.00mmol,) dissolved in THF at RT. After stirring for 2h, the brown solution was evaporated to dryness and the residue was washed with 1 mol/dm³ HCl solution, then with ethanol and finally with diethyl ether. After drying a dark green solid remained, which was identified as the product [$\{\mu\text{-}\eta^5, \eta^5\text{-C}_{14}\text{H}_{16}\}\text{Ti}_2\text{Cp}_2\text{Cl}_4$] 4-09 (11.04g, 80.0%). *Anal. Calc.* for C₂₄H₂₆Cl₄Ti₂: C, 52.17%; H, 4.75%. Found: C, 52.61%; H, 4.92%.

Derivatives of 4-09 were synthesized according to the general method given in the shaded area below. The procedures for the preparation of the lithiated heteroaromatic substrates are given in Table 6.1.

General method for replacing Cl with a heteroaromatic ring ligand

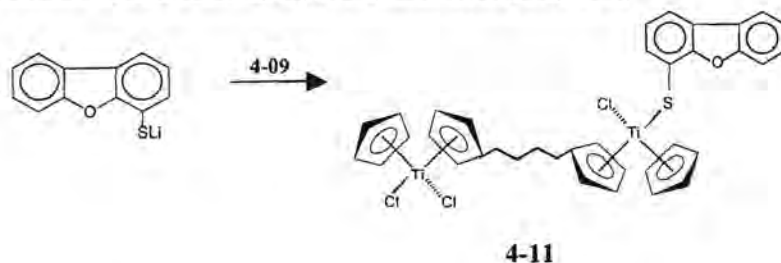
At -50°C the lithiated heteroaromatic substrate was added to a solution of 4-09 (5.52g, 10.0mmol) in THF. A colour change of the reaction mixture was observed almost immediately and stirring was continued at -50°C for 30 minutes. The mixture was allowed to warm to room temperature and it was stirred for another 90 minutes. The solvent was evaporated and the residue was purified using extraction. The products were stored under nitrogen at 5°C.

Synthesis of [$\{\mu\text{-}\eta^5, \eta^5\text{-C}_{14}\text{H}_{16}\}\text{Ti}_2(\text{Dbf})\text{Cp}_2\text{Cl}_3$] 4-10



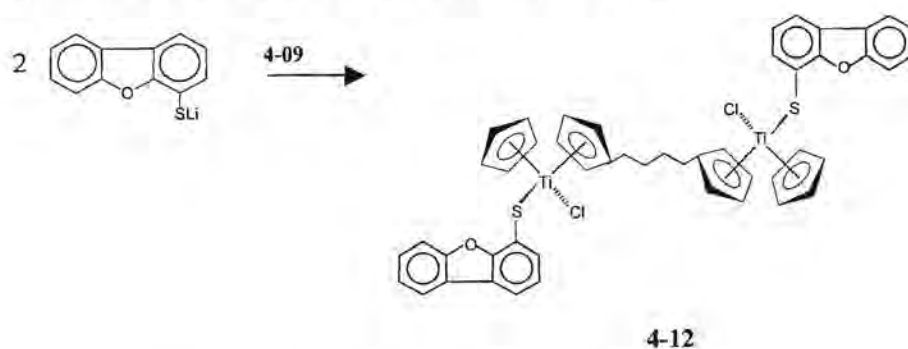
Following the general method with 10.0mmol of the lithiated dibenzofuran, the colour of the reaction mixture changed from dark green to green. The green residue was washed with hexane. The product was extracted using diethyl ether to give a green-yellow solution, which was evaporated to dryness to give $[\{\mu\text{-}\eta^5, \eta^5\text{-C}_{14}\text{H}_{16}\}\text{Ti}_2(\text{Dbf})\text{Cp}_2\text{Cl}_3]$ **4-10** (2.76g, 40.3%). *Anal. Calc.* for $\text{C}_{36}\text{H}_{33}\text{Cl}_3\text{OTi}_2$: C, 63.24%; H, 4.88%. Found: C, 63.75%; H, 5.02%.

Synthesis of $[\{\mu\text{-}\eta^5, \eta^5\text{-C}_{14}\text{H}_{16}\}\text{Ti}_2(\text{Dbf-S})\text{Cp}_2\text{Cl}_3]$ **4-11**



Following the general method with 10.0mmol of dibenzofuran-4-ylthiolate, the colour of the reaction mixture changed from dark green to brown-yellow. The brown residue was washed with hexane and a brown residue remained. The product was extracted from the residue by using diethyl ether to give an orange-yellow solution, which was evaporated to dryness to give an orange-yellow solid, $[\{\mu\text{-}\eta^5, \eta^5\text{-C}_{14}\text{H}_{16}\}\text{Ti}_2(\text{Dbf-S})\text{Cp}_2\text{Cl}_3]$ **4-11** (3.15g, 44.0%). *Anal. Calc.* for $\text{C}_{36}\text{H}_{33}\text{Cl}_3\text{OSTi}_2$: C, 60.41%; H, 4.66%. Found: C, 60.80%; H, 4.82%.

Synthesis of $[\{\mu\text{-}\eta^5, \eta^5\text{-C}_{14}\text{H}_{16}\}\{\text{Ti}(\text{Dbf-S})\text{CpCl}\}_2]$ **4-12**



Following the general method with 20.0mmol of the dibenzofuran-4-ylthiolate, the colour of the solution changed from dark green to red. The green residue was washed with hexane and a purple residue remained. The residue was subjected to column chromatography on silica gel by starting with 1:1 hexane:dichloromethane mixture as eluent and increasing the polarity with time. The purple fraction was identified as $[\{\mu\text{-}\eta^5, \eta^5\text{-C}_{14}\text{H}_{16}\}\{\text{Ti}(\text{Dbf-S})\text{CpCl}\}_2]$ **4-12** (3.16g, 35.9%). *Anal. Calc.* for $\text{C}_{48}\text{H}_{40}\text{Cl}_2\text{O}_2\text{S}_2\text{Ti}_2$: C, 65.52%; H, 4.59%. Found: C, 65.88%; H, 4.80%.

6.5 *In vitro* tests

The *in vitro* tests were executed using cell cultures with CoLo (colorectal carcinoma) cells and HeLa (human cervix epithelioid carcinoma) cells. The cells were incubated in an oven at 37 °C for 3h and the cell concentration was determined on day 0 by counting the cells on a grid. A specified volume of cells was mixed with a solution of the complex in various concentrations. The solutions of the complexes were prepared by making a stock solution of each and through dilution the desired concentrations were obtained. The concentrations ranged from 0.01 μ M titanium up to 100 μ M titanium. The stock solutions were prepared by weighing the complexes in sterile tubes and then dissolving them in DMSO, where after the solution was diluted with an aqueous NaCl solution. The ratio was kept at 1:9 DMSO:NaCl(aq). The cells were incubated for three days at body temperature and afterwards the cells were dyed and the intensity of the color was measured. The color intensity was directly proportional to the number of living cells. It was then possible to plot the results and make comparisons. Each experiment was done in triplicate and the average value was recorded as shown in Appendix D. The results were graphically presented and discussed in Section 5.2.

6.6 Studies related to the antitumor activities of the complexes

Intercalation studies

The intercalation tests were done in triplicate by an application of a technique derived from flow cytometry and results were expressed as an average of three experiments. A human cervix epithelial cell line (HeLa:ATCC CC42) was grown as monolayer cultures using Minimum Essential Medium (MEM) supplemented with 10% fetal calf serum (FCS). For the flow cytometry assays, cells were made up in HEPES buffer (HBSS-HEPES buffer) containing 0.4mg/ml propidium iodide. Each sample was treated with a different concentration (0.03 - 0.01 μ g/ml) of the intercalator or metal complex. To measure the damage to the DNA a nucleoid sedimentation technique using a flow cytometer (Coulter XL-MCL)-based laser light scattering system was used¹⁰. The measurement was done after a 30 minute treatment at 4°C, with the exception of H₂O₂ (incubated for 15 minutes at 37°C). The median for the forward and side scatter was calculated for each concentration and was reported as the median channel number. The results are tabulated in Appendix E and discussed in Section 5.5.

Ligand substitution in aqueous medium

The displacement of ligands from the coordination sphere of the titanium in aqueous solution was studied with NMR. During this experiment, titanocene dichloride and the mono and bis substituted

10. A. E. Milner, A. T. M. Vaughan, I. P. Clark, *Radiation Research*, 1987, 110, 108.

thiolates derivatives were compared. A titanium compound concentration of 0.25M was prepared for each complex in a mixture of DMSO and 32% saline D₂O in a 1:4 ratio. The samples were kept in a water bath at 37 °C. Samples were run for 64 scans on a Bruker AC-300 spectrometer and over eight time intervals: 0h, 1h, 2h, 4h, 6h, 10h, 20h, 30h and 60h. The data is shown in Appendix F and discussed in Section 5.4.

6.7 Crystal structure determinations

Complex 2-05

The X-ray intensity data set for complex 2-05 was collected on a novel 1K SMART Siemens CCD area detector system using Mo radiation¹¹. X-rays were generated using a regular sealed tube and an X-ray generator operating at 50kV 30mA. The 9cm wide CCD area detector was mounted 4.5cm from the crystal and the data set collected at low temperature (-100°C). A graphite monochromator followed by a 5mm collimator was used. The selected crystal was mounted on a thin glass fibre.

In order to obtain an initial set of cell parameters and an orientation matrix for data collection, reflections from three sets of 15 frames each were collected, covering three perpendicular sectors of space. The data collection nominally covered over a hemisphere of reciprocal space, by a combination of 3 sets of exposures of 1271 frames. Each set had a different ϕ angle for the crystal and each exposure covered 0.3° in ω , with 10 seconds exposure per frame. In order to monitor crystal and instrument stability and to enable crystal decay corrections, the first 50 frames of the first set were measured again at the end of the data collection. Crystal decay was found to be negligible after analysing the duplicate reflections. The final data set after scaling consisted of 16945 reflections to 0.751Å resolution. Coverage of data is 67.87 % complete to at least 28.26° in θ . The data collection took about 5 hours. A detailed presentation of the data collection statistics is given in Table 6.3

H atoms were placed geometrically and refined with a riding model and with U_{iso} constrained to be 0.08Å². Refinement on F^2 for ALL reflections, except for 0 with a very negative F^2 or flagged by the user for potential systematic errors. Weighted R- factors (wR) and all goodness-of-fit (S) are based on F^2 , while conventional R-factors (R) are based on F, with F set to zero for negative F^2 . The observed criterion of $F^2 > 2\sigma(F^2)$ is used only for calculating R-factor observed, etc. and is not relevant to the choice of reflections for refinement. R-factors based on F^2 are statistically about twice as large as those based on F, and R-factors based on ALL data will be even larger.

11. G. M. Sheldrick, *SADABS User Guide*, University of Göttingen, Germany, 1996.

All esd's, except the esd in the dihedral angle between two l. s. planes, were estimated using the full covariance matrix. The cell esds were taken into account individually in the estimation of esd's in distances, angles and torsion angles; correlations between esds in cell parameters were only used when they were defined by crystal symmetry. An approximate (isotropic) treatment of cell esds was used for estimating esds involving l. s. planes.

The determination of the unit cell parameters, crystal orientation and data collection were performed with the SMART package (Siemens 1995)¹². The crystallographic raw data frames were integrated, all reflections extracted, reduced and Lp-corrected using the program SAINT (Siemens 1995)¹³. The cell refinement using all data was also performed by SAINT (Siemens 1995). The program SHELXTL version 5.0 (Siemens 1995) was used for the structure solution, refinement, molecular graphics and publication preparation¹⁴. The crystal data and structure refinement for **2-05** is shown in Table 6.3. In Appendix A the complete tables of the fractional atomic coordinates and equivalent isotropic displacement parameters, bond lengths, bond angles, anisotropic displacement parameters, hydrogen coordinates and isotropic displacement parameters of complex **2-05** are listed.

Complexes 2-02 and 3-09

The intensity data for the compounds were collected on a Nonius KappaCCD diffractometer, using graphite-monochromated Mo-K α radiation. Data were corrected for Lorentz and polarization effects, but not for absorption effects^{15,16}. The structures were solved by direct methods (SHELXS¹⁷) and refined by full-matrix least squares techniques against Fo² (SHELXL-97¹⁸). The hydrogen atoms were included at calculated positions with fixed thermal parameters. All nonhydrogen atoms were refined anisotropically¹⁸. XP (SIEMENS Analytical X-ray Instruments, Inc.) was used for structure representations. The crystal data and structure refinement for **2-02** and **3-09** is shown in Table 6.4 and

-
12. Siemens (1996) *SMART Reference Manual*, Siemens Analytical X-ray Instruments Inc., Madison, Wisconsin, USA, 1996.
 13. Siemens (1995b) *ASTRO and SAINT. Data Collection and Processing for the SMART System*, Siemens Analytical X-ray Instruments Inc., Madison, Wisconsin, USA, 1995.
 14. Siemens (1995a) *SHELXTL Version 5.0 (Dos version) - Structure Determination Programme*, Siemens Analytical X-ray Instruments Inc., Madison, Wisconsin, USA, 1995.
 15. *COLLECT. Data Collection Software*; Nonius B.V., Netherlands, 1998.
 16. Z. Otwinowski, W. Minor, „Processing of X-Ray Diffraction Data Collected in Oscillation Mode”, in *Methods in Enzymology, Macromolecular Crystallography, Part A*, C.W. Carter & R.M. Sweet (eds), Academic Press, 1997, 276, 307-326.
 17. G. M. Sheldrick, *Acta Crystallogr. Sect. A*, 1990, 46, 467-473.
 18. G. M. Sheldrick, SHELXL-97 (Release 97-2), University of Göttingen, Germany, 1997.

Table 6.3. Crystal data and structure refinement for **2-05**.

Empirical formula	C ₃₃ H ₄₁ ClO ₃ Ti	
Molecular weight	569.01	
Temperature, K	296(2)	
Wavelength, Å	0.71073	
Space group	P2(1)/n	
Unit cell dimensions:	a = 10.0318(5)Å b = 17.6700(10)Å c = 15.3214(8)Å	α = 90° β = 103.728(1)° γ = 90°
Z	4	
Volume, Å ³	2638.3(2)	
Density (calculated), Mg/m ³	1.433	
Absorption coefficient, mm ⁻¹	0.461	
F(000)	1208	
Crystal size, mm	0.28 x 0.36 x 0.44	
Scan range (θ°)	1.79 ≤ θ ≤ 28.26	
Zone collected	-12 ≤ h ≤ 9 ; -22 ≤ k ≤ 21 ; -19 ≤ l ≤ 20	
Reflections collected	16714	
Independent reflections	6010	
R _{int}	0.0209	
Data / restraints / parameters	6010 / 0 / 411	
Goodness-of-fit on F ²	1.840	
Final R indices [I > 2σ(I)]	R1 = 0.0610; wR2 = 0.2122	
R indices (all data)	R1 = 0.0674; wR2 = 0.2187	
Residual electron density, (eÅ ⁻³)	Max = 1.564; Min = -0.710	

Table 6.5 respectively. In Appendix B and Appendix C the complete tables of the fractional atomic coordinates and equivalent isotropic displacement parameters, bond lengths, bond angles, anisotropic displacement parameters, hydrogen coordinates and isotropic displacement parameters of complexes **2-02** and **3-09** are listed respectively.



Table 6.4. Crystal data and structure refinement for 2-02.

Identification code	FO1047	
Empirical formula	C ₃₄ H ₂₄ O ₂ Ti	
Formula weight	512.43	
Temperature	183(2) K	
Wavelength	0.71073 Å	
Crystal system	Monoclinic	
Space group	P2(1)/c	
Unit cell dimensions	a = 12.4323(6) Å b = 12.6852(7) Å c = 31.796(1) Å	a = 12.4323(6) Å b = 12.6852(7) Å c = 31.796(1) Å
Volume	4988.6(4) Å ³	
Z	8	
Density (calculated)	1.365 g/cm ³	
Absorption coefficient	0.374 mm ⁻¹	
F(000)	2128	
Crystal size	0.28 x 0.22 x 0.10 mm ³	
Theta range for data collection	3.11 to 30.99°.	
Index ranges	-17 ≤ h ≤ 17, -7 ≤ k ≤ 18, -44 ≤ l ≤ 44	
Reflections collected	19160	
Independent reflections	13869 [R(int) = 0.1240]	
Completeness to theta = 27.48°	87.4 %	
Absorption correction	0.9636 and 0.9026	
Max. and min. transmission	Full-matrix least-squares on F ²	
Refinement method	13869 / 0 / 667	
Data / restraints / parameters	0.987	
Goodness-of-fit on F ²	R1 = 0.1099, wR2 = 0.1448	
Final R indices [I > 2σ(I)]	R1 = 0.2918, wR2 = 0.1941	
R indices (all data)	0.303 and -0.370 e.Å ⁻³	
Largest diff. peak and hole	2128	

**Table 6.5.** Crystal data and structure refinement for 3-09.

Identification code	fo1042	
Empirical formula	C ₂₂ H ₁₇ ClS ₂ Ti	
Formula weight	428.83	
Temperature	183(2) K	
Wavelength	0.71073 Å	
Crystal system	Monoclinic	
Space group	P2(1)/c	
Unit cell dimensions	a = 11.1309(5) Å b = 7.8238(3) Å c = 21.946(1) Å	α = 90°. β = 96.464(2)°. γ = 90°.
Volume	1899.0(1) Å ³	
Z	4	
Density (calculated)	1.500 g/cm ³	
Absorption coefficient	0.814 mm ⁻¹	
F(000)	880	
Crystal size	0.28 x 0.22 x 0.18 mm ³	
Theta range for data collection	3.19 to 27.48°.	
Index ranges	-14 ≤ h ≤ 14, -9 ≤ k ≤ 10, -28 ≤ l ≤ 28	
Reflections collected	7637	
Independent reflections	4277 [R(int) = 0.0424]	
Completeness to theta = 27.48°	98.2 %	
Absorption correction	None	
Max. and min. transmission	0.8673 and 0.8041	
Refinement method	Full-matrix least-squares on F ²	
Data / restraints / parameters	4277 / 0 / 235	
Goodness-of-fit on F ²	1.022	
Final R indices [I > 2σ(I)]	R1 = 0.0424, wR2 = 0.0877	
R indices (all data)	R1 = 0.0705, wR2 = 0.0967	
Largest diff. peak and hole	0.267 and -0.469 e.Å ⁻³	

Appendix A

Crystallographic data for $[TiCp_2(Dbf)_2]$ 2-02.

Table 1. Fractional atomic coordinates ($\times 10^4$) and equivalent isotropic displacement parameters ($\text{Å}^2 \times 10^3$) for $[TiCp_2(Dbf)_2]$.

Atom	x	y	z	U_{eq}
Ti	7485(1)	1706(1)	235(1)	20(1)
Cl	5763(1)	2640(1)	708(1)	36(1)
S(1)	8951(1)	3370(1)	871(1)	26(1)
S(2)	11721(1)	2761(1)	1440(1)	28(1)
C(1)	9282(2)	2608(3)	1637(1)	26(1)
C(2)	8418(2)	2336(3)	2040(1)	29(1)
C(3)	8767(2)	1864(3)	2652(1)	31(1)
C(4)	9978(2)	1651(3)	2870(1)	28(1)
C(5)	10869(2)	1903(3)	2474(1)	24(1)
C(6)	12182(2)	1743(3)	2591(1)	25(1)
C(7)	12906(2)	1190(3)	3122(1)	30(1)
C(8)	14144(2)	1099(3)	3126(1)	39(1)
C(9)	14698(3)	1548(4)	2607(1)	45(1)
C(10)	14012(2)	2083(4)	2074(1)	39(1)
C(11)	12758(2)	2166(3)	2070(1)	27(1)
C(12)	10498(2)	2398(3)	1865(1)	24(1)
C(13)	8627(2)	-562(3)	758(1)	32(1)
C(14)	7481(2)	-559(3)	970(1)	34(1)
C(15)	6612(2)	-980(3)	468(1)	33(1)
C(16)	7225(2)	-1219(3)	-51(1)	30(1)
C(17)	8477(2)	-936(3)	125(1)	29(1)
C(18)	6493(3)	3620(4)	-522(1)	38(1)
C(19)	6692(2)	2050(4)	-810(1)	33(1)
C(20)	7955(2)	1827(3)	-802(1)	29(1)
C(21)	8533(2)	3230(3)	-493(1)	33(1)
C(22)	7621(3)	4321(3)	-314(1)	37(1)

U_{eq} is defined as one third of the trace of the orthogonalized U_{ij} tensor.



Table 2. Bond lengths [Å] for [TiCp₂(Dbf)₂].

TiA-C(13A)	2.210(4)	TiB-C(13B)	2.218(4)
TiA-C(1A)	2.218(5)	TiB-C(1B)	2.229(4)
TiA-C(27A)	2.335(4)	TiB-C(32B)	2.341(4)
TiA-C(32A)	2.366(4)	TiB-C(26B)	2.360(4)
TiA-C(26A)	2.385(4)	TiB-C(27B)	2.378(4)
TiA-C(31A)	2.392(4)	TiB-C(33B)	2.391(4)
TiA-C(25A)	2.398(5)	TiB-C(31B)	2.392(4)
TiA-C(28A)	2.400(5)	TiB-C(29B)	2.395(5)
TiA-C(29A)	2.404(5)	TiB-C(28B)	2.400(4)
TiA-C(33A)	2.406(5)	TiB-C(25B)	2.402(5)
TiA-C(30A)	2.410(5)	TiB-C(34B)	2.405(4)
TiA-C(34A)	2.418(5)	TiB-C(30B)	2.419(4)
O(1A)-C(11A)	1.398(5)	O(1B)-C(11B)	1.393(5)
O(1A)-C(12A)	1.405(5)	O(1B)-C(12B)	1.404(5)
O(2A)-C(23A)	1.388(5)	O(2B)-C(23B)	1.397(5)
O(2A)-C(24A)	1.418(4)	O(2B)-C(24B)	1.400(5)
C(1A)-C(12A)	1.410(6)	C(1B)-C(2B)	1.406(6)
C(1A)-C(2A)	1.415(6)	C(1B)-C(12B)	1.401(6)
C(2A)-C(3A)	1.422(6)	C(2B)-C(3B)	1.397(6)
C(3A)-C(4A)	1.382(7)	C(3B)-C(4B)	1.386(6)
C(4A)-C(5A)	1.393(7)	C(4B)-C(5B)	1.387(6)
C(5A)-C(12A)	1.410(6)	C(5B)-C(12B)	1.407(6)
C(5A)-C(6A)	1.450(7)	C(5B)-C(6B)	1.470(6)
C(6A)-C(11A)	1.395(6)	C(6B)-C(11B)	1.388(6)
C(6A)-C(7A)	1.422(7)	C(6B)-C(7B)	1.400(6)
C(7A)-C(8A)	1.372(8)	C(7B)-C(8B)	1.407(7)
C(8A)-C(9A)	1.363(8)	C(8B)-C(9B)	1.370(7)
C(9A)-C(10A)	1.400(7)	C(9B)-C(10B)	1.384(6)
C(10A)-C(11A)	1.375(7)	C(10B)-C(11B)	1.384(6)
C(13A)-C(24A)	1.391(5)	C(13B)-C(14B)	1.404(6)
C(13A)-C(14A)	1.422(5)	C(13B)-C(24B)	1.408(6)
C(14A)-C(15A)	1.390(6)	C(14B)-C(15B)	1.408(6)
C(15A)-C(16A)	1.383(6)	C(15B)-C(16B)	1.390(6)
C(16A)-C(17A)	1.391(6)	C(16B)-C(17B)	1.388(7)
C(17A)-C(24A)	1.404(5)	C(17B)-C(24B)	1.397(6)
C(17A)-C(18A)	1.459(6)	C(17B)-C(18B)	1.452(6)
C(18A)-C(19A)	1.392(6)	C(18B)-C(23B)	1.387(7)
C(18A)-C(23A)	1.398(6)	C(18B)-C(19B)	1.410(6)
C(19A)-C(20A)	1.372(6)	C(19B)-C(20B)	1.374(8)
C(20A)-C(21A)	1.392(7)	C(20B)-C(21B)	1.398(8)
C(21A)-C(22A)	1.399(6)	C(21B)-C(22B)	1.403(6)
C(22A)-C(23A)	1.379(6)	C(22B)-C(23B)	1.386(7)
C(25A)-C(26A)	1.384(6)	C(25B)-C(29B)	1.388(6)
C(25A)-C(29A)	1.421(6)	C(25B)-C(26B)	1.410(6)
C(26A)-C(27A)	1.400(6)	C(26B)-C(27B)	1.406(6)
C(27A)-C(28A)	1.397(6)	C(27B)-C(28B)	1.401(6)
C(28A)-C(29A)	1.391(6)	C(28B)-C(29B)	1.410(6)



C(30A)-C(31A)	1.393(6)	C(30B)-C(31B)	1.387(6)
C(30A)-C(34A)	1.420(6)	C(30B)-C(34B)	1.416(6)
C(31A)-C(32A)	1.415(6)	C(31B)-C(32B)	1.421(6)
C(32A)-C(33A)	1.396(6)	C(32B)-C(33B)	1.402(6)
C(33A)-C(34A)	1.397(6)	C(33B)-C(34B)	1.394(6)

Symmetry transformations used to generate equivalent atoms:

#1 $-x+2, -y, -z+1$

Bestpfe.com



Table 3. Bond angles [°] for [TiCp₂(Dbf)₂].

C(13A)-TiA-C(1A)	104.96(16)	C(13B)-TiB-C(1B)	104.01(17)
C(13A)-TiA-C(27A)	97.27(17)	C(13B)-TiB-C(32B)	132.14(15)
C(1A)-TiA-C(27A)	131.74(17)	C(1B)-TiB-C(32B)	95.17(15)
C(13A)-TiA-C(32A)	131.67(16)	C(13B)-TiB-C(26B)	93.10(16)
C(1A)-TiA-C(32A)	96.17(16)	C(1B)-TiB-C(26B)	131.76(16)
C(27A)-TiA-C(32A)	100.07(17)	C(32B)-TiB-C(26B)	106.02(16)
C(13A)-TiA-C(26A)	130.79(17)	C(13B)-TiB-C(27B)	76.91(15)
C(1A)-TiA-C(26A)	106.16(17)	C(1B)-TiB-C(27B)	106.25(17)
C(27A)-TiA-C(26A)	34.49(14)	C(32B)-TiB-C(27B)	138.45(17)
C(32A)-TiA-C(26A)	81.07(17)	C(26B)-TiB-C(27B)	34.53(15)
C(13A)-TiA-C(31A)	107.63(16)	C(13B)-TiB-C(33B)	108.40(16)
C(1A)-TiA-C(31A)	130.25(17)	C(1B)-TiB-C(33B)	77.40(15)
C(27A)-TiA-C(31A)	79.58(17)	C(32B)-TiB-C(33B)	34.45(14)
C(32A)-TiA-C(31A)	34.59(15)	C(26B)-TiB-C(33B)	138.85(16)
C(26A)-TiA-C(31A)	78.92(17)	C(27B)-TiB-C(33B)	172.89(17)
C(13A)-TiA-C(25A)	127.96(17)	C(13B)-TiB-C(31B)	109.09(16)
C(1A)-TiA-C(25A)	76.08(16)	C(1B)-TiB-C(31B)	129.72(15)
C(27A)-TiA-C(25A)	56.70(16)	C(32B)-TiB-C(31B)	34.92(13)
C(32A)-TiA-C(25A)	98.95(18)	C(26B)-TiB-C(31B)	83.25(16)
C(26A)-TiA-C(25A)	33.65(14)	C(27B)-TiB-C(31B)	117.26(17)
C(31A)-TiA-C(25A)	109.78(18)	C(33B)-TiB-C(31B)	56.92(15)
C(13A)-TiA-C(28A)	76.77(16)	C(13B)-TiB-C(29B)	131.37(15)
C(1A)-TiA-C(28A)	111.54(17)	C(1B)-TiB-C(29B)	78.73(17)
C(27A)-TiA-C(28A)	34.28(14)	C(32B)-TiB-C(29B)	94.96(16)
C(32A)-TiA-C(28A)	133.91(16)	C(26B)-TiB-C(29B)	57.04(16)
C(26A)-TiA-C(28A)	56.68(16)	C(27B)-TiB-C(29B)	56.57(15)
C(31A)-TiA-C(28A)	111.79(17)	C(33B)-TiB-C(29B)	119.27(16)
C(25A)-TiA-C(28A)	56.41(17)	C(31B)-TiB-C(29B)	104.54(17)
C(13A)-TiA-C(29A)	93.72(17)	C(13B)-TiB-C(28B)	98.36(16)
C(1A)-TiA-C(29A)	79.21(17)	C(1B)-TiB-C(28B)	75.56(16)
C(27A)-TiA-C(29A)	56.79(15)	C(32B)-TiB-C(28B)	129.01(17)
C(32A)-TiA-C(29A)	133.19(18)	C(26B)-TiB-C(28B)	57.30(17)
C(26A)-TiA-C(29A)	56.68(16)	C(27B)-TiB-C(28B)	34.09(15)
C(31A)-TiA-C(29A)	133.66(16)	C(33B)-TiB-C(28B)	145.70(17)
C(25A)-TiA-C(29A)	34.44(15)	C(31B)-TiB-C(28B)	133.02(17)
C(28A)-TiA-C(29A)	33.67(15)	C(29B)-TiB-C(28B)	34.20(15)
C(13A)-TiA-C(33A)	109.75(17)	C(13B)-TiB-C(25B)	127.38(15)
C(1A)-TiA-C(33A)	77.69(16)	C(1B)-TiB-C(25B)	110.97(16)
C(27A)-TiA-C(33A)	133.21(16)	C(32B)-TiB-C(25B)	82.77(16)
C(32A)-TiA-C(33A)	34.00(15)	C(26B)-TiB-C(25B)	34.44(14)
C(26A)-TiA-C(33A)	113.47(17)	C(27B)-TiB-C(25B)	56.54(15)
C(31A)-TiA-C(33A)	56.44(16)	C(33B)-TiB-C(25B)	116.59(16)
C(25A)-TiA-C(33A)	120.78(18)	C(31B)-TiB-C(25B)	76.65(16)
C(28A)-TiA-C(33A)	167.48(16)	C(29B)-TiB-C(25B)	33.64(14)
C(29A)-TiA-C(33A)	150.52(18)	C(28B)-TiB-C(25B)	56.45(17)
C(13A)-TiA-C(30A)	76.60(16)	C(13B)-TiB-C(34B)	77.17(15)
C(1A)-TiA-C(30A)	130.16(18)	C(1B)-TiB-C(34B)	97.13(17)



C(27A)-TiA-C(30A)	96.24(18)	C(32B)-TiB-C(34B)	56.98(15)
C(32A)-TiA-C(30A)	56.96(16)	C(26B)-TiB-C(34B)	130.83(17)
C(26A)-TiA-C(30A)	109.12(17)	C(27B)-TiB-C(34B)	148.51(17)
C(31A)-TiA-C(30A)	33.73(15)	C(33B)-TiB-C(34B)	33.80(14)
C(25A)-TiA-C(30A)	142.25(18)	C(31B)-TiB-C(34B)	56.49(16)
C(28A)-TiA-C(30A)	117.00(18)	C(29B)-TiB-C(34B)	151.43(16)
C(29A)-TiA-C(30A)	150.41(18)	C(28B)-TiB-C(34B)	170.42(17)
C(33A)-TiA-C(30A)	56.48(16)	C(25B)-TiB-C(34B)	132.93(16)
C(13A)-TiA-C(34A)	78.00(17)	C(13B)-TiB-C(30B)	77.86(15)
C(1A)-TiA-C(34A)	96.33(17)	C(1B)-TiB-C(30B)	130.62(16)
C(27A)-TiA-C(34A)	130.33(17)	C(32B)-TiB-C(30B)	56.94(14)
C(32A)-TiA-C(34A)	56.55(17)	C(26B)-TiB-C(30B)	96.76(17)
C(26A)-TiA-C(34A)	133.94(16)	C(27B)-TiB-C(30B)	121.67(17)
C(31A)-TiA-C(34A)	56.27(16)	C(33B)-TiB-C(30B)	56.42(15)
C(25A)-TiA-C(34A)	153.93(19)	C(31B)-TiB-C(30B)	33.51(14)
C(28A)-TiA-C(34A)	146.28(18)	C(29B)-TiB-C(30B)	136.80(18)
C(29A)-TiA-C(34A)	169.36(16)	C(28B)-TiB-C(30B)	153.80(17)
C(33A)-TiA-C(34A)	33.67(15)	C(25B)-TiB-C(30B)	105.10(17)
C(30A)-TiA-C(34A)	34.21(16)	C(34B)-TiB-C(30B)	34.14(15)
C(11A)-O(1A)-C(12A)	106.3(4)	C(11B)-O(1B)-C(12B)	106.0(3)
C(23A)-O(2A)-C(24A)	105.9(3)	C(23B)-O(2B)-C(24B)	106.0(3)
C(12A)-C(1A)-C(2A)	110.3(4)	C(2B)-C(1B)-C(12B)	111.1(4)
C(12A)-C(1A)-TiA	126.3(3)	C(2B)-C(1B)-TiB	122.4(3)
C(2A)-C(1A)-TiA	123.3(4)	C(12B)-C(1B)-TiB	126.4(3)
C(1A)-C(2A)-C(3A)	123.9(5)	C(3B)-C(2B)-C(1B)	124.5(4)
C(4A)-C(3A)-C(2A)	121.5(5)	C(4B)-C(3B)-C(2B)	121.4(5)
C(3A)-C(4A)-C(5A)	118.1(5)	C(3B)-C(4B)-C(5B)	117.1(5)
C(4A)-C(5A)-C(12A)	117.9(5)	C(4B)-C(5B)-C(12B)	119.3(4)
C(4A)-C(5A)-C(6A)	135.6(5)	C(4B)-C(5B)-C(6B)	134.7(5)
C(12A)-C(5A)-C(6A)	106.2(4)	C(12B)-C(5B)-C(6B)	106.0(4)
C(11A)-C(6A)-C(7A)	117.4(5)	C(11B)-C(6B)-C(7B)	119.6(4)
C(11A)-C(6A)-C(5A)	106.6(4)	C(11B)-C(6B)-C(5B)	105.7(4)
C(7A)-C(6A)-C(5A)	135.9(5)	C(7B)-C(6B)-C(5B)	134.7(5)
C(8A)-C(7A)-C(6A)	117.8(6)	C(6B)-C(7B)-C(8B)	117.3(5)
C(9A)-C(8A)-C(7A)	123.2(6)	C(9B)-C(8B)-C(7B)	121.4(5)
C(8A)-C(9A)-C(10A)	120.7(6)	C(8B)-C(9B)-C(10B)	121.9(5)
C(11A)-C(10A)-C(9A)	116.2(5)	C(9B)-C(10B)-C(11B)	116.7(5)
C(10A)-C(11A)-O(1A)	124.9(5)	C(10B)-C(11B)-C(6B)	123.1(4)
C(10A)-C(11A)-C(6A)	124.4(5)	C(10B)-C(11B)-O(1B)	125.0(4)
O(1A)-C(11A)-C(6A)	110.7(5)	C(6B)-C(11B)-O(1B)	111.9(4)
C(5A)-C(12A)-O(1A)	110.1(4)	C(1B)-C(12B)-O(1B)	123.2(4)
C(5A)-C(12A)-C(1A)	127.9(4)	C(1B)-C(12B)-C(5B)	126.3(4)
O(1A)-C(12A)-C(1A)	122.0(4)	O(1B)-C(12B)-C(5B)	110.4(4)
C(24A)-C(13A)-C(14A)	110.9(4)	C(14B)-C(13B)-C(24B)	110.8(4)
C(24A)-C(13A)-TiA	126.4(3)	C(14B)-C(13B)-TiB	122.3(3)
C(14A)-C(13A)-TiA	122.6(3)	C(24B)-C(13B)-TiB	126.7(3)
C(15A)-C(14A)-C(13A)	124.3(4)	C(13B)-C(14B)-C(15B)	124.9(5)
C(16A)-C(15A)-C(14A)	121.2(4)	C(16B)-C(15B)-C(14B)	120.7(5)



C(15A)-C(16A)-C(17A)	118.0(4)	C(17B)-C(16B)-C(15B)	117.4(5)
C(16A)-C(17A)-C(24A)	118.4(4)	C(16B)-C(17B)-C(24B)	119.3(5)
C(16A)-C(17A)-C(18A)	135.1(4)	C(16B)-C(17B)-C(18B)	134.2(5)
C(24A)-C(17A)-C(18A)	106.6(4)	C(24B)-C(17B)-C(18B)	106.5(4)
C(19A)-C(18A)-C(23A)	118.8(4)	C(23B)-C(18B)-C(19B)	118.8(5)
C(19A)-C(18A)-C(17A)	135.4(4)	C(23B)-C(18B)-C(17B)	106.2(4)
C(23A)-C(18A)-C(17A)	105.8(4)	C(19B)-C(18B)-C(17B)	135.1(5)
C(20A)-C(19A)-C(18A)	119.2(5)	C(20B)-C(19B)-C(18B)	118.1(5)
C(19A)-C(20A)-C(21A)	120.7(5)	C(19B)-C(20B)-C(21B)	122.1(5)
C(20A)-C(21A)-C(22A)	122.0(5)	C(20B)-C(21B)-C(22B)	120.8(6)
C(23A)-C(22A)-C(21A)	115.6(4)	C(23B)-C(22B)-C(21B)	115.9(5)
C(22A)-C(23A)-O(2A)	124.6(4)	C(18B)-C(23B)-C(22B)	124.2(5)
C(22A)-C(23A)-C(18A)	123.7(4)	C(18B)-C(23B)-O(2B)	111.1(4)
O(2A)-C(23A)-C(18A)	111.8(4)	C(22B)-C(23B)-O(2B)	124.7(5)
C(13A)-C(24A)-C(17A)	127.2(4)	C(17B)-C(24B)-O(2B)	110.3(4)
C(13A)-C(24A)-O(2A)	122.8(4)	C(17B)-C(24B)-C(13B)	126.8(5)
C(17A)-C(24A)-O(2A)	110.0(3)	O(2B)-C(24B)-C(13B)	122.9(4)
C(26A)-C(25A)-C(29A)	108.2(4)	C(29B)-C(25B)-C(26B)	108.4(4)
C(26A)-C(25A)-TiA	72.7(3)	C(29B)-C(25B)-TiB	72.9(3)
C(29A)-C(25A)-TiA	73.0(3)	C(26B)-C(25B)-TiB	71.1(3)
C(25A)-C(26A)-C(27A)	107.7(4)	C(27B)-C(26B)-C(25B)	107.0(4)
C(25A)-C(26A)-TiA	73.7(3)	C(27B)-C(26B)-TiB	73.4(3)
C(27A)-C(26A)-TiA	70.8(2)	C(25B)-C(26B)-TiB	74.4(3)
C(26A)-C(27A)-C(28A)	108.6(4)	C(28B)-C(27B)-C(26B)	108.8(4)
C(26A)-C(27A)-TiA	74.7(3)	C(28B)-C(27B)-TiB	73.8(2)
C(28A)-C(27A)-TiA	75.4(3)	C(26B)-C(27B)-TiB	72.0(2)
C(29A)-C(28A)-C(27A)	107.9(4)	C(27B)-C(28B)-C(29B)	107.2(4)
C(29A)-C(28A)-TiA	73.3(3)	C(27B)-C(28B)-TiB	72.1(2)
C(27A)-C(28A)-TiA	70.3(3)	C(29B)-C(28B)-TiB	72.7(2)
C(28A)-C(29A)-C(25A)	107.5(4)	C(25B)-C(29B)-C(28B)	108.5(4)
C(28A)-C(29A)-TiA	73.0(3)	C(25B)-C(29B)-TiB	73.5(3)
C(25A)-C(29A)-TiA	72.6(3)	C(28B)-C(29B)-TiB	73.1(3)
C(31A)-C(30A)-C(34A)	107.4(4)	C(31B)-C(30B)-(34B)	108.1(4)
C(31A)-C(30A)-TiA	72.4(3)	C(31B)-C(30B)-TiB	72.2(2)
C(34A)-C(30A)-TiA	73.2(3)	C(34B)-C(30B)-TiB	72.4(2)
C(30A)-C(31A)-C(32A)	108.4(4)	C(30B)-C(31B)-(32B)	C107.9(4)
C(30A)-C(31A)-TiA	73.9(3)	C(30B)-C(31B)-TiB	74.3(3)
C(32A)-C(31A)-TiA	71.7(2)	C(32B)-C(31B)-TiB	70.6(2)
C(33A)-C(32A)-C(31A)	107.6(4)	C(33B)-C(32B)-(31B)	107.7(4)
C(33A)-C(32A)-TiA	74.5(3)	C(33B)-C(32B)-TiB	74.7(2)
C(31A)-C(32A)-TiA	73.7(3)	C(31B)-C(32B)-TiB	74.5(2)
C(34A)-C(33A)-C(32A)	108.5(4)	C(34B)-C(33B)-(32B)	108.2(4)
C(34A)-C(33A)-TiA	73.7(3)	C(34B)-C(33B)-TiB	73.6(2)
C(32A)-C(33A)-TiA	71.5(3)	C(32B)-C(33B)-TiB	70.8(2)
C(33A)-C(34A)-C(30A)	107.9(4)	C(33B)-C(34B)-(30B)	108.0(4)
C(33A)-C(34A)-TiA	72.7(3)	C(33B)-C(34B)-TiB	72.6(2)
C(30A)-C(34A)-TiA	72.6(3)	C(30B)-C(34B)-TiB	73.5(2)

Symmetry transformations used to generate equivalent atoms: #1 -x+2,-y,-z+1



Table 4. Anisotropic displacement parameters ($\text{Å}^2 \times 10^3$) for $[\text{TiCp}_2(\text{Dbf})_2]$.

Atom	U(11)	U(22)	U(33)	U(23)	U(13)	U(12)
Ti	20(1)	20(1)	20(1)	1(1)	1(1)	1(1)
Cl	27(1)	45(1)	36(1)	-6(1)	8(1)	7(1)
S(1)	31(1)	24(1)	22(1)	3(1)	-3(1)	-4(1)
S(2)	33(1)	33(1)	20(1)	2(1)	4(1)	-2(1)
C(1)	33(1)	22(1)	21(1)	-1(1)	-2(1)	-1(1)
C(2)	27(1)	27(1)	31(2)	0(1)	2(1)	0(1)
C(3)	35(1)	31(1)	27(1)	3(1)	9(1)	-2(1)
C(4)	38(2)	27(1)	19(1)	2(1)	2(1)	2(1)
C(5)	31(1)	19(1)	21(1)	-2(1)	0(1)	-2(1)
C(6)	31(1)	20(1)	22(1)	-2(1)	1(1)	-2(1)
C(7)	38(1)	25(1)	24(1)	-1(1)	-2(1)	-2(1)
C(8)	37(2)	37(2)	39(2)	-1(1)	-9(1)	-2(1)
C(9)	28(2)	54(2)	52(2)	3(2)	-4(1)	-3(1)
C(10)	35(2)	45(2)	38(2)	4(1)	10(1)	-6(1)
C(11)	32(1)	25(1)	24(1)	1(1)	1(1)	-2(1)
C(12)	31(1)	19(1)	21(1)	-2(1)	2(1)	-3(1)
C(13)	36(1)	21(1)	37(2)	4(1)	-6(1)	5(1)
C(14)	52(2)	24(1)	28(2)	5(1)	11(1)	-2(1)
C(15)	35(1)	26(1)	39(2)	0(1)	11(1)	-11(1)
C(16)	33(1)	20(1)	36(2)	-2(1)	3(1)	-2(1)
C(17)	28(1)	20(1)	38(2)	0(1)	5(1)	3(1)
C(18)	42(2)	45(2)	25(1)	9(1)	-1(1)	19(1)
C(19)	32(1)	47(2)	20(1)	0(1)	-3(1)	-2(1)
C(20)	38(2)	29(1)	20(1)	3(1)	7(1)	5(1)
C(21)	35(1)	39(2)	24(1)	16(1)	2(1)	-3(1)
C(22)	65(2)	22(1)	23(1)	7(1)	0(1)	4(1)

The anisotropic displacement factor exponent takes the form:

$$-2 \pi^2 [h^2 a^{*2} U(11) + \dots + 2 h k a^* b^* U(12)]$$

Table 5. Hydrogen coordinates ($\times 10^4$) and isotropic displacement parameters ($\text{Å}^2 \times 10^3$) for $[\text{TiCp}_2(\text{Dbf})_2]$.

Atom	x	y	z	U_{eq}
H(2A)	7585	2470	1899	34
H(3A)	8166	1688	2920	37
H(4A)	10203	1337	3285	34
H(7A)	12541	879	3477	35
H(8A)	14627	727	3486	46
H(9A)	15553	1485	2619	54
H(10A)	14385	2384	1720	47
H(13A)	9418	-432	1019	39
H(14A)	7319	-432	1407	41
H(15A)	5733	-1201	491	40
H(16A)	6858	-1649	-459	35
H(17A)	9142	-1146	-136	34
H(18A)	5691	4182	-503	45
H(19A)	6055	1320	-1038	40
H(20A)	8362	907	-1020	34
H(21A)	9419	3482	-453	39
H(22A)	7758	5476	-124	44

Appendix B

Crystallographic data for [TiCp₂(Dbz)Cl] 2-05.

Table 1. Fractional atomic coordinates ($\times 10^4$) and equivalent isotropic displacement parameters ($\text{Å}^2 \times 10^3$) for [TiCp₂(Dbz)Cl].

Atom	x/a	y/b	z/c	U _{eq}
Ti	1229(1)	1961(1)	9799(1)	21(1)
Cl	1952(1)	838(1)	10619(1)	31(1)
O(1)	2028(2)	3106(1)	8226(2)	35(1)
C(1)	7618(4)	-1127(2)	3281(2)	51(1)
C(2)	8098(4)	-395(2)	3483(3)	54(1)
O(2)	4402(2)	3185(1)	7529(1)	34(1)
C(3)	9038(4)	-183(2)	4235(3)	49(1)
C(4)	9411(3)	573(2)	4360(2)	35(1)
O(3)	-1151(3)	4258(1)	8588(2)	58(1)
C(5)	10390(4)	748(2)	5150(3)	49(1)
C(6)	10785(4)	1493(2)	5308(3)	55(1)
C(7)	11771(5)	1709(2)	6094(4)	68(1)
C(8)	-739(3)	1180(2)	9250(2)	42(1)
C(9)	-1170(3)	1931(2)	9220(2)	41(1)
C(10)	-589(3)	2321(2)	8592(2)	36(1)
C(11)	189(3)	1793(2)	8235(2)	32(1)
C(12)	114(3)	1096(2)	8648(2)	38(1)
C(13)	506(4)	2732(2)	10858(3)	47(1)
C(14)	822(4)	3215(2)	10205(2)	47(1)
C(15)	2234(4)	3156(2)	10279(2)	38(1)
C(16)	2769(3)	2642(2)	10971(2)	40(1)
C(17)	1694(4)	2404(2)	11325(2)	45(1)
C(18)	2950(3)	2049(1)	9134(2)	22(1)
C(19)	4044(3)	1542(2)	9384(2)	27(1)
C(20)	5194(3)	1567(2)	9014(2)	31(1)
C(21)	5295(3)	2107(2)	8385(2)	28(1)
C(22)	4242(3)	2626(2)	8134(2)	26(1)
C(23)	3090(3)	2589(1)	8490(2)	24(1)
C(24)	3240(3)	3597(2)	7155(2)	29(1)
C(25)	2060(3)	3545(1)	7487(2)	28(1)
C(26)	3276(3)	4080(2)	6448(2)	33(1)
C(27)	2128(3)	4509(2)	6064(2)	37(1)
C(28)	938(3)	4444(2)	6382(2)	37(1)
C(29)	901(3)	3957(2)	7083(2)	33(1)
C(30)	-770(5)	5034(3)	8506(4)	77(1)
C(31)	-2008(5)	5398(2)	7920(3)	61(1)
C(32)	-3136(5)	4968(3)	8141(5)	89(2)
C(33)	-2569(5)	4233(3)	8443(5)	87(2)

U_{eq} is defined as one third of the trace of the orthogonalized U_{ij} tensor.

**Table 2.** Bond lengths [Å] for [TiCp₂(Dbz)Cl].

Ti-C(18)	2.208(2)	C(7)-C(1)#1	1.439(6)
Ti-C(10)	2.356(3)	C(8)-C(9)	1.394(5)
Ti-C(9)	2.360(3)	C(8)-C(12)	1.406(5)
Ti-C(14)	2.364(3)	C(9)-C(10)	1.417(5)
Ti-C(13)	2.362(3)	C(10)-C(11)	1.408(4)
Ti-Cl	2.3684(7)	C(11)-C(12)	1.395(4)
Ti-C(15)	2.381(3)	C(13)-C(17)	1.365(6)
Ti-C(11)	2.394(3)	C(13)-C(14)	1.408(6)
Ti-C(8)	2.392(3)	C(14)-C(15)	1.397(5)
Ti-C(16)	2.397(3)	C(15)-C(16)	1.404(5)
Ti-C(12)	2.400(3)	C(16)-C(17)	1.383(5)
Ti-C(17)	2.404(3)	C(18)-C(19)	1.397(4)
O(1)-C(25)	1.379(3)	C(18)-C(23)	1.404(3)
O(1)-C(23)	1.389(3)	C(19)-C(20)	1.403(4)
C(1)-C(2)	1.391(5)	C(20)-C(21)	1.376(4)
C(1)-C(7)#1	1.439(6)	C(21)-C(22)	1.383(4)
C(2)-C(3)	1.356(5)	C(22)-C(23)	1.392(3)
O(2)-C(24)	1.378(3)	C(24)-C(26)	1.387(4)
O(2)-C(22)	1.389(3)	C(24)-C(25)	1.397(4)
C(3)-C(5)#1	1.398(5)	C(25)-C(29)	1.387(4)
C(3)-C(4)	1.388(4)	C(26)-C(27)	1.388(4)
C(4)-C(5)	1.400(5)	C(27)-C(28)	1.398(4)
O(3)-C(33)	1.387(6)	C(28)-C(29)	1.383(4)
O(3)-C(30)	1.437(5)	C(30)-C(31)	1.494(7)
C(5)-C(6)	1.380(6)	C(31)-C(32)	1.467(7)
C(5)-C(3)#1	1.398(5)	C(32)-C(33)	1.449(6)
C(6)-C(7)	1.417(7)		

Symmetry transformations used to generate equivalent atoms: #1 -x+2,-y,-z+1



Table 3. Bond angles [°] for [TiCp₂(Dbz)Cl].

C(18)-Ti-C(10)	99.42(10)	C(3)-C(2)-C(1)	125.5(4)
C(18)-Ti-C(9)	131.90(11)	C(24)-O(2)-C(22)	115.7(2)
C(10)-Ti-C(9)	34.98(12)	C(2)-C(3)-C(5)#1	117.9(4)
C(18)-Ti-C(14)	104.94(12)	C(2)-C(3)-C(4)	119.5(3)
C(10)-Ti-C(14)	78.65(12)	C(5)#1-C(3)-C(4)	122.6(3)
C(9)-Ti-C(14)	84.01(13)	C(3)-C(4)-C(5)	116.3(3)
C(18)-Ti-C(13)	132.65(11)	C(33)-O(3)-C(30)	107.5(3)
C(10)-Ti-C(13)	94.38(13)	C(6)-C(5)-C(3)#1	120.5(4)
C(9)-Ti-C(13)	79.56(12)	C(6)-C(5)-C(4)	118.4(3)
C(14)-Ti-C(13)	34.67(14)	C(3)#1-C(5)-C(4)	121.1(3)
C(18)-Ti-Cl	97.42(7)	C(5)-C(6)-C(7)	121.3(4)
C(10)-Ti-Cl	136.53(8)	C(6)-C(7)-C(1)#1	118.4(4)
C(9)-Ti-Cl	109.72(9)	C(9)-C(8)-C(12)	108.2(3)
C(14)-Ti-Cl	134.10(9)	C(9)-C(8)-Ti	71.7(2)
C(13)-Ti-Cl	102.94(11)	C(12)-C(8)-Ti	73.2(2)
C(18)-Ti-C(15)	76.09(10)	C(8)-C(9)-C(10)	108.1(3)
C(10)-Ti-C(15)	101.24(12)	C(8)-C(9)-Ti	74.2(2)
C(9)-Ti-C(15)	117.09(12)	C(10)-C(9)-Ti	72.4(2)
C(14)-Ti-C(15)	34.26(13)	C(11)-C(10)-C(9)	107.2(3)
C(13)-Ti-C(15)	56.79(11)	C(11)-C(10)-Ti	74.3(2)
Cl-Ti-C(15)	121.68(9)	C(9)-C(10)-Ti	72.7(2)
C(18)-Ti-C(11)	75.54(10)	C(12)-C(11)-C(10)	108.3(3)
C(10)-Ti-C(11)	34.47(11)	C(12)-C(11)-Ti	73.3(2)
C(9)-Ti-C(11)	57.16(11)	C(10)-C(11)-Ti	71.3(2)
C(14)-Ti-C(11)	108.55(11)	C(11)-C(12)-C(8)	108.1(3)
C(13)-Ti-C(11)	128.85(13)	C(11)-C(12)-Ti	72.9(2)
Cl-Ti-C(11)	115.69(8)	C(8)-C(12)-Ti	72.6(2)
C(15)-Ti-C(11)	118.11(11)	C(17)-C(13)-C(14)	108.3(3)
C(18)-Ti-C(8)	123.28(11)	C(17)-C(13)-Ti	75.1(2)
C(10)-Ti-C(8)	57.28(12)	C(14)-C(13)-Ti	72.8(2)
C(9)-Ti-C(8)	34.11(13)	C(15)-C(14)-C(13)	107.0(3)
C(14)-Ti-C(8)	117.03(14)	C(15)-C(14)-Ti	73.5(2)
C(13)-Ti-C(8)	102.27(12)	C(13)-C(14)-Ti	72.6(2)
Cl-Ti-C(8)	80.02(9)	C(14)-C(15)-C(16)	108.0(3)
C(15)-Ti-C(8)	150.98(13)	C(14)-C(15)-Ti	72.2(2)
C(11)-Ti-C(8)	56.57(11)	C(16)-C(15)-Ti	73.6(2)
C(18)-Ti-C(16)	82.80(10)	C(17)-C(16)-C(15)	107.4(3)
C(10)-Ti-C(16)	133.93(12)	C(17)-C(16)-Ti	73.6(2)
C(9)-Ti-C(16)	135.35(12)	C(15)-C(16)-Ti	72.3(2)
C(14)-Ti-C(16)	56.82(12)	C(13)-C(17)-C(16)	109.3(3)
C(13)-Ti-C(16)	56.20(12)	C(13)-C(17)-Ti	71.6(2)
Cl-Ti-C(16)	87.75(9)	C(16)-C(17)-Ti	73.0(2)
C(15)-Ti-C(16)	34.17(12)	C(19)-C(18)-C(23)	115.2(2)
C(11)-Ti-C(16)	149.62(12)	C(19)-C(18)-Ti	118.5(2)
C(8)-Ti-C(16)	152.22(12)	C(23)-C(18)-Ti	126.2(2)
C(18)-Ti-C(12)	89.17(10)	C(18)-C(19)-C(20)	122.4(2)



C(10)-Ti-C(12)	57.09(11)	C(21)-C(20)-C(19)	120.7(2)
C(9)-Ti-C(12)	56.89(12)	C(20)-C(21)-C(22)	118.4(2)
C(14)-Ti-C(12)	135.33(12)	C(21)-C(22)-O(2)	117.1(2)
C(13)-Ti-C(12)	134.97(12)	C(21)-C(22)-C(23)	120.7(2)
Cl-Ti-C(12)	83.52(8)	O(2)-C(22)-C(23)	122.2(2)
C(15)-Ti-C(12)	151.82(11)	C(22)-C(23)-O(1)	120.4(2)
C(11)-Ti-C(12)	33.85(11)	C(22)-C(23)-C(18)	122.6(2)
C(8)-Ti-C(12)	34.12(12)	O(1)-C(23)-C(18)	117.1(2)
C(16)-Ti-C(12)	167.29(12)	C(26)-C(24)-O(2)	118.3(2)
C(18)-Ti-C(17)	115.65(11)	C(26)-C(24)-C(25)	120.4(3)
C(10)-Ti-C(17)	127.63(12)	O(2)-C(24)-C(25)	121.3(2)
C(9)-Ti-C(17)	108.53(13)	C(29)-C(25)-O(1)	118.7(2)
C(14)-Ti-C(17)	56.25(12)	C(29)-C(25)-C(24)	119.8(2)
C(13)-Ti-C(17)	33.28(13)	O(1)-C(25)-C(24)	121.5(2)
Cl-Ti-C(17)	78.00(9)	C(24)-C(26)-C(27)	119.6(3)
C(15)-Ti-C(17)	55.97(11)	C(26)-C(27)-C(28)	119.9(3)
C(11)-Ti-C(17)	162.10(12)	C(29)-C(28)-C(27)	120.3(3)
C(8)-Ti-C(17)	118.92(13)	C(25)-C(29)-C(28)	119.9(3)
C(16)-Ti-C(17)	33.47(12)	O(3)-C(30)-C(31)	105.2(4)
C(12)-Ti-C(17)	150.56(12)	C(32)-C(31)-C(30)	102.4(4)
C(25)-O(1)-C(23)	116.3(2)	C(33)-C(32)-C(31)	105.8(4)
C(2)-C(1)-C(7)#1	116.5(4)	O(3)-C(33)-C(32)	109.4(4)

Symmetry transformations used to generate equivalent atoms:

#1 $-x+2, -y, -z+1$



Table 4. Anisotropic displacement parameters ($\text{Å}^2 \times 10^3$) for $[\text{TiCp}_2(\text{Dbz})\text{Cl}]$.

Atom	U(11)	U(22)	U(33)	U(23)	U(13)	U(12)
Ti	20(1)	20(1)	23(1)	-1(1)	7(1)	-3(1)
Cl	38(1)	27(1)	31(1)	6(1)	12(1)	0(1)
O(1)	34(1)	33(1)	45(1)	16(1)	23(1)	10(1)
C(1)	66(2)	41(2)	46(2)	-5(2)	14(2)	2(2)
C(2)	47(2)	47(2)	62(2)	-10(2)	5(2)	5(2)
O(2)	30(1)	38(1)	40(1)	16(1)	18(1)	4(1)
C(3)	55(2)	39(2)	53(2)	-2(2)	11(2)	3(2)
C(4)	43(2)	24(1)	32(1)	4(1)	-5(1)	0(1)
O(3)	46(2)	38(1)	86(2)	0(1)	9(1)	11(1)
C(5)	47(2)	48(2)	54(2)	9(2)	15(2)	4(1)
C(6)	60(2)	51(2)	57(2)	5(2)	22(2)	10(2)
C(7)	65(3)	38(2)	120(4)	8(2)	57(3)	10(2)
C(8)	37(2)	49(2)	36(2)	2(1)	0(1)	-24(1)
C(9)	18(1)	62(2)	43(2)	-13(1)	9(1)	-5(1)
C(10)	29(1)	36(2)	37(2)	3(1)	-2(1)	4(1)
C(11)	25(1)	42(2)	26(1)	-2(1)	3(1)	-4(1)
C(12)	40(2)	31(2)	36(2)	-9(1)	-5(1)	-3(1)
C(13)	43(2)	47(2)	58(2)	-27(2)	29(2)	-11(1)
C(14)	60(2)	27(1)	47(2)	-15(1)	-2(2)	11(1)
C(15)	52(2)	31(1)	38(2)	-14(1)	21(1)	-19(1)
C(16)	35(2)	43(2)	38(2)	-20(1)	3(1)	-4(1)
C(17)	71(2)	39(2)	30(1)	-10(1)	18(2)	-8(2)
C(18)	21(1)	23(1)	22(1)	-3(1)	7(1)	-3(1)
C(19)	24(1)	24(1)	34(1)	6(1)	7(1)	1(1)
C(20)	25(1)	31(1)	37(1)	5(1)	9(1)	7(1)
C(21)	19(1)	32(1)	35(1)	0(1)	10(1)	-1(1)
C(22)	24(1)	27(1)	27(1)	3(1)	9(1)	-2(1)
C(23)	24(1)	22(1)	28(1)	1(1)	10(1)	2(1)
C(24)	31(1)	24(1)	34(1)	4(1)	14(1)	-1(1)
C(25)	31(1)	23(1)	32(1)	6(1)	11(1)	0(1)
C(26)	39(2)	31(1)	31(1)	3(1)	15(1)	-5(1)
C(27)	47(2)	34(2)	32(1)	6(1)	10(1)	-5(1)
C(28)	37(2)	30(1)	39(2)	5(1)	3(1)	-1(1)
C(29)	28(1)	26(1)	43(2)	4(1)	7(1)	-1(1)
C(30)	64(3)	59(3)	112(4)	-32(3)	29(3)	-10(2)
C(31)	83(3)	38(2)	61(2)	-3(2)	13(2)	-1(2)
C(32)	59(3)	85(4)	118(4)	36(3)	12(3)	25(2)
C(33)	58(3)	76(3)	134(5)	31(3)	38(3)	10(2)

The anisotropic displacement factor exponent takes the form:

$$-2 \pi^2 [h^2 a^{*2} U(11) + \dots + 2 h k a^* b^* U(12)]$$

Table 5. Hydrogen coordinates ($\times 10^4$) and isotropic displacement parameters ($\text{Å}^2 \times 10^3$) for $[\text{TiCp}_2(\text{Dbz})\text{Cl}]$.

Atom	x	y	z	U_{eq}
H(8)	-939(59)	925(31)	9595(39)	89(17)
H(9)	-1709(39)	2100(20)	9474(27)	41(10)
H(10)	-720(45)	2910(23)	8459(30)	57(11)
H(11)	687(40)	1861(20)	7814(28)	45(10)
H(12)	525(45)	652(24)	8615(29)	56(11)
H(13)	-366(45)	2654(23)	10910(28)	50(11)
H(14)	107(50)	3538(27)	9875(33)	66(14)
H(15)	2764(48)	3289(26)	9936(32)	70(13)
H(16)	3635(35)	2511(19)	11143(23)	31(8)
H(17)	1600(67)	2033(31)	11747(47)	103(21)
H(19)	3969(40)	1167(23)	9786(27)	51(10)
H(20)	5916(44)	1193(25)	9162(27)	57(11)
H(21)	5986(40)	2170(20)	8093(26)	42(9)
H(26)	4094(42)	4119(21)	6236(28)	49(10)
H(27)	2175(38)	4798(21)	5586(26)	42(9)
H(28)	83(37)	4772(21)	6121(24)	42(9)
H(29)	28(38)	3881(20)	7359(24)	41(9)
H(30A)	7(5)	5067(3)	8233(4)	93
H(30B)	-530(5)	5276(3)	9090(4)	93
H(31A)	-2061(5)	5930(2)	8064(3)	73
H(31B)	-2009(5)	5347(2)	7289(3)	73
H(32A)	-3467(5)	5220(3)	8611(5)	107
H(32B)	-3892(5)	4916(3)	7616(5)	107
H(33A)	-2822(5)	4096(3)	8996(5)	104
H(33B)	-2937(5)	3853(3)	7994(5)	104

Appendix C

Crystallographic data for $[TiCp_2(DbS)Cl]$ 2-16.

Table 1. Fractional atomic coordinates ($\times 10^4$) and equivalent isotropic displacement parameters ($\text{Å}^2 \times 10^3$) for $[TiCp_2(DbS)Cl]$.

Atom	x	y	z	U_{eq}
Ti	7485(1)	1706(1)	235(1)	20(1)
Cl	5763(1)	2640(1)	708(1)	36(1)
S(1)	8951(1)	3370(1)	871(1)	26(1)
S(2)	11721(1)	2761(1)	1440(1)	28(1)
C(1)	9282(2)	2608(3)	1637(1)	26(1)
C(2)	8418(2)	2336(3)	2040(1)	29(1)
C(3)	8767(2)	1864(3)	2652(1)	31(1)
C(4)	9978(2)	1651(3)	2870(1)	28(1)
C(5)	10869(2)	1903(3)	2474(1)	24(1)
C(6)	12182(2)	1743(3)	2591(1)	25(1)
C(7)	12906(2)	1190(3)	3122(1)	30(1)
C(8)	14144(2)	1099(3)	3126(1)	39(1)
C(9)	14698(3)	1548(4)	2607(1)	45(1)
C(10)	14012(2)	2083(4)	2074(1)	39(1)
C(11)	12758(2)	2166(3)	2070(1)	27(1)
C(12)	10498(2)	2398(3)	1865(1)	24(1)
C(13)	8627(2)	-562(3)	758(1)	32(1)
C(14)	7481(2)	-559(3)	970(1)	34(1)
C(15)	6612(2)	-980(3)	468(1)	33(1)
C(16)	7225(2)	-1219(3)	-51(1)	30(1)
C(17)	8477(2)	-936(3)	125(1)	29(1)
C(18)	6493(3)	3620(4)	-522(1)	38(1)
C(19)	6692(2)	2050(4)	-810(1)	33(1)
C(20)	7955(2)	1827(3)	-802(1)	29(1)
C(21)	8533(2)	3230(3)	-493(1)	33(1)
C(22)	7621(3)	4321(3)	-314(1)	37(1)

U_{eq} is defined as one third of the trace of the orthogonalized U_{ij} tensor.

**Table 2.** Bond lengths [Å] for [TiCp₂(Dbt-S)Cl].

Ti-C(17)	2.368(2)	C(4)-C(5)	1.403(3)
Ti-C(19)	2.378(2)	C(5)-C(12)	1.408(3)
Ti-C(16)	2.382(2)	C(5)-C(6)	1.460(3)
Ti-C(22)	2.387(2)	C(6)-C(7)	1.408(3)
Ti-C(20)	2.393(2)	C(6)-C(11)	1.411(3)
Ti-Cl	2.3948(7)	C(7)-C(8)	1.379(4)
Ti-C(14)	2.398(2)	C(8)-C(9)	1.400(4)
Ti-C(15)	2.395(2)	C(9)-C(10)	1.388(4)
Ti-C(21)	2.398(2)	C(10)-C(11)	1.396(4)
Ti-C(13)	2.398(2)	C(13)-C(17)	1.411(4)
Ti-S(1)	2.4068(7)	C(13)-C(14)	1.407(3)
Ti-C(18)	2.410(3)	C(14)-C(15)	1.420(4)
S(1)-C(1)	1.782(2)	C(15)-C(16)	1.405(4)
S(2)-C(12)	1.757(2)	C(16)-C(17)	1.421(3)
S(2)-C(11)	1.762(2)	C(18)-C(22)	1.399(4)
C(1)-C(2)	1.394(3)	C(18)-C(19)	1.411(4)
C(1)-C(12)	1.400(3)	C(19)-C(20)	1.415(3)
C(2)-C(3)	1.404(4)	C(20)-C(21)	1.407(4)
C(3)-C(4)	1.389(4)	C(21)-C(22)	1.415(4)

Symmetry transformations used to generate equivalent atoms: #1 -x+2,-y,-z+1

Table 3. Bond angles [°] for [TiCp₂(Dbt-S)Cl].

C(17)-Ti-C(19)	97.31(9)	Cl-Ti-C(18)	77.39(7)
C(17)-Ti-C(16)	34.81(8)	C(14)-Ti-C(18)	152.57(10)
C(19)-Ti-C(16)	80.45(9)	C(15)-Ti-C(18)	121.79(10)
C(17)-Ti-C(22)	129.79(9)	C(21)-Ti-C(18)	56.76(9)
C(19)-Ti-C(22)	56.92(9)	C(13)-Ti-C(18)	165.16(9)
C(16)-Ti-C(22)	134.70(9)	S(1)-Ti-C(18)	106.97(7)
C(17)-Ti-C(20)	77.50(9)	C(1)-S(1)-Ti	114.89(8)
C(19)-Ti-C(20)	34.49(8)	C(12)-S(2)-C(11)	91.06(12)
C(16)-Ti-C(20)	79.69(9)	C(2)-C(1)-C(12)	117.6(2)
C(22)-Ti-C(20)	56.87(9)	C(2)-C(1)-S(1)	124.43(19)
C(17)-Ti-Cl	135.67(7)	C(12)-C(1)-S(1)	117.75(18)
C(19)-Ti-Cl	98.93(7)	C(1)-C(2)-C(3)	120.7(2)
C(16)-Ti-Cl	109.12(6)	C(4)-C(3)-C(2)	120.9(2)
C(22)-Ti-Cl	93.23(7)	C(3)-C(4)-C(5)	119.7(2)
C(20)-Ti-Cl	132.18(6)	C(4)-C(5)-C(12)	118.3(2)
C(17)-Ti-C(14)	57.30(9)	C(4)-C(5)-C(6)	130.0(2)
C(19)-Ti-C(14)	134.76(9)	C(12)-C(5)-C(6)	111.7(2)
C(16)-Ti-C(14)	57.14(9)	C(7)-C(6)-C(11)	118.2(2)
C(22)-Ti-C(14)	168.00(9)	C(7)-C(6)-C(5)	129.7(2)
C(20)-Ti-C(14)	133.36(9)	C(11)-C(6)-C(5)	112.0(2)
Cl-Ti-C(14)	82.59(7)	C(8)-C(7)-C(6)	120.0(2)
C(17)-Ti-C(15)	57.39(9)	C(7)-C(8)-C(9)	120.8(3)
C(19)-Ti-C(15)	100.95(9)	C(10)-C(9)-C(8)	120.7(3)
C(16)-Ti-C(15)	34.20(9)	C(9)-C(10)-C(11)	118.3(3)
C(22)-Ti-C(15)	155.51(9)	C(10)-C(11)-C(6)	122.0(2)
C(20)-Ti-C(15)	112.06(9)	C(10)-C(11)-S(2)	125.7(2)
Cl-Ti-C(15)	79.10(7)	C(6)-C(11)-S(2)	112.36(18)
C(14)-Ti-C(15)	34.48(9)	C(1)-C(12)-C(5)	122.7(2)
C(17)-Ti-C(21)	95.69(9)	C(1)-C(12)-S(2)	124.54(19)
C(19)-Ti-C(21)	57.12(9)	C(5)-C(12)-S(2)	112.75(18)
C(16)-Ti-C(21)	110.89(9)	C(17)-C(13)-C(14)	108.4(2)
C(22)-Ti-C(21)	34.40(9)	C(17)-C(13)-Ti	71.63(13)
C(20)-Ti-C(21)	34.17(9)	C(14)-C(13)-Ti	72.92(14)
Cl-Ti-C(21)	127.59(7)	C(13)-C(14)-C(15)	107.8(2)
C(14)-Ti-C(21)	148.65(9)	C(13)-C(14)-Ti	72.97(14)
C(15)-Ti-C(21)	144.91(9)	C(15)-C(14)-Ti	72.67(14)
C(17)-Ti-C(13)	34.42(9)	C(16)-C(15)-C(14)	108.0(2)
C(19)-Ti-C(13)	131.63(9)	C(16)-C(15)-Ti	72.38(13)
C(16)-Ti-C(13)	57.12(9)	C(14)-C(15)-Ti	72.85(14)
C(22)-Ti-C(13)	144.63(9)	C(15)-C(16)-C(17)	108.1(2)
C(20)-Ti-C(13)	108.88(9)	C(15)-C(16)-Ti	73.42(14)
Cl-Ti-C(13)	115.15(7)	C(17)-C(16)-Ti	72.07(13)
C(14)-Ti-C(13)	34.11(8)	C(13)-C(17)-C(16)	107.6(2)
C(15)-Ti-C(13)	56.93(9)	C(13)-C(17)-Ti	73.95(13)
C(21)-Ti-C(13)	114.55(9)	C(16)-C(17)-Ti	73.12(13)
C(17)-Ti-S(1)	103.77(6)	C(22)-C(18)-C(19)	107.8(2)
C(19)-Ti-S(1)	130.70(7)	C(22)-C(18)-Ti	72.16(14)



C(16)-Ti-S(1)	136.62(6)	C(19)-C(18)-Ti	71.65(14)
C(22)-Ti-S(1)	75.64(7)	C(18)-C(19)-C(20)	107.9(2)
C(20)-Ti-S(1)	108.90(6)	C(18)-C(19)-Ti	74.08(14)
Cl-Ti-S(1)	96.13(3)	C(20)-C(19)-Ti	73.34(14)
C(14)-Ti-S(1)	93.55(7)	C(21)-C(20)-C(19)	108.0(2)
C(15)-Ti-S(1)	127.98(7)	C(21)-C(20)-Ti	73.09(14)
C(21)-Ti-S(1)	76.63(7)	C(19)-C(20)-Ti	72.17(14)
C(13)-Ti-S(1)	80.49(6)	C(20)-C(21)-C(22)	107.5(2)
C(17)-Ti-C(18)	130.92(9)	C(20)-C(21)-Ti	72.75(14)
C(19)-Ti-C(18)	34.27(9)	C(22)-C(21)-Ti	72.39(14)
C(16)-Ti-C(18)	112.52(9)	C(18)-C(22)-C(21)	108.6(2)
C(22)-Ti-C(18)	33.90(9)	C(18)-C(22)-Ti	73.93(15)
C(20)-Ti-C(18)	56.82(9)	C(21)-C(22)-Ti	73.21(13)

Symmetry transformations used to generate equivalent atoms:

#1 -x+2,-y,-z+1

Table 4. Anisotropic displacement parameters ($\text{Å}^2 \times 10^3$) for $[\text{TiCp}_2(\text{Dbt-S})\text{Cl}]$.

Atom	U(11)	U(22)	U(33)	U(23)	U(13)	U(12)
Ti	20(1)	20(1)	20(1)	1(1)	1(1)	1(1)
Cl	27(1)	45(1)	36(1)	-6(1)	8(1)	7(1)
S(1)	31(1)	24(1)	22(1)	3(1)	-3(1)	-4(1)
S(2)	33(1)	33(1)	20(1)	2(1)	4(1)	-2(1)
C(1)	33(1)	22(1)	21(1)	-1(1)	-2(1)	-1(1)
C(2)	27(1)	27(1)	31(2)	0(1)	2(1)	0(1)
C(3)	35(1)	31(1)	27(1)	3(1)	9(1)	-2(1)
C(4)	38(2)	27(1)	19(1)	2(1)	2(1)	2(1)
C(5)	31(1)	19(1)	21(1)	-2(1)	0(1)	-2(1)
C(6)	31(1)	20(1)	22(1)	-2(1)	1(1)	-2(1)
C(7)	38(1)	25(1)	24(1)	-1(1)	-2(1)	-2(1)
C(8)	37(2)	37(2)	39(2)	-1(1)	-9(1)	-2(1)
C(9)	28(2)	54(2)	52(2)	3(2)	-4(1)	-3(1)
C(10)	35(2)	45(2)	38(2)	4(1)	10(1)	-6(1)
C(11)	32(1)	25(1)	24(1)	1(1)	1(1)	-2(1)
C(12)	31(1)	19(1)	21(1)	-2(1)	2(1)	-3(1)
C(13)	36(1)	21(1)	37(2)	4(1)	-6(1)	5(1)
C(14)	52(2)	24(1)	28(2)	5(1)	11(1)	-2(1)
C(15)	35(1)	26(1)	39(2)	0(1)	11(1)	-11(1)
C(16)	33(1)	20(1)	36(2)	-2(1)	3(1)	-2(1)
C(17)	28(1)	20(1)	38(2)	0(1)	5(1)	3(1)
C(18)	42(2)	45(2)	25(1)	9(1)	-1(1)	19(1)
C(19)	32(1)	47(2)	20(1)	0(1)	-3(1)	-2(1)
C(20)	38(2)	29(1)	20(1)	3(1)	7(1)	5(1)
C(21)	35(1)	39(2)	24(1)	16(1)	2(1)	-3(1)
C(22)	65(2)	22(1)	23(1)	7(1)	0(1)	4(1)

The anisotropic displacement factor exponent takes the form:

$$-2 \pi^2 [h^2 a^{*2} U(11) + \dots + 2 h k a^* b^* U(12)]$$

Table 5. Hydrogen coordinates ($\times 10^4$) and isotropic displacement parameters ($\text{Å}^2 \times 10^3$) for $[\text{TiCp}_2(\text{Dbt})\text{Cl}]$.

Atom	x	y	z	U_{eq}
H(2A)	7585	2470	1899	34
H(3A)	8166	1688	2920	37
H(4A)	10203	1337	3285	34
H(7A)	12541	879	3477	35
H(8A)	14627	727	3486	46
H(9A)	15553	1485	2619	54
H(10A)	14385	2384	1720	47
H(13A)	9418	-432	1019	39
H(14A)	7319	-432	1407	41
H(15A)	5733	-1201	491	40
H(16A)	6858	-1649	-459	35
H(17A)	9142	-1146	-136	34
H(18A)	5691	4182	-503	45
H(19A)	6055	1320	-1038	40
H(20A)	8362	907	-1020	34
H(21A)	9419	3482	-453	39
H(22A)	7758	5476	-124	44

Appendix D

Results of the preclinical tests of the selected complexes on CoLo and HeLa cells

Table 1. Inhibition of HeLa and CoLo cells by S-01, 2-08, 3-09, 2-05 and 3-05.

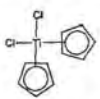
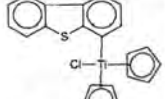
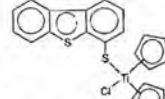
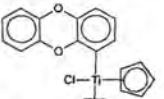
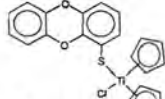

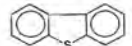
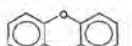
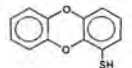
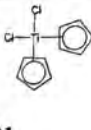
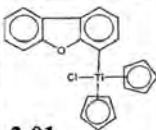
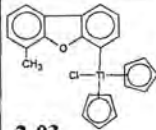
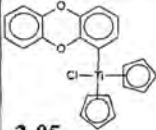
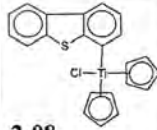
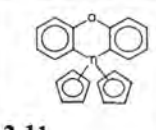
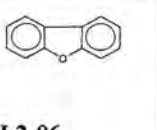
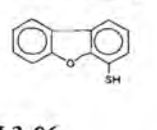
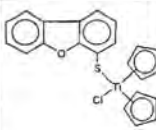
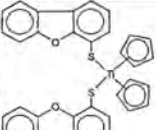
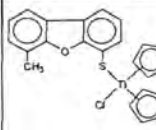
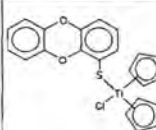
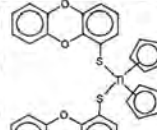
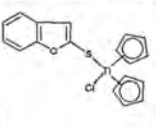
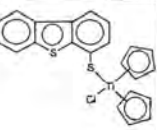
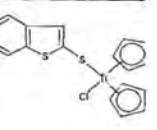
Conc. µg/ml	 S-01		 2-08		 3-09		 2-05		 3-05	
	% Cell Growth									
	HeLa	CoLo	HeLa	CoLo	HeLa	CoLo	HeLa	CoLo	HeLa	CoLo
0	100	100	100	100	100	100	100	100	100	100
0.05	100	100	100	100	100	100	96	91	48	69
0.1	100	100	100	100	100	100	87	85	47	50
0.2	100	100	100	100	100	100	75	80	40	49
0.4	100	100	98	100	85	100	48	50	41	40
0.8	100	100	93	100	84	100	40	43	41	45
1.5	100	100	88	100	81	97	-	-	-	-
3	99	98	85	97	68	91	-	-	-	-
6	95	101	70	93	63	89	-	-	-	-
12	78	82	56	78	50	55	-	-	-	-
25	53	57	48	56	42	54	-	-	-	-
Conc. µg/ml	 3-10		 L2-01		 L2-03		 L3-03			
	% Cell Growth									
	HeLa	CoLo	HeLa	CoLo	HeLa	CoLo	HeLa	CoLo	HeLa	CoLo
0	100	100	100	100	100	100	100	100	100	
0.05	100	100	100	100	100	100	96	91		
0.1	100	100	100	100	100	100	87	85		
0.2	100	100	100	100	100	100	75	80		
0.4	100	100	100	100	85	100	48	50		
0.8	100	100	100	100	100	100	100	100		
1.5	100	99	96	98	95	97	98	99		
3	98	97	95	97	94	95	96	98		
6	97	95	93	96	92	94	95	97		
12	95	93	92	95	90	92	94	96		
25	91	90	90	93	88	90	92	95		



Table 2. Inhibition of CoLo cells by S-01, 2-01, 2-03, 2-05, 2-08, 2-11, L2-06, L3-06, 3-01, 3-02, 3-03, 3-05, 3-06, 3-07, 3-09 and 3-13.

Conc. μM								
	S-01	2-01	2-03	2-05	2-08	2-11	L2-06	L3-06
% Cell Growth								
0	100	100	100	100	100	100	100	100
0.04	100	100	100	100	100	100	100	100
0.08	100	100	100	100	100	100	100	100
0.16	100	100	100	100	100	100	100	100
0.33	100	100	100	100	100	100	100	100
0.75	100	100	100	100	100	100	100	100
1.5	99	95	83	96	97	98	95	97
3	98	83	71	95	94	84	87	98
6	97	75	64	87	92	86	75	97
12	95	55	52	65	87	86	85	91
25	100	43	18	57	84	70	88	100
50	100	8	5	6	8	14	90	96
100	96	5	5	4	5	4	84	100
Conc. μM								
	3-01	3-02	3-03	3-05	3-06	3-07	3-09	3-13
% Cell Growth								
0	100	100	100	100	100	100	100	100
0.04	75	100	90	96	100	100	100	100
0.08	46	100	88	95	100	100	100	100
0.16	8	100	86	76	100	100	100	100
0.33	6	100	55	63	100	100	100	100
0.75	4	100	29	11	100	100	100	100
1.5	-	90	100	-	100	83	90	94
3	-	81	-	-	89	72	92	80
6	-	50	-	-	87	66	86	88
12	-	25	-	-	85	54	84	81
25	-	17	-	-	74	22	50	80
50	-	18	-	-	60	8	16	84
100	-	-	-	-	26	2	9	77

Appendix E

Results of the intercalation tests of the selected complexes.

Table 1. Intercalation of ethidium bromide, doxorubicin, propidium iodide, S-01, 3-01 and L2-06.

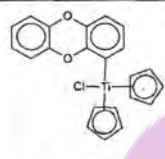
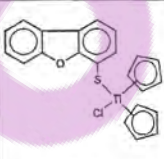
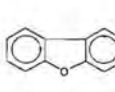
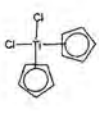
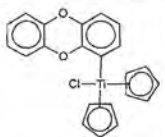
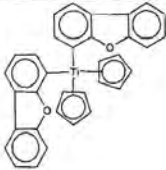
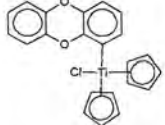
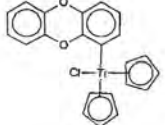
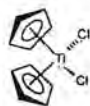
Conc. µg/ml	Ethidium bromide	Doxorubicin		Propidium iodide		 S-01		Conc. µg/ml	 3-01		 L2-06			
		Scattering (Median Channel Number)								Scattering (Median Channel Number)				
		SS	FS	SS	FS	SS	FS		SS	FS	SS	FS	SS	FS
0	0	0	100	100	100	100	0	0	0	0	0	0		
0.03	1	1	100	100	100	100	1	1	0.3	4	4	7	13	
0.06	2	3	100	100	100	100	2	3	0.6	0	2	7	12	
0.12	5	6	100	100	100	104	5	6	1.2	3	3	2	12	
0.24	10	12	101	101	101	101	10	12	2.4	9	4	0	11	
0.49	20	25	102	102	102	102	12	10	4.9	6	3	125	10	
0.98	40	50	103	103	103	103	10	8	9.8	9	8	11	11	
2	60	55	115	115	103	105	6	7	19.6	10	9	13	8	
3.9	110	50	123	115	118	113	5	10	39.1	10	10	11	5	
7.8	60	32	115	108	127	105	5	12	59.1	10	10	12	7	
15.6	20	28	105	103	100	102	5	8	78.1	8	12	9	3	
31.2	3	8	101	100	100	100	5	8	156.2	15	12	13	7	
62.5	2	40	120	120	100	100	5	10	312.5	17	13	13	5	
125	3	80	220	525	100	103	3	5	625	16	17	11	1	
250	5	120	-	-	100	125	5	3	1250	14	23	12	0	
500	10	250	-	-	100	145	6	3	2500	16	26	15	0	
1000	60	750	-	-	100	190	8	3	5000	17	33	21	2	

Table 2. Inhibition of CoLo cells by S-01, 2-02, 2-05, 3-01 and 3-09.

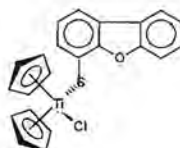
Conc. µg/ml					
	S-01	2-05	2-02	3-09	3-01
Side Scatter (Median Channel Number)					
0	5	5	5	5	5
0.1	5	5	5	5	5
0.2	5	5	5	5	5
0.4	5	5	5	5	5
0.8	5	5	5	5	5
1.5	5	5	5	5	5
3	5	5	5	5	5
6	5	5	5	5	5
12	5	5	5	5	5
25	5	6	6	7	13
50	5	7	8	12	36
100	5	23	27	37	93

Appendix F

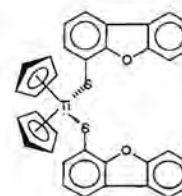
Cp hydrolysis of S-01, 3-01 and 3-02.



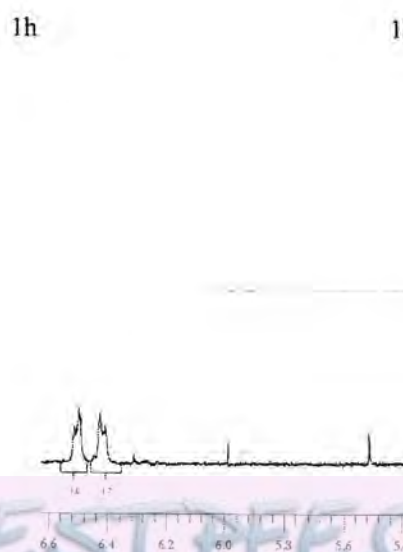
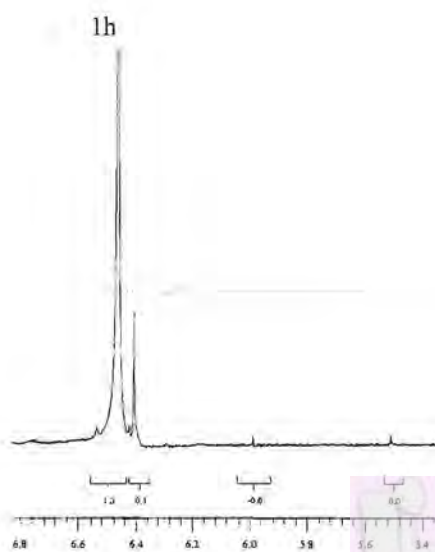
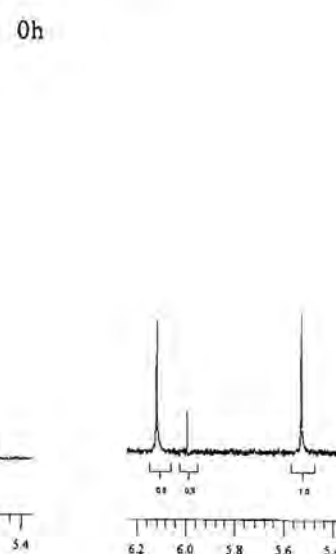
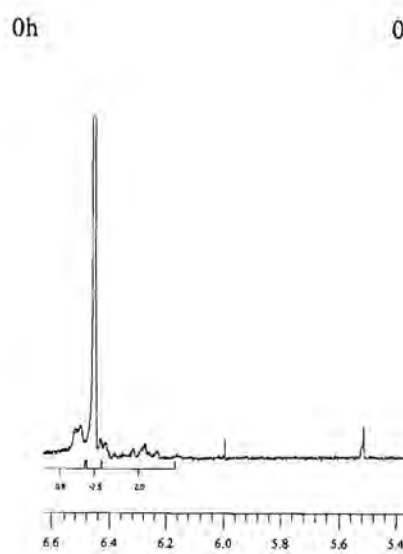
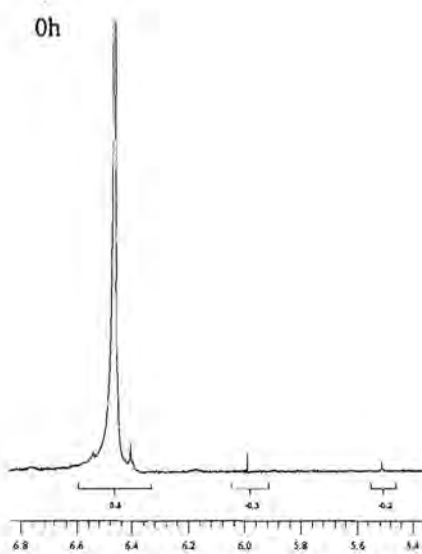
S-01

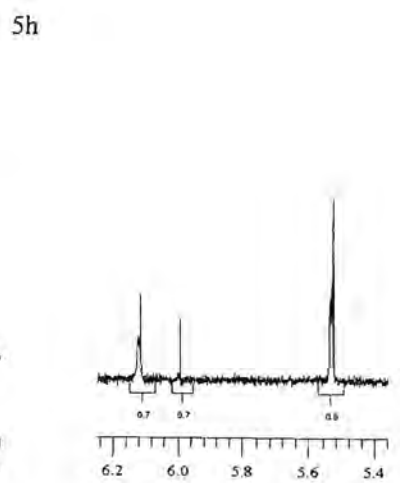
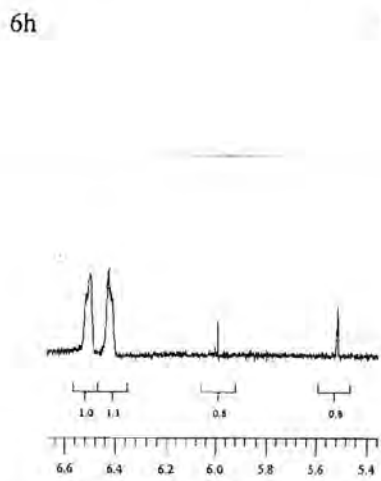
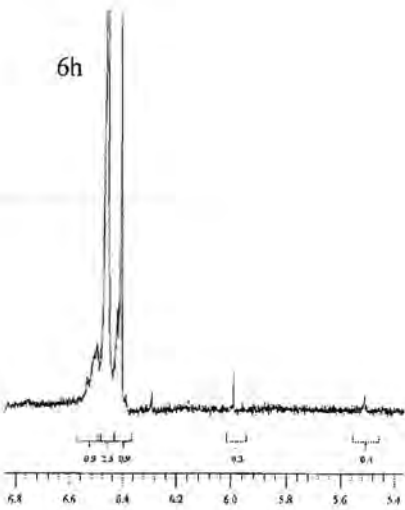
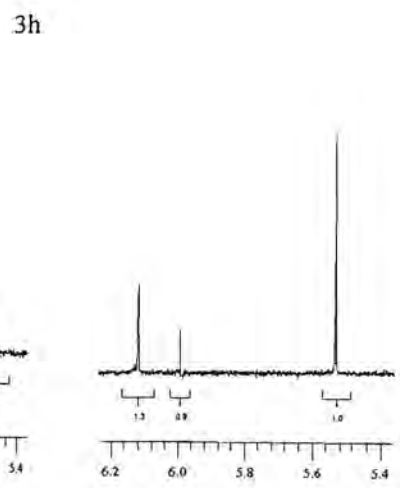
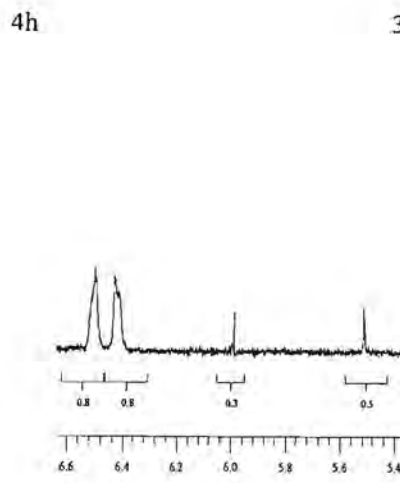
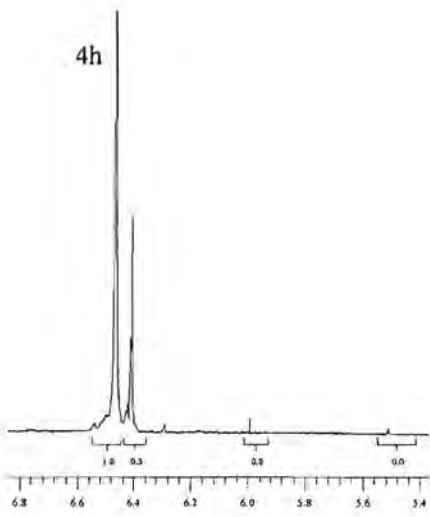
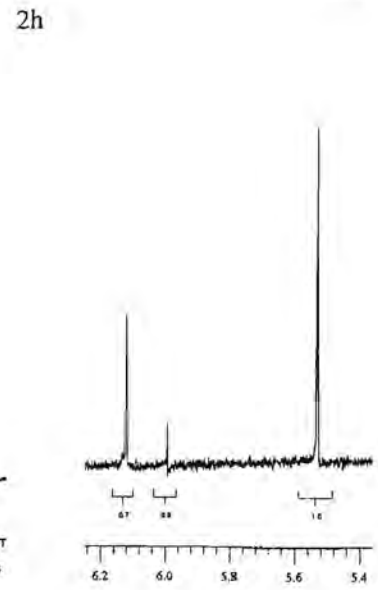
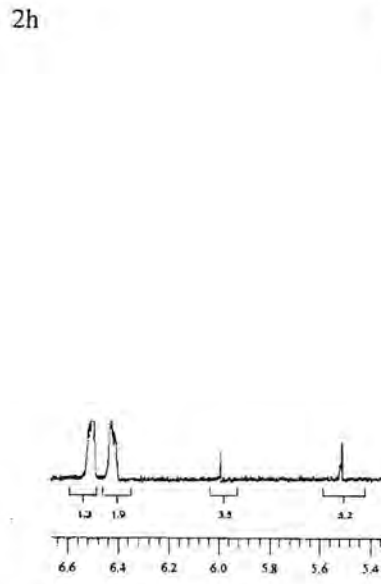
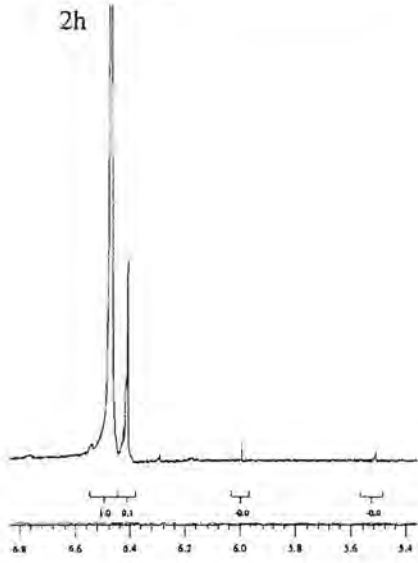


3-01



3-02





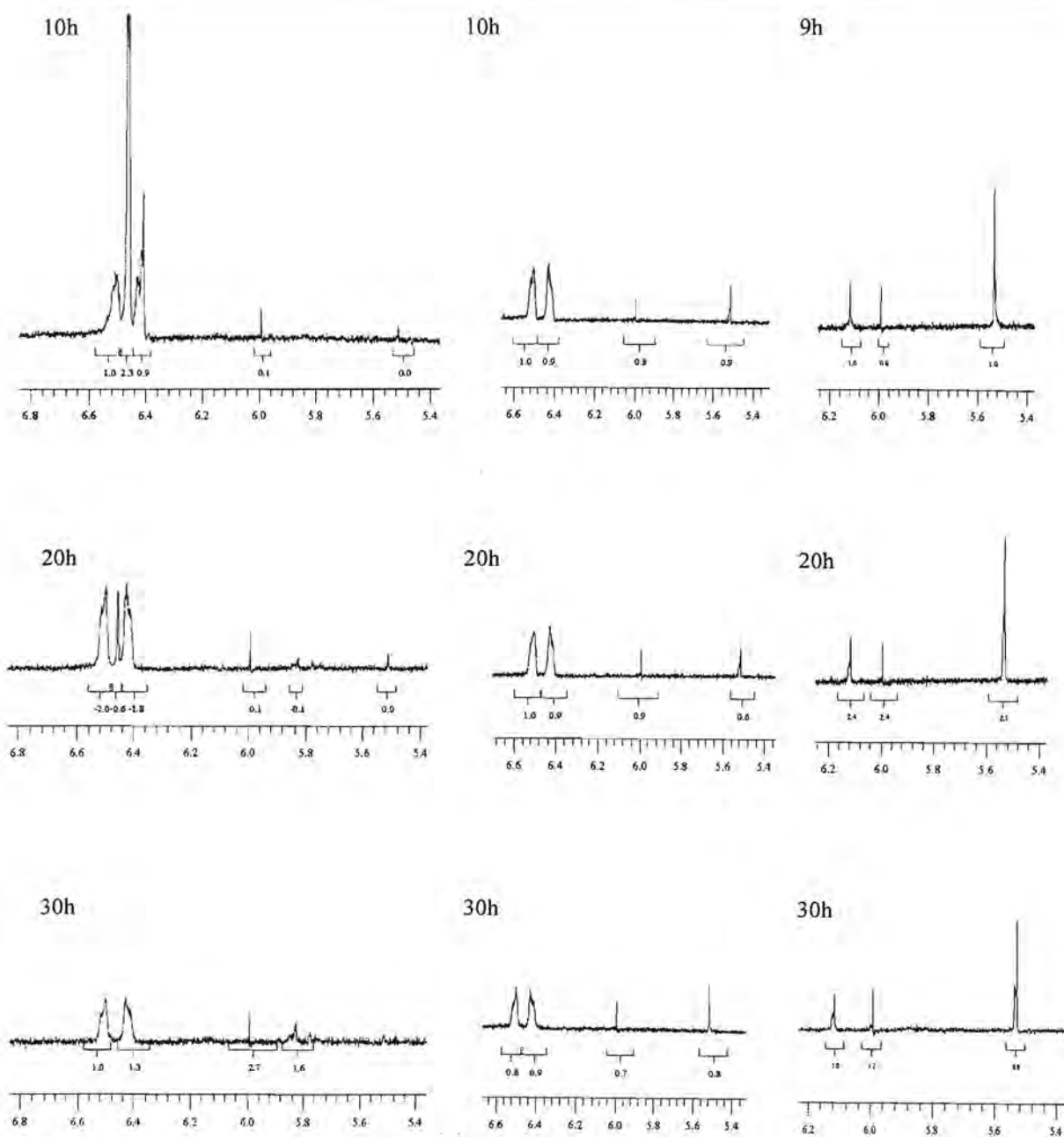
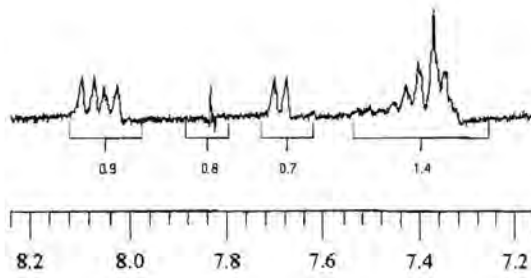


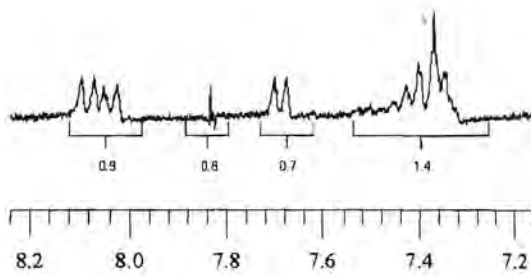
Figure 1. Experiment comparing Cp hydrolysis of S-01, 3-01 and 3-02.

Substitution of the thiolato ligand of complex 3-01.

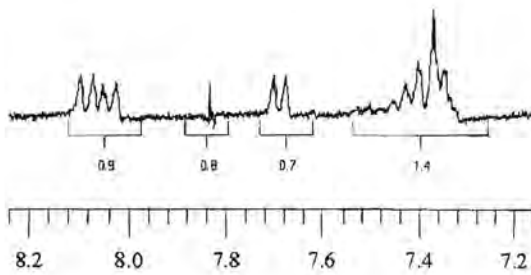
0h



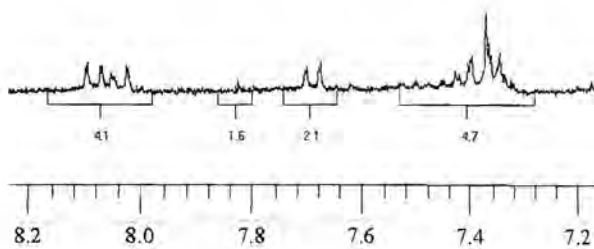
2h



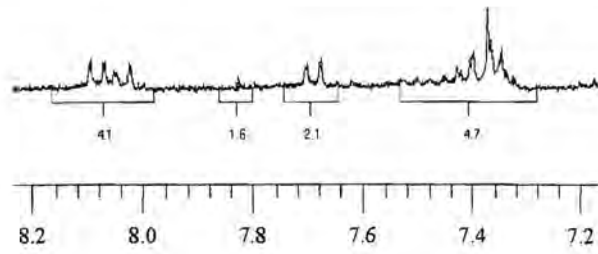
4h



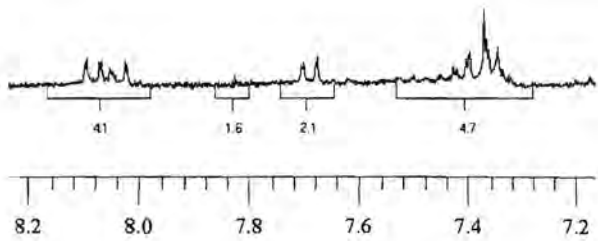
6h



10h



20h



30h

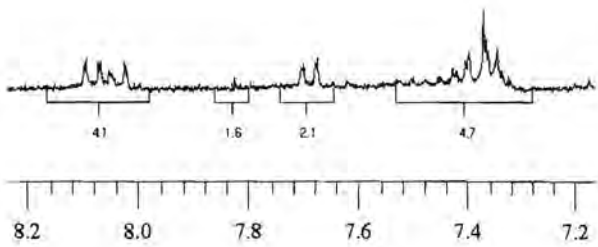
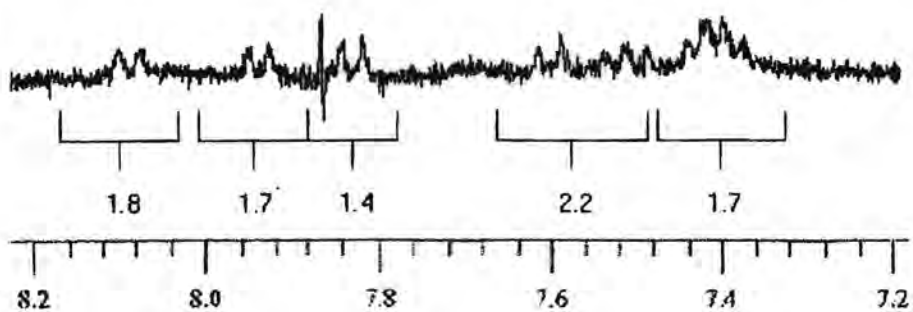


Figure 2. ¹H NMR resonances in the aromatic region of **3-01**.

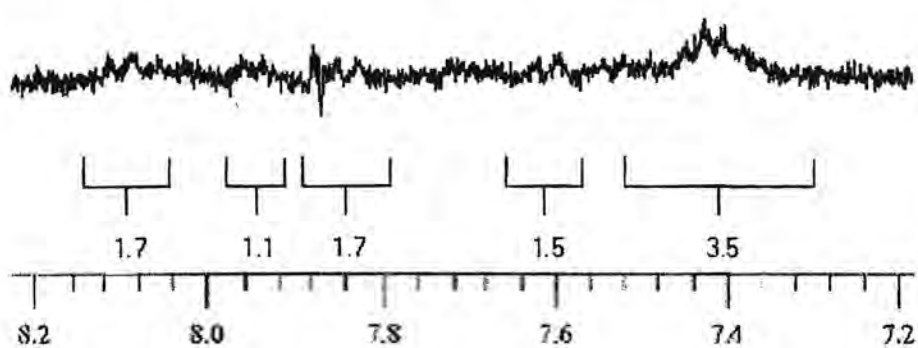


Substitution of the thiolato ligand of complex 3-02.

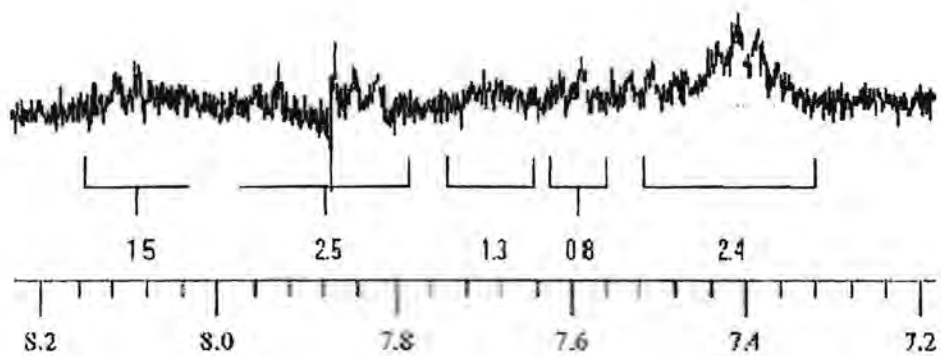
0h



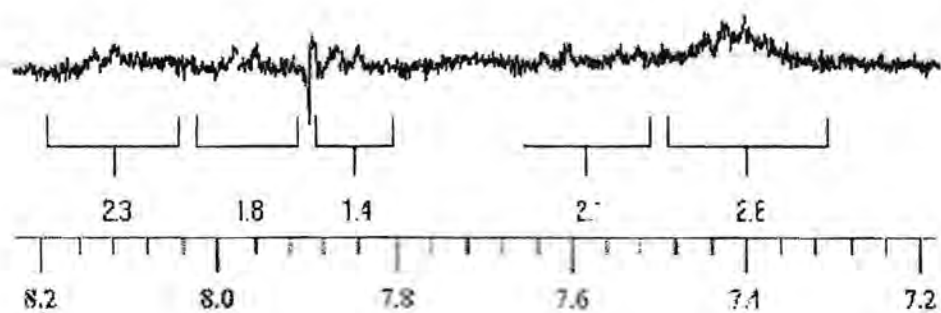
1h



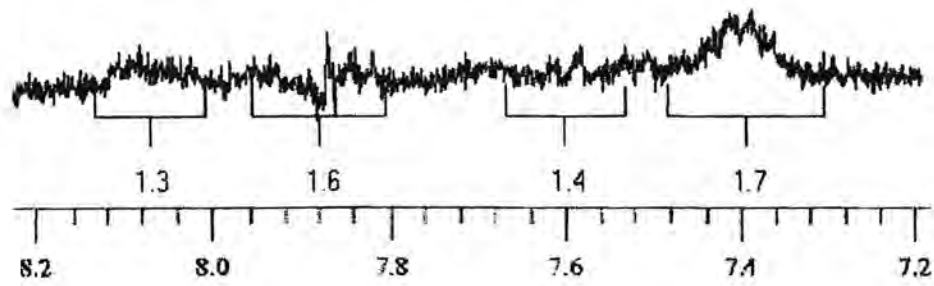
2h



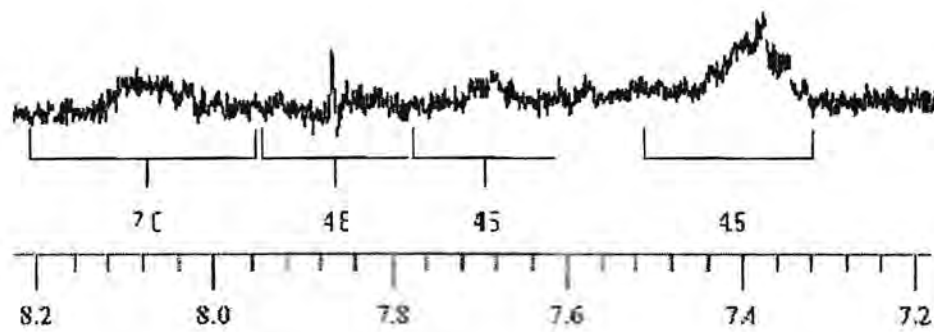
3h



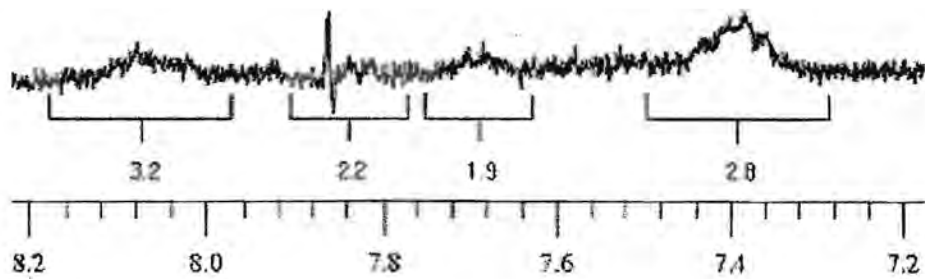
7h



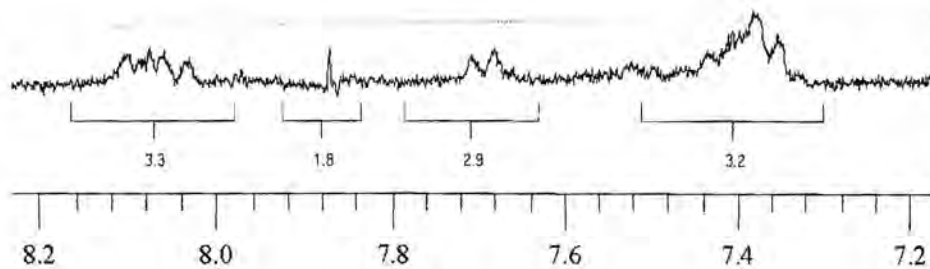
9h



20h



30h





60h

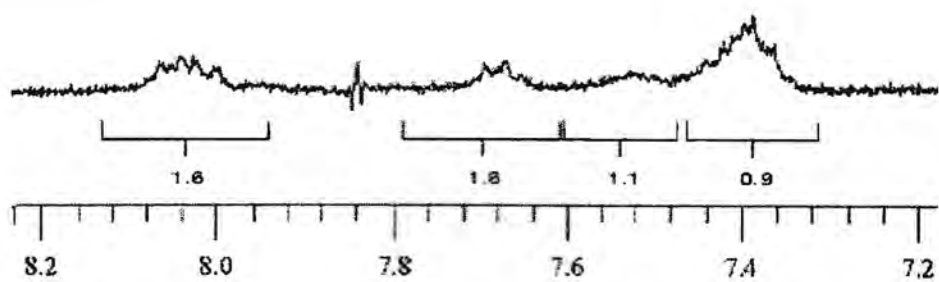


Figure 3. Substitution of the thiolato ligand of complex 3-02.